ISSN 1519-1397

PHYLLOMEDUSA

Journal of Herpetology

Volume 24 Number 2 December 2025

PHYLLOMEDUSA
Journal of Herpetology

ISSN 1519-1397 (print) / ISSN 2316-9079 (online)

Correspondence to:
Jaime Bertoluci
Departamento de Ciências Biológicas – ESALQ – USP
Av. Pádua Dias, 11 – 13418-900, Piracicaba – SP - BRAZIL
E-mail: phyllomedusa@usp.br

Cover: A male *Ninia sebae* from Veracruz, Mexico.
Photo: Víctor Vásquez-Cruz

ISSN 1519-1397 (print)
ISSN 2316-9079 (online)

PHYLLOMEDUSA

Journal of Herpetology

VOLUME 24 - NUMBER 2
JULY–DECEMBER 2025

Phyllomedusa

IS PUBLISHED BY **UNIVERSIDADE DE SÃO PAULO,**
ESCOLA SUPERIOR DE AGRICULTURA "LUIZ DE QUEIROZ"

PIRACICABA BIANNUAL

CREDENCIAMENTO E APOIO FINANCEIRO:
PROGRAMA DE APOIO ÀS PUBLICAÇÕES CIENTÍFICAS PERIÓDICAS DA USP
COMITÊ CIENTÍFICO

AGÊNCIA DE BIBLIOTECAS E COLEÇÕES DIGITAIS
DA UNIVERSIDADE DE SÃO PAULO

Phyllomedusa	Piracicaba	v.24	n.2	pp. 149–340	Jul–Dec 2025

PHYLLOMEDUSA
Journal of Herpetology

Phyllomedusa: Journal of Herpetology—Vol. 5, No. 1, 2006—Piracicaba, SP, Brazil: Departamento de Ciências Biológicas, Escola Superior de Agricultura "Luiz de Queiroz", Universidade de São Paulo.

v.; il

Vol. 1 (2002) to Vol. 3 (2004) published by Melopsittacus Publicações Científicas, Belo Horizonte, MG, Brazil.

Vol. 1 (2002) to Vol. 5 (2006) Phyllomedusa: Journal of Neotropical Herpetology

Biannual

Articles and abstracts in English; additional abstracts in Portuguese, Spanish, French, Italian, or German are optional.

ISSN 1519-1397 (print) ISSN 2316-9079 (online)
1. Herpetology CDU - 598

Phyllomedusa 24(2):151–173, 2025

ISSN 1519-1397 (print) / ISSN 2316-9079 (online)
doi: http://dx.doi.org/10.11606/issn.2316-9079.v24i2p151-173

A new lizard of the *Liolaemus walkeri* clade (Squamata: Liolaemidae) endemic to northern Chile

Jaime Troncoso-Palacios,[1] Roy Santa-Cruz,[2] Michael Venegas Ponce,[3] and Cesar Aguilar-Puntriano[4,5]

[1] Universidad de Chile, Facultad de Medicina, Programa de Fisiología y Biofísica. Av. Independencia 1027, Santiago, Chile. E-mail: jtroncosopalacios@gmail.com.

[2] Universidad Nacional de San Agustín de Arequipa, Museo de Historia Natural, Av. Alcides Carrión s/n, Arequipa, C.P. 04002, Peru. E-mail: lsantacruzf@unsa.edu.pe.

[3] Conciencia Soluciones Ambientales SPA. Avenida Apoquindo N°4700, Of. 1102A, Santiago, Chile. E-mail: mvenegas@concienciambiental.cl.

[4] Universidad Nacional Mayor de San Marcos, Museo de Historia Natural, Departamento de Herpetología. Av. Arenales 1256, Lima, Peru. E-mail: caguilarp@unmsm.edu.pe.

[5] Universidad Nacional Mayor de San Marcos, Facultad de Ciencias Biológicas, Laboratorio de Sistemática y Ecología de Vertebrados. Av. Carlos Germán Amezaga 375, Lima, Peru. E-mail: caguilarp@unmsm.edu.pe.

Abstract

A new lizard of the *Liolaemus walkeri* clade (Squamata: Liolaemidae) endemic to northern Chile. The *Liolaemus walkeri* clade comprises small, slender lizards, most species of which exhibit ventral melanism and a fragmented dark vertebral line. These lizards inhabit high Andean zones of Peru, although two field guide include photographs of *L. tacnae* from northern Chile, without voucher specimens or published scientific studies to support this taxonomic assignment. We recently examined specimens labeled *L.* cf. *tacnae* from Quebrada Blanca, Tarapacá Region, Chile, and performed morphological analyses, providing the first taxonomic assessment of a population of the *L. walkeri* clade outside Peru. Males of this population exhibit melanism on the throat and belly, and both sexes lack precloacal pores, among other diagnostic traits. We propose that this population represents a new species and highlight morphological characters of the *L. walkeri* clade that do not match those of the subgenus *Liolaemus* (*sensu stricto*). The *L. walkeri* clade lacks two of the three external characters used to diagnose the subgenus and does not exhibit some of the defining characters of the *L. alticolor-bibronii* group, where this clade is currently been placed by some studies. This observations suggest the need to evaluate the existence of a third subgenus of *Liolaemus* in future research.

Keywords: Andes, *Liolaemus tacnae*, Melanism, Precloacal pores, Tarapacá.

Resumen

Una nueva lagartija del clado de *Liolaemus walkeri* (Squamata: Liolaemidae) endémico del norte de Chile. El clado de *Liolaemus walkeri* comprende lagartijas pequeñas, esbeltas, en las cuales la mayoría de las especies presenta melanismo ventral y una línea vertebral oscura fragmentada.

Received 10 December 2024
Accepted 22 October 2025
Distributed December 2025

Estas lagartijas habitan en los altos Andes del Perú, aunque dos guías de campo de fauna incluyen fotografías de *L. tacnae*, del norte de Chile, sin especímenes de referencia o estudios científicos publicados para apoyar esta designación taxonómica. Recientemente nosotros examinamos especímenes etiquetados como *L.* cf. *tacnae* de Quebrada Blanca, Región de Tarapacá, Chile, y realizamos análisis morfológicos para proveer el primer estudio taxonómico de una población del clado de *L. walkeri* de fuera del Perú. Los machos de esta población presentan melanismo en el vientre y en la garganta, y ambos sexos carecen de poros precloacales, entre otras características de diagnóstico. Nosotros proponemos que esta población es una especie nueva y llamamos la atención sobre algunos caracteres morfológicos del clado de *L. walkeri* que no coinciden con los del subgénero *Liolaemus* (*sensu stricto*). El clado de *L. walkeri* carece de dos de los tres caracteres externos que diagnostican el subgénero, ni tampoco presenta algunos de los caracteres que definen el grupo de *L. alticolor-bibronii*, en donde algunos estudios actualmente sitúan a este clado. Esto levanta la necesidad de evaluar la pertinencia de un tercer subgénero de *Liolaemus* en un estudio futuro.

Palabras claves: Andes, *Liolaemus tacnae*, Melanismo, Poros precloacales, Tarapacá.

Resumo

Um novo lagarto do clado de *Liolaemus walkeri* (Squamata: Liolaemidae) endêmico no norte do Chile. O clado *Liolaemus walkeri* é composto por lagartos pequenos e esguios, e a maioria das espécies apresenta melanismo ventral e uma linha vertebral escura fragmentada. Esses lagartos habitam zonas andinas elevadas do Peru, embora dois guias de campo da fauna incluam fotografias de *L. tacnae* do norte do Chile, sem espécimes de referência ou estudos científicos publicados que apoiem essa classificação taxonômica. Recentemente, examinamos espécimes etiquetados como *L.* cf. *tacnae* de Quebrada Blanca, região de Tarapacá, Chile, e realizamos análises morfológicas, fornecendo a primeira avaliação taxonômica de uma população do clado *L. walkeri* fora do Peru. Os machos dessa população apresentam melanismo na região do mento e no ventre, e ambos os sexos não apresentam poros pré-cloacais, entre outras características diagnósticas. Propomos que essa população represente uma nova espécie e destacamos as características morfológicas do clado *L. walkeri* que não correspondem às do sub-gênero *Liolaemus* (*sensu stricto*). O clado *L. walkeri* não possui duas das três características externas utilizadas para diagnosticar o sub-gênero e não apresenta algumas das características definidoras do grupo *L. alticolor-bibronii*, em que esse clado está atualmente incluído por alguns estudos. Isso levanta a necessidade de avaliar a pertinência de um terceiro sub-gênero de *Liolaemus* em pesquisas futuras.

Palavras-chave: Andes, *Liolaemus tacnae*, Melanismo, Poros pré-cloacais, Tarapacá.

Introduction

Liolaemus is an extraordinarily diverse lizard genus, with nearly 300 described species (Abdala *et al.* 2021, Avila *et al.* 2021). Several new species continue to be discovered each year (Abdala *et al.* 2023, Campos-Soto *et al.* 2023, Sánchez *et al.* 2023, Troncoso-Palacios and Contreras-Piderit 2023). This remarkable diversity has been divided into two subgenera, *Eulaemus* and *Liolaemus* (*sensu stricto*), each further subdivided into several species groups (e.g. Avila *et al.* 2020). The *L. walkeri* clade consists of small, slender lizards, with black pigmentation on the throat (reticulation or melanism); and the lack of precloacal pores in some species (Aguilar *et al.* 2013, 2015).

Two alternative hypotheses have been proposed regarding the higher taxonomy of the *L. walkeri* clade. First, based on four mitochondrial (mtDNA) and six nuclear (nDNA) loci, Esquerré *et al.* (2019) placed the *L. walkeri* clade as sister to the node that separated the subgenera *Eulaemus* and *Liolaemus* (*sensu stricto*), a proposal also commented on in Esquerré *et al.* (2022). Second, Portelli and

Quinteros (2018) using a total-evidence phylogeny that combined two mitochondrial markers (mtDNA) and 167 morphological characters, placed the *L. walkeri* clade as a derived group within the subgenus *Liolaemus* (*sensu stricto*). Despite this disagreement, the monophyly of the group is not in question. It currently comprises six species (Aguilar *et al.* 2013, Santa-Cruz *et al.* 2025): *L. chavin* Aguilar, Wood, Cusi, Guzmán, Huari, Lundberg, Mortensen, Ramírez, Robles, Suárez, Ticona, Vargas, Venegas and Sites, 2013; *L. misti* Santa-Cruz, Canazas-Terán, Bejarano, López, Morales, von May, Catenazzi and Aguilar-Puntriano, 2025; *L. pachacutec* Aguilar, Wood, Cusi, Guzmán, Huari, Lundberg, Mortensen, Ramírez, Robles, Suárez, Ticona, Vargas, Venegas, and Sites, 2013; *L. tacnae* (Shreve, 1941); *L. walkeri* Shreve, 1938; and *L. wari* Aguilar, Wood, Cusi, Guzmán, Huari, Lundberg, Mortensen, Ramírez, Robles, Suárez, Ticona, Vargas, Venegas, and Sites, 2013.

Most species are currently considered endemic to Peru (Aguilar *et al.* 2013), although an undescribed species is suspected to inhabit Bolivia (I. De la Riva personal communication to CAP). In addition, *L. tacnae* and *L. walkeri* have been reported for Chile. In the case of *L. walkeri,* the record from Chile (Donoso-Barros 1961, 1966) was based on a misidentification of the unrelated species *L. puna* Lobo and Espinoza, 2004 (Lobo *et al.* 2010). However, the record of *L. tacnae* from Chile is more problematic. This species was described from three specimens (MCZ R-45806–08) collected at Toquepala Mine, sixty kilometers east of Moquegua, Department of Tacna, Peru (Shreve 1941), which is the southernmost Department of Peru, near the border with Chile. Additional information on the type series was later provided by Lobo and Espinoza (2004). Later, Aguilar *et al.* (2013) offered the most comprehensive characterization of this species to date, expanding its distribution to the Moquegua and Arequipa Departments from Peru, including DNA data from eight individuals made available in GenBank. Meanwhile, Lobo and Espinoza (1999) listed *L. tacnae* from Chile based on a female specimen (SDSU 1924) from Chapiquiña, 4080 m a.s.l., 3 km east of Portezuelo, Arica-Parinacota Region (near the border with Peru). The same authors later noted that this specimen is not referable to *L. tacnae* (Lobo and Espinoza 2004). Pincheira-Donoso and Núñez (2005) also listed *L. tacnae* for Chile, based on the same female specimen (SDSU 1924), without mentioning the early record (Lobo and Espinoza 1999) or its subsequent correction (Lobo and Espinoza 2004). Troncoso-Palacios and Etheridge (2012) re-examined the taxonomic status of this specimen and concluded that it should not be assigned to *L. tacnae* pending further data. Additionally, two books (Demangel 2016, Mella 2017) included photographs labelled as *L. tacnae* from Chile, but without providing supporting evidence for this species identification. Ruiz-de-Gamboa (2020), in an updated list of Chilean Squamata, recommended excluding *L. tacnae* from the Chilean fauna, citing the lack of reliable data.

More recently, Esquerré *et al.* (2022) included three individuals labelled as *L.* cf. *tacnae* from two localities in Chile, separated by more than 290 km, in their DNA phylogenetic analyses. One sample was from Quebrada Allane (18°02' S, 69°23' W, Arica-Parinacota Region) and two samples were from Quebrada Blanca (21°03' S, 68°51' W, Tarapacá Region). The novel DNA data by Esquerré *et al.* (2022) are not yet available in Genbank or any other repository. Their analyses, however, included DNA data from two individuals of *L. tacnae* (Genbank), but no additional species of the *L. walkeri* clade. Using mtDNA data, they found that all of these samples diverged from the same node. Thus, the *L.* cf. *tacnae* specimens from Chile undoubtedly belong to the *L. walkeri* clade, although their precise phylogenetic relationships within the clade remain unsolved.

We studied lizard specimens labelled as *Liolaemus* cf. *tacnae* in the herpetological collection of the Pontificia Universidad Católica

de Chile, which corresponded to an unexpected field discovery carried out in Quebrada Blanca (21°00' S, 68°49' W) by one of us (MVP) in 2021. Both samples (Esquerré *et al.* 2022 and this study) came from the Quebrada Blanca locality; but from two different coordinates separated by approximately 5.5 km straight line. The large geographic distance (more than 450 km straight line) between the type locality of *L. tacnae* and Quebrada Blanca raises doubts about the correct taxonomic assignment of this population. To clarify the status of the *L.* cf. *tacnae* population from Quebrada Blanca, hereafter referred to as *Liolaemus* sp. QuebradaBlanca, we conducted morphological analyses comparing it with all other known species of the *L. walkeri* clade.

Materials and Methods

Specimens of *Liolaemus* sp. QuebradaBlanca were collected in the field (21°00' S, 68°49' W, 15 November 2021) by hand or with a noose and euthanized with an injection of lidocaine 4% (Núñez *et al.* 2010). We examined specimens of all species of the *Liolaemus walkeri* clade. In total, 142 specimens were studied, which are listed in Appendix I, along with the acronyms used throughout this publication. Morphological characters commonly used in *Liolaemus,* described mainly by Etheridge (1995), Lobo (2005) and Aguilar *et al.* (2013), were analyzed. Body measurements were taken with a digital caliper to the nearest ± 0.02 mm. Scales were observed under different magnifying lenses.

Only adult males were used in the multivariate analysis to avoid confounding effects of intraspecific allometric variation (Losos 1990), and because for some species only a few adult females were available. All bilateral characters were recorded on the right side of each specimen.

The following morphometric traits were used in a principal component analysis (PCA): snout–vent length (SVL), head length, head width, snout length, auditory meatus width, auditory meatus length, rostral width, rostral depth, and axilla-groin distance. The following meristic characters were counted for statistical analyses: number of scales around midbody (SAM), number of dorsal scales between the occiput and the level of the anterior edge of the thigh (DS), number of ventral scales (VS), scales between the nasal and the canthal (NC), scales between the nasal and the subocular (NS), dorsal head scales (Hellmich Index, DHS), and scales around the interparietal scale (SAI).

For visualization and exploratory analysis, a PCA was performed using the R Package Facto Mine R (Lê *et al.* 2008) to compare almost all species of the *Liolaemus walkeri* clade with the candidate species *Liolaemus* sp. QuebradaBlanca. These analyses were carried out in R version 3.2.3 (R Development Core Team 2016). To assess the shape variation, the effect of size was removed by using the residuals of each character regressed on SVL in a correlation matrix. To better visualize any size effect, an additional analysis including SVL was also performed. Missing data were imputed using the function from the Miss MDAR package (Josse and Husson 2012).

For the meristic variables (square root transformed), as well the SVL to test the size differences among adult males, we performed the normality test (Shapiro-Wilk) and the homoscedasticy test (Levene). When assumptions were met, we used one-way ANOVA followed by a Holm-Sidak *post hoc* test. When normality or homoscedasticity assumptions were not met, we used the Kruskal-Wallis one-way analysis of variance on ranks, followed by a Dunn Test (Zar 2010).

We also considered qualitative traits, such as the color pattern and the shape of the scales, following Aguilar *et al.* (2013), and Lobo and Espinoza (1999).

Results

Morphometric analyses revealed clear differentiation among the studied species. In the PCA performed on the residuals of each character

regressed on SVL, the first four components cumulatively accounted for 74.0% of the variation (Table 1). The first axis (PC1, 30.7 %) was mainly influenced by head length, rostral width and rostral depth. PC2 (17.7 %, Table 1) primary reflected variation in auditory meatus length, head width and rostral depth. PC3 (13.6 %, Table 1) mostly represented variation in auditory meatus width, snout length and rostral depth. Finally, PC4 accounted for 11.9 % of the variation (Table 1). PCA plots (Figure 1) included 95.0% confidence ellipses around the centroid of each species and illustrated the morphometric differences among species. Across all PC plots, *Liolaemus* sp. QuebradaBlanca does not overlap with *L. tacnae,* but partially overlapped with *L. pachacutec* and *L. wari* (PC1 vs. PC2); and with *L. chavin* and *L. walkeri* (PC2 vs. PC3), whereas no overlap was observed in the PC1 vs. PC3 graph (Figure 1).

When body size (SVL) was included in the analysis, patterns of morphometric differentiation among species changed, revealing partial overlaps not detected in the residual-based PCA.

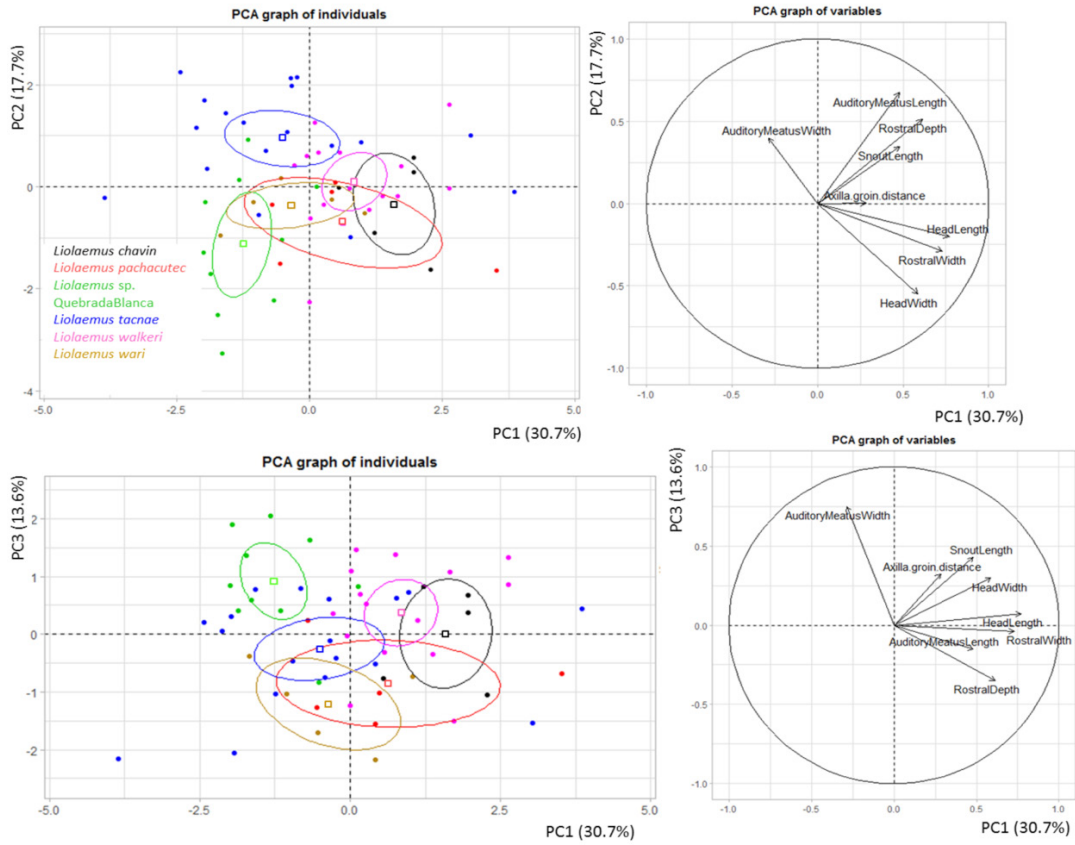

Figure 1. Principal Component Analysis (PCA) plots of males of almost all species of the *L. walkeri* clade, performed using the residuals of each character regressed on snout–vent length. In the left panels, individuals are colored according to their species, as shown on the legend at the bottom left corner. Ellipses represent the 95% confidence interval around the centroid for each species. Each axis is labeled with the PC number and the percentage of the total variance it explains. The right panels show variable plots, illustrating the contribution of each variable to the construction of the axes.

Table 1. Principal component (PC) axis loadings of continuous characters (males only) for *Liolaemus* sp. QuebradaBlanca (*N* = 10), *L. chavin* (*N* = 5), *L. pachacutec* (*N* = 5), *L. tacnae* (*N* = 18), *L. walkeri* (*N* = 15) and *L. wari* (*N* = 5). Eigenvectors, eigenvalues, and percentage of variance explained for the first three principal components based on data from putative species of the *L. walkeri* clade, with the exception of *L. misti*.

PCA of the residuals of each character in a regression with the snout–vent length				
Axes	**PC1**	**PC2**	**PC3**	**PC4**
Percentage variation accounted for	30.7	17.7	13.6	11.9
Eigenvalue	2.46	1.41	1.08	0.95
Head length	0.76	-0.20	0.07	-0.13
Head width	0.58	-0.54	0.29	-0.04
Axilla-groin distance	0.28	0.01	0.32	0.88
Snout length	0.47	0.34	0.42	-0.35
Rostral width	0.72	-0.29	-0.03	-0.08
Rostral depth	0.61	0.51	-0.35	0.03
Auditory meatus width	-0.28	0.39	0.74	-0.11
Auditory meatus length	0.47	0.67	-0.14	0.11
PCA including the snout–vent length				
Axes	**PC1**	**PC2**	**PC3**	
Percentage variation accounted for	50.7	12.6	11.0	
Eigenvalue	4.57	1.13	0.99	
Snout–vent length	0.85	0.16	-0.16	
Head length	0.76	-0.18	-0.11	
Head width	0.81	-0.01	-0.39	
Axilla-groin distance	0.67	0.17	-0.17	
Snout length	0.74	0.22	0.12	
Rostral width	0.86	-0.10	-0.18	
Rostral depth	0.57	-0.28	0.67	
Auditory meatus width	-0.09	0.94	0.13	
Auditory meatus length	0.70	0.10	0.50	

In the PCA including the SVL as a variable (Figure 2), the first three components cumulatively explained 74.4% of the variation (Table 1). PC1 (50.7 %) was mainly influenced by rostral width, snout vent length, and head width. PC2 (12.6 %, Table 1) primary reflected variation in auditory meatus width, rostral depth, and snout length. PC3 (11.0 %, Table 1) mostly represented variation in rostral depth, auditory meatus length, and head width. *Liolaemus* sp. QuebradaBlanca partially overlaped with *L. tacnae* (PC1 *vs.* PC2 graph) and with *L. pachacutec* (PC1 *vs.* PC3 graph),

while no overlap was observed in the PC2 *vs.* PC3 graph (Figure 2). Notably, the partial overlaps with *L. tacnae* were observed only in PCA including the SVL, but not in the PCA based on residuals.

Meristic and diagnostic characters further supported the distinctiveness of *Liolaemus* sp. QuebradaBlanca relative to other members of the *L. walkeri* clade. Statistical analyses of meristic characters and SVL revealed significant differences in seven of the eight variables analyzed (Table 2). At least one character differed significantly between *Liolaemus* sp. QuebradaBlanca and all other species of the *L. walkeri* clade, with the exception of *L. chavin*. Additionally, differences were observed between *Liolaemus* sp. QuebradaBlanca and all other species in binary diagnostic characters mentioned by Aguilar *et al.* (2013), including a novel color character unique to *Liolaemus* sp. QuebradaBlanca. Collectively, these results supported the recognition of *Liolaemus* sp. QuebradaBlanca as a distinct species, which we formally describe below.

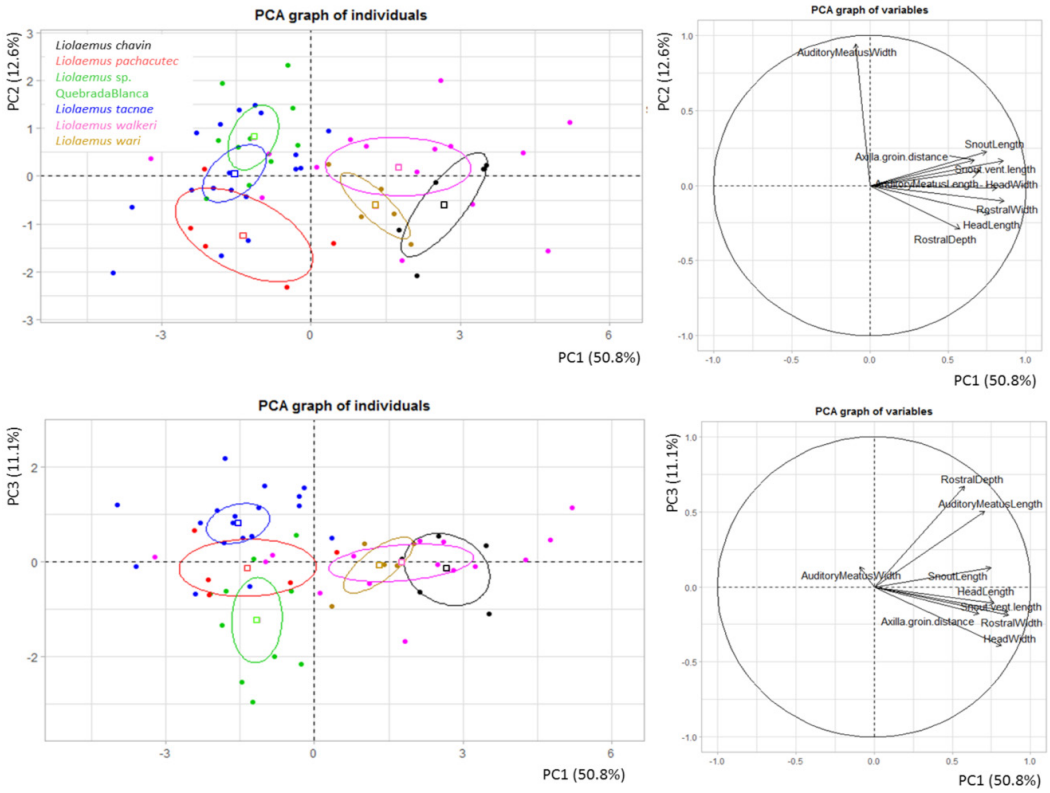

Figure 2. Principal Component Analysis (PCA) plots of males of almost all species of the *L. walkeri* clade, performed using the snout–vent length as a variable. In the left panels, individuals are colored according to their species, as shown on the legend at the top left corner. Ellipses represent the 95% confidence interval around the centroid for each species. Each axis is labeled with the PC number and the percentage of the total variance it explains. The right panels show variable plots, illustrating the contribution of each variable to the construction of the axes.

Table 2. Statistical results for meristic characters and snout vent length (SVL) in males of all species belonging to the *Liolaemus walkeri* clade. DHS = dorsal head scales, DS = dorsal scales, NC = scales between the nasal and the canthal, NS = scales between the nasal and the subocular, SAI = scales around the interparietal scale, SAM = scales around midbody and VS = ventral scales.

	One Way ANOVA			Holm-Sidak method
DHS	***F***	***p***	***df***	
	3.8	< 0.01	6	*Liolaemus* sp. QuebradaBlanca > *L. tacnae*; *L. chavin* > *L. tacnae*
	Kruskal-Wallis test			**Dunn Test**
DS	***H***	***p***	***df***	
	37.8	< 0.01	6	*Liolaemus* sp. QuebradaBlanca > *L. wari*; *L. chavin* > *L. wari*; *L. misti* > *L. pachacutec, L. tacnae, L. wari*; *L. walkeri* > *L. wari*
NC	45.2	< 0.01	6	*Liolaemus* sp. QuebradaBlanca > *L. pachacutec, L. wari, L. walkeri*; *L. misti* > *L. pachacutec, L. wari, L. walkeri*
NS	No significant result			
SAI	24.7	< 0.01	6	*Liolaemus chavin* > *L. pachacutec, L. tacnae*; *L. wari* > *L. pachacutec*
SAM	31.3	< 0.01	6	*Liolaemus chavin* > *L. pachacutec, L. tacnae*; *L. misti* > *L. pachacutec, L. tacnae*; *L. walkeri* > *L. pachacutec, L. tacnae*
SVL	38.5	< 0.01	6	*Liolaemus wari* > *L. misti, L. pachacutec, L. tacnae*; *L. chavin* > *L. misti, L. pachacutec, L. tacnae*; *L. walkeri* > *L. misti, L. pachacutec, L.*
VS	25.6	< 0.01	6	*Liolaemus* sp. QuebradaBlanca > *L. misti, L. pachacutec, L. tacnae*

***Liolaemus tunupa* sp. nov.**
(Figures 3 and 4)

LSID:Zoobank.org:pub:8CDAE041-C543-461D-AEDB-42271513A2BD

2016 *Liolaemus tacnae* (in part), Demangel. Reptiles en Chile, p. 42.

2017 *Liolaemus tacnae* (in part), Mella. Guía de campo reptiles de Chile, Volume 2, p. 28.

2020 *Liolaemus tacnae*, Ruiz de Gamboa. Boletín Chileno de Herpetología 7, p. 8.

2022 *Liolaemus* cf. *tacnae* (in part), Esquerré, Keogh, Demangel, Morando, Avila, Sites, Ferri-Yáñez and Leaché. Systematic Biology 71, p. 287.

Holotype.—SSUC Re 798. Adult male (Figure 3A, B). Quebrada Blanca (21°00'10" S, 68°49'50" W, 4280 m a.s.l.), approximately 120 km SE Pozo Almonte town, Tarapacá Region, Chile. Collector: M. Venegas. 15 November 2021.

Paratypes.—SSUC Re 799-807, nine males (Figure 3C, D). SSUC Re 808-813, six females (Figure 4). Same collection data as the holotype.

Etymology.—The species is named after the Andean divinity Tunupa, god of volcanoes and thunder, who was venerated by the Aymara people. It is most probable that the Tarapacá Region of Chile, in which *Liolaemus tunupa* sp. nov. inhabit, is also named after the god Tunupa.

Diagnosis.—DNA phylogenetic evidence provided by Esquerré *et al.* (2022) shows that *Liolaemus tunupa* sp. nov. is a member of the *L. walkeri* clade. It exhibits the morphological features characteristic of this group (Aguilar *et al.* 2013): it is a small (maximum SVL = 52.7 mm), slender lizard, which has black pigmentation on the throat (reticulation or melanism; Figure 3) and lacks precloacal pores in both sexes (Figure 5G, H). In addition, it lacks an upward curved, elongated supralabial scale (Figure 5A–C), has dorsolateral nostrils, and has parietal that scales are variable in size (smaller, similar, or larger than the interparietal).

Liolaemus tunupa sp. nov. and *L. chavin* are similar in scale counts and coloration. *Liolaemus tunupa* sp. nov. differs from *L. chavin* in that most males of *L. tunupa* sp. nov. have reddish coloration on the lateral sides and the venter, and all have a black lateral band over the shoulder (some specimens have white scales dispersed on the band). Males of *L. tunupa* sp. nov. have a fragmented vertebral line, whereas in *L. chavin* the line is continuous (Table 3). PCA analyses further show that both species only marginally overlap in few graphs of the first three PCs (Figures 1 and 2). Finally, *L. chavin* is the northernmost species of the clade, whereas *L. tunupa* sp. nov. is the southernmost.

Liolaemus tunupa sp. nov. has more ventral scales than *L. misti* (82.6 ± 3.7 *vs.* 76.2 ± 2.7); most males of *L. tunupa* sp. nov. exhibit reddish coloration on the lateral and ventral fields, whereas this trait is absent in males of *L. misti,* which exhibit reddish coloration in the dorsal and ventral side of the last half of the tail. In most males of *L. tunupa* sp. nov. the paravertebral stripe and the dorso-lateral stripes are barely visible, whereas in males of *L. misti* these stripes are evident.

Liolaemus tunupa sp. nov. has more ventral scales than *L. pachacutec* (82.6 ± 3.7 *vs.* 73.4 ± 2.9, Table 4) and more scales between the nasal and the canthal (2 *vs.* 1, Tables 2 and 4). In addition, males of *L. pachacutec* have precloacal pores (4–5), which are absent in *L. tunupa* sp. nov. Males and females of *L. pachacutec* lack regular spots on the lateral field, whereas these are present in both sexes in *L. tunupa* sp. nov. or are replaced by a black lateral band in males. Most males of *L. tunupa* sp. nov. have reddish color on the lateral and ventral fields, which is completely absent in males of *L. pachacutec*. Both species show only marginal overlap in some PCA graphs (Figures 1 and 2).

Liolaemus tunupa sp. nov. has more ventral scales than *L. tacnae* (82.6 ± 3.7 *vs.* 72.8 ± 7.0, Tables 2 and 4) and more dorsal head scales (15.7 ± 1.5 *vs.* 13.4 ± 0.9, Tables 2 and 4). Males of *L. tacnae* lack reddish coloration on lateral and ventral fields (reddish color is restricted to the sides of the tail); while most males of *L. tunupa* sp. nov. exhibit reddish coloration on the lateral and ventral fields. Males of *L. tacnae* have dark ventral rings on the tail, which are absent in *L. tunupa* sp. nov. (Table 3). We note that both species show only marginal overlap in some PCA graphs (Figures 1 and 2).

Liolaemus tunupa sp. nov. has more scales between the nasal and the canthal (2 *vs.* 1.2 ± 0.4, Tables 2 and 4) than *L. walkeri*. Moreover, males of *L. walkeri* have precloacal pores (3–6), which are absent in *L. tunupa* sp. nov. Males of *L. tunupa* sp. nov. have fragmented vertebral line, whereas in males of *L. walkeri* it is continuous (Table 3). In addition, males of *L. walkeri* lack reddish coloration on the lateral and ventral fields. Both species show only marginal overlap in some PCA graphs (Figures 1 and 2).

Liolaemus tunupa sp. nov. has more dorsal scales than *L. wari* (52.5 ± 2.1 *vs.* 45.1 ± 3.0, Tables 2 and 4) and more scales between the nasal and the canthal (2 *vs.* 1, Tables 2 and 4). Males of *L. wari* have precloacal pores (4–5), which are absent in *L. tunupa* sp. nov. In addition, males of *L. wari* have a continuous vertebral line, whereas in males of *Liolaemus tunupa* sp. nov. have a fragmented line. Males of *L. wari* lack reddish coloration on the lateral sides and venter. Males of *L. wari* have dark ventral rings on the tail, which are absent in *L. tunupa* sp. nov. Both species show only partial

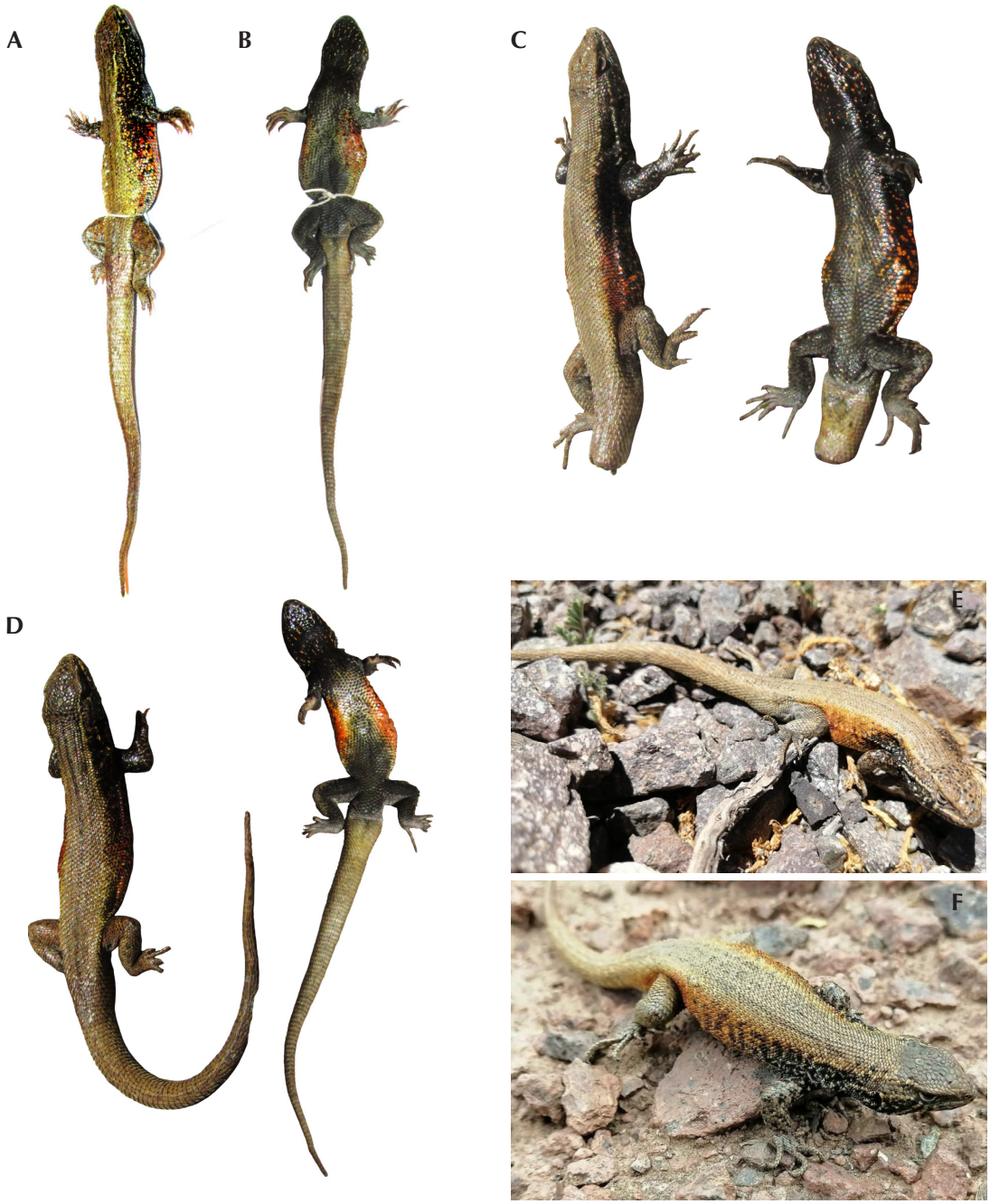

Figure 3. Some male specimens of *Liolaemus tunupa* sp. nov. (**A, B**) Holotype SSUC Re 798 (SVL = 50.6 mm) in dorsal and ventral view, respectively. Note the presence of some discolored dorsal scales (light gray). (**C**) Paratype SSUC Re 800 (SVL = 52.2 mm) in dorsal and ventral view. (**D**) Paratype SSUC Re 805 (SVL = 52.7 mm, largest male in the sample) in dorsal and ventral view. (**E, F**) Male individuals not vouchered.

Figure 4. Some female specimens of *Liolaemus tunupa* sp. nov. (**A**) Paratype SSUC Re 813 (SVL = 49.3 mm) in dorsal and ventral view. (**B**) Paratype SSUC Re 812 (SVL = 44.8 mm) in dorsal and ventral view. (**C**) Paratype SSUC Re 809 (SVL = 48.5 mm) in dorsal and ventral view.

overlap in some PCA graphs (Figures 1 and 2).

A summary of the morphological features used for comparison is provided in Table 4. Due to its size and shape, *L. tunupa* sp. nov. might be confused with *L. puna,* a species of the *L. alticolor-bibronii* group of the *Liolaemus* (*sensu stricto*) subgenus, which also inhabits the Tarapacá Region of Chile. However, all species of the *L. walkeri* clade, including *L. tunupa* sp. nov., lack an upward curved, elongated supralabial scale (Figure 5A–C), and have dorsolateral nostrils. All other species of *Liolaemus* (*sensu stricto*), have an upward curved, elongated supralabial (usually the fourth) and lateral nostrils (Etheridge 1995; Figure 5D–E of this study), including *L. puna* (Lobo and Espinoza

2004, Pincheira-Donoso and Núñez 2005). Species of the *L. walkeri* clade have parietal scales that are variable in size (smaller, similar or larger than the interparietal), but in *L. puna* and at least the Chilean and Peruvian species of the *L. alticolor-bibronii* group the interparietal scale is always smaller than the parietals (Pincheira-Donoso and Núñez 2005, CAP and JTP unpublished data). Finally, in males of Chilean species of the *L. alticolor-bibronii* group, including *L. puna,* precloacal pores are always present (Pincheira-Donoso and Núñez 2005, named as *L. bibronii* group), whereas they are absent in males of *L. tunupa* sp. nov.

Description of holotype.—Adult male. SVL = 50.6 mm. Horizontal diameter of the eye: 2.8 mm. Subocular length: 3.0 mm. Length of the fourth supralabial: 2.2 mm. Head length (from the anterior border of the auditory meatus to the tip of the snout): 11.3 mm. Head height (at the level of ear openings): 5.6 mm. Head width (distance between the two ear openings): 10.3 mm. Neck width: 8.9 mm. Interorbital distance: 4.6 mm. Ear-eye distance: 3.6 mm. Internasal distance: 1.9 mm. Ear width: 1.2 mm. Ear height: 1.5 mm. Axilla-groin distance: 21.4 mm. Body width: 14.4 mm. Forelimb length: 17.9 mm. Hindlimb length (the fourth toe is partially amputated): 20.7 mm. Tail length (not autotomized): 77.0 mm; tail length/SVL ratio = 1.5. Rostral scale wider (2.4 mm) than high (0.6 mm).

Two postrostrals and four internasals present. The interparietal is pentagonal, with a small central spot marking the position of the parietal eye. The interparietal scale is larger than the parietals and is surrounded by eight scales. Parietal scales partially in contact. Nine scales between the interparietal and rostral. Thirteen scales between the occiput and the rostral. Orbital semicircles complete, each formed by 11 scales. Four supraoculars on both sides. Seven superciliary scales. The frontal area is divided into five scales (2, 1 and 2, from anterior to posterior). Preocular separated from the lorilabials by one loreal scale. Two scales between nasal and canthal. The nasal is in contact with the rostral and surrounded by six scales (including the rostral). One row of lorilabials between the supralabials and the subocular. Six supralabials, fourth elongated; but not curved upward; the fifth oriented diagonally, like slash symbol (/). Five infralabials. Mental pentagonal, in contact with four scales. Few pairs of enlarged post-mental scales, only two pairs distinguishable: the first in contact and the second separated by two scales. The temporal scales variable in shape, slightly keeled or smooth, mainly juxtaposed, with few subimbricate. Seven temporal scales are between the level of superciliary scales and the level of the mouth commissure. Two projected scales on the anterior edge of the ear, not covering the auditory meatus. Differentiated auricular scale, quadrangular, located on the upper section of the auditory meatus. Thirty-six gular scales between the auditory meatuses. Dorsolateral neck fold "Y" shaped. SAM: 50. Dorsal scales lanceolate, subimbricate, keeled, without mucron; few interstitial granules. Dorsal scales larger than ventral scales. DS: 51. Ventral scales rounded, smooth, subimbricate, with interstitial granules. VS: 84. No precloacal pores. Supra-antebrachial scales rounded, imbricate, keeled, some mucronate. Infra-antebrachials rounded, imbricate, smooth. Supra-femoral scales lanceolate, imbricate, keeled, some mucronate. Infra-femoral scales rounded, smooth, imbricate. Dorsal scales of the first third of the tail rhomboidal, imbricate, keeled, mucronate. Ventral scales: in the first third of the tail lanceolate, smooth, imbricate. Finger lamellae: I: 8, II: 14, III: 17, IV: 19, V: 10. Toes lamellae (partially amputated toes omitted): V: 16. The left foot also has partially amputated toes, with the exception of the second.

Color of holotype in ethanol.—Dorsal pattern as follows. Dorsal surface of the head is brown, scattered with black small spots. The interparietal, rostral and mental scales are light brown. The temporal region and the cheeks are black with

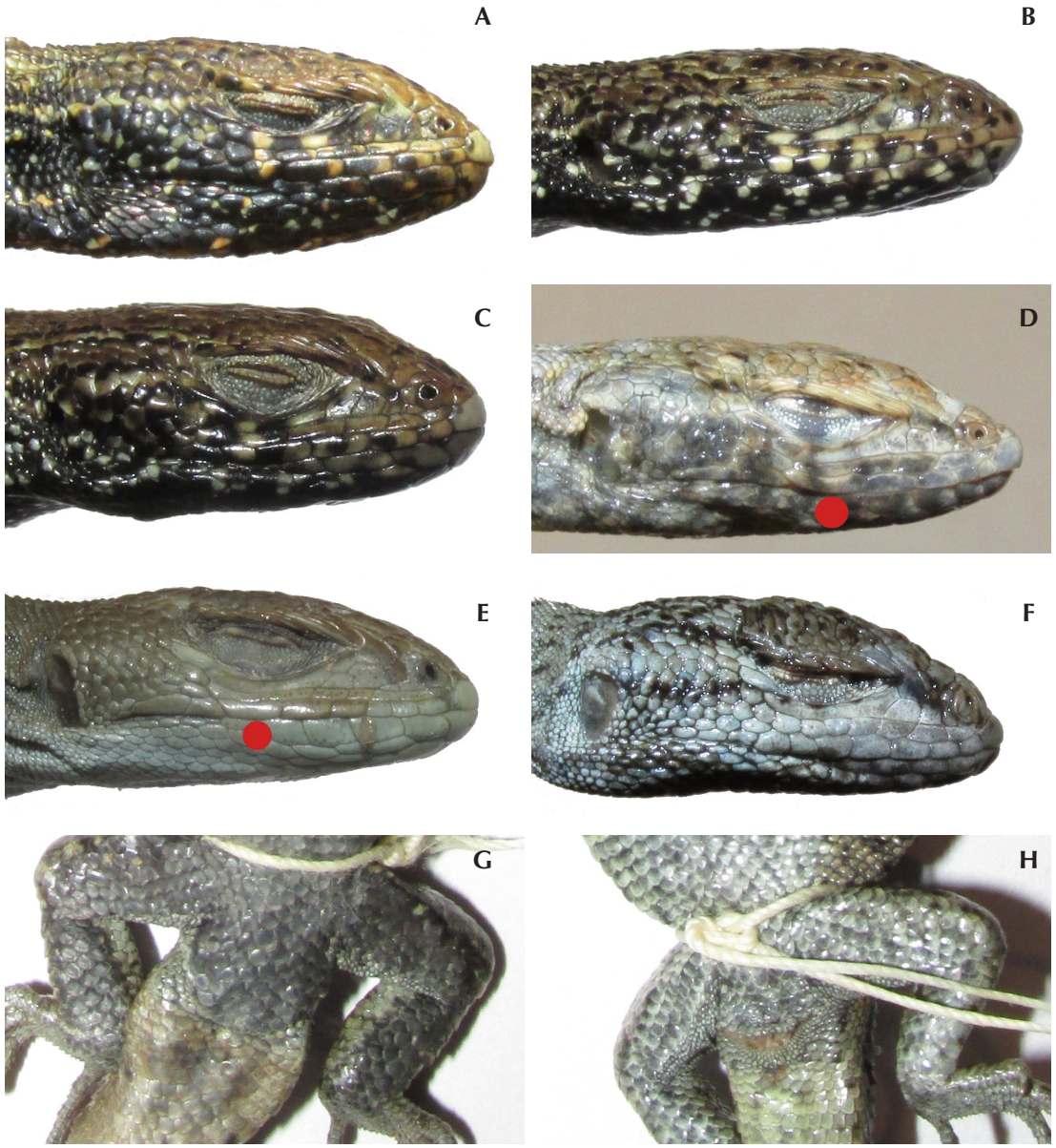

Figure 5. (**A**) Lateral view of the head of the holotype of *Liolaemus tunupa* sp. nov. (SSUC Re 798), without an enlarged upward curved supralabial scale and dorsolateral nostril. (**B, C**) Lateral head view of two paratypes of *L. tunupa* sp. nov., SSUC Re 799 (male) and SSUC Re 805 (male), respectively, both without an enlarged upward curved supralabial scale and with dorsolateral nostril. (**D**) Specimen of *L. constanzae* SSUC Re 343, *Liolaemus* (*sensu stricto*) subgenus, with the fourth supralabial curved upward (above the red dot) and lateral nostril. (**E**) Specimen of *L. janequeoae* SSUC Re 650, *Liolaemus* (*sensu stricto*) subgenus, with the sixth supralabial curved upward (above the red dot) and lateral nostril. (**F**) Specimen of *L. rosenmanni* SSUC Re 149, *Eulaemus* subgenus, without an enlarged upward curved supralabial scale and dorsolateral nostril. Cloacal region of (**G**) a male paratype (SSUC Re 805) and (**H**) a female paratype (SSUC Re 812) of *L. tunupa* sp. nov.

Table 3. Binary characters for adult males of the *Liolaemus walkeri* clade. Data are from Aguilar *et al.* (2013), plus *L. tunupa* sp. nov. (this study), and *L. misti* (from Santa-Cruz *et al.* 2025). Only characters that may be used as diagnostic between species are shown. The vertebral line is presented as a not binary character.

	***L. tunupa* sp. nov. (*N* = 10)**	***L. chavin* (*N* = 12)**	***L. misti* (*N* = 13)**	***L. pachacutec* (*N* = 8)**	***L. tacnae* (*N* = 18)**	***L. walkeri* (*N* = 21)**	***L. wari* (*N* = 10)**
Precloacal pores	No	No	No	Yes (4–5)	No	Yes (3–6)	Yes (4–5)
Regular spots in lateral field	Yes	Yes	Yes	No	Yes/No	Yes/No	Yes
Complete or partial melanistic belly	Yes	Yes	Yes/No	Yes	Yes/No	Yes	Yes/No
Ventral tail with ringed pattern	No	Yes/No	No	No	Yes	No	Yes
Reddish lateral color on trunk	Yes/No	No	No	No	No	No	No
Vertebral line	Fragmented/ Absent	Unfragmented	Fragmented	Unfragmented/ Absent	Fragmented	Unfragmented	Unfragmented

dispersed light-yellow dots. The trunk is brown with yellowish shades. A fragmented black vertebral line runs from the occiput along the entire tail, though it is inconspicuous between the base and the tip of the tail. Fragmented and inconspicuous black paravertebral stripes run from the occiput to the base of the tail. A light brown dorsolateral stripe runs from the upper posterior border of the eye to the shoulder, and a ventrolateral stripe runs from the lower posterior border of the eye but ends on the neck, before reaching the shoulder. As noted, a lateral black band extends from the cheeks through the temporal region of the head, along the neck, and terminates at the shoulder. Whitish scales are present on the antehumeral pocket. Five black transverse dorsolateral stripes are present on the trunk. Dorsolateral and ventrolateral regions of the trunk are reddish. The forelimbs are black with scattered whitish scales. The hindlimbs are brown with dispersed dark brown spots. Tail is brown, lacking rings.

Ventral coloration as follows. Throat is black with a few whitish stripes. The chest, central belly, and cloacal region are dark gray. The sides of the belly are reddish with dispersed dark gray spots. Forelimbs and hindlimbs are dark gray. The tail is whitish and unpatterned.

Variation.—Based on ten adult males (including the holotype): SVL: 47.4–52.7 mm (50.6 ± 1.7). Axilla-groin distance: 19.0–24.5 mm (21.3 ± 1.9). Head length: 10.5–12.1 mm (11.3 ± 0.4). Head width: 8.3–10.3 mm (9.7 ± 0.6). Head height: 4.9–6.0 mm (5.6 ± 0.4). Forelimb length: 16.4–17.9 mm (16.9 ± 0.7). Hindlimb length: 25.2–28.1 mm (26.3 ± 1.1). Foot length: 13.3–14.8 mm (14.3 ± 0.5). Tail length: 77.0–85.0 mm (81.3 ± 3.9, four specimens measured, autotomized in the remainder). Tail length/SVL ratio = 1.5–1.6. No precloacal pores. In six adult females: SVL: 44.8–52.2 mm (47.9 ± 2.7). Axilla-groin distance: 20.2–26.2 mm (22.9 ± 2.2). Head length: 9.4–10.6 mm (10.0 ± 0.4). Head width: 8.1–8.6 mm (8.5 ± 0.2). Head height: 4.5–5.5 mm (5.0 ± 0.4).

Forelimb length: 14.4–16.3 mm (15.3 ± 0.7). Hindlimb length: 22.4–25.5 mm (24.6 ± 1.2). Foot length: 13.0–14.1 mm (13.7 ± 0.4). Tail length: 63.0–69.0 mm (66.0 ± 3.0, three specimens measured, autotomized in the remainder). Tail length/SVL ration = 1.2–1.5. Precloacal pores absent.

The variation in squamation in adult males is as follows. SAM: 46–54 (50.4 ± 3.5). DS: 49–56 (52.5 ± 2.1). VS: 78–88 (82.6 ± 3.7). Fourth finger lamellae: 16–19 (17.9 ± 1.2). Fourth toe lamellae: 20–23 (21.3 ± 1.2). Supralabial scales: 6–7 (6.2 ± 0.4). Infralabial scales: 5–6 (5.2 ± 0.4). Variation in adult females is as follows. SAM: 44–56 (50.7± 4.7). DS: 49–57 (53.3 ± 3.3). VS: 79–86 (82.0 ± 2.8). Fourth finger lamellae: 17–19 (17.3 ± 0.8). Fourth toe lamellae: 20–23 (21.3 ± 1.4). Supralabial scales: 6. Infralabial scales: 5. In adult specimens of both sexes, the interparietal scale is triangular, pentagonal or hexagonal. It is bordered by 6–8 scales (7.1 ± 0.8). The parietal scales are highly variable in size, being smaller than, similar to or larger than the interparietal. Parietals are separated, partially in contact, or in contact. Nasal and rostral scales are in contact or separated by one scale. No upward curved supralabial. Precloacal pores absent.

Adult male paratypes have a color pattern similar to the holotype (Figure 3). However, the trunk is brown without the yellowish shades in most specimens. The fragmented black vertebral line and the fragmented black paravertebral stripes are more pronounced than in the holotype in some specimens, whereas they are as inconspicuous as in the holotype in most specimens. The light brown dorsolateral and ventrolateral stripes are entirely absent in some specimens. The lateral black band starts on the cheeks or anterior to the shoulder and may extended to the groin, sometimes with scattered white scales. Reddish dorsolateral and ventrolateral coloration of the trunk is absent in some specimens. Tail without rings. Ventrally, the throat shows complete melanism or is black with whitish stripes, some specimens also have reddish scales instead of white. Ventral melanism varies from complete to restricted to the posterior belly, especially the cloacal region. The sides of the belly are reddish or yellowish. The ventral surface of the tail is whitish and unpatterned. In the adult females (Figure 4), the dorsal surface of the head is brown with some scattered black spots. The temporal area and sides of the neck are brown. A black or dark brown fragmented vertebral line runs from the occiput to almost the tip of the tail or at least two-thirds of it, accompanied by black or dark brown fragmented paravertebral lines, extending over the same area. In some specimens the vertebral and paravertebral lines are almost indistinguishable. A dorsolateral and a ventrolateral light brown stripe runs from the posterior border of the eye to the base of the tail. A lateral band formed by several black or dark brown spots runs from the posterior border of the ear to the groin (or extends to the middle of the trunk), although it is inconspicuous in some specimens. Some specimens have few reddish scales on the lateral sides. Forelimbs and hindlimbs are brown with black or dark brown spots or short stripes; however, in some specimens the limbs are uniformly brown. Ventrally, the throat is gray, yellowish, or reddish with black stripes that extend onto the chest. The belly is gray. Of six females, one has orange on the sides of the belly, and the others have yellow on the sides or over the entire belly. The ventral surfaces of the limbs are gray or gray-yellow, immaculate or with black spots. The cloacal area is gray or gray-yellow. The ventral surface of the tail is light gray and unpatterned.

Distribution and natural history.— There are two confirmed records for *L. tunupa* sp. nov. (Figure 6), both from the same locality, Quebrada Blanca, approximately 120 km SE Pozo Almonte city, Tarapacá Region, Chile. However, these records have different coordinates, separated by approximately 5.5 km in a straight line. The type locality is in Quebrada Blanca (21°00'10" S, 68°49'50" W, 4280 m, this study), and Esquerré

Table 4. Squamation and morphological characteristics of species of the *Liolaemus walkeri* clade. Adult males are shown in the upper row and adult females in the lower row. Since few females were examined for some species and characters, PCA and statistical analyses were performed only on males. Values are presented as mean ± standard deviation. Measurements in mm.

	L. chavin M = 11, F = 18	***L. misti*** M = 11	***L. pachacutec*** M = 5, F = 4	***L. tacnae*** M = 16, F = 25	***L. tunupa* sp. nov.** M = 10, F = 6	***L. walkeri*** M = 21, F = 27	***L. wari*** M = 7, F = 10
Meristic characters							
Scales around midbody (SAM)	48–62 (55.8 ± 7.3) 48–66 (57.5 ± 5.0)	49–58 (52.4 ± 2.7)	39–46 (43.6 ± 2.7) 42–51 (47.0 ± 3.7)	43–57 (47.8 ± 4.1) 40–58 (46.9 ± 3.4)	46–54 (50.4 ± 3.5) 44–56 (50.7 ± 4.7)	45–62 (53.7 ± 4.1) 47–62 (53.7 ± 3.8)	48–55 (50.9 ± 2.9) 46–54 (49.8 ± 2.6)
Dorsal scales (DS)	43–66 (54.0 ± 7.2) 45–65 (57.0 ± 6.1)	53–59 (55.7 ± 1.8)	42–50 (45.8 ± 3.3) 43–50 (46.5 ± 3.5)	40–53 (47.1 ± 4.0) 42–54 (47.2 ± 2.9)	49–56 (52.5 ± 2.1) 49–57 (53.3 ± 3.3)	45–59 (52.5 ± 3.8) 49–66 (56.2 ± 4.8)	41–50 (45.1 ± 3.0) 40–50 (45.7 ± 2.9)
Ventral scales (VS)	71–87 (79.2 ± 3.9) 70–87 (79.1 ± 4.7)	72–81 (76.1 ± 2.5)	69–77 (73.4 ± 2.9) 73–79 (77.0 ± 2.8)	60–85 (72.8 ± 7.0) 68–87 (77.7 ± 4.1)	78–88 (82.6 ± 3.7) 79–86 (82.0 ± 2.8)	72–84 (78.7 ± 4.2) 73–96 (82.6 ± 5.6)	73–88 (77.6 ± 5.4) 71–83 (76.6 ± 3.4)
Scales between the nasal and the canthal (NC)	1–2 (1.4 ± 0.5) 1–2 (1.7 ± 0.5)	2	1 1	1–2 (1.8 ± 0.4) 1–2 (1.8 ± 0.4)	2 1–2 (1.8 ± 0.4)	1–2 (1.2 ± 0.4) 1–2 (1.3 ± 0.5)	1 1–2 (1.1 ± 0.3)
Scales between the nasal and the subocular (NS)	3–5 (3.8 ± 0.8) 2–5 (3.4 ± 0.7)	3–4 (3.8 ± 0.4)	4–5 (4.8 ± 0.4) 3–5 (4.0 ± 0.8)	4–5 (4.2 ± 0.4) 3–5 (4.0 ± 0.3)	4 4	2–5 (3.8 ± 0.8) 3–5 (3.9 ± 0.7)	3–5 (4.0 ± 0.6) 2–5 (3.7 ± 1.1)
Dorsal head scales (DHS)	13–18 (15.5 ± 1.8) 10–19 (14.1 ± 2.3)	13–17 (15.2 ± 1.4)	13–16 (14.6 ± 1.3) 12–14 (12.5 ± 1.1)	11–15 (13.4 ± 1.1) 11–17 (13.9 ± 1.7)	13–18 (15.7 ± 1.5) 13–16 (14.8 ± 1.5)	10–19 (14.2 ± 2.1) 10–17 (13.3 ± 1.5)	12–16 (13.7 ± 1.4) 11–17 (13.1 ± 2.2)
Scales around the interparietal (SAI)	7–10 (8.3 ± 0.9) 5–10 (7.5 ± 1.2)	5–9 (7.3 ± 1.3)	4–7 (5.6 ± 1.1) 6–8 (6.8 ± 1.0)	5–8 (6.7 ± 0.9) 6–10 (7.0 ± 1.1)	6–8 (7.2 ± 0.8) 6–8 (6.8 ± 1.7)	6–9 (7.2 ± 0.9) 5–9 (7.2 ± 0.9)	7–9 (7.9 ± 0.9) 7–9 (7.4 ± 0.8)

Table 4. *Continued.*

	L. chavin M = 11, F = 18	***L. misti*** M = 11	***L. pachacutec*** M = 5, F = 4	***L. tacnae*** M = 16, F = 25	***L. tunupa* sp. nov.** M = 10, F = 6	***L. walkeri*** M = 21, F = 27	***L. wari*** M = 7, F = 10
Continuous characters							
Snout–vent length (SVL)	56.3–57.9 (55.4 ± 1.9) 44.6–57.1 (53.0 ± 3.5)	41.5–49.3 (45.9 ± 2.3)	44.8–51.9 (47.3 ± 2.9) 47.2–52.0 (48.8 ± 2.3)	44.1–54.9 (49.2 ± 2.7) 42.6–56.6 (50.1 ± 3.4)	47.4–52.7 (50.6 ± 1.7) 44.8–52.2 (47.9 ± 2.7)	46.9–54.9 (55.0 ± 3.9) 47.0–64.4 (56.4 ± 4.4)	55.4–56.8 (55.6 ± 1.1) 50.0–61.4 (56.0 ± 3.5)
Head length	12.4–13.7 (13.1 ± 0.6) 10.7–11.9 (11.4 ± 0.4)	9.4–10.9 (10.2 ± 0.5)	10.6–16.9 (12.1 ± 2.7) 9.9–10.7 (10.2 ± 0.3)	9.7–11.4 (10.7 ± 0.5) 9.4–12.0 (10.6 ± 0.7)	10.5–12.1 (11.4 ± 0.3) 9.4–10.6 (10.0 ± 0.4)	11.5–14.2 (12.8 ± 0.8) 10.2–13.3 (12.0 ± 0.9)	11.3–12.7 (12.2 ± 0.6) 10.3–11.9 (11.0 ± 0.6)
Head width	10.4–11.4 (11.0 ± 0.4) 8.4–9.7 (9.2 ± 0.4)	7.4–8.5 (8.0 ± 0.3)	7.8–9.1 (8.3 ± 0.5) 7.5–8.3 (7.9 ± 0.3)	7.3–9.1 (8.1 ± 0.5) 5.7–9.3 (8.0 ± 0.9	8.3–10.3 (9.7 ± 0.6) 8.1–8.6 (8.5 ± 0.2)	8.5–11.6 (10.2 ± 0.9) 7.8–11.5 (9.7 ± 1.0)	9.2–10.6 (10.0 ± 0.6) 8.1–10.2 (9.1 ± 0.6)
Snout length	5.2–6.3 (5.7 ± 0.4) 4.2–5.6 (5.1 ± 0.4)	1.9–2.5 (2.2 ± 0.2)	3.9–4.7 (4.4 ± 0.3) 3.7–4.3 (4.0 ± 0.3)	4.0–5.5 (4.9 ± 0.4) 3.7–5.3 (4.5 ± 0.4)	2.8–4.4 (3.8 ± 0.5) 3.3–3.7 (3.6 ± 0.2)	4.7–6.9 (5.4 ± 0.6) 4.3–6.2 (5.2 ± 0.5)	4.5–4.8 (4.6 ± 0.1) 4.0–4.8 (4.2 ± 0.3)
Auditory meatus width	0.7–1.2 (1.0 ± 0.2) 0.6–1.2 (1.0 ± 0.2)	0.9–1.2 (1.1 ± 0.1)	0.8–1.2 (1.0 ± 0.2) 0.8–1.0 (1.0 ± 0.1)	0.8–1.5 (1.2 ± 0.2) 0.5–1.5 (1.1 ± 0.2)	1.0–1.6 (1.3 ± 0.2) 1.0–1.7 (1.3 ± 0.2)	0.7–1.6 (1.2 ± 0.2) 0.6–1.6 (1.2 ± 0.2)	0.9–1.1 (1.0 ± 0.1) 0.7–1.2 (1.0 ± 0.2)
Auditory meatus length	2.1–2.4 (2.3 ± 0.1) 1.7–2.7 (2.2 ± 0.3)	1.7–2.3 (2.0 ± 0.2)	1.6–2.2 (1.9 ± 0.2) 1.5–1.8 (1.6 ± 0.1)	1.4–2.4 (2.0 ± 0.2) 1.5–2.1 (1.8 ± 0.1)	1.4–2.2 (1.8 ± 0.3) 1.3–1.9 (1.6 ± 0.2)	1.7–2.6 (2.3 ± 0.3) 1.4–2.5 (2.1 ± 0.3)	1.9–2.4 (2.2 ± 0.2) 1.7–2.5 (2.0 ± 0.2)
Rostral width	2.4–3.0 (2.8 ± 0.2) 2.2–2.7 (2.5 ± 0.1)	1.9–2.4 (2.1 ± 0.1)	2.3–2.7 (2.5 ± 0.1) 2.1–2.5 (2.3 ± 0.2)	1.8–2.6 (2.3 ± 0.2) 1.9–2.8 (2.3 ± 0.2)	2.2–2.7 (2.5 ± 0.2) 1.8–2.2 (2.0 ± 0.2)	2.3–3.1 (2.8 ± 0.3) 1.9–3.0 (2.6 ± 0.3)	2.6–2.9 (2.8 ± 0.1) 2.0–2.8 (2.4 ± 0.2)
Rostral depth	1.0–1.2 (1.1 ± 0.1) 0.9–1.2 (1.0 ± 0.1)	0.8–1.1 (0.9 ± 0.1)	0.9–1.1 (1.0 ± 0.1) 0.8–2.4 (1.2 ± 0.7)	0.8–1.3 (1.0 ± 0.1) 0.8–1.3 (1.3 ± 0.8)	0.6–1.0 (0.8 ± 0.1) 0.6–0.8 (0.7 ± 0.1)	0.9–1.3 (1.1 ± 0.1) 0.7–1.2 (1.0 ± 0.1)	0.9–1.2 (1.1 ± 0.1) 0.8–1.1 (1.0 ± 0.1)
Axilla-groin distance	20.4–25.3 (23.1 ± 2.2) 19.2–29.6 (25.3 ± 3.1)	19.2–22.4 (20.5 ± 1.1)	18.4–24.0 (21.1 ± 2.3) 21.2–27.4 (23.3 ± 2.4)	15.8–25.4 (20.4 ± 3.1) 18.8–29.4 (23.4 ± 2.7)	19.0–24.5 (21.3 ± 1.9) 20.2–26.2 (22.9 ± 2.2)	20.9–28.1 (23.9 ± 2.0) 20.3–31.9 (26.5 ± 3.1)	21.4–23.8 (22.8 ± 1.0) 22.3–32.3 (28.0 ± 3.3)

et al. (2022) recorded this species from a nearby site (21°03' S, 68°51' W). The species is abundant; although only one day was dedicated to collecting the sample, several additional individuals were observed beyond those collected. The habitat is rocky, mainly composed of small and medium-sized rocks with few bushes. The only other species of *Liolaemus* (*sensu stricto*) that inhabits the Tarapacá Region is *L. puna,* recorded north of Quebrada Blanca in the locality of Chiapa (19°32' S, 69°12' W); and also in several localities of the Antofagasta Region (Lobo and Espinoza 2004). Thus, both species might at least share the geographic range, if not the habitat. We do not have field data for *L. puna* that is sympatric with *L. tunupa* sp. nov. Mella (2017) provided other photographic records assignable to *L. tunupa* sp. nov.: Cerro Pabellón del Inca (20°55' S, 68°36' W) and Quebrada El Escorial (20°58' S, 68°47' W). Mella (2017) further included photographs of specimens from Quebrada El Zorro (p. 187), listed as Quebrada Zorro in the coordinate appendix (20°58' S, 68°46' W; p. 303). Mella (2017) also provided a photograph of one individual from Michincha, listed in the coordinate appendix as Salar de Michincha (20°59' S, 68°33' W; J. Mella pers. comment). All these records are located less than 20 km away from Quebrada Blanca.

Liolaemus tunupa sp. nov. is a viviparous species. At the time of collection (November), three females had two embryos, one had one embryo and two had 1–5 oocytes of at least 1.5 mm.

Discussion

Two hypotheses have been proposed regarding the phylogenetic position of the *L. walkeri* clade within *Liolaemus.* Esquerré *et al.* (2019) placed the *L. walkeri* clade outside both subgenera, *Eulaemus* and *Liolaemus* (*sensu stricto*). In contrast, Portelli and Quinteros (2018) positioned the *L. walkeri* clade within *Liolaemus* (*sensu stricto*), specifically as part of the *L. alticolor-bibronii* group. Although resolving this issue is not the focus of our study, we note that species of the *L. walkeri* clade do not match in two of the three characters used to diagnose the species of the *Liolaemus* (*sensu stricto*) subgenus: lack an elongated, upward curved supralabial scale and the presence of dorsolateral nostrils (Figure 5A–C). The only diagnostic character of the subgenus *Liolaemus* (*sensu stricto*), as established by Laurent (1992) and Etheridge (1995), present in all known species of the *Liolaemus* (*sensu stricto*) subgenus (Abdala *et al.* 2021; Figure 5D–E of this study) and also present in species of the *L. walkeri* clade is the reduction in the number or lack of precloacal pores. We note that species of the *Eulaemus* subgenus also lack an elongated, upward curved supralabial scale and have dorsolateral nostrils (Figure 5F). Notably, Portelli and Quinteros (2018) include the *L. walkeri* clade in the *L. alticolor-bibronii* group of the *Liolaemus* (*sensu stricto*) subgenus. However, in the Chilean and Peruvian species of the *L. alticolor-bibronii* group, the interparietal scale is consistently smaller than the parietals (JTP and CAP, unpublished data), whereas in the *L. walkeri* clade the parietals are highly variable among individuals (smaller than, similar to, or larger than the interparietal). These characters might prove useful in future studies on the taxonomic status and the phylogenetic position of the *L. walkeri* clade. At present, we emphasize the possibility that establishing a third subgenus of *Liolaemus* to accommodate the *L. walkeri* clade cannot be ruled out.

Aguilar *et al.* (2013) reported the presence of *Liolaemus tacnae* in several localities of southern Peru, near the Chilean border. Records of *L. tacnae* exist from two Chilean regions (Esquerré *et al.* 2022): Arica-Parinacota and Tarapacá. All Tarapacá Region records are described here or assigned to *L. tunupa* sp. nov. In Arica-Parinacota, three records exist. The first is from Chapiquiña, 4080 m a.s.l., 3 km east of Portezuelo (approximately 85 km south from the Peruvian border, 18°23' S, 69°31' W, estimated coordinates), based on one adult female specimen (Lobo and Espinoza 1999, Pincheira-Donoso and Núñez 2005). This record was later

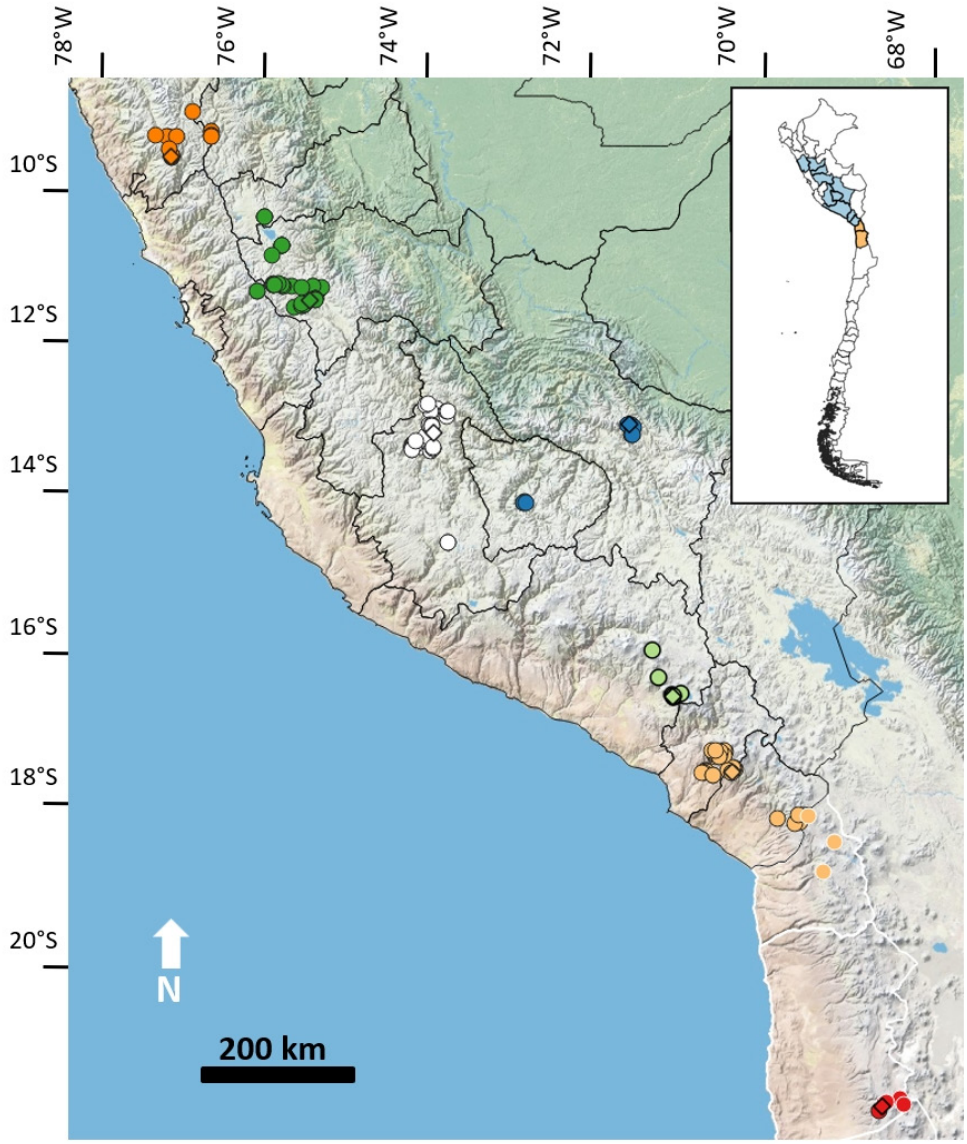

Figure 6. Distribution map of species of the *L. walkeri* clade. Administrative borders of Peru are shown in black and administrative borders of Chile in white. Diamonds indicate type localities, and circles indicate additional records. All records from Peru are based on coordinates provided by Aguilar *et al.* (2013) and Santa-Cruz *et al.* (2025). Orange: *L. chavin.* Green: *L. walkeri.* White: *L. wari.* Blue: *L. pachacutec.* Light green: *L. misti.* Light orange: *L. tacnae.* Chilean records assigned to *L. tacnae* (light orange circles with white border line) are from north to south: Tacora, Chapiquiña and Quebrada Allane. Red: *Liolaemus tunupa* sp. nov. Two samples are known from Quebrada Blanca, but with different coordinates, the type locality (diamond, this study) and by Esquerré *et al.* (2022, circle). Records based on photographs (Mella 2017, red dots with white border line) are from north to south: Cerro Pabellón del Inca, Quebrada El Zorro and Salar de Michincha.

reassigned to *Liolaemus* sp. due to the absence of additional specimens and data (Lobo and Espinoza 2004, Troncoso-Palacios and Etheridge 2012). The second record is supported by DNA data (Esquerré *et al.* 2022) and photographs (Demangel 2016) from Quebrada Allane (18°02' S, 69°23' W, approximately 55 km from Peruvian southern border). Finally, Demangel (2016) provided photographs from Tacora, near the border with Peru, but without additional data or precise coordinates. Esquerré *et al.* (2022) confirmed that at least the Quebrada Allane population belongs to the *L. walkeri* clade. The color pattern of the Chapiquiña specimen resembles that of *L. tacnae* females and differs from *L. chungara* Quinteros, Valladares, Semham, Acosta, Barrionuevo, and Abdala, 2014, the only other *Liolaemus* (*sensu stricto*) recorded in Arica-Parinacota region. Given the geographic proximity to the type locality of *L. tacnae,* we tentatively assign all Arica-Parinacota populations to *L. tacnae* until more evidence, particularly collected specimens, become available. As a useful reference for future studies, we examined a photograph of the male holotype of *L. chungara* (FML 26505, published here for the first time, Figure 7). Diagnostic color characters described by Quinteros *et al.* (2014) allow easy differentiation from *L. tacnae* or *L. tunupa* sp. nov., including: an almost continuous dark brown vertebral line, paravertebral dark brown stripes, dorsolateral and ventrolateral light brown stripes, and absence of ventral melanism. The males of *L. chungara* possess both, precloacal pores and supernumerary precloacal pores, whereas males of *L. tacnae* and *L. tunupa* sp. nov. lack such pores.

The species of the *L. walkeri* clade show latitudinal variation in the presence or absence of precloacal pores in males, depending on whether the species inhabits occidental or oriental side of the Andes (from north to south, Table 3): *L. chavin* (absent, inhabits occidental Andes), *L. wari* (present, inhabits oriental Andes), *L. walkeri* (present, inhabits oriental Andes), *L. pachacutec* (present, inhabits oriental Andes), *L. misti* (absent, inhabits occidental Andes), *L. tacnae* (absent, inhabits occidental Andes) and *L. tunupa* sp. nov. (absent, inhabits occidental Andes). Several authors have attempted to interpret the evolutionary significance of pore absence in *Liolaemus* males (see Esquerré *et al.* 2013). Other *Liolaemus* lack precloacal pores, either in well-defined monophyletic groups such as the *L. lineomaculatus* group (as defined by Breitman *et al.* 2011), *L. cristiani, L. neuquensis, L. punmahuida,* and *L. villaricensis* groups (as defined by Esquerré *et al.* 2022), or sporadically in some members of the *L. elongatus* group (as defined by Esquerré *et al.* 2022). Therefore, the *L. walkeri* clade represents an excellent model for studying the evolution of pore absence in males of the genus *Liolaemus.*

Figure 7. Holotype of *Liolaemus chungara* (FML 26505, photograph by C. S. Abdala and S. A. Quinteros). Note the almost continuous dark brown vertebral line, dark brown paravertebral stripes, and light brown dorsolateral and ventrolateral stripes. Ventral melanism is absent.

Acknowledgments

We thank D. Kotoras, E. Palma and B. Rosende for allowing us to review and deposit material in the collection under their care (SSUC, Pontificia Universidad Católica de Chile). Troncoso-Palacios J. thanks M. Penna, from the Physiology and Biophysics Program, Faculty of Medicine, University of Chile, for his support. Thanks to J. Mella for clarifying some distributional records of *L. tunupa* sp. nov. We are also grateful to the Servicio Agrícola y Ganadero (SAG) for the collecting permit (Nº 309). We thank A. S. Quinteros and C. S. Abdala for providing photographs of the holotype of *L. chungara*. Finally, we thank two anonymous reviewers and to the Editors C. Koch and J. Bertoluci, for all their constructive suggestions to improve the manuscript, and to J. Caldwell for review the English.

References

Abdala, C. S., A. Laspiur, G. Scrocchi, R. V. Semhan, F. Lobo, and P. Valladares-Faundez. 2021. *Las Lagartijas de la Familia Liolaemidae. Sistemática, Distribución e Historia Natural de Una de las Familias de Vertebrados Más Diversas del Cono Sur de Sudamérica.* Tapa Blanca. RIL Editorial, Universidad de Tarapacá. 848 pp.

Abdala, C. S., P. A. Chafrat, J. C. Chaparro, I. E. Procheret, J. Valdes, V. Lannutti, L. Perez, and S. Quinteros. 2023. A new species of *Liolaemus* (Iguania: Liolaemidae) from the hot deserts of northern Patagonia, Argentina. *European Journal of Taxonomy 890:* 136–164.

Aguilar, C., M. R. Stark, J. A. Arroyo, M. D. Standing, S. Rios, T. Washburn, and J. W. Sites Jr. 2015. Placental morphology in two sympatric Andean lizards of the genus *Liolaemus* (Reptilia: Liolaemidae). *Journal of Morphology 276:* 1205–1217.

Aguilar, C., P. L. Wood Jr., J. C. Cusi, A. Guzmán, F. Huari, M. Lundberg, E. Mortensen, C. Ramírez, D. Robles, J. Suárez, A. Ticona, V. J. Vargas, P. J. Venegas, and J. W. Sites Jr. 2013. Integrative taxonomy and preliminary assessment of species limits in the *Liolaemus walkeri* complex (Squamata, Liolaemidae) with descriptions of three new species from Peru. *ZooKeys 364:* 47–91.

Avila, L.J., A. González, J. Troncoso-Palacios, K.I. Sánchez, C.H.F. Pérez, and M. Morando. 2020. Naming the diversity: taxonomy of current species of Patagonian lizards. Pp. 123–188 *in* M. Morando and L. J. Avila (eds.), *Lizards of Patagonia. Diversity, Systematics, Biogeography and Biology of the Reptiles at the End of the World.* Cham. Springer Nature Switzerland AG.

Avila, L. J., J. E. Vrdoljak, C. D. Medina, J. García, J. C. H. Fulvio, J. W. Sites Jr., and M. Morando. 2021. A new species of *Liolaemus* (Reptilia: Squamata) of the *Liolaemus capillitas* clade (Squamata, Liolaemini, *Liolaemus elongatus-kriegi* group) from Sierra de Velasco, La Rioja Province, Argentina. *Zootaxa 4903:* 194–216.

Breitman, M. F., M. Parra, C.H. Fulvio Pérez, and J. W. Sites Jr. 2011. Two new species of lizards from the *Liolaemus lineomaculatus* section (Squamata: Iguania: Liolaemidae) from southern Patagonia. *Zootaxa 3120:* 1–28.

Campos-Soto, R., E. Rodríguez-Valenzuela, Y. Bruna, G. Díaz-Campusano, F. Cianferoni, D. Boric-Bargetto, and F. Torres-Pérez. 2023. Phylogenetic analyses of lizards from the Chilean Humboldt archipelago reveal a new species for the Chañaral Island (Squamata: Liolaemidae). *Animals 13:* 3576.

Demangel, D. 2016. *Reptiles en Chile.* Santiago. Fauna Nativa Ediciones. 619 pp.

Donoso-Barros, R. 1961. Three new lizards of the genus *Liolaemus* from the highest Andes of Chile and Argentina. *Copeia 1961:* 387–391.

Donoso-Barros, R. 1966. *Reptiles de Chile.* Santiago. Ediciones de la Universidad de Chile. 458 pp.

Esquerré, D., H. Núñez, and J. A. Scolaro. 2013. *Liolaemus carlosgarini* and *Liolaemus riodamas* (Squamata: Liolaemidae), two new species of lizards lacking precloacal pores, from Andean areas of central Chile. *Zootaxa 3619:* 428–452.

Esquerré D, I. G. Brennan, R. A. Catullo, F. Torres-Pérez, and J. S. Keogh. 2019. How mountains shape biodiversity: the role of the Andes in biogeography, diversification, and reproductive biology in South America's most species-rich lizard radiation (Squamata: Liolaemidae). *Evolution 73:* 214–230.

Esquerré, D., J. S. Keogh, D. Demangel, M. Morando, L. J. Avila, J. W. Sites, F. Ferri-Yáñez, and A. D. Leaché. 2022. Rapid radiation and rampant reticulation: phylogenomics of South American *Liolaemus* lizards. *Systematic Biology 71:* 286–300.

Etheridge, R. 1995. Redescription of *Ctenoblepharys adspersa* Tschudi, 1845, and the taxonomy of Liolaeminae (Reptilia: Squamata: Tropiduridae).

American Museum Novitates 3142: 1–34.

Josse, J. and F. Husson. 2012. Handling missing values in exploratory multivariate data analysis methods. *Journal de la Société Française de Statistique 153:* 79–399.

Laurent, R. F. 1992. On some overlooked species of the genus *Liolaemus* Wiegmann (Reptilia: Tropiduridae) from Peru. *Breviora 494:* 1–33.

Lê, S., J. Josse, and F. Husson. 2008. FactoMineR: an R Package for multivariate analysis. *Journal of Statistical Software 25:* 1–18.

Lobo, F. 2005. Las relaciones filogenéticas dentro grupo *chiliensis* (Iguania: Liolaemidae: *Liolaemus*): sumando nuevos caracteres y taxones. *Acta Zoologica Lilloana 49:* 65–87.

Lobo, F. and R. E. Espinoza. 1999. Two new cryptic species of *Liolaemus* (Iguania: Tropiduridae) from northwestern Argentina: resolution of the purported reproductive bimodality of *Liolaemus alticolor*. *Copeia 1999:* 122–140.

Lobo, F. and R. E. Espinoza. 2004. Further resolution of purported reproductive bimodality in *Liolaemus alticolor* (Iguania: Tropiduridae) with descriptions of two new species from the Puna region of Argentina and Chile. *Copeia 2004:* 850–867.

Lobo, F., R. E. Espinoza, and S. A. Quinteros. 2010. A critical review and systematic discussion of recent classification proposals for liolaemid lizards. *Zootaxa 2549:* 1–30.

Losos, J. B. 1990. Ecomorphology, performance capability, and scaling of West Indian *Anolis* lizards: and evolutionary analysis. *Ecological Monographs 60:* 369–388.

Mella, J. E. 2017. *Guía de Campo de Reptiles de Chile. Tomo 2, Zona Norte.* Volume II. Santiago. Alejandro P. Peñaloza G. Edición. 316 pp.

Núñez, H., A. Veloso, P. Espejo, C. Veloso, A. Cortés, and S. Araya. 2010. Nuevas especies de *Phymaturus* (grupo *palluma*) para la zona Cordillerana Central de Chile (Reptilia, Sauria, Liolaemidae). *Boletín del Museo Nacional de Historia Natural de Chile 59:* 41–74.

Pincheira-Donoso, D. and H. Núñez. 2005. Las especies chilenas del género *Liolaemus* Wiegmann, 1834 (Iguania: Tropiduridae: Liolaeminae). Taxonomía, sistemática y evolución. *Publicación Ocasional del Museo Nacional de Historia Natural de Chile 59:* 1–486.

Portelli, S. N. and S. A. Quinteros. 2018. Phylogeny, time divergence, and historical biogeography of the South American *Liolaemus alticolor–bibronii* group (Iguania: Liolaemidae). *PeerJ 6:* e4404.

Quinteros, A. S., P. Valladares, R. Semhan, J. L. Acosta, S. Barrionuevo, and C. S. Abdala. 2014. A new species of *Liolaemus* (Iguania: Liolaemidae) of the *alticolor–bibronii* group from northern Chile. *South American Journal of Herpetology 9:* 20–29.

R Development Core Team. 2016. R: A Language and Environment for Statistical Computing. Vienna, Austria: R Foundation for Statistical Computing. URL: http://www.r-project.org. Captured on 19 March 2024.

Ruiz-de-Gamboa, M. 2020. Estados de conservación y lista actualizada de los reptiles nativos de Chile. *Boletín Chileno de Herpetología 7:* 1–11.

Sánchez, K. I., M. Morando, and L. J. Avila. 2023. A new lizard species of the *Liolaemus kingi* group (Squamata: Liolaemidae) from northwestern Chubut province (Argentina). *Zootaxa 5264:* 235–255.

Santa-Cruz, R., A. Canzas-Terán, R. Bejarano, E. López, A. Morales, R. von May, A. Catenazzi, and C. Aguilar-Puntriano. 2025. A new species of the *Liolaemus walkeri* clade (Squamata: Liolaemidae) in the volcanic chain of Arequipa, Peru. *Salamandra 61*: 115–131.

Shreve, B. 1941. Notes on Ecuadorian and Peruvian reptiles and amphibians with description of new forms. *Proceedings of the New England Zoological Club 18:* 71–83.

Troncoso-Palacios, J. and F. Contreras-Piderit. 2023. A new species of the *Liolaemus nigroviridis* group from the Andes of Central Chile (Iguania: Liolaemidae). *Acta Zoológica Lilloana 671:* 233–259.

Troncoso-Palacios, J. and R. Etheridge. 2012. Distributional range of the poorly known *Liolaemus tacnae* (Shreve 1941). *Herpetological Bulletin 121:* 35–38.

Zar, J. H. 2010. *Biostatistical Analysis.* 5th Edition. Upper Saddle River. Prentice-Hall/Pearson. 944 pp.

Editor: Claudia Koch

Appendix I. *Adult specimens of the* Liolaemus walkeri *clade examined for morphological analyses. Acronyms used are: BYU (Brigham Young University), CORBIDI (Centro de Ornitología y Biodiversidad, Peru), FML (Fundación Miguel Lillo), MUSA (Museo de Historia Natural de la Universidad Nacional de San Agustín de Arequipa, Peru), MUSM (Museo de Historia Natural de San Marcos, Peru), MVZ (Museum of Vertebrate Zoology, USA), SSUC Re (Reptile collection of the Pontificia Universidad Católica, Chile) and ZSM (The Bavarian State Collection of Zoology, formerly Zoologische Staatssammlung München, Germany).*

Liolaemus chavin (29). Males: CORBIDI 10439, 10441–10443, 10450, 10452. Peru, Ancash Department, Pampas de Huamani. MUSM 20141, 20143, 20146, 25417. Peru, Ancash Department, Conococha. MUSM 20147. Peru, Ancash Department, Carpa. Females: CORBIDI 10437–10438, 10440, 10445, 10449, 10451. Peru, Ancash Department, Pampas de Huamani. MUSM 20145, 25324, 25327–25328, 25331, 25333–25334, 25340, 25412, 25423, 30812–30813. Peru, Ancash Department, Conococha.

Liolaemus chungara (1). FML 26505. Chile, Arica-Parinacota Region, Entrada a Putre.

Liolaemus constanzae (1). SSUC Re 343. Chile, Antofagasta Region, Barros Arana.

Liolaemus janequeoae (1). SSUC Re 650. Chile, Araucanía Region, Laguna Verde, approximately 13.5 km NW from Tolhuaca Volcano.

Liolaemus misti (13). Males: MUSA 1239. Peru, Arequipa Department, Huito-Moche. MUSA 4728–4729, 4734, 5708, 5844–5845. Peru, Arequipa Department, Simbral. MUSA 4581–4583, 4588. Peru, Arequipa Department, Toccra. MUSM 40545–46. Peru, Arequipa Department, Simbral.

Liolaemus pachacutec (9). Males: MUSM 29664. Peru, Cuzco Department, Pampallacta Alta. MUSM 29665, 29668. Peru, Cuzco Department, Huarqui. MUSM 29681, 29683. Peru, Cuzco Department, Ttio Grande. Females: MUSM 29680, 29682, 29689. Peru, Cuzco Department, Ttio Grande. MUSM 29688. Peru, Cuzco Department, Pampallacta Alta.

Liolaemus rosenmanni (1). SSUC Re 149. Chile, Atacama Region, Salar de Pedernales.

Liolaemus tacnae (33). Males: MUSM 21331–21332. Peru, Moquegua Department (unspecified locality). MUSA 4357, 5710, 5769–5770, 5773, 5779, 5782. Peru, Moquegua Department, Torata. MUSM 29599, 29602. Peru, Tacna Department, Zona Arqueologica Cuajone. MUSM 29615. Peru, Tacna Department, Cocotea Baja, Cuajone. MUSA 4358. Peru, Tacna Department (unspecified locality). MVZ 45806–45807. Peru, Tacna Department, Toquepala Mine, 60 km east of Moquegua. Females: MUSA 5771, 5774–5778. Peru, Moquegua Department, Torata. MUSM 29612–29613, 29625–29626. Peru, Moquegua Department, Reservorio Pampa de Vaca, Toquepala. MUSM 29600–29601. Peru, Tacna Department, Zona Arqueologica, Cuajone. MUSM 29603. Peru, Tacna Department, Ichupampa, Cuajone. MUSM 29604. Peru, Tacna Department, Cocotea Baja, Cuajone. MUSM 29605. Peru, Tacna Department, Chujulay, Cuajone. MUSM 29606. Peru, Tacna Department, Cerca de Tajo de Toquepala. MUSM 29610. Peru, Tacna Department, Quebrada Cimarron, Toquepala. MUSM 29611. Peru, Tacna Department, Quebrada Muñane, Toquepala.

Liolaemus tunupa sp. nov. (16). Males: SSUC Re 798–807. Chile, Tarapacá Region, Quebrada Blanca, approximately 120 km SE Pozo Almonte city. Females: SSUC Re 808–813. Chile, Tarapacá Region, Quebrada Blanca, approximately 120 km SE Pozo Almonte city.

Liolaemus walkeri (34). Males: MUSM 18062, 18068, 18076. Peru, Pasco Department, Ninacaca. MUSM 13446, 13454, 13456. Peru, Junin Department (unspecified locality). MUSM 22039. Peru, Junin Department, Carhuamayo. MUSM 29574–75. Peru, Junin Department, Pichcapuquio. MUSM 1961, 13451. Peru, Lima Department, Ticlio. MUSM 23660, 29644. Peru, Lima Department, Chicla. Females: MUSM 18075, 18079. Peru, Pasco Department, Ninacaca. ZSM 10/1952/2. Peru, Junin Department, Llocllapampa. MUSM 20559. Peru, Junin Department, Mina Santa Sabina. MUSM 22041–42. Peru, Junin Department, Carhuamayo. MUSM 29576, 30814, 30816–30818. Peru, Junin Department, Pichcapuquio. MUSM 30815. Peru, Junin Department, Tunanmarca. MUSM 1985, 13447. Peru, Lima Department, Ticlio. MUSM 23622–23623, 23657, 23659, 23662, 29643. Peru, Lima Department, Chicla.

Liolaemus wari (17). Males: BYU 50184–50185. Peru, Ayacucho Department, Abra Toccto. MUSM 25703–25704. Peru, Ayacucho Department, Yanacocha Lake. MUSM 30823, 30837. Peru, Ayacucho Department, Abra Toccto. MUSM 30834. Peru, Ayacucho Department, Parte alta del Santuario Historico Pampas. Females: MUSM 25702. Peru, Ayacucho Department, Yanacocha Lake. MUSM 25719. Peru, Ayacucho Department, Huaychao. MUSM 30243–30244. Peru, Ayacucho Department, Tambo. BYU 50189. Peru, Ayacucho Department, Acosvinchos-Huaychao. BYU 50186, 50243. Peru, Ayacucho Department, Abra Toccto. MUSM 30824, 30826, 30828. Peru, Ayacucho Department, Abra Toccto.

Phyllomedusa 24(2):175–200, 2025

ISSN 1519-1397 (print) / ISSN 2316-9079 (online)
doi: http://dx.doi.org/10.11606/issn.2316-9079.v24i2p175-200

Spatial distribution models for the *Micrurus divaricatus* complex (Serpentes: Elapidae) in Nuclear Central America with emphasis on Honduras

Jorge Luis Montoya, Anthonie Ivanovish Andino-Mazariegos, Julio Enrique Mérida, and Gustavo Adolfo Cruz

Universidad Nacional Autónoma de Honduras, Museo de Historia Natural. Boulevard Suyapa, Tegucigalpa, Honduras.
E-mail: jlmontoya.jlmf@gmail.com.

Abstract

Spatial distribution models for the *Micrurus divaricatus* complex (Serpentes: Elapidae) in Nuclear Central America with emphasis on Honduras. This study modeled the distribution of the *M. divaricatus* complex in Nuclear Central America (NCA) by testing multiple modeling techniques and identifying crucial bioclimatic predictors. We used 178 occurrence records and seven variables selected for ecological relevance and low collinearity. Validating the eight techniques using AUC, TSS, Cohen's Kappa, sensitivity, specificity, COR, and CA. Random Forest, Support Vector Machines, Generalized Additive Models, and Maximum Entropy Modeling performed best, with Random Forest showing the highest predictive accuracy. Main predictors were temperature seasonality, precipitation of the driest month, and precipitation seasonality. Projections indicated high suitability along the Pacific and Caribbean slopes and in parts of the Mosquitia, and low suitability in the Chortís Block highlands. Lowland and premontane moist forests were identified as critical habitats. The Chortís Block highlands represent a transitional zone for the three subspecies. These results, obtained via a multi-model approach to reduce uncertainty, provide relevant insights for taxonomy and conservation planning of the *M. divaricatus* complex and the genus *Micrurus* in NCA.

Keywords: *Micrurus divaricatus* complex, Nuclear Central America, Species distribution models.

Resumen

Modelos potenciales de distribución espacial para el complejo *Micrurus divaricatus* (Serpentes: Elapidae) en Centroamérica Nuclear con énfasis en Honduras. Este estudio modelo la distribución del complejo *M. divaricatus* en Centroamérica Nuclear (CAN) mediante la evaluación de multiples técnicas de modelización e identificación de predictores bioclimáticos cruciales. Se utilizaron 178 registros de ocurrencia y siete variables seleccionadas por su relevancia ecológica y baja colinealidad. Validando las ocho técnicas con las metricas AUC, TSS, Kappa de Cohen, sensibilidad, especificidad, COR y CA. Random Forest, Support Vector Machines, Generalized

Received 30 September 2024
Accepted 30 April 2025
Distributed December 2025

Additive Models y Maximum Entropy Modeling mostraron mejor desempeño, destacando Random Forest por su mayor precisión predictiva. Los predictores más importantes fueron la estacionalidad de la temperatura, la precipitación del mes más seco y la estacionalidad de la precipitación. Las proyecciones indicaron alta idoneidad en las vertientes del Pacífico y Caribe y en partes de la Mosquitia, mientras que se predijo baja idoneidad en las tierras altas del Bloque Chortís. Los bosques húmedos de tierras bajas y premontanos fueron identificados como hábitats críticos. Las tierras altas del Bloque Chortís representan una zona de transición para las tres subespecies. Estos resultados, obtenidos mediante un enfoque multimodelo reduce la incertidumbre, proporcionan información relevante para la taxonómia y la conservación del complejo *M. divaricatus* y género *Micrurus* en CAN.

Palabras claves: Centroamerica Nuclear, Complejo *M. divaricatus,* Modelos de distribución de especies.

Resumo

Modelos de distribuição espacial para o complexo *Micrurus divaricatus* (Serpentes: Elapidae) na América Central Nuclear com ênfase em Honduras. Este estudo modelou a distribuição do complexo *M. divaricatus* na América Central Nuclear (CAN) testando múltiplas técnicas de modelagem e identificando preditores bioclimáticos chave. Foram utilizados 178 registros de ocorrência e sete variáveis selecionadas por relevância ecológica e baixa colinearidade Validando as oito técnicas usando AUC, TSS, Kappa de Cohen, sensibilidade, especificidade, COR e CA. Random Forest, Support Vector Machines, Generalized Additive Models e Maximum Entropy Modeling apresentaram melhor desempenho, com Random Forest mostrando a maior precisão preditiva. Os preditores principais foram a sazonalidade da temperatura, precipitação do mês mais seco e sazonalidade da precipitação. As projeções indicaram alta adequação ao longo das encostas do Pacífico e Caribe e em partes da Mosquitia, e baixa adequação nas terras altas do Bloco Chortís. Florestas úmidas de baixas altitudes e premontanas foram identificadas como habitats críticos. As terras altas do Bloco Chortís representam uma zona de transição para as três subespécies. Estes resultados, obtidos via abordagem multimodelo para reduzir a incerteza, fornecem informações relevantes para a taxonomia e conservação do complexo *M. divaricatus* e do gênero *Micrurus* na CAN.

Palavras-chave: América Central Nuclear, Complexo *M. divaricatus,* Modelos de distribuição de espécies.

Introduction

Biological species modeling has become the primary statistical technique for predicting the potential distribution of a taxon by considering the abiotic and biotic conditions necessary for its establishment and persistence in a given territory (Guisan and Zimmermann 2000, Guisan and Thuiller 2005, Elith and Leathwick 2009, Mateo *et al.* 2011, Guisan *et al.* 2013, Elith and Franklin 2017). Species distribution models (SDMs) are a valuable tool for elucidating or anticipating the distribution patterns of a taxon. The development of SDMs relies on the use of historical or contemporary occurrence records (coordinates/location), biotic and abiotic predictor variables, and elevation models (raster files) (Franklin 1995, Guisan and Zimmermann 2000, Phillips *et al.* 2006, Mateo *et al.* 2011, Elith and Franklin 2017).

The application of SDM has proven to be a valuable instrument for addressing problems at a systematic and taxonomic level by providing a quantitative and spatial framework for understanding the relationship between species and their environment (Lissovsky *et al.* 2021,

Rodríguez-Gómez *et al*. 2021). This assertion is supported by the proposal of biogeographic delimitations, thereby enhancing our comprehension of historical and evolutionary processes operating at the species and subspecies level (Rodríguez-Gómez *et al.* 2021). A key advantage of SDMs is their ability to identify new occurrence areas, significant transition zones, and critical regions for understanding the presence and movement patterns of these taxa (Mizsei *et al.* 2016). Furthermore, they help elucidate the factors influencing our understanding of ecological and morphometric variation in taxa. Consequently, they provide a comprehensive global perspective of the taxonomic landscape.

Beyond their ecological and taxonomic applications, SDMs play a crucial role in conservation planning and have significant implications for medical research. In regions with a high prevalence of venomous snakebites, they contribute to the development of conservation strategies, medical treatments, and preparation of antidotes (Fernández *et al.* 2011, Archis *et al.* 2018, Guerra *et al.* 2019, Rodríguez-Gómez, *et al.* 2021, Al Haidar *et al.* 2023, Jowers *et al.* 2023). Reptiles are a group of ectothermic organisms, comprising lizards, snakes, and turtles, that are currently facing challenges due to habitat alteration and destruction (Archis *et al.* 2018). A recent study by Biber *et al.* (2023) suggests a potential global decline in the richness of this group, based on an analysis of distribution patterns and bioclimatic variables. This analysis entailed the generation of 6,296 models for diverse reptile species, including 2,305 taxa classified within snakes. Understanding the distribution limits of a snake taxon is essential for analyzing biogeographic processes, ecological conservation, and medical relevance (Mota-Vargas and Rojas-Soto 2012, Archis *et al.* 2018, Guerra *et al.* 2019, Martín *et al.* 2022). Coral snakes represent a diverse group of species within the genus *Micrurus*, as classified by Wagler in 1824 (Roze 1982). Currently, approximately 85 species of *Micrurus* are documented across the Americas (Jowers *et al.* 2023).

These snakes are distinguished by their distinctive coloration patterns in addition to their potent venom that is predominantly neurotoxic (Köhler 2003, Stazi *et al.* 2022). They belong to the Family Elapidae and exhibit a wide distribution in America, ranging from southwestern Oaxaca, Mexico, to northwestern Colombia (Roze 1996, Köhler 2008, McCranie 2011). This territory is inhabited by five distinct subspecies: *M. nigrocinctus babaspul* Roze, 1967, *M. nigrocinctus coibensis* Schmidt, 1936, *M. nigrocinctus divaricatus* Hallowell, 1855, *M. n. nigrocinctus* Girard, 1854, and *M. n. zunilensis* Schmidt, 1932. These subspecies display tricolor (red, yellow, and black) and bicolor (red and black) ring patterns, as documented by Köhler (2008) and McCranie (2011). Their diet consists of other snakes, lizards, and caecilians, and they reproduce via oviparous means. They exhibit a marked preference for dry forest, humid forest, and tropical rainforest habitats, with an altitude range of 0 to 1,640 m a.s.l. (Roze 1996, Köhler 2003, Köhler 2008, McCranie 2011).

Currently recognized as *Micrurus nigrocinctus* (Girard, 1854), this species is considered a complex (Köhler 2003, 2008, Campbell and Lamar 2004, Fernández *et al.* 2011, McCranie 2011, Jowers *et al.* 2023). A phylogenetic analysis conducted by Jowers *et al.* (2023) proposed three lineages. The first lineage includes the *M. nigrocinctus nigrocinctus* populations from Panama. The second lineage contains *M. nigrocinctus divaricatus* and *M. ruatanus* Günther, 1895 from Honduras. The third lineage comprises *M. nigrocinctus zulinensis* and *M. nigrocinctus nigrocinctus* populations from Chiapas, Guatemala, Honduras, Nicaragua, and Costa Rica. Notably, the first lineage exhibits a significant degree of genetic divergence from lineages two and three. According to the findings of Jowers *et al.* (2023), no specific taxonomic classification exists for Nuclear Central America (NCA) populations due to the presence of genetic evidence indicating

that *Micrurus nigrocinctus* Girard, 1854 is restricted to Panamá. Meanwhile, the second and third lineages represent a subspecies complex whose nominal status remains undetermined (for further details, please refer to Figure 2 in Jowers *et al.* 2023).

Consequently, the NCA populations are classified as a subspecies complex that currently lacks a taxonomic species designation and will henceforth be referred to as the *M. divaricatus* complex. This designation is because the name *M. divaricatus* was first used by Hallowell in 1854, making it the oldest name among these lineages. Given the absence of a well-defined classification system for this taxon in southern Mexico and Central America, the study species will be informally treated at the level of the previously used name *Micrurus divaricatus* Hallowell, 1854.

Several studies have focused on distribution modeling for different species of *Micrurus* (Terribile *et al.* 2007, Archis *et al.* 2018, Hidalgo-García *et al.* 2018, Guerra *et al.* 2019, Lara-Galván *et al.* 2023), particularly in context of NCA, according to the work of Hidalgo-García *et al.* (2018) and Lara-Galván *et al.* (2023). This genus holds both medical and taxonomic significance, as evidenced by the proposal of multiple lineages for NCA by Jowers *et al.* (2023). Developing distribution models for the *M. divaricatus* complex is highly valuable, as it enhances the current understanding of the generic distribution across the Americas. It also plays a crucial role in identifying suitable areas, areas with potential new records, and bioclimatic and ecological factors, which are essential for future studies of the *M. divaricatus* complex in NCA.

The objective of this study is to develop a distribution model for the *M. divaricatus* complex in NCA, with a particular focus on Honduras, given that the three subspecies comprising this complex are found in that country, along with an abundant number of presence records for these taxa. The study will entail a comparison of different algorithms for the generation of SDMs, with the objective of selecting the techniques with the best performance in function of predictive variables according to bioclimatic and ecological aspects that contribute to the explanation of the distribution of the *M. divaricatus* complex, as well as detecting the bioclimatic variables and ecological aspects that influence this group of snakes.

Materials and Methods

Study Area

The study area was defined as the zone extending eastward from the Isthmus of Tehuantepec and the mountainous region of Chiapas (southern Mexico), Guatemala, El Salvador, and Honduras, encompassing the depression of Nicaragua between the Santa Elena Peninsula and the Hessian Escarpment. This region is geologically part of the Maya and Chortís blocks. The Nuclear Central America region is situated between the North American and Caribbean Plates (Figure 1) (Brineman and Vinson 1961, Savage 1966, Banks 1975, Donnelly *et al.* 1990, James 2007, Marshall 2007, Cano *et al.* 2018).

This region is a suitable area for the study of venomous snakes because it is considered a historical transition zone with remarkable richness and diversity, being an area of importance for the endemism of this reptile group in the Americas (Russell *et al.* 1997, Köhler 2003, Mata-Silva *et al.* 2019). Consequently, the generation of SDMs on *M. divaricatus* in this area contributes new information about historical, ecological, and evolutionary biogeographic patterns in this reptile group, specifically for the genus *Micrurus* and this subspecies complex. The existence of a significant number of catalogued records in museums, private collections, and numerous bibliographic references for this region facilitates the generation of SDMs that allow us to obtain more precise and rigorous results.

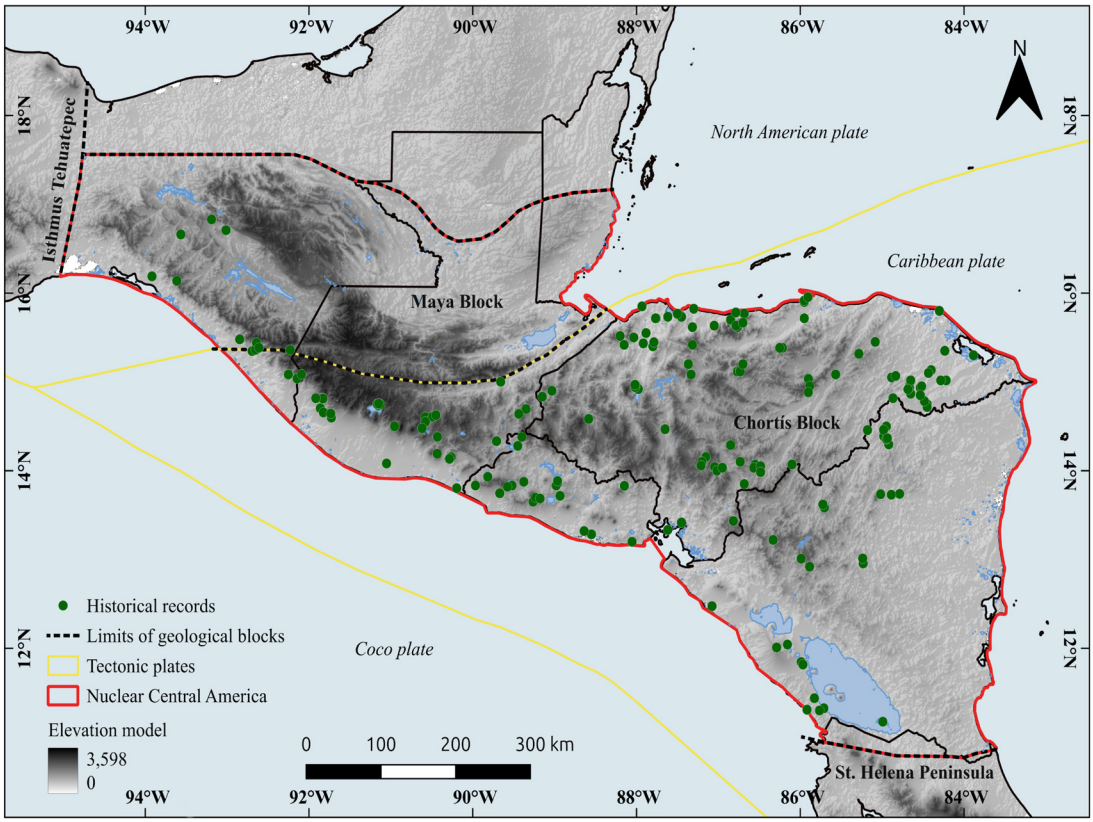

Figure 1. Historical records of the study species in NCA and delimitation of the Mayan and Chortís geological blocks. Map generated in QGIS 3.28.

Occurrence Records

To obtain the georeferenced occurrence records of the study species, several databases were consulted: VertNet.org. 2016, (http://portal.vertnet.org/search); Global Biodiversity Information Facility, 2023 (GBIF.org, https://www.gbif.org/); Portal de Biodiversidad de Guatemala (https://biodiversidad.gt/portal/index.php) (Orellana and López 2023). The latter digital platform links to databases of the reptile collections of the University of Michigan Museum of Zoology UMMZ-Vertebrates, Smithsonian National Museum of Natural History NMNH-Vertebrates, University of Texas-Arlington Herpetology UTA, Universidad del Valle de Guatemala UVG-UVGR, American Museum of Natural History AMNH-Vertebrates, Field Museum of Natural History FMNH-Zoology, Florida Museum of Natural History UF-Vertebrates, Museum of Comparative Zoology, Harvard University MCZ-Vertebrates, Museum of Vertebrate Zoology, University of California Berkeley MVZ-Herp, Muséum National d'Histoire Naturell MNHN-Vertebrates and Natural History Museum (London) NHM-Vertebrates; Taxonomic Catalog of the Biota of Mexico [CONABIO (comp) 2023], (https://www.snib.mx/taxonomia/descarga/). The following records were considered: those with specimens

conserved in museums, private biological collections, and data cited in scientific articles, as well as records of specimens deposited by one of the authors in the Museum of Natural History of the Universidad Nacional Autónoma de Honduras.

Appropriate records were considered to be data with the following considerations: (1) data with vouchers in biological collections, with catalog number of or collector code; (2) data with a geographical reference or a detailed description of the collection location; (3) records cited in scientific papers that have not yet been deposited in biological collections nor available in online databases, but which have been published in prestigious journals on this group. Data with only observation records were excluded. The selection of reliable records for the study area serves to eliminate the possibility of bias due to misidentifications that can occur in the various digital platforms that publish visual records.

The selected data were stored in a spreadsheet containing the following fields: a numerical code, the country or region of collection, geographic reference (longitude, latitude, in decimal degrees), and a bibliography of reference of the specimen record (Appendix I). Subsequently, the geographic references were refined and corrected with the help of relevant publications, scientific research articles, and books that provided detailed descriptions of the localities where the specimens were collected (Schmidt 1932, 1933, Gaige *et al.* 1937, Smith and Taylor 1945, Landy *et al.* 1966, Roze 1967, 1982, 1996, Seib 1984, Köhler 2001, 2003, 2008, Jansen and Köhler 2003, Köhler *et al.* 2006, Sunyer 2009, Illescas *et al.* 2011, McCranie 2011, Scott *et al.* 2011, Travers *et al.* 2011, Jowers *et al.* 2023).

Using the geospatial software Quantum GIS 3.28 (QGIS Development Team 2023), Google Earth Pro (Google 2023), and ACME mapper 2.2. (ACME 2024), the geographic points were coupled in a vector layer of southern Mexico and Central America and a satellite imagery layer (QuickMapServices add-on in QGIS) for verification and rectification of the localities and geographic references of each record. Those with anomalies or incorrect geographic references or data that could not be georeferenced were discarded. Data with duplicated geographic references were considered as one record.

Climate Variables

The selection of bioclimatic variables was based on ecological factors such as temperature and precipitation, as indicated by Marques *et al.* (2006), Mizsei *et al.* (2016), and Archis *et al.* (2018). Temperature and precipitation have been identified as significant ecological and biological factors that influence ectothermic species and the composition of surrounding vegetation, highlighting their crucial role in environmental dynamics. This statement is corroborated by McCranie (2011), who notes that distribution of these species in Honduras is predominantly concentrated in lowland rainforest, lowland dry forest, premontane rainforest, premontane wet forest, premontane dry forest, and low montane rainforest. These formations are delimited based on Holdridge's classification of life zones, which are determined by mean annual temperature, mean annual precipitation, humidity, and altitude. Bioclimatic variables were used in potential distribution studies for species of the genus *Micrurus* in different regions of the Americas, including the southern United States, southern Mexico, Central America, Rio de Janeiro, and southeastern Brazil (Terribile *et al.* 2007, Archis *et al*. 2018, Hidalgo-García *et al.* 2018, Guerra *et al.* 2019, Lara-Galván *et al.* 2023).

Consequently, a set of 13 bioclimatic variables and a digital elevation model (DEM) were obtained. This set of predictor variables was reduced to seven through a process that included the selection of the most frequently used variables in previous studies on species of the genus (Terribile *et al.* 2007, Archis *et al*. 2018, Hidalgo-García *et al*. 2018, Guerra *et al*. 2019, Lara-Galván *et al*. 2023). The application of a

collinearity analysis used the pairwise correlation coefficient and the variance inflation factor (VIF) to mitigate the bias introduced by highly correlated variables (more details in the section on identification of collinearity of the predictor variables).

The analysis showed that the mean diurnal range, temperature seasonality, mean temperature of the driest quarter, annual precipitation, precipitation seasonality, precipitation of the warmest quarter, and precipitation of the driest month exhibited the lowest correlation values. Although prior research indicated that the mean annual temperature is a significant factor in the modeling for taxa in this genus, it was excluded due to its high correlation in relation to the other variables. Bioclimatic variable files and digital elevation models were obtained from Worldclim.org (https://www.worldclim.org/data/index.html) (Worldclim.org. 2023), "bio30s" and "elev30s," both with a spatial resolution of 1 km^2 (Fick and Hijmans 2017). The files were edited by making a raster mask at geographic extent between longitudes -95°02'23.70" W, -83°07'08.36" E, and latitude 10°46'11.96" S, 17°33'41.65" N in the software QGIS. For each variable, all files had the same pixel size (30"), with a size of ≈0.93 km, in latitude orientation.

Pseudo-absence

Pseudo-absences were created to meet the requirements of Species Distribution Models (SDMs) that need them. The criteria used for generating these pseudo-absences included: (1) utilizing occurrence records from other species within the same genus, as advised by Phillips *et al.* (2009); (2) identifying and considering regions lacking valid occurrence records, such as the eastern highlands of the Chiapas Mountains in southern Mexico (cf. Johnson *et al.* 2015 classification), southern Petén in Guatemala, and southern Belize (Cayo, Stann Creek, and Toledo), for Honduras based on the distribution of *M. divaricatus* and its relationship with the Holdridge life zones for Honduras, where this complex is absent, as proposed by McCranie (2011). A manual procedure was employed to generate pseudo-absences at random in these zones. Vector layers delineating boundaries within the specified regions were utilized, and an elevation layer was used to restrict the generation of pseudo-absences to a higher range of 0 to 1,900 m a.s.l. These actions were executed in the QGIS program. (3) In addition, pseudo-absences were generated along the study area, with the help of the background function (SDM), through the eDist method, using the occurrence records and a layer stack of the predictive variables that had been previously selected. It was determined that all pseudo-absences situated within a 0.1° radius of each occurrence record should be excluded.

Modeling Process

The processing and execution of the models was conducted using R project software, version 4.3.0 (R Core Team 2023), RStudio version 2023.6.1.524 (Posit Team 2023), through the SDM package (Naimi and Araújo 2021). This package allowed adaptability in developing different modeling techniques and was flexible for generating SDMs, helping to reduce errors in the construction of species distribution models, as well as being easy to use (Naimi and Araújo 2016). The following steps were applied: (1) data loading into the RStudio interface (occurrences, pseudo-absences, and predictor variables); (2) identification collinearity of the predictor variables; (3) model processing, fitting, and evaluation; and (4) generation and preparation of predictions.

Data import into the RStudio interface.—The occurrence, pseudo-absence, and predictor variables (climatic) records were loaded into the RStudio interface. The predictor variables were then grouped into an ensemble file using the raster package (Hijmans 2023). The occurrence and pseudo-absence data were subsequently identified in a binary manner (1 = occurrence

and 0 = pseudo-absence) and converted to SpatialPointsDataFrame format using the "coordinates" function (sdm package).

Identification of collinearity of the predictor variables.—Typically, a threshold of VIF < 10 is used for the exclusion of correlated variables (Dormann *et al*. 2013, Naimi *et al.* 2013, Mpakairi *et al.* 2017, Arenas-Castro *et al.* 2022). Cobos *et al.* (2019) employed a different approach by setting the threshold at VIF < 5, which prompted a review of alternative cutoffs to assess their impact on model performance. To this end, a series of multicollinearity analyses were conducted, examining the impact of various VIF thresholds (VIF < 3, VIF < 5, VIF < 7, and VIF < 10) in the set of 14 pre-selected variables. These analyses indicated that the elimination of predictor variables with VIF values greater than 3 significantly reduced the set of predictor variables and decreased the performance of the models.

Analyses employing VIF < 5 and VIF < 7 thresholds identified the same set of predictor variables, with models exhibiting moderate performance in comparison to exclusion with a VIF threshold < 3. The set of predictor variables obtained in the analysis at a threshold of VIF < 10 exerted a favorable influence on model performance. Each set of predictive variables obtained at different VIF thresholds is evaluated by the performance of the models, using the sensitivity and specificity metrics.

This process allowed selection of the most optimal threshold, which groups the best set of variables. Consequently, the optimal threshold for excluding predictor variables with a high degree of correlation was determined to be a threshold of VIF < 10. During this last analysis, the variables BIO2, BIO4, BIO9, BIO12, BIO15, and BIO18 were not excluded on the basis that they are regarded as essential bioclimatic variables within the genus. The "sdmata" object was then constructed, containing information on occurrences, pseudo-absences in binary form, and predictor variables. For these analyses, the "vifstep" function of the USDM package (Naimi 2023) was used to identify variables with high correlations, and the "keep" argument was utilized for the set of variables that should not be excluded. This function facilitates identification of collinearity between predictor variables through the use of VIF, an effective method to elucidate the relationship between a variable and multiple variables considered in the development of SDMs (Dormann *et al.* 2013, Naimi and Araújo 2016).

Processing, model fitting, and evaluation.—A wide variety of techniques is available for the development of SDMs. Elith *et al.* (2006), Pliscoff and Fuentes-Castillo (2011), Guisan *et al.* (2017) and Hijmans and Elith (2017) classified them into the following three groups: (a) profile or "envelope" methods: based on ranges of minimum and maximum values of climatic variables and values in the location of known occurrences, or mathematical distances to determine the possible occurrence of a species in an established area; (b) regression-based: this technique makes use of occurrence and absence data through multiple regressions, logistic regression, or poisson regression, and describes the relationship between predictor variables, occurrence, and absence; (c) machine learning: uses occurrence data, background data or absence/pseudo absence, predictive variables; within this group there are different techniques, some based on clustering trees and regressions, maximum entropy, and finally, a combination of simple linear method, regression, and outlier detection and class categorization such as support vector machines.

Among the profiling methods, the Bioclim (BIOC), Domain (DOM), and Mahalanobis (MAH) approaches were considered. The Bioclim method employs a straightforward algorithm based on Boolean operators (Busby 1991). In contrast, the Domain (Carpenter *et al.* 1993) and Mahalanobis (Mahalanobis 1936) methods rely on mathematical distances and the similarity of climatic characteristics to identify

potential new locations for occurrence (Elith *et al.* 2006, Hernández *et al.* 2006, Guisan *et al.* 2017). Conversely, regression techniques are predicated on the analysis of the relationship between occurrence data and predictor variables using regression methods. The following methodologies were employed: the generalized linear model (GLM) and the generalized additive model (GAM) (Guisan *et al.* 2002, Elith and Franklin 2013, Guisan *et al.* 2017). The machine learning approach entailed the implementation of random forest (RF), support vector machines (SVM), and maximum entropy modeling (MaxEnt) methods. These models are founded on the principles of classification and regression trees (Breiman 2001). The SVM technique can be applied to regression analysis, outlier detection, and class categorization to predict the areas of presence (Tax and Duin 2004, Guo *et al*. 2005, Hijmans and Elith 2017). According to Zhang and Li (2017), MaxEnt is an approach that employs a maximum entropy framework to contrast presences with predictor variables and to similarly consider absences. This allows the classification of areas with potential presence or absence of a taxon (Phillips *et al.* 2006, Hernández *et al.* 2006, Dudík *et al.* 2007, Guisan *et al.* 2017).

The eight modeling techniques described above were used for the modeling of *M. divaricatus*, with the algorithms for Bioclim, Mahalanobis, and Dominance being those fitted in the Dismo package (Hijmans *et al.* 2023) and MaxEnt implemented using the same framework as the Java package 'MaxEnt', version 3.4.0. While each modeling technique makes different assumptions based on their algorithms when generating SDMs, it is important to review the predictive response from different approaches due to the high environmental, biogeographical, and dataset variation obtained for the study area. This also allows the selection of models that reveal more suitable information for the distribution of this complex. The predictive responses are evaluated using the most common statistics in the evaluation of SDMs (Shabani *et al.* 2018), allowing us to identify the best model to fit our data and study area.

They also allow for an assembly of the models with the best predictive responses, grouping areas with better suitability and reducing the uncertainties of the different models (Araujo and New 2007, Thuiller *et al.* 2009). This approach will provide more robust boundaries of the distribution of the *M. divaricatus* complex in NCA. The following structure was used for each modeling technique: "sdm(bi~BIO2+BIO4+BIO9+BIO12 +BIO14+BIO15+BIO18, data = "Presence – Pseudoabsence," methods = "Models," dep.test, replication = boot, N = 10)" modifying only the "methods" argument. The "sdm" function (sdm package) was used to fit the models, and replications of the different models were performed using the bootstrap method.

To validate the models, a subset of the data prepared for training the models was selected using the bootstrapping technique. This was done to perform validation with dependent test data and to determine the proportion of test data to be used for validating the different models under consideration. Publications on SDMs have proposed that the proportion of test data should be within the range of 20% to 40% for this purpose (Hidalgo-García *et al.* 2018, Stevens and Conway 2019, Interiano *et al.* 2024, Montero and Velasco 2024). In accordance with the aforementioned guideline, five models were executed with test data partitions of 20%, 25%, 30%, 35%, and 40%, comprising 10 replication iterations and 100 repetitions for each modeling method. The models generated with varying percentages of test data partitions were evaluated using the following metrics: the area under the ROC curve (AUC), the true skill statistic (TSS), and the point-biserial correlation coefficient (COR). For each technique, the test data proportions yielding the highest mean values for these metrics were selected, employing the criterion max(se + sp) as the threshold.

The statistical analyses employed to assess the adequacy of the various models were

executed using the "getEvaluation" and "evalates" functions of the SDM packages (Naimi and Araujo 2021). This assessment contributes to the calibration of the models, during which the aforementioned metrics, along with sensitivity and specificity, were employed. The integration of diverse metrics was based on prevalence (AUC and COR), threshold-independent, and threshold-dependent confounding matrix-based statistics (TSS, Kappa, Sensitivity and Specificity), enabling a more rigorous validation process and facilitating a multifaceted evaluation of the SDMs (Fielding and Bell 1997, Segurado and Araújo 2004, Allouche *et al*. 2006, Elith *et al.* 2006, Franklin 2009, Mouton *et al.* 2010, Naimi and Araújo 2016, Guisan *et al*. 2017, Shabani *et al.* 2018).

Considering optimal values between 0.8–0.89 as good, values above 0.9–0.99 are considered very good, and 1 as perfect, for AUC, in the case of TSS and Kappa ≥ 0.7–0.79 good, 0.8–0.99 very good, and 1 perfect, while sensitivity and specificity range between 0–1, with ≥ 0.8–1 being acceptable values, for COR and CA close to 1 (Vaughan and Ormerod 2005, Pearson 2010, Phillips and Elith 2010, Zhang *et al.* 2015, Komac *et al*. 2016, Guisan *et al.* 2017). During the evaluation processes, a total of 30 rounds of runs were executed. These consisted of adjusting the number of pseudoabsences required and the selection of predictor variables at different VIF thresholds (VIF < 3, VIF < 5, VIF < 7, VIF < 10), according to the values of the metrics established, considering the number of pseudoabsences and the VIF threshold with optimal results for the different models. In addition, the variables with the highest relative importance and response were calculated with AUC, using the "rcurve" and "getVarImp" functions (SDM package).

Elaboration of predictions and maps.—Eight predictions for the considered models were generated using the "predict" function (SDM package), from the average of the ten models corresponding to each technique, with the following structure: "predict (RF10, newdata = layer, mean = T)." In addition, an average prediction of the most efficient models was generated on a scale from 0 to 1 to delimit the zones of occurrence. Following the example of the method proposed by Hijmans and Elith (2017), modifying the threshold of 0.5 by an average value of the thresholds obtained by max (se+sp) for the considered models. Subsequently, a second validation was performed using the projections of the generated predictions (transformed to binary) and the occurrence and pseudo-absence data. The same metrics used in the initial evaluation were applied, augmented with the inclusion of the Kappa coefficient and the calibration statistic (CA). This was done to evaluate the discrimination and calibration of the predictions.

The calibration statistic was calculated according to the methodology described in the SDM package. The remaining metrics AUC, TSS, Kappa, COR, Sensitivity (SEN), and Specificity (SPE) were obtained using the "absence.accuracy" and "ecospat.meva.table" functions from the PresenceAbsence and ecospat packages (Broennimann and Di Cola 2023, Freeman 2023). The projections of predictions were selected based on the values resulting from the second round of evaluation. The coefficient of variation was calculated to illustrate areas of agreement between the models. This was achieved by utilizing the "cv" function (raster package). These projections were exported in TIF format using the "writeRaster" function (raster package) and processed in QGIS 3.22 to prepare the potential distribution maps of the *M. divaricatus* complex. The predicted area for Holdridge life zones (Holdridge 1978) for Honduras was also calculated from the average prediction of models with good performance on a scale of 0–1, according to the example presented by Hijmans and Elith (2017). With the help of geospatial tools and the Group Stats add-on in the QGIS program, the area of overlap of life zones and area of possible occurrence of the *M. divaricatus* complex was estimated. The

methodology described above is designed to align with the recommendations made by Zurell *et al.* (2020) during the development of SDMs. The objective is to facilitate the creation of more reliable, reproducible, and efficient models.

Results

The models were derived from a dataset comprising 178 occurrence records obtained from the different localities in various countries (16 from southern México, 28 from Guatemala, 19 from El Salvador, 87 for Honduras, and 28 from Nicaragua) and 306 pseudo-absences, also generated for study area (97 from southern Mexico, 19 from Belize, 61 from Guatemala, 17 from El Salvador, 53 from Honduras, and 59 from Nicaragua). The collinearity analysis conducted on the 14 predictor variables, which were initially chosen based on studies of taxa from the genus *Micrurus,* identified six bioclimatic variables and the elevation model as having a high degree of correlation. As a result, these variables were excluded from further analysis, leading to the development of the models based on seven variables (BIO2, BIO4, BIO9, BIO12, BIO14, BIO15, and BIO18) and the dataset described above (occurrence and pseudo-absences).

The findings derived from the metrics employed during the model fitting and evaluation processes identified four models with acceptable performance levels. Among these, the RF model stood out as the top performer, surpassing SVM, GAM, and MaxEnt. The RF model achieved values of AUC = 0.97, TSS = 0.86, and COR = 0.85, revealing very good performance. While the SVM, GAM, and MaxEnt models also demonstrated good performance with values of AUC $\geq$ 0.87, the rest of the metrics showed values of TSS $\geq$ 0.70 and COR $\geq$ 0.67, indicating good predictive capability. These values, collectively, indicate that all four models possess sufficient accuracy to forecast the potential distribution of the *M. divaritacus* complex. MaxEnt consistently exhibited lower TSS and COR values compared to the other three models (refer to Table 1).

The second evaluation of the generated predictions reinforced the initial results, with the RF model again demonstrating superior performance. It achieved the highest scores: AUC = 0.99, TSS = 0.91, Kappa = 0.89, COR = 0.90, CA = 0.75, SEN = 0.98, and SPE = 0.93, indicating very good predictive capacity. In comparison, the SVM and GAM models exhibited strong results across the board, with AUC $\geq$ 0.93, TSS $\geq$ 0.71, Kappa $\geq$ 0.66, COR $\geq$ 0.74, CA $\geq$ 0.84, SEN $\geq$ 0.88, and SPE $\geq$ 0.76, delivering good predictions. Meanwhile, MaxEnt demonstrated slightly weaker results with an AUC = 0.90, TSS = 0.66, Kappa = 0.63, COR = 0.68, CA = 0.84, SEN = 0.87, and SPE = 0.79. These metrics reflected satisfactory values for the MaxEnt models and demonstrated acceptable

Table 1. The values obtained in the first evaluation were based on a subsample of the training data for use in the validation of the different models, applying the AUC, TSS, and COR metrics. The best performing models are presented in bold. These acronyms are also used in the following sub-section: Processing, Model Fitting, and Evaluation.

	RF	SVM	GAM	MaxEnt	MAH	GLM	DOM	BIOC
AUC	**0.97**	**0.91**	**0.87**	**0.89**	0.91	0.80	0.76	0.73
TSS	**0.86**	**0.73**	**0.70**	**0.70**	0.67	0.57	0.46	0.41
COR	**0.85**	**0.72**	**0.69**	**0.67**	0.38	0.50	0.42	0.28
TH	0.44	0.31	0.52	0.46	-0.17	0.31	0.54	0.02

Table 2. The second evaluation yielded the following values, which were calculated using the prediction projections and the entire training data set for validation. The following metrics were applied: AUC, TSS, Kappa, COR, CA, SEN, and SPE. The best performing models are indicated in bold.

	RF	SVM	GAM	MaxEnt	MAH	GLM	DOM	BIOC
AUC	**0.99**	**0.93**	**0.97**	**0.90**	0.93	0.79	0.76	0.73
TSS	**0.91**	**0.71**	**0.72**	**0.66**	-0.04	0.54	0.30	0.38
Kappa	**0.89**	**0.66**	**0.70**	**0.63**	-0.03	0.49	0.29	0.33
COR	**0.90**	**0.74**	**0.84**	**0.68**	0.36	0.49	0.31	0.39
CA	**0.75**	**0.87**	**0.84**	**0.84**	-0.02	0.77	-0.17	0.76
SEN	**0.98**	**0.94**	**0.88**	**0.87**	0.95	0.89	0.66	0.84
SPE	**0.93**	**0.76**	**0.84**	**0.79**	0.01	0.65	0.64	0.54

performance. Nevertheless, the slightly lower values suggest reduced predictive accuracy compared to the other three models (Table 2).

The evaluations underscored the importance of utilizing a diverse range of metrics such as AUC, TSS, Kappa, COR, SEN, and SPE for a more holistic and rigorous assessment through tailored statistical methodologies specific to each metric. For instance, the MAH model demonstrated suboptimal performance for COR and CA values despite achieving high scores for metrics like AUC, TSS, and Kappa. Models where SPE exceeded SEN were deemed less favorable (Tables 1 and 2). Similarly, models such as Bioclim, Domain, and Generalized Linear Model were excluded due to their failure to meet optimal criteria across these metrics. These models produced inaccurate and low-quality predictions regarding the distribution of the *M. divaricatus* complex, further validating the significance of this multi-metric approach in model evaluation. During these validations, various proportions of test data were assessed to determine optimal performance levels. The analysis suggested that the following percentages of test data delivered the best results: 20% MAH, 30% for RF and BIOC, 35% for GAM, GLM, and DOM, 40% for SVM and MaxEnt (Appendix II). Although performance differences across these percentages were minimal, the models showed their highest accuracy within these ranges. This was demonstrated by the average values recorded for key metrics such as AUC, TSS, and COR (refer to Appendix II for statistics).

Projections from various models revealed significant differences in how this complex is distributed. This can be seen through the values of the coefficient of variation obtained from predictions made by RF, GAM, and MaxEnt (Figure 2). The MaxEnt model primarily shows a Pacific prevalence for NCA, with areas of moderate to high suitability. The Sierra Madre de Chiapas displayed less suitability, characterized by low values. Conversely, the highlands of the Chortís Block in Honduras and Nicaragua projected areas with low suitability. In contrast yet again, the Caribbean slope regions of Honduras exhibited high suitability, while the Honduran Mosquitia and Nicaraguan Mosquitia regions presented areas of half suitability (Figure 3A). In contrast, the RF model showed a reduction in areas corresponding to the highlands of the Chortís block, with low suitability values. The Pacific slopes of Nicaragua exhibited larger areas with low and medium suitability, with certain specific zones of high suitability such as the Pacific coast of El Salvador. Similar patterns

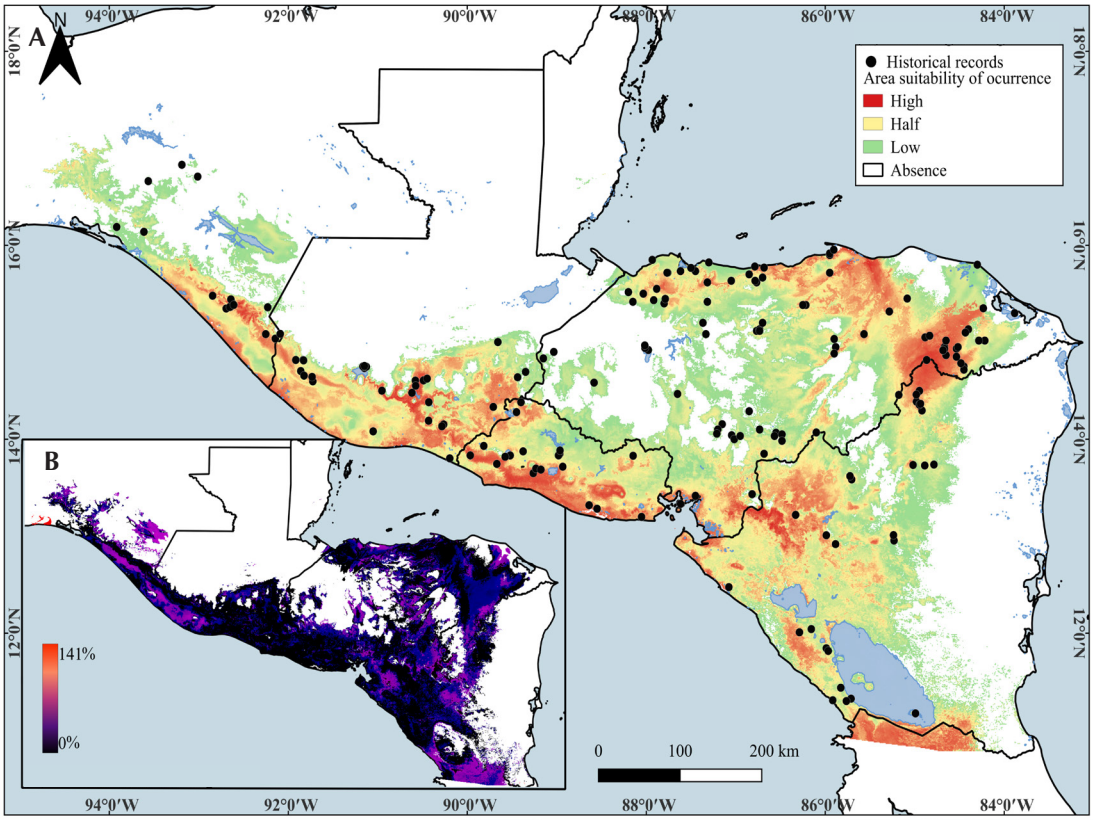

Figure 2. (**A**) Projected average of the RF, GAM, and MaxEnt models, along with historical records for the *M. divaricatus* complex in the NCA. (**B**) Coefficients of variation for the suitability areas indicated by the models.

were observed for the Caribbean slope of Honduras and the Mosquitia region, where the lowlands showed high suitability (Figure 3B).

The SVM model presented a distribution similar to MaxEnt, but it indicated larger areas with high suitability for the Pacific slope of NCA and an increase in suitable areas with low values in the Sierra Madre de Chiapas. On the other hand, the lowlands of the Caribbean side of Honduras and the Mosquitia revealed high suitability. Meanwhile, the highlands of the Chortís block projected a broad area of low suitability values for Honduras and high suitability in the Chortís lands of Nicaragua (Figure 3C). This model identified a small area of suitability conditions in the highlands of Belize. The GAM model produced a varied distribution of areas with values ranging from low to medium and high suitability. The regions demonstrating favorable suitability for the presence of this complex are consistent, both on the Pacific slope and in the Caribbean areas of Honduras and Mosquitia. Notably, the Chortís block region exhibited a broad area of high suitability, contrasting with projections from MaxEnt, RF, and SVM models.

This model acknowledged favorable suitability areas in the Belize highlands and predicted high suitability in the Sierra Madre de Chiapas and the Chiapas highlands (Figure 3D). Areas identified with negative suitability included the northern Sierra Madre Mountains in Chiapas,

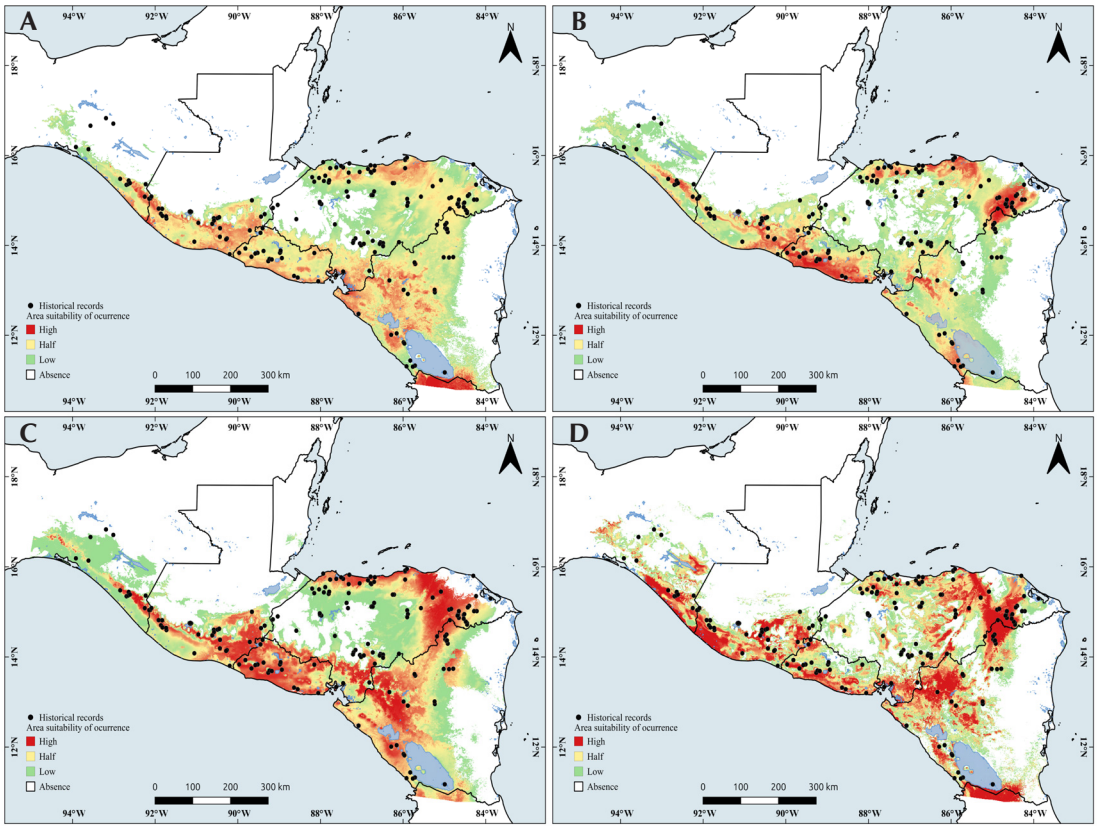

Figure 3. Predictions of the potential distribution of *M. divaricatus* complex in NCA using MaxEnt (**A**), RF (**B**), SVM (**C**), and GAM (**D**). Map generated in QGIS 3.28.

southern Belize, the Petén highlands, the high mountains of Guatemala, the region north of the Polochic-Jocotán and Motagua faults, and the northwestern Mosquitia region of Honduras. Sections of the Chortís Block highlands and most of the Caribbean coast of Nicaragua also displayed negative suitability. The differences in predicted distribution and suitability areas across the models highlight significant variability in estimating suitable regions for various ecosystems in Holdridge's classification for Honduras.

Among the models analyzed, MaxEnt identified large regions of suitability for most ecosystems, including Lowland Arid Forest. It showed restricted suitability areas for Lower Montane Moist Forest. In contrast, the RF, SVM, and GAM models exhibited a gradual reduction in the extent of suitable areas across the ecosystems. Premontane Moist Forests and Lowland Dry Forests were associated with a reduced portion of suitable areas in these models. The Lowland Arid Forest and Lower Montane Moist Forest displayed very minimal suitable regions. On the other hand, the Lowland Moist Forest demonstrated extensive suitability across all four modeling approaches, with only minor variation observed between models. This finding underscores the importance of the Lowland Moist Forest, likely serving as a critical ecosystem for the species complex within Honduras.

The overlap analysis of Holdridge life zones and the average projections generated by the RF,

GAM, and MaxEnt models provided an estimated area of overlap and potential habitat for these ecosystems in Honduras, relative to the distribution of the *M. divaricatus* complex. The results identified overlapping areas of 23,289.12 km² for Lowland Moist Forest, 10,135.04 km² for Lowland Dry Forest, 10,951.40 km² for Premontane Moist Forest, 17,622.18 km² for Premontane Wet Forest, 1,285.53 km² for Premontane Dry Forest, and 1,114.99 km² for Lower Montane Moist Forest. Collectively, these findings suggest that the *M. divaricatus* complex primarily spans six ecosystems within the Honduran territory, covering a potential area of 63,236.1 km².

The assessment of response patterns to predictor variables across four modeling approaches revealed that variables BIO4, BIO14, and BIO15 exert significant influence on the distribution of the *M. divaricatus* complex. While BIO12 notably impacted models generated by SVM, other predictor variables exhibited moderate effects. For the MaxEnt, SVM, and GAM, response values varied from 0.8 to 0.97, contrasting with RF, which exhibited a lower response value of 0.69 (Figure 4). In the analysis of variable importance, BIO4, BIO14, and BIO15 emerged as key factors for predicting the distribution of this complex. BIO4 was identified by RF, SVM, GAM, and MaxEnt as the variable with the greatest contribution in the distribution patterns generated by these approaches for the *M. divaricatus* complex (Figure 5). Additionally,

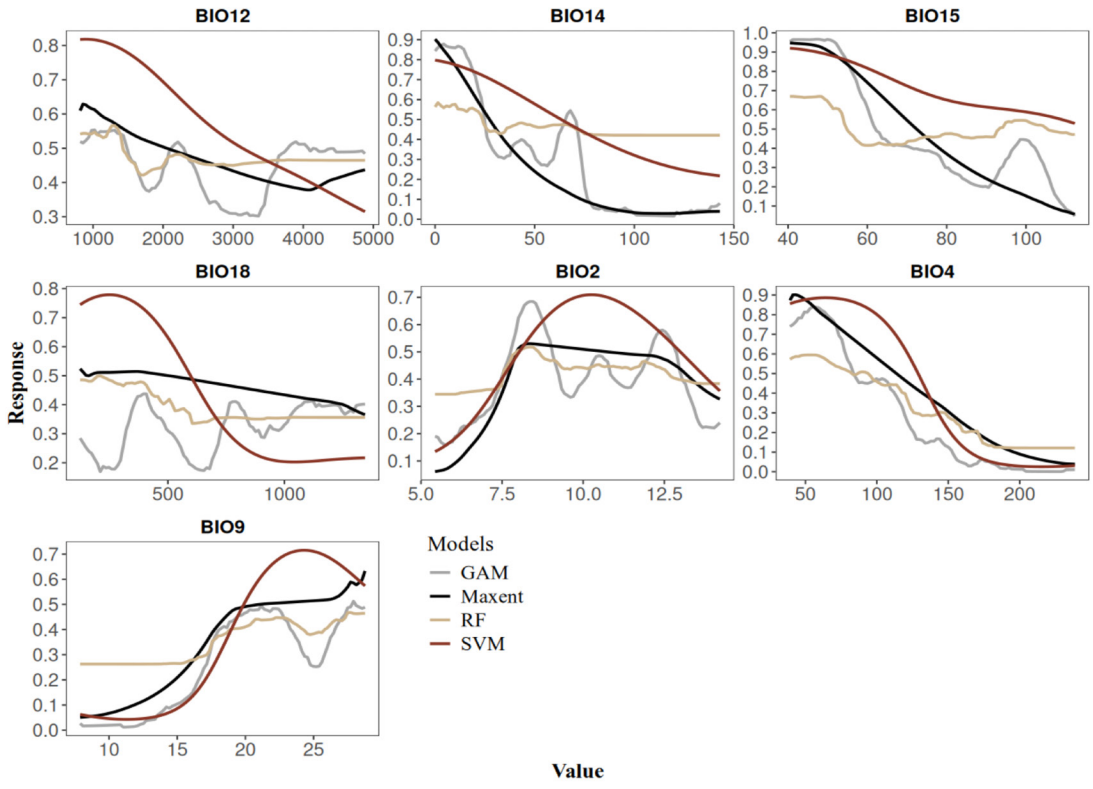

Figure 4. Illustrates the response curves that depict the influence of predictor variables in the top-performing models. The x-axis displays the values of these predictor variables, while the y-axis represents the response rate of the models on a scale from 0 to 1.

both GAM and MaxEnt underscored the relative importance of BIO14 and BIO15 over other variables. These findings indicate that BIO4, BIO14, and BIO15 are essential for comprehending the distribution patterns and ecological factors influencing the *M. divaricatus* complex. Furthermore, a set of preferred values was determined, which is favorable for the occurrence of this complex (for more details on these ranges, refer to Appendix III).

Discussion

The findings indicated that Random Forest (RF), Support Vector Machine (SVM), Generalized Additive Models (GAM), and Maximum Entropy (MaxEnt) are the most effective tools for modeling the distribution of the *M. divaricatus* complex, with RF showing the highest performance. These outcomes align with other research studies on modeling techniques, such as those by Van Strien (2008) and Pliscoff and Fuentes-Castillo (2011). These approaches delimited an area of distribution which spans from the Isthmus of Tehuantepec to the end of the Nicaraguan depression. The models suggest a restricted distribution for the complex north of the Motagua-Polochic-Jocotán fault and predict lower distribution probabilities in the highlands of the Chortís block. They also identify high transition potential between the Pacific and Caribbean slope zones of both

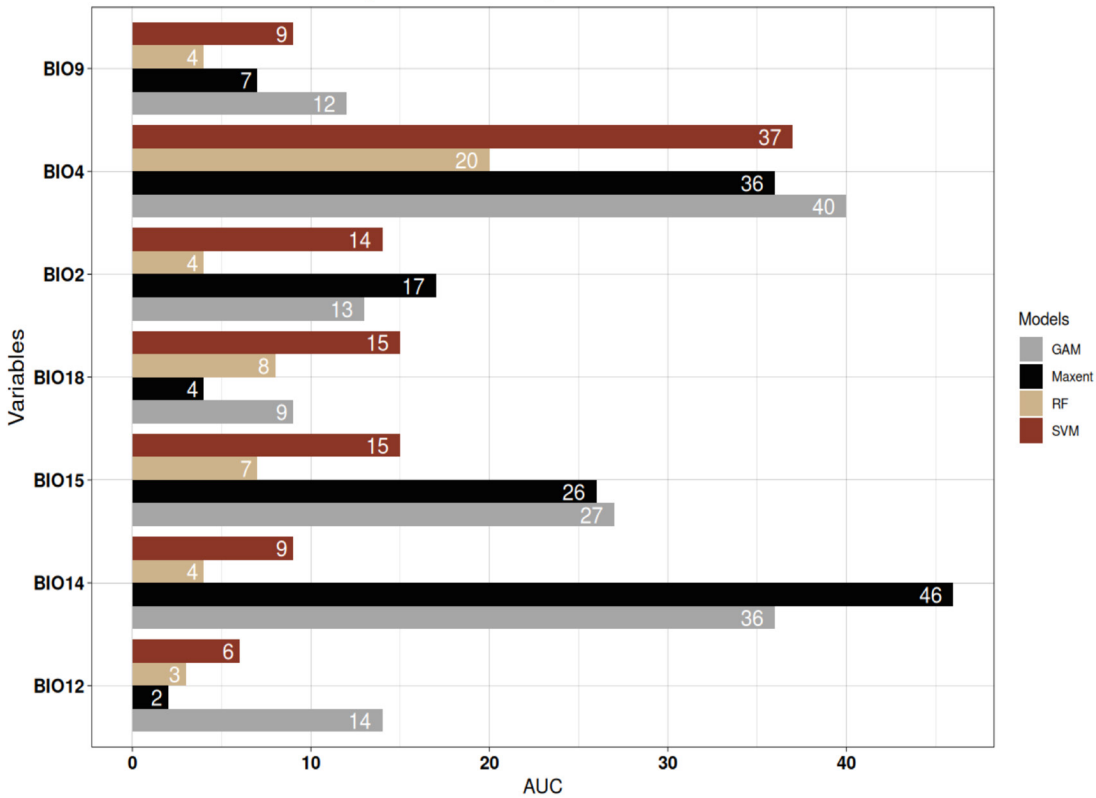

Figure 5. Displays the findings from analyzing the variables with the highest relative importance across four models that demonstrated strong performance for the *M. divaricatus* complex, using the AUC metric method. The bars illustrate the percentage contribution of each variable within these models.

Honduras and Nicaragua (Figure 2). RF, SVM, and GAM are found to more precisely define the distribution range, as the probabilities of presence decrease toward ecological boundaries compared to MaxEnt results.

All models consistently highlight the lowland and mid-elevation areas as particularly suitable for the occurrence of this complex, especially on the Pacific slope of NCA, the Caribbean slope of Honduras, and the Mosquitia regions in both Honduras and Nicaragua. In these locales, the combination of high temperatures and moderate precipitation seems favorable for the prevalence of these taxa. On the other hand, while the highlands of the Chortís block might significantly influence movement patterns, high precipitation levels could render these environments less suitable for occurrence. Similar challenges might arise north of the Motagua-Polochic-Jocotán fault, along Nicaragua's Caribbean coast, and in the highlands of Chiapas, where a disproportionate balance of temperature and precipitation likely restricts the presence of these species. This is supported by results regarding the response and significance of the bioclimatic variables employed.

In the context of this study, the variables BIO4, BIO14, and BIO15 showed valuable insights, suggesting a high likelihood that this complex is linked to NCA regions. This association is marked by BIO4 values ranging from 43.25 to 135.87, BIO14 values between 1.4 to 83.8, and BIO15 values spanning 40.5 to 112.3 (Appendix III). These parameters reflect the preference of the *M. divaricatus* complex for tropical rainforest and dry forest ecosystems, as previously documented by Köhler (2003) and McCranie (2011). These regions typically experience brief periods of seasonal rainfall, while temperatures seldom drop below 75.20 °F. Among these variables, BIO4 is considered crucial in explaining the distribution of the complex, though BIO14 and BIO15 also play significant roles in understanding the genus and distribution patterns of other taxa of *Micrurus*. This observation aligns with findings by Hidalgo-García *et al.* (2018), who analyzed *M. diastema* (Duméril, Bibron, and Duméril, 1854) and *M. elegans* Jan, 1858 within the region.

Research conducted by Hidalgo-García *et al.* (2018) and Lara-Galván *et al.* (2023) on *M. diastema*, *M. elegans*, and *M. distans* Kennicott, 1860 revealed distribution patterns that align with the defined negative suitability zones for the *M. divaricatus* complex. Observed overlap occurs in the Maya Mountains region of Belize, the highlands of Chiapas, and the western Chortís Block. A more extensive overlap was identified west of the Sierra Madre and in the Pacific regions of Chiapas, near the Isthmus of Tehuantepec. These findings suggest that competitive interactions among these species may significantly impact their spatial boundaries in these areas. Further investigation is necessary to explore specific niche dynamics and ecological competition in regions where overlaps are most pronounced.

To confirm the effectiveness of our distribution models for this complex, field evaluations are recommended, following the methodology outlined by Mizsei *et al*. (2016). These evaluations involve field sampling to assess species presence and the functionality of predicted values in key areas, particularly those lacking previous records. This approach also aids in gathering new ecological data. Incorporating biotic variables could enhance predictive accuracy in certain regions, a factor not addressed in this study. Future research should explore the identification of abiotic and biotic tolerance ranges to achieve a more precise ecological characterization of this complex along the NCA corridor. Understanding these ecological relationships will clarify how they affect the distribution of each subspecies within the complex. Additionally, investigating the role of diet as a pivotal biotic factor influencing distribution is an important avenue for future studies.

In accordance with the aforementioned points, ascertaining dietary preference and levels of predation among the three subspecies within

the NCA biogeographic area could facilitate a more profound comprehension of their competitive feeding interactions and underscore regions exhibiting elevated predation rates. These factors are of paramount importance, as they contribute to ecological characterizations and facilitate a more precise delineation of the distribution of this species complex. Subspecies-level venom studies have the potential to identify unique taxonomic and ecological characteristics for each subspecies in this region. This research could provide valuable information for medical treatments by establishing toxicity levels and proteomic data among populations residing in Honduras. A salient example is the findings on *M. ruatanus* (Günther, 1895)(a population from the Caribbean islands of Honduras), which is believed to have evolved recently from *M. divaricatus* but shows a high toxicity level compared to other groups in Central America (Lippa *et al*. 2019, Jowers *et al.* 2023).

In accordance with the IUCN's 2024 classification system for species protection, this complex is currently designated as Least Concern (LC). This status is subject to re-evaluation in light of recent findings by Jowers *et al.* (2023). In Honduras and the nearby region, an alternative system focused on species protection is in place: the Environmental Vulnerability Score (EVS) proposed by Wilson and McCranie (2004). This system assigns a value of EVS = 9, placing it in the low range. Conversely, Johnson *et al.* (2015) have proposed an EVS value of 12 for NCA, which falls within the medium range. While the latter evaluation appears more suitable, it is recommended that the EVS for this species complex be re-evaluated, taking into account the level of subspecies as a criterion. This recommendation is because each subspecies may be subject to different types of negative impacts or a higher degree of vulnerability in various regions of NCA. This species complex exhibits an intriguing genetic richness, and it would be beneficial to expand the components of the EVS by including the significance of the genetic pool presented by the subspecies within a taxon.

The differences observed between the models highlight the importance of integrating multiple approaches when studying species distributions, which helps reduce uncertainty in the final projection for a taxon. The results indicate that the bioclimatic variables Temperature Seasonality (BIO4), Precipitation of Driest Month (BIO14), and Precipitation Seasonality (BIO15) are essential for understanding the ecological distribution and characterizations of the *M. divaricatus* complex in NCA. The overlapping ecosystems and spatial distribution reaffirm the significance of Lowland Moist Forest and Premontane Moist Forest as critical ecosystems and habitats for this species complex. This information is crucial for ecological conservation and management, emphasizing the need to protect these types of forests. Considering the historical distribution patterns proposed by Campbell and Lamar (2004), Köhler (2008), and IUCN (2024), along with comparisons to those generated in this study, we obtained favorable predictive responses. The distributional patterns are similar to those proposed empirically, with only slight discrepancies.

Honduras possesses a significant expanse of suitable habitat along the Caribbean slope, a characteristic that distinguishes it from other regions within NCA. These similarities with empirical distribution patterns underscore the crucial role of modeling in achieving more accurate delineations and validating boundaries proposed by experts. This approach facilitates the identification of ecological aspects and zones of particular importance crucial for the presence of specific taxa. As previously mentioned, the transition zone in the highlands of the Chortís Block, located between Honduras and Nicaragua, is of particular significance. Consequently, it is imperative to undertake a more profound examination of the influence of biotic and abiotic factors on the distribution and adaptation of various subspecies within this complex. Such studies promise to significantly enhance our

understanding of specialization processes and clarify the taxonomy of this group of coral snakes in Nuclear Central America.

Acknowledgments

We thank the MHN-UNAH-CU volunteers; Allyson A. Oviedo and for their contributions to the linguistic revision of the manuscript; Ashly M. Gody and Juan C. Hernández for providing us with their laptops for editing figures; and Jose L. Rodríguez Corleto for granting us internet access during the field trip for editing and submission of the manuscript. Additionally, we express our gratitude to two anonymous reviewers for their corrections, comments, and suggestions, which significantly contributed to the manuscript's development, and to editor Jaime Bertoluci for his continuous communication and guidance and finally, Janalee P. Caldwell, for her insightful feedback on the final version of the manuscript.

References

ACME Mapper 2.2. 2024. Acme Mapper. Version 2.2. URL https://mapper.acme.com/. Captured on 22 July 2024.

Al Haidar, I. K., A. Ghose, M. Noman, M. M. Rahman, S. Rudra, A. Auawal, R. Islam, A. Uddin, R. A. Efran, A. A. Sayeed, R. Amin, F. Ahsan, A. Faiz, and M. A. Wahed. 2023. Implementation of ecological distribution of venomous snakes for clinical management of snakebite in Bangladesh. *Journal of Medicine 24:* 139–151.

Allouche, O., A. Tsoar, and R. Kadmon. 2006. Assessing the accuracy of species distribution models: prevalence, Kappa and the true skill statistic (TSS). *Journal of Applied Ecology 43:* 1223–1232.

Araujo, M. B. and M. New. 2007. Ensemble forecasting of species distributions. *Trends in Ecology and Evolution 22:* 42–47.

Archis, J. N., C. Akcali, B. L. Stuart, D. Kikuchi, and A. J. Chunco. 2018. Is the future already here? The impact of climate change on the distribution of the eastern coral snake (*Micrurus fulvius*). *PeerJ 6:* 1–25.

Arenas-Castro, S., A. Regos, and P. González-Moreno. 2022. Modelos de distribución de especies en ecosistemas forestales. Pp. 1–45 *in* R. M. Navarro, F. J. Mesas, Ó. Pérez, F. J. Ruiz, G. Palacios, P. González-Moreno, and V. Rodríguez (eds.), *Geomática y Ciencia de Datos Aplicadas a la Gestión Forestal: Nuevos Avances y Perspectivas.* Córdoba. Geoforest.

Banks, P. O. 1975. Basement rocks bordering the Gulf of Mexico and the Caribbean sea. Pp. 181–199 *in* A. E. M. Nairn and F. G. Stehli. (eds.), *The Gulf of Mexico and the Caribbean.* New York and London. Plenum Press.

Biber, M. F., A. Voskamp, and C. Hof. 2023. Potential effects of future climate change on global reptile distributions and diversity. *Global Ecology and Biogeography: A Journal of Macroecology 32:* 519–534.

Breiman, L. 2001. Random Forests. *Machine Learning 45:* 5–32.

Brineman, J. H. and G. L. Vinson. 1961. Nuclear Central America hub of Antillean transverse belt: abstract. *AAPG Bulletin 45:* 411–412.

Broennimann, O. and V. Di Cola. 2023. Ecospat: Spatial Ecology miscellaneous methods, an online reference. Electronic Database accessible at https://cran.r-project.org/web/packages/ecospat/ecospat.pdf. Captured on 10 April 2023.

Busby, J. R. 1991. Bioclim: a bioclimate analysis and prediction system. *Plant Protection Quarterly 6:* 8–9.

Campbell, J. A. and W. W. Lamar (eds.). 2004. *The Venomous Reptiles of the Western Hemisphere.* Ithaca. Comstock Publishing, Cornell University Press. 870 pp.

Cano, E. B., J. C. Schuster, and J. Morrone. 2018. Phylogenetics of *Ogyges* Kaup and the biogeography of Nuclear Central America (Coleoptera, Passalidae). *ZooKeys 737:* 81–111.

Carpenter, G., A. N. Gillison, and J. Winter. 1993. DOMAIN: a flexible modelling procedure for mapping potential distributions of plants and animals. *Biodiversity and Conservation 2:* 667–680.

Cobos, M. E., A. T. Peterson, L. Osorio-Olvera, and D. Jiménez-García. 2019. An exhaustive analysis of heuristic methods for variable selection in ecological niche modeling and species distribution modeling. *Ecological Informatics 53:* 1–10.

CONABIO (comp). 2023. Catalog of taxonomic authorities of flora and fauna species with distribution in Mexico: an online reference. Electronic Database accessible at https://www.snib.mx/taxonomia/descarga/. Captured on 22 February 2023.

Donnelly, T., G. S. Horne, R. C. Finch, and E. L. Ramos. 1990. Northern Central America; the Maya and Chortís

blocks. Pp. 1–39 *in* G. Dengo and J. E. Case (eds.). *The Caribbean Region.* Boulder. Geological Society of America.

Dormann, C. F., J. Elith, S. Bacher, C. Buchmann, G. Carl, G. Carré, J. R. Garcia-Marquéz, B. Gruber, B. Lafourcade, P. J. Leitão, T. Münkemüller, C. McClean, P. E. Osborne, B. Reineking, B. Schröder, A. K. Skidmore, D. Zurell, and S. Lautenbach. 2013. Collinearity: a review of methods to deal with it and a simulation study evaluating their performance. *Ecography 36:* 27–46.

Dudík, M., S. J. Phillips, and R. E. Schapire. 2007. Maximum entropy density estimation with generalized regularization and an application to species distribution modeling. *Journal of Machine Learning Research 8:* 1217–1260.

Elith, J. and J. Franklin. 2013. Species distribution modeling. *Encyclopedia of Biodiversity 6:* 692–705.

Elith, J. and J. Franklin. 2017. Species Distribution Modeling. *Reference Module in Life Sciences:* 1–15.

Elith, J. and J. R. Leathwick. 2009. Species distribution models: ecological explanation and prediction across space and time. *Annual Review of Ecology, Evolution, and Systematics 40:* 677–697.

Elith, J., C. H. Graham, R. P. Anderson, K. M. Dudi, S. Ferrier, A. Guisan,R. J. Hijmans, F. Huettmann, J. R. Leathwick, A. Lehmann, J. Li, L. G. Lohmann, B. A. Loiselle, G. Manion,C. Moritz, M. Nakamura, Y. Nakazawa, J. McC. Overton, A. T. Peterson, S. J. Phillips, K. S. Richardson, R. Scachetti-Pereira, R. E. Schapire, J. Soberon, S. Williams, M. S. Wisz, and N. E. Zimmermann. 2006. Novel methods improve prediction of species' distributions from occurrence data. *Ecography 29:* 129–151.

Fernández, J., A. Alape, Y. Angulo, L. Sanz, J. M. Gutiérrez, J. J. Calvete, and B. Lomonte. 2011. Venomic and antivenomic analyses of the Central American coral snake, *Micrurus nigrocinctus* (Elapidae). *Journal of Proteome Research 10:* 1816–1827.

Fick, S. E. and R. J. Hijmans. 2017. WorldClim 2: new 1-km spatial resolution climate surfaces for global land areas. *International Journal of Climatology 37:* 4302–4315.

Fielding, A. H. and J. F. Bell. 1997. A review of methods for the assessment of prediction errors in conservation presence/absence models. *Environmental Conservation 24:* 38–49.

Franklin, J. 1995. Predictive vegetation mapping: geographic modelling of biospatial patterns in relation to environmental gradients. *Progress in Physical Geography 19:* 474–499.

Franklin, J. (ed.). 2009. *Mapping Species Distributions: Spatial Inference and Prediction.* Cambridge. Cambridge University Press. 320 pp.

Freeman, E. 2023. Presence Absence: Presence-Absence Model Evaluation: an online reference. Electronic Database accessible at https://cran.r-project.org/web/packages/PresenceAbsence/PresenceAbsence.pdf. Captured on 10 April 2023.

Gaige, H. T., N. Hartweg, and L. C. Stuart. 1937. Notes on a collection of amphibians and reptiles from eastern Nicaragua. *Occasional papers of the Museum of Zoology, University of Michigan 357:* 1–18.

GBIF.org 2023. The Global Biodiversity Information Facility: an Online Reference. Version 278deb0 (26 february 2022). Electronic Database accessible at https://www.gbif.org. Captured on 10 February 2023.

Google. 2023. Google Earth Pro. Version 7.3.2. URL: https://www.google.com/earth/versions/#earth-pro.

Guerra, G. F., L. G. Da Silva, C. Machado, and D. S. Fernandes. 2019. Potential geographic distribution of the genus *Micrurus* Wagler, 1824 (Serpentes: Elapidae) and antivenom supply in Rio de Janeiro state, Brazil. *Oecologia Australis 23*: 496–506.

Guisan, A. and N. E. Zimmermann. 2000. Predictive habitat distribution models in ecology. *Ecological Modelling 135:* 147–186.

Guisan, A. and W. Thuiller. 2005. Predicting species distribution: offering more than simple habitat models. *Ecology Letters 8:* 993–1009.

Guisan, A., R. Tingley, J. B. Baumgartner, I. Naujokaitis-Lewis, P. R. Sutcliffe, A. I. Tulloch, T. J. Regan, L. Brotons, E. McDonald-Madden, C. Mantyka-Pringle, T. G. Martin, J. R. Rhodes, R. Maggini, S. A. Setterfield, J. Elith, M. W. Schwartz, B. A. Wintle, O. Broennimann, M. Austin, S. Ferrier, M. R. Kearney, H. P. Possingham, Y. M. Buckley, and H. Arita. 2013. Predicting species distributions for conservation decisions. *Ecology Letters 16:* 1424–1435.

Guisan, A., T. C. Edwards, and T. Hastie. 2002. Generalized linear and generalized additive models in studies of species distributions: setting the scene. *Ecological Modelling 157:* 89–100.

Guisan, A., W. Thuiller. And N. E. Zimmermann (eds.). 2017. *Habitat Suitability and Distribution Models with Applications in R.* Cambridge. Cambridge University Press. 461 pp.

Guo, Q., M. Kelly, and C. H. Graham, 2005. Support Vector

Machines for predicting distribution of sudden oak death in California. *Ecological Modelling 182:* 75–90.

Hernandez, P. A., C. H. Graham, L. L. Master, and D. L. Albert. 2006. The effect of sample size and species characteristics on performance of different species distribution modeling methods. *Ecography 29:* 773–785.

Hidalgo-García, J. A., J. R. Cedeño-Vázquez, R. Luna-Reyes, and D. González-Solís. 2018. Modelaje de la distribución geográfica de cuatro especies de serpientes venenosas y su percepción social en el sureste de la Altiplanicie de Chiapas. *Acta Zoológica Mexicana 34:* 1–20.

Hijmans, R. J. 2023. Raster: geographic data analysis and modeling: an online reference. Electronic Database acessible at https://cran.r-project.org/web/packages/raster/raster.pdf. Captured on10 April 2023.

Hijmans, R. J. and J. Elith. 2017. Species distribution modeling with R: an online reference. Electronic Database accessible at http://cran.nexr.com/web/packages/dismo/vignettes/sdm.pdf. Captured on 10 April 2023.

Hijmans, R. J., S. Phillips, J. Leathwick, and J. Elith. 2023. Dismo: Species Distribution Modeling: an online reference. Electronic Database accessible at https://cran.r-project.org/web/packages/dismo/dismo.pdf. Captured on 10 June 2023.

Holdridge, L. R. (ed.). 1978. *Ecologia: Basada en Zonas de Vida.* San José. Instituto Intermericano de Ciencias Agricolas. 216 pp.

Illescas, M. J., M. Dix, and M. L. Maldonado. 2011. *Inventario de Especies de Herpetofauna de las Colecciones Zoológicas en Guatemala. Informe Final: Sistema Guatemalteco de Información Sobre Biodiversidad (SGIB) para la Planificación de Manejo de Vida Silvestre y Áreas Protegidas (Fase IV): Anfibios y Reptiles.* Guatemala. Proyecto FODECYT (FD18-2006), Secretaría Nacional de Ciencia y Tecnología. 223 pp.

Interiano, A. L., D. Herrera, H. Orellana-Carrera, R. N. D. Monroy, P. García, J. E. López, and R. A. Jiménez. 2024. Interaction intensity as determinant of geographic range overlap between ant-following birds and army ants. *Neotropical Biology and Conservation 19:* 137–186.

IUCN (International Union for Conservation of Nature). 2024. The IUCN Red List of Threatened Species. https://www.iucnredlist.org. Captured on 16 April 2025.

James, K. H. 2007. Structural geology: from local elements to regional synthesis. Pp 1–45 *in* J. Bundschuh and G. E. Alvarado (eds.), *Central America: Geology, Resources and Hazards, Vol. II.* New York. CRC Press, Taylor y Francis Press.

Jansen, M. and G. Köhler. 2003. Biogeografische Analyse der Herpetofauna von ausgewählten Hochlandgebieten Nicaraguas. *Salamandra 38:* 269–286.

Johnson, J. D., V. Mata-Silva, E. García-Padilla, and L. D. Wilson. 2015. The herpetofauna of Chiapas, Mexico: composition, physiographic distribution, and conservation status. *Mesoamerican Herpetology 2:* 272–329.

Jowers, M. J., U. Smart, S. Sánchez-Ramírez, J. C. Murphy, A. Gómez, R. J. Bosque, G. C. Sarker, B. P. Noonan, J. F. Faria, D. J. Harris, N. J. Da Silva, A. L. Prudente, J. Weber, P. J. Kok, G. A. Rivas, R. C. Jadin, M. Sasa, A. Muñoz-Mérida, G. Moreno-Rueda, and E. N. Smith. 2023. Unveiling underestimated species diversity within the Central American coralsnake, a medically important complex of venomous taxa. *Scientific Reports 13:* 11674.

Köhler, G. 2001. *Anfibios y Reptiles de Nicaragua.* Offenbach. Herpeton-Verl. 208 pp.

Köhler, G. 2003. *Reptiles de Centroamérica.* Offenbach. Herpeton-Verl. 367 pp.

Köhler, G. 2008. *Reptiles of Central América.* Offenbach. Herpeton-Verl. 393 pp.

Köhler, G., M. Veselý, and E. Greenbaum. 2006. *The Amphibians and Reptiles of El Salvador.* Malabar. Krieger Publishing. 238 pp.

Komac, B., P. Esteban, L. Trapero, and R. Caritg. 2016. Modelization of the current and future habitat suitability of *Rhododendron ferrugineum* using potential snow accumulation*. PLoS ONE 11:* 1–18.

Landy, M. J., D. A. Langebartel, E. O. Moll, and H. M. Smith. 1966. A collection of snakes from Volcan Tacana, Chiapas, México. *Journal of the Ohio Herpetological Society 5:* 93–101.

Lara-Galván, J. L., M. Montesino-San Martin, J. F. Martínez-Montoya, J. J. Sigala-Rodríguez, J. A. Bañuelos-Alamillo, and M. Barbosa. 2023. Assessing the distribution of the West Mexican Coralsnake, *Micrurus distans* Kennicott, 1860, in Zacatecas State, Mexico, using modelling based on multiple data sources. *Herpetology Notes 16:* 827–836.

Lippa, E., F. Török, A. Gómez, G. Corrales, D. Chacón, M. Sasa, J. M. Gutiérrez, B. Lomonte, and J. Fernández. 2019 First look into the venom of Roatan Island's critically endangered coral snake *Micrurus ruatanus:* proteomic characterization, toxicity, immunorecognition and neutralization by an antivenom. *Journal of*

Proteomics 198: 177–185.

Lissovsky, A. A., S. V. Dudov, and E. V. Obolenskaya. 2021. Species-distribution modeling: advantages and limitations of its application; 1. General approaches. *Biology Bulletin Reviews 11:* 254–264.

Mahalanobis, P. C. 1936. On the generalised distance in statistics. *Proceedings of the National Institute of Science of India 2:* 49–54.

Marques, O. A. V., S. M. Almeida-Santos, and M. G. Rodrigues. 2006. Activity patterns in coral snakes, genus *Micrurus* (Elapidae) in south and southeastern Brazil. *South American Journal of Herpetology 1*: 114–120.

Marshall, J. S. 2007. The Geomorphology and Physiographic Provinces of Central America. Pp 1–50 in J. Bundschuh and G. E. Alvarado (eds.), Central America: Geology, Resources and Hazards. Vol. II. New York. CRC Press, Taylor y Francis Press.

Martín, G., J. Erinjery, R. Gumbs, R. Somaweera, D. Ediriweera, P. J. Diggle, A. Kasturiratne, H. J. De Silva, D. G. Lalloo, T. Iwamura, and K. A. Murray. 2022. Integrating snake distribution, abundance and expert-derived behavioural traits predicts snakebite risk. *Journal of Applied Ecology 59*: 611–623.

Mata-Silva, V., D. L. DeSantis, E. García-Padilla, D. Jerry, J. D. Johnson, and L. D. Wilson. 2019. The endemic herpetofauna of Central America: a casualty of anthropocentrism. *Amphibian and Reptile Conservation 13:* 1–64.

Mateo, R. G., Á. M. Felicísimo, and J. Muñoz. 2011. Modelos de distribución de especies: una revisión sintética. *Revista Chilena de Historia Natural 84:* 217–240.

McCranie, J. R. 2011. The snakes of Honduras: systematics, distribution, and conservation. *Society for the Study of Amphibians and Reptiles 26:* 1–714.

Mizsei, E., B. Uveges, B. Vági, M. Szabolcs, S. Lengyel, W. P. Pfliegler, Z. T. Nagy, and J. P. Tóth. 2016. Species distribution modelling leads to the discovery of new populations of one of the least known European snakes, *Vipera ursinii graeca,* in Albania. *Amphibia-Reptilia 37:* 55–68.

Montero, J. M. and J. Velasco. 2024. Herramientas para el análisis en ciencia de datos. Pp. 153–170 *in* G. Fernández-Avilés and J. M. Montero (eds.), *Fundamentos de Ciencia de Datos con R.* Madrid. McGraw Hill Interamericana de Espana, SL.

Mota-Vargas, C. and O. R. Rojas-Soto. 2012. The importance of defining the geographic distribution of species for conservation: the case of the Bearded Wood-Partridge. *Journal for Nature Conservation 20:* 10–17.

Mouton, A. M., B. De Baets, and P. L. Goethals. 2010. Ecological relevance of performance criteria for species distribution models. *Ecological Modelling 221:* 1995–2002.

Mpakairi, K. S., H. Ndaimani, P. Tagwireyi, T. W. Gara, M. Zvidzai, and D. Madhlamoto. 2017. Missing in action: species competition is a neglected predictor variable in species distribution modelling. *PLoS ONE 12:* 1–14.

Naimi, B. 2023. usdm: Uncertainty Analysis for Species Distribution Models: an Online Reference. Electronic Database accessible at https://cran.r-project.org/web/packages/usdm/usdm.pdf. Captured on 20 April 2023.

Naimi, B. and M. B. Araújo. 2016. sdm: a reproducible and extensible R platform for species distribution modelling. *Ecography 39:* 368–375.

Naimi, B. and M. B. Araujo. 2021. sdm: Species Distribution Modellingd: an Online Reference. Electronic Database accessible at https://cran.r-project.org/web/packages/sdm/sdm.pdf. Captured on 20 April 2023.

Naimi, B., N. A. S. Hamm, T. A. Groen, A. K. Skidmore, and A. G. Toxopeus. 2013. Where is positional uncertainty a problem for species distribution modelling? *Ecography 37:* 191–203.

Orellana, S. and Z. López. (eds.). 2023. Portal de Biodiversidad de Guatemala: Digitalización y Manejo de Colecciones Biológicas. Electronic Database accessible at https://biodiversidad.gt/portal/index.php, Guatemala. Captured on 30 April 2023.

Pearson, R. G. 2010. Species' distribution modeling for conservation educators and practitioners. *Lessons in Conservation 3: 54–89*.

Phillips, S. J. and J. Elith. 2010. POC plots: calibrating species distribution models with presence-only data. *Ecology 91*: 2476–2484.

Phillips, S. J., M. Dudík, J. Elith, C. H. Graham, A. Lehmann, J. Leathwick, and S. Ferrier. 2009. Sample selection bias and presence-only distribution models: implications for background and pseudo-absence data. *Ecological Applications 19:* 181–197.

Phillips, S. J., R. P. Anderson, and R. E. Schapire. 2006. Maximum entropy modeling of species geographic distributions. *Ecological Modelling 190:* 231–259.

Pliscoff, P. and T. Fuentes-Castillo. 2011. Modelación de la distribución de especies y ecosistemas en el tiempo y en el espacio: una revisión de las nuevas herramientas y enfoques disponibles. *Revista de Geografía Norte*

Grande 48: 61–79.

Posit Team 2023. RStudio: Integrated Development Environment for R. Version 2023.6.1.524. URL: http://www.posit.co/.

QGIS Development Team. 2023. QGIS un Sistema de Información Geográfica Libre y de Código Abierto. Version 3.28. URL: http://qgis.osgeo.org.

R Core Team. 2023. R: A Language and Environment for Statistical Computing. R. Version 4.3.0. URL: https://www.R-project.org/.

Rodríguez-Gómez, F., Y. Licona-Vera, L. Silva-Cárdenas, and J. F. Ornelas. 2021. Phylogeography, morphology and ecological niche modelling to explore the evolutionary history of Azure-crowned Hummingbird (*Amazilia cyanocephala,* Trochilidae) in Mesoamerica. *Journal of Ornithology 162:* 529–547.

Roze, J. A. 1967. A check list of the new world venomous coral snakes (Elapidae), with descriptions of new forms. *American Museum Novitates 2287:* 1–60.

Roze, J. A. 1982. New world coral snakes (Elapidae): a taxonomic and biological summary. *Memórias do Instituto Butantan 46:* 305–338.

Roze, J. A. 1996. *Coral Snakes of the Americas: Biology, Identification, and Venoms.* Malabar. Krieger Publishing Company. 328 pp.

Russell, F. E., F. G. Walter, T. A. Bey, and M. C. Fernandez. 1997. Snakes and snakebite in Central America. *Toxicon 35:* 1469–1522.

Savage, J. M. 1966. The origins and history of the Central American Herpetofauna. *Copeia 1966:* 719–766.

Schmidt, K. P. 1932. Stomach contents of some American Coral snakes, with the description of a new species of *Geophis. Copeia 1932: 6–9.*

Schmidt, K. P. 1933. Preliminary account of the coral snakes of Central America and México. *Zoological Series of Field Museum of Natural History, Chicago 20:* 29–40.

Scott, T. L., S. Doucette-Riise, L. A. Obando, and J. H. Townsend. 2011. *Micrurus nigrocinctus* (central American coral snake). Cannibalism. *Herpetological Bulletin 115:* 31–32.

Segurado, P. and M. B. Araújo. 2004. An evaluation of methods for modelling species distributions. *Journal of Biogeography 31:* 1555–1568.

Seib, R. L. 1984. Prey use in three syntopic Neotropical racers. *Society for the Study of Amphibians and Reptiles 18:* 412–420.

Shabani, F., L. Kumar, and M. Ahmadi. 2018. Assessing accuracy methods of species distribution models: AUC, specificity, sensitivity, and the true skill statistic. *Global Journals 18:* 6–18.

Smith, H. M. and E. H. Taylor. 1945. An annotated checklist and key to the snakes of Mexico. *Bulletin of the United States National Museum 187*: 1–239.

Stazi, M., F. Fabris, J. Fernández, G. D'Este, M. Rigoni, A. Megighian, J. M. Gutiérrez, B. Lomonte, and C. Montecucco. 2022. Recovery from the neuroparalysis caused by the *Micrurus nigrocinctus* venom is accelerated by an agonist of the CXCR4 receptor. *Toxins 14:* 1–13.

Stevens, B. S. and C. J. Conway. 2019. Predicting species distributions: unifying model selection and scale optimization for multi-scale occupancy models. *Ecosphere 10:* 1–25.

Sunyer, J. 2009. Taxonomy, zoogeography, and conservation of the herpetofauna of Nicaragua. Unpublished Doctoral, Dissertation. Goethe University, Frankfurt am Main, Germany.

Tax, D. M. and R. P. Duin, 2004. Support vector data description. *Machine Learning 54:* 45–6.

Terribile, L. C., T. C. S. Anacleto, N. J. Silva Jr., and J. A. F. Diniz-Filho. 2007. Potential geographic distribution of the coral snake *Micrurus decoratus* Jan, 1858 (Serpentes, Elapidae) in the Atlantic Rainforest of Brazil. *Arquivos do Museu Nacional 65:* 217–223.

Thuiller, W., B. Lafourcade, R. Engler, and M. Araujo. 2009. BIOMOD, a platform for ensamble forecasting of species distributions. *Ecography 32:* 369–373.

Travers, S. L., J. H. Townsend, J. Sunyer, L. A. Obando, L. D. Wilson, and A. N. Max. 2011. New and noteworthy records of amphibians and reptiles from Reserva de la Biósfera Bosawas, Nicaragua. *Herpetological Review 42:* 399–403.

Van Strien, M. 2008. Best practice species distribution modelling protocol. Version 1.0. Lausanne. Ecospat-Spatial Ecology Group, University of Lausanne.

Vaughan, I. P. and S. J. Ormerod, 2005. The continuing challenges of testing species distribution models. *Journal of Applied Ecology 42:* 720–730.

VertNet.org. 2016. Search VertNet: an Online Reference. Version 2016-09-29 (04 July 2020). Electronic database accessible at: http://portal.vertnet.org/search. Captured on 28 February 2023.

Wilson, L. D. and J. R. McCranie. 2004. The conservation status of the herpetofauna of Honduras. *Amphibian and*

Reptile Conservation 3: 6–33.

Worldclim.org. 2023. WorldClim: an Online Reference. Version 2020-2022. Electronic Database accessible at https://www.worldclim.org/data/index.html. Captured on 17 April 2023.

Zhang, J. and S. Li. 2017. A review of Machine Learning Based Species' Distribution Modelling. Pp. 199–206 *in* J. E. Guerrero (ed.), *2017 International Conference on Industrial Informatics, Computing Technology, Intelligent Technology, Industrial Information Integration (ICIICII).* Wuhan. IEE Computer Society, Conference Publishing Services (CPS).

Zhang, L., S. Liu, P. Sun, T. Wang, G. Wang, X. Zhang, and L. Wang. 2015. Consensus forecasting of species distributions: the effects of niche model performance and niche properties. *PLoS ONE 10:* 1–18.

Zurell, D., J. Franklin, C. König, P. J. Bouchet, C. F. Dormann, J. Elith, G. Fandos, X. Feng, G. Guillera-Arroita, A. Guisan, J. J. Lahoz-Monfort, P. J. Leitão, D. S. Park, A. T. Peterson, G. Rapacciuolo, D. R. Schmatz, B. Schröder, J. M. Serra-Diaz, W. Thuiller, K. L. Yates, N. E. Zimmermann, and C. Merow 2020. A standard protocol for reporting species distribution models. *Ecography 43:* 1261–1277.

Editor: Jaime Bertoluci

Appendix I. *Historical records of the* Micrurus divaricatus *species complex, along with their geographical references in decimal degrees format, are used as presence data. Data are presented as Code (latitude, longitud).*

El Salvador; Köhler *et al.* 2006: 1 (13.93098, -89.81564), 2 (13.71667, -88.93333), 3 (13.85, -88.96667), 4 (13.83333, -88.98056), 5 (13.64949, -89.26276), 6 (13.87487, -89.37644), 7 (14.2791, -89.45), 8 (13.696969, -89.233333), 9 (13.686482, -89.177341), 10 (13.745379, -89.669616), 11 (13.83333, -89.9666), 12 (13.283333, -88.55), 13 (13.199025, -88.053147), 14 (14.38087, -89.399929), 15 (13.88374, -88.963933), 16 (13.829419, -88.147227), 17 (13.832662, -89.520137), 18 (13.81905, -89.576632), 19 (13.31957, -88.63889).

Guatemala; Orellana, S. and Z. López. (eds.). 2023: 20 (14.7028, -91.8611), 21 (14.6042, -90.5806), 22 (14.6556, -91.8247), 23 (14.0811, -91.0522), 24 (14.733333, -91.15), 25 (14.152309, -90.26342), 26 (14.75, -91.166667), 27 (14.746946, 91.128027), 28 (14.816667, -91.833333), 29 (14.190873, -90.433333), 30 (14.133333, -90.283333), 31 (14.75508, -91.149313), 32 (14.812773, -91.829879), 33 (14.6065, -90.4901), 34 (14.5511, -90.5772), 35 (14.5, -90.9542), 36 (14.3814, -90.4306), 37 (14.5511, -90.5772), 38 (14.8167, -91.9167), 39 (14.6247, -90.4494), 40 (15.0017, -89.6583), 41 (14.4783, -90.6189), 42 (14.6941, -89.3485), 43 (13.8028, -90.1956), 44 (14.6389, -89.4376), 45 (14.5967, -91.7264), 46 (14.3328, -89.7094), 47 (14.6425, -91.7344).

Honduras; McCranie 2011: 48 (14.8333, -89.15), 49 (14.5833, -88.5833), 50 (14.9, -89.0333), 51 (14.9194, -87.9771), 52 (13.85, -86.6833), 53 (14.0667, -86.55), 54 (15.0333, -85.9), 55 (15.1333, -84.4), 56 (15.8, -84.3), 57 (14.9333, -84.5333), 58 (14.8667, -84.65), 59 (14.8167, -84.8667), 60 (15.6167, -87.3167), 61 (15.9, -85.95), 62 (14.041316, -87.045327), 63 (14.07, -86.1), 64 (15.4167, -88.15), 65 (15.8235, -87.30032), 66 (14.4667, -87.65), 67 (15.77, -86.6833), 68 (15.3833, -86.2167), 69 (14.0333, -86.5667), 70 (15.0833, -85.5667), 71 (15.0167, -84.2167), 72 (15.5167, -88.2), 73 (15.1167, -86.7667), 74 (14.9406, -88.0146), 75 (14.1, -86.7333), 76 (15.4, -87.8), 77 (14.0, -87.0167), 78 (15.45, -85.0833), 79 (15.7, -86.85), 80 (15.7167, -85.95), 81 (15.7167, -87.76), 82 (14.95, -84.6667), 83 (13.3333, -87.6167), 84 (14.9333, -84.6667), 85 (15.05, -84.8833), 86 (15.781249, -86.786535), 87 (14.95, -85.8833), 88 (15.4167, -87.3167), 89 (15.4333, -87.9167), 90 (14.05, -86.4833), 91 (15.55, -87.8833), 92 (15.7333, -87.45), 93 (15.0667, -84.8333), 94 (14.0333, -86.95), 95 (14.15475, -87.1513), 96 (15.6167, -86.7667), 97 (13.9833, -86.4833), 98 (14.75, -84.45), 99 (15.0167, -84.2833), 100 (15.1333, -86.7333), 101 (14.2886, -86.85), 102 (15.2, -87.3667), 103 (14.9667, -88.0167), 104 (14.8833, -85.9), 105 (15.0833, -87.3333), 106 (15.7667, -87.499993), 107 (15.6333, -86.7833), 108 (15.1167, -86.7333), 109 (15.3167, -85.2833), 110 (15.1, -84.4333), 111 (15.3833, -86.25), 112 (15.6667, -86.7), 113 (14.7167, -84.45), 114 (13.4167, -87.45), 115 (13.4333, -86.8167), 116 (15.5, -88.0333), 117 (14.95, -84.5167), 118 (15.6333, -87.05), 119 (14.7833, -84.4833), 120 (15.3, -83.8833), 121 (14.85, -84.53333333), 122 (14.1, -87.2), 123 (15.2, -86.7), 124 (15.0167, -84.65), 125 (15.7167, -87.7667), 126 (15.91636, -85.94941), 127 (15.7333, -87.6167), 128 (14.9167, -84.6833), 129 (15.35, -84.2333), 130 (14.9167, -84.6833), 131 (15.44669964, -87.78699951), 132 (14.0573, -87.2114), 133 (15.85, -87.9333), 134 (15.954053, -85.90452).

Mexico; CONABIO (comp). 2023: 135 (15.0372394, -92.1452034), 136 (15.08611, -92.09028), 137 (15.36, -92.23), 138 (15.347222, -92.693889), 139 (16.661111, -93.565278), 140 (15.083333, -92.252222), 141 (16.188611, -93.918056), 142 (16.138806, -93.614055), 143 (15.479167, -92.846667), 144 (15.41, -92.63), 145 (16.83, -93.19), 146 (16.7080556, -93.0133333), 147 (15.365278, -92.644444), 148 (15.3625, -92.654167), 149 (15.441667, -92.641667), 150 (15.384722, -92.609722).

Appendix I. *Continued.*

Nicaragua; Köhler 2001, Sunyer 2009: 151 (12.955222, -85.230889), 152 (11.3080278, -85.9164167), 153 (11.324154, -85.711263), 154 (11.844167, -85.988056), 155 (11.816667, -85.966667), 156 (12.041868, -86.155722), 157 (12.008864, -86.287994), 158 (14.3535, -84.942), 159 (12.918273, -85.884966), 160 (11.29972, -85.764063), 161 (12.474348, -87.076823), 162 (14.296217, -84.918517), 163 (13.738586, -84.784889), 164 (14.387767, -84.979917), 165 (11.172778, -84.990833), 166 (13.728917, -84.887361), 167 (14.355833, -84.947778), 168 (14.498056, -84.9475), 169 (13.585518, -85.704848), 170 (14.456931, -85.177629), 171 (13.011389, -85.236556), 172 (13.22, -86.330833), 173 (13.734722, -85.018056), 174 (13.01, -85.988056), 175 (13.61963, -85.72331), 176 (14.459847, -84.981499), 177 (14.36533, -84.93495), 178 (11.43716, -85.82633).

Appendix II. *Analysis for the selection of test data, based on the AUC, the TSS, and the COR, for the different models considered. The values presented in bold are of greater magnitude.*

RF	**AUC_{mean}**	**TSS_{mean}**	**COR_{mean}**	**MAH**	**AUC_{mean}**	**TSS_{mean}**	**COR_{mean}**
$Data_{test}$ 20	0.97182	0.85728	0.84672	$Data_{test}$ 20	**0.9174**	**0.6989**	**0.3657**
$Data_{test}$ 25	0.97203	0.85819	0.84711	$Data_{test}$ 25	0.9155	0.6978	0.3605
$Data_{test}$ 30	**0.97373**	**0.86438**	**0.85175**	$Data_{test}$ 30	0.9133	0.6933	0.3610
$Data_{test}$ 35	0.97151	0.86135	0.84840	$Data_{test}$ 35	0.9095	0.6777	0.3576
$Data_{test}$ 40	0.97227	0.86030	0.84849	$Data_{test}$ 40	0.9149	0.7027	0.3640
SVM	**AUC_{mean}**	**TSS_{mean}**	**COR_{mean}**	**MAH**	**AUC_{mean}**	**TSS_{mean}**	**COR_{mean}**
$Data_{test}$ 20	0.91274	0.72769	0.71894	$Data_{test}$ 20	0.8044	0.5820	0.5039
$Data_{test}$ 25	0.91470	0.73157	0.72311	$Data_{test}$ 25	0.8048	0.5840	0.5043
$Data_{test}$ 30	0.91453	0.72854	0.72212	$Data_{test}$ 30	0.8044	0.5834	0.5035
$Data_{test}$ 35	0.91447	0.73125	0.72281	$Data_{test}$ 35	**0.8082**	**0.5897**	**0.5100**
$Data_{test}$ 40	**0.91540**	**0.73182**	**0.72485**	$Data_{test}$ 40	0.8043	0.5818	0.5035
GAM	**AUC_{mean}**	**TSS_{mean}**	**COR_{mean}**	**MAH**	**AUC_{mean}**	**TSS_{mean}**	**COR_{mean}**
$Data_{test}$ 20	0.87562	0.69883	0.68402	$Data_{test}$ 20	0.7186	0.3937	0.3770
$Data_{test}$ 25	0.87274	0.69094	0.67934	$Data_{test}$ 25	0.7202	0.3948	0.3797
$Data_{test}$ 30	0.87644	0.68765	0.68765	$Data_{test}$ 30	0.7181	0.3925	0.3770
$Data_{test}$ 35	**0.87848**	**0.70516**	**0.69000**	$Data_{test}$ 35	**0.7219**	**0.3990**	**0.3812**
$Data_{test}$ 40	0.87689	0.69725	0.68092	$Data_{test}$ 40	0.7195	0.3950	0.3781
MaxEnt	**AUC_{mean}**	**TSS_{mean}**	**COR_{mean}**	**MAH**	**AUC_{mean}**	**TSS_{mean}**	**COR_{mean}**
$Data_{test}$ 20	0.88535	0.68305	0.66135	$Data_{test}$ 20	0.4264	0.7305	0.2810
$Data_{test}$ 25	0.88934	0.69280	0.66690	$Data_{test}$ 25	0.4271	0.7290	0.2767
$Data_{test}$ 30	0.88462	0.68475	0.65757	$Data_{test}$ 30	**0.4280**	**0.7317**	**0.2865**
$Data_{test}$ 35	0.88865	0.68230	0.66361	$Data_{test}$ 35	0.4269	0.7286	0.2795
$Data_{test}$ 40	**0.88881**	**0.69639**	**0.66743**	$Data_{test}$ 40	0.4272	0.7302	0.2849

Appendix III. *Suggested ranges for the seven variables used in model generation. Values for variables that significantly influenced distribution of the* Micrurus divaricatus *complex are highlighted in bold.*

	BIO2		**BIO4**		**BIO9**		**BIO12**		**BIO14**		**BIO15**		**BIO18**	
	Min	Max	Min	Max	Min	Max	Min	Max	Min	Max	Min	Max	Min	Max
SVM	7.5	10.5	**63.4**	**135.9**	18.9	24.3	899.1	424.2	**1.4**	**83.8**	**40.5**	**112.3**	246.5	678.9
MaxEnt	7.7	12.8	**43.3**	**121.8**	18.6	28.8	899.1	2828.5	**1.4**	**30.3**	**40.5**	**75.3**	123	913
GAM	10.7	8.4	**105.7**	**55.3**	20.1	28.8	817	2335.9	**1.4**	**24.5**	**41.9**	**63**	123	133.6
RF	8.4	12.5	**55.3**	**115.7**	20.5	27.7	1309.6	1761.2	**1.4**	**78**	**40.5**	**70.2**	209.5	456.5

Phyllomedusa 24(2):201–221, 2025

ISSN 1519-1397 (print) / ISSN 2316-9079 (online)
doi: http://dx.doi.org/10.11606/issn.2316-9079.v24i2p201-221

Cephalic fossae and pits in the parietal shields of caenophidian snakes and their correspondence in the braincase

Alessandro Paterna

OPHIS Museo Paleontologico e Centro Erpetologico, 64100 Teramo, Italy. E-mail: alessandro.paterna@hotmail.com.

Abstract

Cephalic fossae and pits in the parietal shields of caenophidian snakes and their correspondence in the braincase. Anatomical and osteological analyses in several species of ophidians belonging to the clade Caenophidia have led to the identification of different structures present in the cephalic shields of these reptiles. These structures are observed expressed mainly in the parietal shields, manifesting themselves in different forms. “Major parietal pits,” generally symmetrical, occur in the center of the parietal shields, more or less medially distanced to each other. These may appear circular, linear, separated, conjunct, or in contact with the lateral margin of the parietal shield by a slit. Together with the pits, a new distinct trait has been observed in the parietal shields of different species of colubroids, here named “parietal fossae.” Parietal pits and fossae are situated in correspondence with the paired foramina on the parietal bone’s dorsal plane, which in turn correspond ventrally with the epiphysis, and the contact between the cephalic hemispheres and the optic lobes. Other fossae may be present in certain species, occurring more posteriorly in the parietal shields, or in the supraocular shields, in correspondence with neurovascular foramina and fossae present in the underlying cranial bones. A second category of pits has also been found, here named “minor pits,” which appear randomly within the cephalic shields, and are also linked to neurovascular foramina present in the corresponding cranial bones. A third type of pit, distinct from the others, is the “medial posterior pit”, which has been found in aquatic snakes. This pit occurs in the posterior half of the medial contact of the parietal shields, and corresponds to a large central foramen in the posterior apex of the parietal bone’s plane, ventrally opening within a canal between the two fossae covering the optic lobes. All of these traits have been observed in a large number of snakes belonging to the families Colubridae, Natricidae, Psammophiidae, Atractaspididae, Pareidae, Xenodermidae, Micrelapidae and Elapidae. These do not occur in all individuals within the examined taxa, but rather affect part of the specimens of a given species. Fossae and pits appear to be sporadic surface structures that correspond to neurovascular foramina present in the underlaying cranial bones.

Keywords: Cranial anatomy, Parietal pits, Parietal fossae, Parietal foramen, Colubroidea.

Received 21 August 2024
Accepted 21 January 2025
Distributed December 2025

Resumo

Fossetas e cavidades cefálicas nos escudos parietais das serpentes Caenophidia e sua correspondência na caixa craniana. Análises anatômicas e osteológicas em várias espécies de serpentes pertencentes ao clado Caenophidia levaram à identificação de diferentes estruturas presentes nos escudos cefálicos. Estas estão presentes principalmente nos escudos parietais, manifestando-se de diferentes formas. "Fossetas parietais maiores", geralmente simétricas, ocorrem no centro dos escudos parietais, mais ou menos distanciadas medialmente umas das outras. Estas podem se apresentar circulares, lineares, separadas, conjuntas ou em contato com a margem lateral do escudo parietal por uma fenda. Juntamente com as fossetas, foi observada uma nova característica distinta nos escudos parietais de diferentes espécies de colubróides, aqui denominada "fossetas parietais". As fossas e fossetas parietais estão situadas em correspondência com os forâmenes emparelhados no plano dorsal do osso parietal, que por sua vez correspondem ventralmente à epífise e ao contato entre os hemisférios cefálicos e os lobos ópticos. Outras fossas podem estar presentes em certas espécies, ocorrendo mais posteriormente nos escudos parietais ou nos escudos supraoculares, em correspondência com as forâmenes e fossas neurovasculares presentes nos ossos cranianos subjacentes. Uma segunda categoria de fossas também foi encontrada, aqui denominadas "fossetas menores", que aparecem aleatoriamente dentro dos escudos cefálicos e também estão ligadas às forâmenes neurovasculares presentes nos ossos cranianos correspondentes. Um terceiro tipo de fosseta, distinto dos outros, é a "fosseta posterior medial", que foi encontrada em serpentes aquáticas. Esta ocorre na metade posterior do contato medial dos escudos parietais e corresponde a um grande forâmen central no ápice posterior do plano do osso parietal, abrindo-se ventralmente dentro de um canal entre as duas fossetas que cobrem os lobos ópticos. Todas essas características foram observadas em um grande número de serpentes pertencentes às famílias Colubridae, Natricidae, Psammophiidae, Atractaspididae, Pareidae, Xenodermidae, Micrelapidae e Elapidae. Estas não representam uma constante dentro dos táxons examinados, mas ocorre em uma parte dos espécimes de uma determinada espécie. As fossas e cavidades parecem ser expressões superficiais esporádicas correspondentes a forâmenes neurovasculares presentes nos ossos cranianos subjacentes.

Palavras-chave: Anatomia craniana, Colubroidea, Fossa parietal, Fosseta parietal, Forâmen parietal.

Introduction

Many of the more derived snakes, such as colubroids, present enlarged cephalic scales, defined as shields, which are larger and distinct from the dorsal scales. These shields have a specific shape and the cephalic dorsal ones are usually organized in a number that can vary from nine to 11 (Schulz, 1996). Recent studies have been dedicated to examined the presence of pits within the parietal shields that have been observed in several species belonging to five genera of the family Psammophiidae (De Haan 2003, 2006, Cottone and Bauer 2011). The presence of similar cephalic structures has been previously mentioned for several species in the genera *Alsophis, Dasypeltis, Mehelya,* and *Tropidonophis* (Underwood 1967, Malnate and Underwood 1988), but parietal pits were described in detail for the first time by De Haan (2003). In addition to psammophiids, these traits have been found in an Asian natricid species, *Atretium schistosum* (Daudin, 1803) (Miralles and Ineich 2006). In these studies, among the various hypotheses generated of a possible sensorial nature, the authors support the conclusion that these pits could be an expression of ancestral traits present in the analyzed species (de Haan 2006, Miralles and Ineich 2006, Cottone and Bauer 2011) and a surface manifestation originating from underlying structures (Miralles and Ineich 2006, Cottone and Bauer 2011).

The present study examines some species of Old World snakes belonging to the clade Caenophidia in which similar structures to the pits described in psammophiids have been identified in the parietal shields. Anatomical and osteological analyses were performed on 19

representative species belonging to the families Colubridae, Natricidae, Psammophiidae, Elapidae, and Viperidae, where the relationship between the cephalic shields, the braincase, and the encephalon was investigated. The resulting study represents a preliminary analysis of the cephalic traits present in the shields of snakes belonging to the clade Caenophidia. Three new distinct traits, and their correspondence with the features of the underlaying cranial bones are described.

Materials and Methods

Osteological and necroscopic analyses were performed at OPHIS Museo Paleontologico e Centro Erpetologico. All deceased specimens belonging to the colubroid, elapoid and viperid clades were donated by private individuals and zoos to OPHIS for research purposes, with the exception of specimens of *Hierophis viridiflavus* (Lacépède, 1789), *Natrix helvetica* (Linnaeus, 1758), and *Zamenis longissimus* (Laurenti, 1768), which consisted of roadkilled individuals collected in Abruzzo (Italy), most of which were used in former studies (Paterna 2023, 2024, 2025, Paterna and Grano 2024). Specimen preparation was performed using surgical tools and solvents. All photographic material relating to anatomical and osteological analyses was produced within OPHIS. Photographs of living specimens belonging to the genera *Hierophis, Zamenis,* and *Natrix* portray both specimens raised in controlled environment and wild ones photographed in nature. Photographs of living specimens belonging to the genera *Elaphe, Hemorrhois, Pituophis, Malpolon,* and *Naja* were taken in controlled environments.

Necroscopic analyses on colubroids have been carried out on seven adult specimens of *H. viridiflavus,* three adult specimens of *Dolichophis caspius* (Gmelin, 1789), five adult specimens of *N. helvetica,* one adult specimen of *Natrix natrix* (Laurenti, 1768), one adult specimen of *Natrix tessellata* (Laurenti, 1768), three adult specimens of *Z. longissimus,* two juvenile specimens of *Elaphe quatuorlineata* (Lacépède, 1789), one adult specimen of *Malpolon moilensis* (Reuss, 1834), one adult specimen of *Pantherophis guttatus* (Linnaeus, 1766), one adult specimen of *Heterodon nasicus* (Baird and Girard, 1852). Necroscopic analyses on elapids were carried out on one specimen of each of the following species: *Naja naja* (Linnaeus, 1758), *Naja atra* (Cantor, 1842), *Naja kaouthia* (Lesson, 1831), *Naja sputatrix* (Boie, 1827), *Naja pallida* (Boulenger, 1896), *Naja haje* (Linnaeus, 1758), and *Aspidelaps lubricus* (Laurenti, 1768). The various steps of anatomical and osteological inspection included a complete preparation and disarticulation of the cranial bones, which were preserved and catalogued at OPHIS. Osteological analyses on European viperids were carried out on the prepared skulls of one adult specimen of *Vipera ammodytes* (Linnaeus, 1758) and two adult specimens of *Vipera aspis* (Linnaeus, 1758). Anatomical analyses in living colubroid specimens raised in a controlled environment were performed at OPHIS on: *H. viridiflavus* (four adults and two subadults), *N. helvetica* (five adults and 23 juveniles), *Z. longissimus* (12 adults, two subadults, and 12 juveniles), *Zamenis scalaris* (Schinz, 1822) (two subadults), *Hemorrhois hippocrepis* (Linnaeus, 1758) (five adults), *M. moilensis* (four adults), *Malpolon insignitus* (Geoffroy Saint-Hilaire, 1827) (two adults), *Elaphe dione* (Pallas, 1773) (two adults, two subadults, and five juveniles), *Elaphe carinata* (Günther, 1864) (four adults and 17 juveniles), *Elaphe bimaculata* (Schmidt, 1925) (15 adults and 18 juveniles), *Elaphe quatuorlineata* (six adults and four juveniles), *Elaphe anomala* (Boulenger, 1916) (one adult), *Ortrhriophis taeniurus* (Cope, 1861) (one adult), *Oreocrypthophis porphyraceus* (Cantor, 1839) (two adults), *Gonyosoma boulengeri* (Mocquard, 1897) (two adults), *Thamnophis marcianus* (Baird and Girard, 1853) (one adult), *Pantherophis guttatus* (16 adults), and *Pituophis catenifer* (Blainville, 1835) (two adults) (Appendix I). Inspection of the external cephalic traits in living European snakes in the wild, belonging to the genera *Elaphe, Hierophis, Dolichophis, Zamenis, Coronella, Natrix,* and *Vipera,* was performed in 2024. Further inspections were possible after the

re-examination of photographic material previously collected portraying both European and extra-European taxa, which were investigated using photographic material present in the literature.

Results

Nomenclature

The term "*pits*" refers to circular, elliptical or longitudinal (slits) incisions present on the parietal shields characterized by well-defined margins. "*Fossae*" refers to small circumscribed depressions inside the shields, in which the surface of the scute remains intact, not showing visible incisions or perforations.

Parietal fossae.—These fossae are usually symmetrical and located at the center of the parietal shields, more or less distant from one another along the transverse axis crossing the medial contact of the shields. They can also appear, always symmetrically, in other cephalic shields (Figure 1A).

Parietal pits (De Hann 2003) or *major parietal pits*.—These pits are usually symmetrical and located at the center of the parietal shields. Equivalent to fossae, these pits can be more or less close together or spaced transversally (Figure 1B).

Conjoined parietal pits.—These major pits are connected to each other by an incision that crosses the parietal shields transversally (Figure 1C).

Parietal slits (De Haan 2003).—These longitudinal incisions occur in the same positions as major parietal pits (Figure 1D, left parietal shield).

Laterally expanded parietal pits.—This condition is the opposite of conjoined pits. Usually symmetrical, these major pits are connected to the lateral margins of the parietal shields by an incision on the surface of the shield, appearing similar to parietal slits (Figure 1D, right parietal shield).

Minor parietal pits.—This type of pit occurs randomly and generally in an asymmetrical manner occupying any position within the parietal shields (Figure 1E).

Medial posterior parietal pit.—This pit occurs singularly near or along the medial contact in the posterior portion of the parietal shields (Figure 1 F).

Colubridae

In adult and subadult individuals of *Hierophis viridiflavus,* a pair of fossae is visible in the parietal shields (Figure 2A). These fossae occur in the center of the shields, and manifest themselves in two laterally compressed depressions that can be more or less extended longitudinally. Other symmetrical depressions are present in the cephalic shields of this species, and can be more or less marked differently in each individual. A second pair of fossae is present in the parietal shields, but in the posterior portion, in contact with the dorsal scales or even involving them (Figure 2A). These fossae are much larger than the previous ones, and develop laterally. A third pair of fossae, with a triangular shape, is found in the posteromedial portion of the supraocular shields, near the contacts with the parietal and frontal shields.

In order to search for connections between the observed cephalic fossae and the underlying structures, the cranial bones of five previously prepared specimens were examined. These fossae occur in correspondence with features present in the dorsal surface of the bones that compose the braincase. The most evident feature is represented by two parietal foramina, which are found in the posterior half of the parietal bone. On the flat and smooth dorsal surface, the presence of two major adjacent foramina, aligned along the transverse axis dorsoventrally crossing the bone, is easily recognizable (Figure 2A). These foramina are located precisely beneath the central fossae present in the parietal shields. Additional foramina are present in the anterolateral portion of the same bone, near the frontal contact,

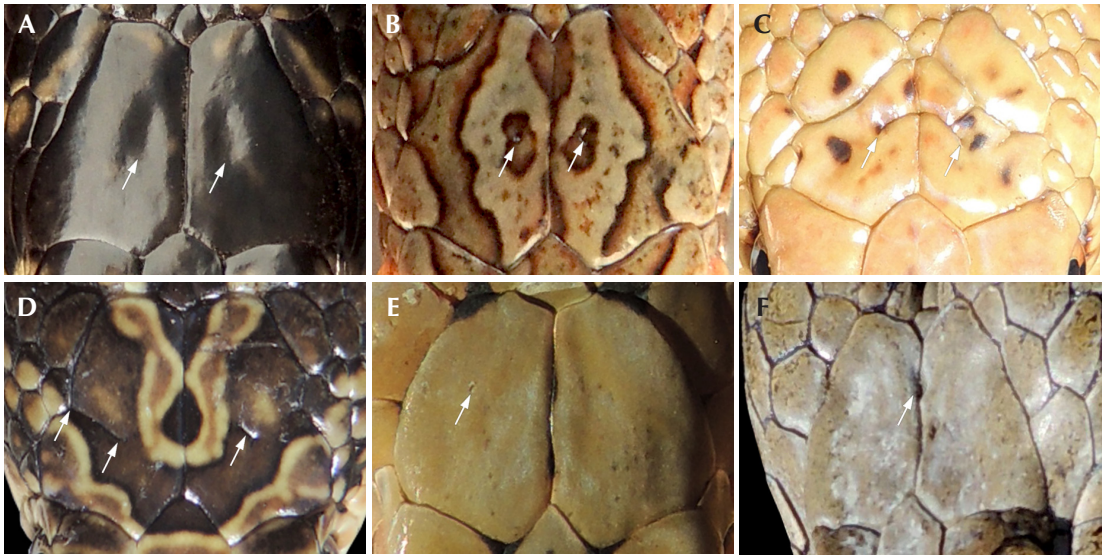

Figure 1. Details of the parietal shields of six colubroid snakes. (**A**), parietal fossae in *Hierophis viridiflavus;* (**B**), major parietal pits in *Elaphe dione;* (**C**); conjoined parietal pits in *Pituophis catenifer;* (**D**) laterally expanded parietal pit (double arrow) and parietal slit (single arrow) in *Hemorrhois hippocrepis;* (**E**), minor parietal pit in *Elaphe carinata;* (**F**), medial posterior parietal pit in *Natrix tessellata*.

where a sequence of large foramina occurs in the lateroposterior portion of these bones (Figure 2A). These features correspond to the fossae that occur in the supraocular shields. Additional foramina in the dorsum of the braincase are present in the supraoccipital bone, where two specular major foramina occur within the two specular fossae. Around these main foramina, smaller foramina may be found, arranged asymmetrically between the two supraoccipital fossae. This third group of foramina corresponds to the fossae present in the posterior portion of the parietal shields and the most anterior dorsal scales. Anomalies have been observed in one of the parietal bones of the prepared specimens, where the right foramen is not located within the respective fossa that should circumscribe it, but is positioned more anteriorly. The foramina in the braincase of the western whipsnake *Hierophis viridiflavus* have been mentioned in prior studies (Racca *et al.* 2020), as well as in other studies on related taxa such as *Dolichophis jugularis* (Linnaeus, 1758) (Sadeghi *et al.* 2014) and *Dolichophis schmidti* (Nikolsky, 1909) (asymmetric case with only one foramen in the left portion of the parietal bone, Rajabizadeh *et al.* 2021). All three pairs of fossae occurring on the shields of the western whipsnake are located in correspondence with neurovascular foramina present in the dorsum of the braincase. The posterior parietal and the supraoccipital fossae are located in correspondence with large foramina present in the cranial bones (situated in the parietal anterior fossae, parietal posterior fossae, and supraoccipital fossae), and develop on the surface of the parietal shields over a larger area than that of the main central parietal fossae, which instead corresponds to the flat plane of the parietal bone (Figure 2A). In the juveniles of *H. viridiflavus,* these cephalic fossae are not always visible. For example, in a young specimen subjected to necropsy these external features were not visible, but the cranial bones had all the foramina observed in adults.

Through the preparation of the samples, it was

possible to observe a further connection of these features between the various levels. The two main parietal foramina not only correspond dorsally to fossae and pits, but ventrally they correspond with the anteroposterior contact between the cerebral hemispheres and the optic lobes, more precisely above the epiphysis (Figure 2B).

A parallel investigation was carried out on a second species of colubrid sympatric with the previous *H. viridiflavus,* the Aesculapian snake *Zamenis longissimus.* Most of the individuals examined have smooth and homogeneous parietal shields, while the parietal bone may feature two medial foramina that are not always well defined, and are positioned close together toward the midline (Figure 3A). The presence of parietal pits and fossae was observed only in some individuals. One adult had symmetrical parietal pits (Figure 3B), and some hatchlings exhibited posterior parietal pits, also symmetrical, and almost in contact with the dorsal scales. In a subadult individual, the presence of a minor pit was found toward the posterior limit of the right parietal shield, and one was found on the left parietal shield (Figure 3C), while another individual, also an adult, showed two symmetrical parietal pits. The same individual had two small pits near the lateral margin of the right parietal shield, corresponding to the anterior portion of the second temporal scale. In one hatchling, the presence of cephalic pits was observed in the frontal shield. Further analyses have been carried out on the cranial bones of different specimens of the whipsnake *Dolichophis caspius,* which appear to be similar to those of *H. viridiflavus,* and on some specimens of the American colubrid *Pantherophis guttatus*, which instead has a condition similar to that of *Z. longissimus.*

Additional analyses were carried out on single individuals or small groups of specimens of different species of colubrids from the Old and New World. In some of these, the presence of major parietal pits was found, but in many different forms from those previously described. The two pits may occur close to each other, immediately after the median contact of the parietal shields, well distanced, or even joined transversally by a groove (Figure 1C). This pit model (conjoined pits) has been observed in *Gonyosoma boulengeri* and in *Pituophis catenifer,* where this feature seems to be common.

The sheds of the species that show these features in the head shields have been examined. As described by De Haan (2003), the pits are found in the exuviae, while the fossae do not always remain imprinted. Exuviae inspection can be used to determine the presence of cephalic pits in species where the background color and the dorsal patterns adorning the shields may be an obstacle in detecting them, as in the case of *Hemorrhois hippocrepis* (Figure 1D). In some species cephalic pits are also visible in hatchlings, as in the case of *Z. longissimus, Orthriophis taeniurus,* and *Telescopus semiannulatus* (Smith, 1849) (pers. obs.).

Natricidae

In this species the fossae on the parietal shields are very visible in hatchlings and juveniles (Figure 4A), and occur near the medial margin of the shields and always in correspondence with the parietal foramina. In this stage the shields are smooth and homogeneous, while in adults the parietal shields undergo deformations that seem to trace the silhouette of the parietal bone. These features associated with ageing can make the fossae difficult to distinguish (Figure 4B–D). The parietal bone of this species has adjacent fossae, where the parietal foramina are present, although in some cases only one of these fossae may host a visible foramen. In the specimens examined, the main parietal foramina may be both symmetrical and asymmetrical, in a number that varies from 1 to 4. The dorsal surface of the parietal bone is not smooth, and may present transverse rugosities. One exception is represented by an adult individual in which, during the preparation phase, the absence of fossae and pits in the shields (Figure 5A) in the epidermis (Figure 5B) and in the parietal bone (Figure 5C) was observed.

During the preparation of a large adult female,

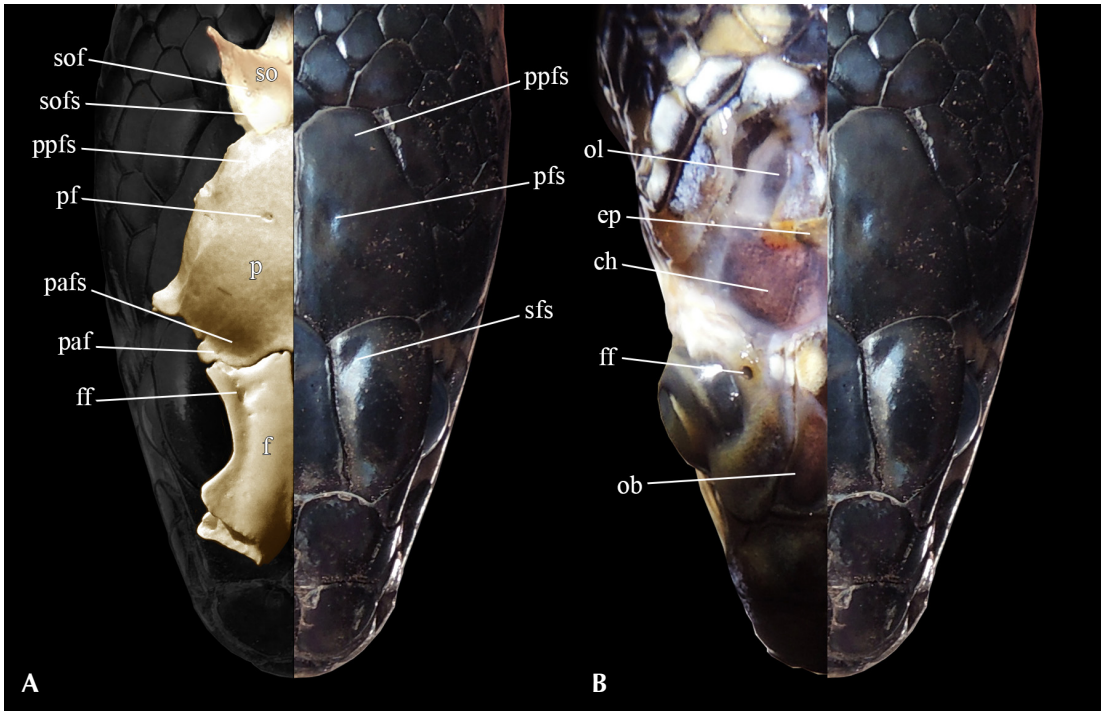

Figure 2. Details of cranial anatomy of *Hierophis viridiflavus*. (**A**), features in the cranial bones and their correspondence in the head shields; (**B**), features of the forebrain and midbrain and their correspondence in the head shields. Abbreviations: ch, cerebral hemisphere; ep, epiphysis; f, frontal; ff, frontal foramina; ob, olfactory bulb; ol, optic lobe; p, parietal; paf, parietal anterior foramina; pafs, parietal anterior fossa; pf, parietal foramen; pfs, parietal fossa; ppfs, parietal posterior fossa; sfs, supraocular fossa; so, supraoccipital; sof, supraoccipital foramina; sofs, supraoccipital fossa.

the presence of several parietal pits of different sizes were observed (Figure 6A). On the epidermis, below the cephalic shields, openings corresponding to the pits above are visible (Figure 6B). In the following preparation step, it was possible to observe how these openings pass through the dermal tissues, where the "hole size" in correspondence with the minor pits are similar to those present dorsally. The larger pits, arranged more laterally in the left shield, are located outside the parietal bone, corresponding to indentations that are present along the bone's left lateral margin (Figure 6 C), and which are absent on the opposite side of the bone (Figure 6A, C).

Parietal pits have also been observed in *Natrix tessellata.* In this species, pits are present adjacent or close to the medial contact of the two parietal shields, together with the occurrence of smaller minor pits. In several specimens, a further large cephalic pit can be noted, set more posteriorly from the central ones, and located in the medial contact of the parietal shields, here referred to as the "medial posterior parietal pit". The presence of corresponding foramina in the parietal bone of this species is documented in the study by Papežíková *et al*. (2024).

Together with the genus *Natrix,* cephalic fossae and pits have been observed in the genus *Thamnophis.* In several species of this genus the parietal pits are found in correspondence with a

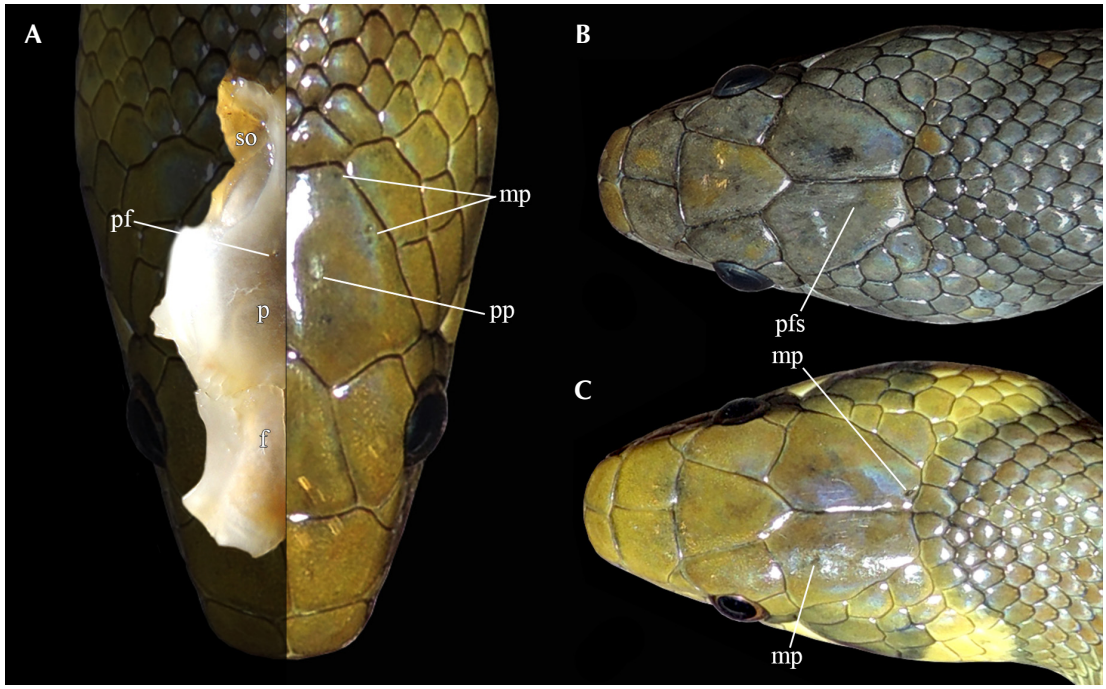

Figure 3. Cranial anatomy and details of cephalic pits and fossae in *Zamenis longissimus*. (**A**), features in the cranial bones and their correspondence in the head shields; (**B**), adult specimen of the *subgrisea* phenotype with parietal fossae; (**C**). adult specimen of the classic phenotype with cephalic minor pits. Abbreviations: f, frontal; m, minor pit; n, nasal; p, parietal; pf, parietal foramen; pfs, parietal fossa; so, supraoccipital.

dorsal pattern, as in the cases of *T. marcianus*, *T. radix* (Baird and Girard, 1853), *T. elegans* (Baird and Girard, 1853), *T. ordinoides* (Baird and Girard, 1852) and *T. sirtalis* (Linnaeus, 1758), where a light-colored circle bordered in black makes them almost unnoticeable at first glance (Mara 1994, Bernstein *et al.* 2024, pers. obs.). As in the case of colubrids, these are easily visible during shedding. The parietal pits appear to be similar to those present in the juveniles of *N. helvetica,* and more visible in adult specimens.

Psammophiidae

Additional inspections were performed in the psammophiids species of the genus *Malpolon* that were not investigated in the previous studies of the parietal pits (De Haan 2003, 2006, Cottone and Bauer 2011). In *Malpolon moilensis* major parietal pits, conjoined parietal pits, minor pits, and even the total absence of pits inside the cephalic shields were observed (Figure 7A). Other pits were identified in the supraocular shields, where they can also appear symmetrically arranged (Figure 7A). The main foramina and minor foramina occur in the parietal bone of this species, all distributed on the parietal plane. A linear series of foramina is always dorsally located along the longitudinal depression that occurs toward the lateral margin of the contact of the parietal bone with the frontals, piercing both cranial bones, and likely corresponding to the minor pits occurring in the supraocular shields. In *Malpolon insignitus* major parietal pits, parietal slits, laterally expanded parietal pits and minor pits were observed (Figure 7B, C). Additional cephalic pits were found in the frontal and supraocular

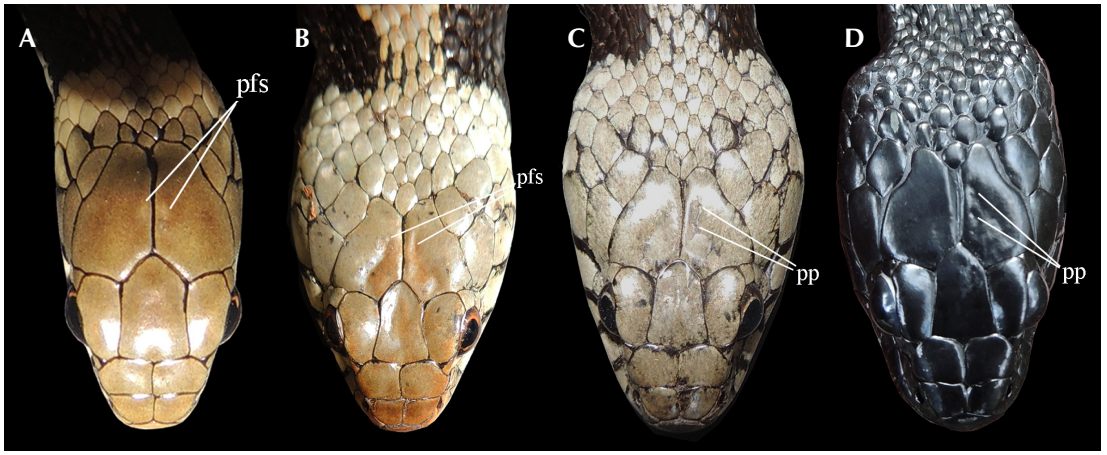

Figure 4. Parietal fossae and pits in *Natrix helvetica*. (**A**) juvenile specimen; (**B**) adult female; (**C**) axanthic adult female; (**D**) melanotic adult male. Abbreviations: pfs, parietal fossa; pp, parietal pit.

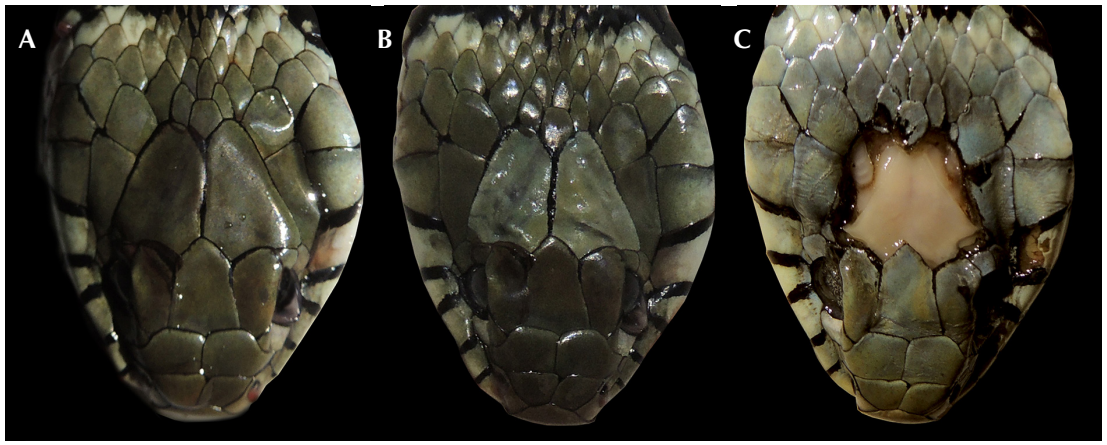

Figure 5. *Natrix helvetica* roadkilled adult specimen presenting no cephalic fossae or pits in the parietal shields (**A**), in the dermal tissues (**B**), and no foramina in the dorsal plane of the parietal bone (**C**).

shields (Figure 7B). Similar to *H. viridiflavus,* fossae are also present in the medioposterior portion of the supraocular and parietal shields.

Elapidae

Specimens belonging to the *Naja, Afronaja,* and *Uraeus* subgenera were analyzed, including *Naja naja, N. atra, N. kaouthia, N. sputatrix, N. pallida,* and *N. haje.* In all of these species the parietal pits are easily distinguishable, and can appear symmetrical, more or less transversally distanced depending on the species, or even asymmetrical. In *N. pallida,* for example, the parietal pits are positioned close together and consequently adjacent to the medial margin of the parietal shields (Figure 8A). A prepared specimen allowed confirmation of what was already observed in the specimens belonging to the other families: the continuity of a small canal that from the surface of the epidermis penetrates the underlying tissues

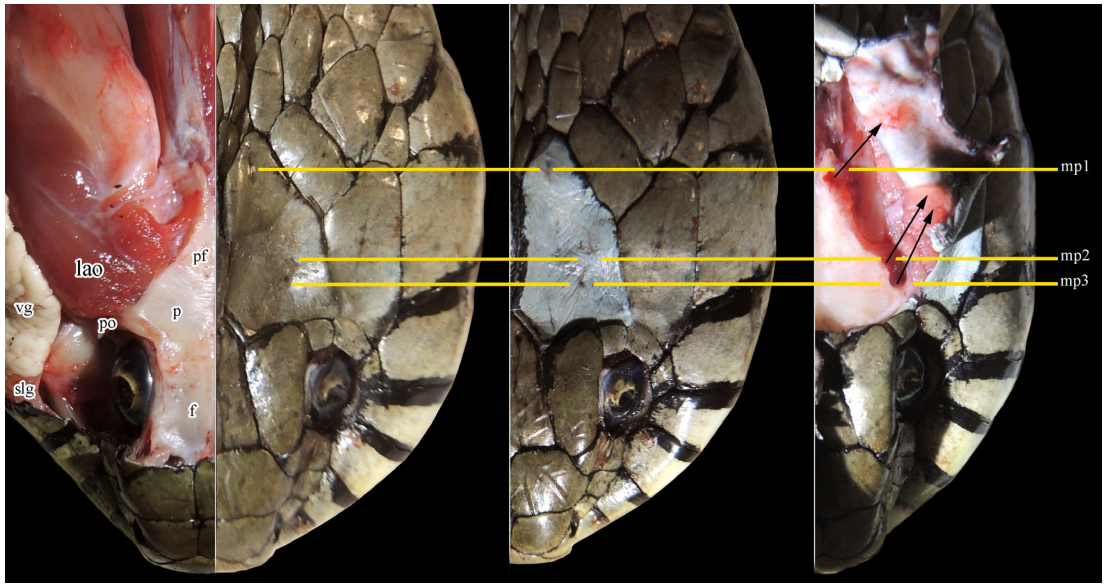

Figure 6. Cephalic pits in a *Natrix helvetica* roadkilled adult specimen. Yellow horizontal lines indicate the position of the minor pits in the different dissection steps. Black arrows indicate underlaying features in correspondence of the minor parietal pits. Abbreviations: f, frontal bone; lao, levator anguli oris; mp, minor pit; p, parietal bone; pf, parietal foramina; po, postorbital bone; slg, supralabial salivary gland; vg, venom gland.

until it enters the parietal foramen (Figure 8B). The same arrangement was observed in *N. sputatrix,* whose pits can be further apart compared to the previous species (Figure 7C). Here, too, in a prepared specimen it was possible to observe the vertical canalization of the cephalic pit, unique and asymmetrical in this individual (Figure 8D). In prepared specimens of the different species, the presence of a pair of main parietal foramina was found, where interspecific variation is present.

Viperidae

The cranial bones of the viperids *Vipera aspis* and *V. ammodytes* were analyzed. These species have a parietal bone with an irregular dorsal surface, unadorned by foramina, as well as the frontal bones, flatter than those of the other species analyzed, that feature a sagittal depression in the center of each bone. Using photographic material acquired in past and recent field observations, it seems that in some European viperids with large parietal shields, cephalic pits may be present as in the case of *Vipera berus* (Linnaeus, 1758) (Meier 2024, pers. obs.).

Parietal Bones

In the dorsal plane of the parietal bones of the specimens examined, the presence of neurovascular foramina was found in correspondence with the fossae and pits present in the parietal shields. There are generally two symmetrical main parietal foramina, but in some individuals these may occur in odd numbers, or be present only on one of the two halves of the bone. These foramina penetrate the entire dorsoventral thickness of the bone, opening ventrally. In colubrids these foramina are small and usually circumscribed by a fossa (Figure 9 A, B). Some irregularities may be present in the arrangement of these foramina. In a specimen of *H. viridiflavus* one of the two fossae that should contain the foramen was located anterioly to it (Figure 9A), and in a

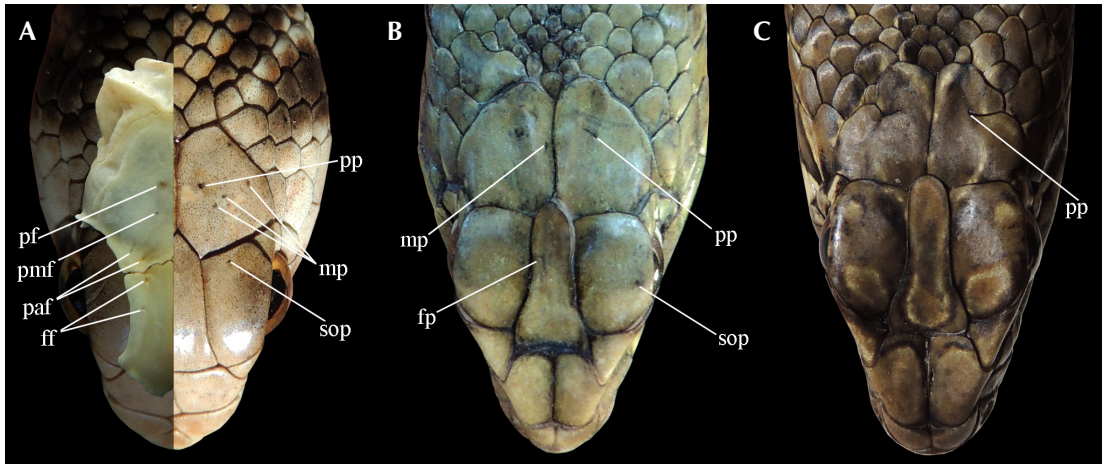

Figure 7. Cephalic pits in psammophiid snakes: (**A**) *Malpolon moilensis* adult male; (**B**) *Malpolon insignitus* adult male; (**C**) *Malpolon insignitus* adult female. Abbreviations: ff, frontal foramina; fp, frontal pit; mp, minor parietal pits; paf, parietal anterior foramina; pf, parietal foramen; pmf, parietal minor foramen; pp, parietal pits; sop, supraoccipital pit.

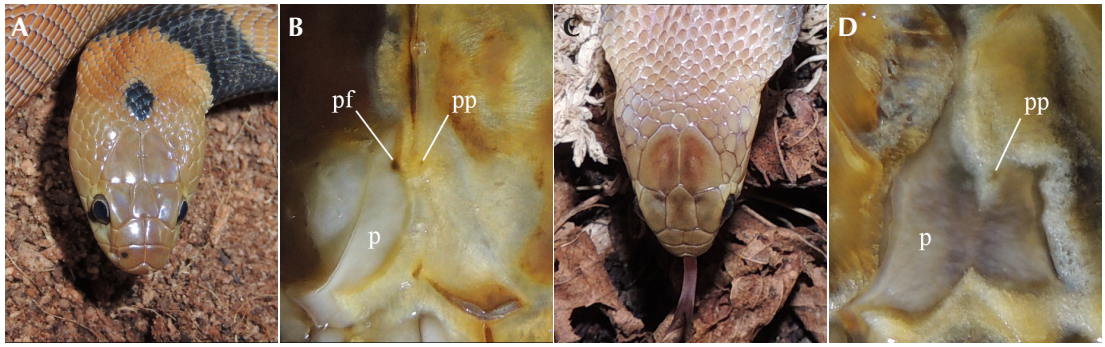

Figure 8. Parietal pits in cobras. (**A**) Subadult specimen of *Naja pallida* showing parietal pits; (**B**) preparation of the skull of an adult specimen of *Naja pallida*; (**C**) juvenile specimen of *Naja sputatrix*; (**D**) preparation of the skull of an adult specimen of *Naja sputatrix*. Abbreviations: p, parietal; pf, parietal foramen; pp, parietal pit.

specimen of *Z. longissimus* a disparity in the foramina in the two halves of the parietal plate was observed, where two more foramina occur posteriorly to the main foramen on the left side, which are absent on the right side (Figure 9B). Additional foramina are present close the anterolateral margins of the bone, in contact with the frontal bones. These foramina are present in almost all analyzed individuals. The lateral margins of the parietal plate of *N. helvetica* are straight and have an angle that gives the posterior half of the bone a dorsal shape of an equilateral triangle. The parietal foramina occur more posteriorly than in the analyzed colubrids, and can vary from one to two pairs, or be asymmetrical (Figure 6A; Figure 9C). The parietal plane of *N. tessellata* is similar in shape to that of *N. helvetica,* with a marked sagittal

depression running along the dorsal parietal plane. The two main foramina are well defined and the wide medioposterior foramen, which corresponds to the medial posterior parietal pit (Figure 1F), is situated at the posterior apex of the bone's dorsal plane. This foramen, as in the paired ones, entirely pierces the bone in a passage from the ventral to the dorsal surface. In elapids of the genus *Naja,* as in *N. helvetica,* the dorsal surface of the parietal bone has a more or less marked transverse sculpting, varying by species. In the species analyzed, there are generally tow main parietal foramina, but even in this family there may be cases of asymmetry (Figure 9E–J). The morphology of the parietal plane varies among the different species, but one thing they have in common is the size of the parietal foramina, which seems to be larger than that of the other species described previously. In the parietals of *V. aspis* and *V. ammodytes* foramina were not found, and the morphology of the parietal bone seems to have important variations between the two species of the same genus (Figure 9K, L).

Discussion

Cephalic pits are mainly divided into two categories: major pits and minor pits. The major pits occur in most cases in even numbers, are symmetrical, and specular at the center of the parietal shields, more or less close together, and in correspondence with the underlying larger parietal foramina. There are cases in which the major pits are asymmetrical, where a single pit is present in only one of the two parietal shields, or in which more than one pit is present in a shield, as occurs for the parietal foramina. The minor pits instead seem to manifest themselves randomly within the shields, and are usually odd and asymmetrical, yet also connected to underlying neurovascular foramina. Neither types of pits are constant within the analyzed species, and seem to affect only some individuals, even within the same bloodline or the same clutch, regardless of factors such as sex and age. The parietal fossae instead seem to be typical of certain species, such as *Hierophis viridiflavus* and *Natrix helvetica,* in which parietal pits can also appear. The fossae can be more or less defined and marked among the various individuals of the same species, and in the different growth phases. These, unlike the pits, always seem to occur in a symmetrical and specular arrangement. Fossae and major pits appear mainly in the same area inside the parietal shields, usually in the central portion of these. Depending on the species, they can be located more or less medially to the contact between the two shields. Fossae and major pits are found in correspondence with the main underlying parietal foramina, in correspondence with the contact between the cephalic hemispheres and the optic lobes. At the same time, in necropsied specimens that did not have parietal pits, no foramina were observed on the parietal plane.

Other fossae can affect the cephalic shields. The posterior ones, occur in the posterior ends of the parietal shields, toward the contact with the dorsal scales, and the anterior ones appear in the supraocular shields near the contacts with the parietals and frontals. These fossae, similarly to the ones described previously, correspond to different features present in the three underlying cranial bones: the posterior ones correspond to the fossae and foramina present in the articulation between the posterior portion of the parietal and the supraoccipital, and the anterior ones correspond to the lateroposterior foramina of the frontal bones and the anterolateral foramina of the parietal bone.

In addition to the species mentioned in the results, parietal pits and fossae are also present in other taxa that I have had the opportunity to observe personally and/or are depicted in literature. The list of species in which these traits occur is long, and includes several genera of the families Elapidae: *Dendroaspis, Hemachatus, Hydrophis, Naja,* and *Notechis* (Cundall and Irish 2008, Palci *et al.* 2019, pers. obs.); Atractaspidae: *Atractaspis* (O'Shea 2018); Micrelapidae: *Micrelapis* (O'Shea 2018); Psammophiidae: *Malpolon, Psammophis,*

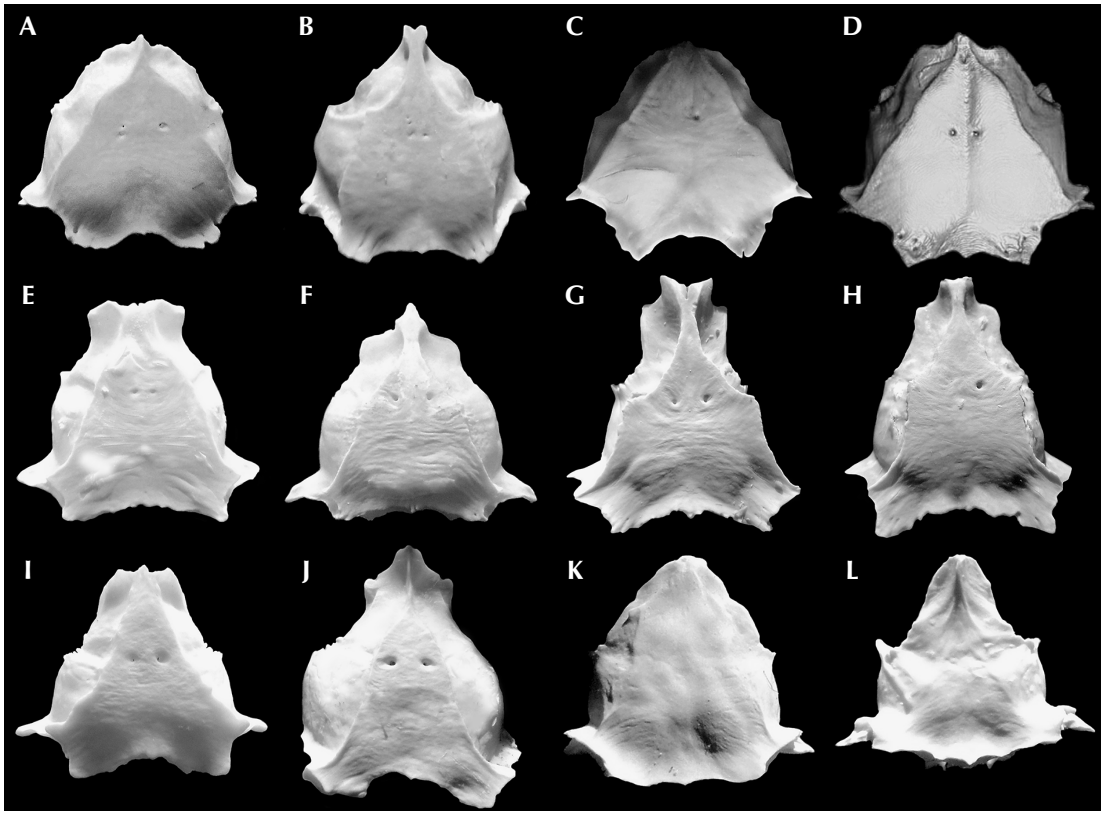

Figure 9. Parietal bones of snakes belonging to the caenophidian clade. Colubridae: (**A**) *Hierophis viridiflavus;* (**B**) *Zamenis longissimus.* Natricidae: (**C**) *Natrix helvtica;* (**D**) *Natrix tessellata;* Elapidae: (**E**) *Naja naja;* (**F**), *Naja atra;* (**G**), *Naja kaouthia;* (**H**), *Naja sputatrix;* (**I**) *Naja haje;* (**J**) *Naja pallida.* Viperidae: (**K**), *Vipera aspis;* (**L**), *Vipera ammodytes.* The parietal bone of *Natrix tessellata* is the specimen DJ4916 described in the study of Papežíková *et al.* (2024), used with permission.

Psammophylax, and *Rhamphiophis* (De Haan 2003, Cottone and Bauer 2011, pers. obs.); Colubridae: *Alsophis, Atretium, Boiga, Coluber, Coelognathus, Crotaphopeltis, Dasypeltis, Dolichophis, Drymarchon, Elaphe, Euprepiophis, Gonyosoma, Hebius, Hemorrhois, Hierophis, Platyceps, Philodryas, Pseudoficimia, Psomophis, Taeniophallus,* and *Zamenis* (Underwood 1967, Marais 2004, Miralles and Ineich 2006, Kreiner 2007, Schulz 2013, O'Shea 2018, pers. obs.); Natricidae: *Natrix, Helophis, Thamnophis, Tropidonophis,* and *Xenochrophis* (Malnate and Underwood 1988, pers. obs.); Viperidae: *Vipera* (Grano *et al.* 2017, Meier 2024, pers. obs.); Pareidae: *Asthenodipsas, Pareas,* and *Xylophis* (Loredo *et al.* 2013, Narayanan 2021, Poyarkov 2022); Xenodermidae: *Achalinus, Fimbrios,* and *Stoliczkia* (Ziegler *et al.* 2008, O'Shea 2018). In addition to photographic material, observations of these traits can be found in illustrations in technical texts, as in the case of *Elaphe carinata yonaguniensis* (Takara, 1962) illustrated by Schulz (1996).

In some cases, however, the identification of cephalic pits may not be easy because some species may have decorative elements in the

parietal portion of the head that resemble pairs of fossae and pits, i.e., *Spalerosophis diadema* (Schlegel, 1837), *Hemorrhois ravergieri* (Ménétries, 1832), *Thamnophis sirtalis,* or a single parietal "eye," i.e., *Thamnophis marcianus* (pers. obs.). Similar patterns are present in some viperids such as *Agkistrodon, Cerastes,* and *Montivipera* (pers. obs.; Figure 10). *Hierophis viridiflavus* may have such decorations, although in the juveniles of this species, the pattern occurring in the parietal shields can be highly variable (Paterna 2015). The difficulty in identifying possible pits also applies to those species that have a complex pattern on the cephalic scales, as in the case of *Elaphe dione* (Figure 1B).

As for the cephalic fossae and pits, numerous texts in the literature illustrate and describe the presence of the parietal foramina in different families of snakes: Elapidae (Scanlon and Lee 2003, Da Silva *et al*. 2018, Palci *et al*. 2019, Patterson *et al*. 2022, Ammresh 2023), Viperidae (Wagner *et al.* 2016, Integrated Sciences for Sustainable Human-Aqua Environment 2024), Atractaspididae (Strong *et al*. 2021), Pseudoxyrhophiidae (Das *et al*. 2024) and Cyclocoridae (Weinell *et al*. 2020), and in several colubroid species (Sadeghi *et al*. 2014, Klaczko *et al*. 2016, Qi *et al*. 2021, Rajabizadeh *et al*. 2021, Pandelis *et al*. 2023, Papežíková *et al*. 2024). Among these, the case of *Natrix tessellata* is extremely interesting. In a recent study by Papežíková *et al*. (2024) on the morphology of two European clades of this species, the specimens had major parietal pits and minor pits in the parietal shields. In the three-dimensional models of the parietal bone of several individuals, a pair of parietal foramina are always present, traversing the bone to open ventrally between the fossae covering the cerebral hemispheres and the optic lobes. Also in the parietal bone, one specimen had a medial foramen at the posterior end of the dorsal plane (Figure 9D) and additional foramina in the anterolateral extremities, close to the frontal contacts. The posterior medial foramen was present in another specimen, which had heavy sculpting consisting of numerous foramina in the right side of the parietal plane. This large foramen, like the paired foramina, opens in the ventral surface of the bone, but in the center of a sagittal canal separating the fossae covering the optic lobes. This foramen also appears to correspond to a pit on the surface as the other pits in the parietal shields. This trait observed in *N. tessellata* corresponds to the third type of pits described, the "medial posterior parietal pit" (Figures 1F and 9D). A similar posterior parietal medial foramen occurs in the aquatic elapid *Hydrophis cyanocinctus* (Daudin, 1803), and is crossed by a parietal blood vessel (Palci *et al*. 2019). This observation confirms that made in *N. helvetica,* where large blood vessels are connected to the minor parietal pits present in the lateral margin of the parietal bone. Palci *et al.* (2019) specify that "no nerve fibers exit the parietal foramen," and add that "such vascular structure draining directly to the brain is likely present in other sea snakes." The authors conclude that this trait is a further elaboration of the sea snakes' cutaneous respiratory anatomy, the most likely function of which is to provide the brain an additional supply of oxygen, thus possibly playing a role during long submersions. The golden sea snake *Aipysurus laevis* (Lacépède, 1804) has both paired foramina and a large posterior medial foramen in the parietal bone (Cundall and Irish 2008). In our case, the structure present in *N. tessellata* appears similar to that observed in marine elapids, considering that they are aquatic ophidians and share multiple adaptations to aquatic life (Paterna 2025).

Many of the cranial bones are perforated by neurovascular foramina, and pits and fossae present in the corresponding shields of these reptiles would appear to be surface expressions of these underlying foramina, which serves as a passage for nerves (Jackson and Doetsch 1977), blood vessels, and emissary veins (O' Donoghue 1921, Palci *et al*. 2019). Of extreme interest is the manifestation of parietal pits and fossae, which occur in correspondence with the paired parietal foramina and the epiphyses of snakes. Within Lepidosauria, many lizards have a parietal eye in the posterior cephalic region, a photosensory organ that occurs as part of the pineal complex in correspondence with a median parietal foramen (Eakin 1973). This structure,

widespread in Paleozoic and early Mesozoic taxa (Benoit *et al*. 2016), was lost in snakes (Labra *et al*. 2010), but developmental vestiges may remain as in the case of some snakes, birds, and mammals (Stebbins and Eakin 1958). Some caenophidian snakes have paired parietal foramina, which analogously are present in humans, where these function as passages for the emissary veins. In humans this feature is expressed only in some individuals (Van der Walt *et al*. 2023). Regarding the pineal complex, nearly all vertebrates present this structure, which is involved in the endocrine regulation of circadian and seasonal cycles. In snakes this structure has a role in courtship and mating (Jackson and Doetsch 1977, Quay 1979, Mendonca *et al*. 1996). It also has a role in thermoregulation and in the production of melatonin (Ralph *et al*. 1979, Lutterschmidt *et al*. 2003). The only structure in the pineal complex of snakes is the median epiphysis or pineal gland (Petit 1951, Tosini 1997), which is probably not photoreceptive as it is morphologically similar to the mammalian pineal gland (Quay *et al*. 1968, Kalsow *et al*. 1991). Stebbins and Eakin (1958) stated that "in snakes the pineal body is usually closely associated with the vascular paraphysis and dorsal sac and may itself be highly vascular, and in reptiles the posterior cerebral vein may be sinus-like and is closely associated with the epiphysis." The parietal pits and fossae, which correspond to these structures, could thus be, or were, linked to these structures. Reichenbach-Klinke and Elkan (1965) describe a specimen of *Natrix natrix* that has two symmetrical lateral and one medial parietal groove. Histological analyses revealed an extreme attenuation in the dorsal plane of the parietal bone corresponding to the two lateral grooves. The authors state that the appearance of accessory parietal organs is extraordinarily common in reptiles, adding statements that note the resemblence to the paired foramina, pits, and fossae in the current study: "attempts at lens and retina formation can clearly be seen in these organs which, in some cases, are paired and often connected with the mesencephalon by a thin strand of optic nerve. There is always a gap in the bony skull dorsal to the parietal eye, matched in some cases by a pitted scale or a pair of pitted scales on the surface." In-depth analyses are needed to determine whether these traits are analogous in all species in which they occur, or wether these may be vestigial traits, traits exclusively linked to the vascular system, or traits involving the neurosensory system.

Figure 10. Juvenile leucistic female of *Agkistrodon contortrix,* found in Montgomery Country, Texas, in 2019 (photo by Daniel Jarvis). Note how the paired parietal dots are the only trait showing black pigmentation beside the eyes.

Conclusions

Cephalic pits and fossae appear to be widespread in the superfamilies Colubroidea and Elapoidea. These features also occur in the more basal families Pareoidea and Xenodermoidea, which indicates that these pits probably include a

larger group of ophidians, the Colubroides. As shown by the observations, it is not certain that the phenomenon involves all genera or all species included in this macrogroup because these traits could have been totally lost during evolution.

Observations of *in vivo* specimens and the anatomical and necroscopic investigations carried out on colubrids, natricids, psammophiids, and elapids highlight that the presence of cephalic pits in the parietal shields of these ophidians can be of different types. The most obvious are the "major" parietal pits and fossae, almost always symmetrical, linked to the paired parietal foramina, which in turn occur in correspondence with the epiphysis at the center of the contact between the optic lobes and the cerebral hemispheres. Others are minor pits, which can occur in asymmetrical positions and in a random number within the cephalic shields, which usually correspond to foramina and fossae occurring in the underlying cranial bones. In some of the cases examined, the presence/visibility of these can also vary based on age, becoming more evident/defined at adult size and age.

A peculiarity observed is that although the main cephalic fossae and pits are "connected" to the parietal foramina through the epidermis and dermis, the presence and number of these features in the bones does not represent a constant in the species where they are expressed. In some specimens the presence of blood vessels occured in correspondence with some pits and cranial features. Regarding the pits occurring in correspondence with the paired parietal foramina, micro-CT scans and histology sections will be necessary to define their nature and/or to define whether any differences are present in the groups in which such traits appear. This would further verify the hypothesis of the formation of parietal organs, and/or their possible functionality in the vascular and/or neuro-sensory field. In addition, more targeted studies involving larger sample sizes, focused on certain species or genera may lead to a better statistical understanding of the phenomenon. At the moment we can affirm that cephalic fossae and pits are sporadic surface manifestations corresponding to neurovascular foramina present in the cranial bones of some individuals belonging to a given species. Following the identification of such traits in a larger number of species, future research should lead to the recognition of fossae and pits in numerous other genera and taxa.

Acknowledgments

I would like to thank all the cited authors whose works have been an important inspiration for this study, the friends who donated to OPHIS part of the specimens used in the anatomical and osteological analyses, and Daniel Jablonski for giving me permission to use the picture obtained with micro-CT of the specimen DJ4916. I thank two anonymous reviewers for their opinions and comments on the manuscript, and Janalee Caldwell for the revision of the text.

References

Acosta-Galvis, A. G. 2000. Ranas, salamandras y caecilias (Tetrapoda: Amphibia) de Colombia. *Biota Colombiana 1:* 289–329.

Ammresh, E. S., V. A. Thomson, M. S. Y. Lee, N. Dunstan, L. Allen, J. Abraham, and A. Palci. 2023. Island tiger snakes (*Notechis scutatus*) gain a 'head start' in life: wow both phenotypic plasticity and evolution underlie skull shape differences. *Evolutionary Biology 50:* 111–126.

Benoit, J., F. Abdala, P. R. Manger, and B. S. Rubidge. 2016. The sixth sense in mammalians forerunners: variability of the parietal foramen and the evolution of the pineal eye in South African Permo-Triassic eutheriodont therapsids. *Acta Palaeontologica Polonica 61:* 777–789.

Bernstein, J. M., M. Clarkson, J. A. Fantuzzi, D. Jablonski, M. J. Jowers, G. Köhler, Z. J. Loughman, J.-J. Mao, K. Mebert, N. Rusli, X. Santos, and M. Segall. 2024. *Aquatic Snakes: Diversity and Natural History*. Will County. John C. Murphy Natural History and Herpetological Conservation International. 729 pp.

Cottone, A. M. and A. M. Bauer. 2011. Variably occurring parietal pits in psammophiid snakes

(Squamata: Serpentes): convergent expression of ancestral skin traits? *Herpetology Notes 4:* 381–385.

Cundall, D. and F. J. Irish. 2008. The snake skull. Pp. 349–692 in C. Gans, A. S. Gaunt, and K. Adler (eds.), *Biology of the Reptilia, vol. 20, Morphology H: The skull of Lepidosauria*. Ithaca. Society for the Study of Amphibians and Reptiles.

Das, S., E. Greenbaum, J. Brecko, O. S.G. Pauwels, S. Ruane, S. Pirro, and J. Merilä. 2024. Phylogenomics of *Psammodynastes* and *Buhoma* (Elapoidea: Serpentes), with the description of a new Asian snake family. *Scientifc Reports 14:* 9489.

Da Silva, F. O., A.-C. Fabre, Y. Savriama, J. Ollonen, K. Mahlow, A. Herrel, J. Müller, and N. Di-Poï. 2018. The ecological origins of snakes as revealed by skull evolution. *Nature Communications 9:* 376.

De Haan, C. C. 2003. Sense-organ-like parietal pits found in Psammophiini (Serpentes, Colubridae). *Comptes Rendus Biologies 326:* 288–293.

De Haan, C. C. 2006. Sense-organ-like parietal pits, sporadically occurring, found in Psammophiinae (Serpentes: Colubridae). Pp. 213–214 *in* M. Vences, J. Köhler, T. Ziegler, and W. Böhme (ed.), *Herpetologia Bonensis II, Proceedings of the 13th Congress of the Societas Europaea Herpetologica*. Koenig, Bonn. Forschungsmuseum.

Eakin, R. M. 1973. *The Third Eye*. Berkely. University of California Press. 157 pp.

Grano, M., G. Meier, and C. Cattaneo. 2017. *Vipere Italiane*. Aicurzio. Gruppo Editoriale Castel Nergrino. 198 pp.

Integrated Sciences for Sustainable Human-Aqua Environment "Aqua Science". 2024. *Gloydius blomhoffii* 3D model created using CT scans. Electronic Database accessible at https://sketchfab.com/3d-models/ct-scan-japanese-pit-viper-d2b1c022759c44adae280231902c6e9f/. Ministry of Education, Culture, Sports, Science and Technology's Grant-in-Aid for Scientific Research (A) for FY2021-2025, "Creating Water Symbiosis Studies through Dynamic Analysis of Water Circulation Systems as a Field of Fluctuations", Kumamoto, Japan. Captured on 21 January 25.

Jackson, M. K. and G. S. Doetsch. 1977. Functional properties of nerve fibers innervating cutaneous corpuscles within cephalic skin of the Texas rat snake. *Experimental Neurology 56:* 63–77.

Kalsow, C. M., S. S. Greenhouse, W. Gern, G. Adamus, P. A. Margrave, L. S. Lang, and L. A. Donoso. 1991. Photoreceptor cell specific proteins of snake pineal. *Journal of Pineal Research 11:* 49–56.

Klaczko, J., E. Sherratt, and E. Z. F. Setz. 2016. Are diet preferences associated to skulls shape diversification in Xenodontine snakes? *PLoS ONE 11:* e0148375.

Kreiner, G. 2007. *The Snakes of Europe*. Frankfurt am Main. Edition Chimaira. 317 pp.

Labra, A., K. L. Voje, H. Seligmann, and T. F. Hansen. 2010. Evolution of the third eye: a phylogenetic comparative study of parietal-eye size as an ecophysiological adaptation in *Liolaemus* lizards. *Biological Journal of the Linnean Society 101:* 870–883.

Loredo, A. I., P. L. Wood Jr., E. S. H. Quah, S. Anuar, L. F. Greer, N. Ahmad, and L. L. Grismer. 2013. Cryptic speciation within *Asthenodipsas vertebralis* (Boulenger, 1900) (Squamata: Pareatidae), the description of a new species from Peninsular Malaysia, and the resurrection of *A. tropidonotus* (Lidth de Jude, 1923) from Sumatra: an integrative taxonomic analysis. *Zootaxa 3664:* 505–524.

Lutterschmidt, D. I., W. I. Lutterschmidt, and V. H. Hutchison. 2003. Melatonin and thermoregulation in ectothermic vertebrates: a review. *Canadian Journal of Zoology 81:* 1–13.

Malnate, E.V. and G. Underwood. 1988. Australasian natricine snakes of the genus *Tropidonophis*. *Proceedings of the Academy of Natural Sciences of Philadelphia 140:* 59–201.

Mara, W. P. 1994. *Garter and Ribbon Snakes*. Neptune City. T. F. H. Publications Inc. 64 pp.

Marais, J. 2004. *A Complete Guide to the Snakes of Southern Africa.* Cape Town. Struik Nature. 360 pp.

Meier, G. 2024. *Alla Scoperta Dei Rettili Del Ticino*. Pregassona-Lugano. Fontana Edizioni. 208 pp.

Mendonca, M. T., A. J. Tousignant, and D. Crews. 1996. Courting and non-courting male garter snakes (*Thamnophis sirtalis parietalis*): plasma melatonin and the effects of pinealectomy. *Hormones and Behavior 30:* 176–185.

Miralles, A. and I. Ineich. 2006. Presence of gular and parietal pits in *Atretium schistosum* (Serpentes, Colubridae), a singular trait not exclusive to psammophine snakes. *Comptes Rendus Biologies 329:* 180–184.

Narayanan, S., P. P. Mohapatra, A. Balan, S. Das, and D. J. Gower. 2021. A new species of *Xylophis* Beddome, 1878 (Serpentes: Pareidae) from the southern Western Ghats of India. *Vertebrate Zoology 71:* 219–230.

O'Donoghue, C. H. 1921. The circulatory system of the common grass-snake (*Tropidonotus natrix*). *Proceedings*

of the Zoological Society of London 82: 612–645.

O'Shea, M. 2018. *The Book of Snakes: A Life-Size Guide to Six Hundred Species from Around the World*. Chicago. University of Chicago Press. 656 pp.

Palci, A., R. S. Seymour, C. Van Nguyen, M. N. Hutchinson, M. S. Y. Lee, and K. L. Sanders. 2019. Novel vascular plexus in the head of a sea snake (Elapidae, Hydrophiinae) revealed by high resolution computed tomography and histology. *Royal Society Open Science 6:* 191099.

Pandelis, G. G., M. C. Grundler, and D. L. Rabosky. 2023. Ecological correlates of cranial evolution in the megaradiation of dipsadine snakes. *BMC Ecology and Evolution 23:* 1–20.

Papežíková, S., M. Ivanov, P. Papežík, A. Javorčík, K. Mebert, and D. Jablonski. 2024. Comparing morphology and cranial osteology in two divergent clades of dice snakes from continental Europe (Squamata: Natricidae: *Natrix tessellata*). *Vertebrate Zoology 74:* 511–531.

Paterna, A. 2015. Morphological traits of hatchlings of the Western Whip snake *Hierophis viridifavus* (Lacépède, 1789) from a central Italian population. *Russian Journal of Herpetology 22:* 179–187.

Paterna, A. 2023. The role of modified teeth in the function of prolonged bites in *Hierophis viridiflavus* (Serpentes: Colubridae). *Phyllomedusa 22:* 121–130.

Paterna, A. 2024. Analyzing and comparing the buccal anatomy of European colubroid snakes: a reassessment of dentition models. *Phyllomedusa 23:* 111–124.

Paterna, A. 2025. Scale sensilla in the snakes of the genus *Natrix,* and in the Old and New World natricids. *Taxonomy 5:* 34.

Paterna, A. and M. Grano. 2024. Morphology of the maxillary bones in the Caspian whipsnake *Dolichophis caspius* (Serpentes: Colubridae) supports the opisthoglyphous model within western palearctic whipsnakes. *Biodiversity Journal 15:* 693–700.

Patterson, M., A. K. Wolfe, P. A. Fleming, P. W. Bateman, M. L. Martin, E. Sherratt, and N. M. Warburton. 2022. Ontogenetic shift in diet of a large elapid snake is facilitated by allometric change in skull morphology. *Evolutionary Ecology 36:* 489–509.

Petit, A. 1971. L'épiphyse d'un serpent: *Tropidonotus natrix* L. *Zeitschrift für Zellforschung und Mikroskopische Anatomie 120:* 94–119.

Poyarkov, N. A., T. V. Nguyen, P. Pawangkhanant, P. V. Yushchenko, P. Brakels, L. H. Nguyen, H. N. Nguyen, C. Suwannapoom, N. Orlov and G. Vogel. 2022. An integrative taxonomic revision of slug-eating snakes (Squamata: Pareidae: Pareineae) reveals unprecedented diversity in Indochina. *PeerJ 10:* e12713

Quay, W. B., J. Ariëns Kappers, and J. F. Jongkind. 1968. Innervation and fluorescence histochemistry of monoamines in the pineal organ of a snake (*Natrix natrix*). *Journal of Neural Transmission 31:* 11–25.

Quay, W. B. 1979. The parietal eye–pineal complex. Pp. 245–406 *in* C. Gans and R. G. Northcutt (eds*.), Biology of Reptilia. A*. London. Academic Press.

Qi, S., J-S. Shi, Y-B. Ma, Y-F. Gao, S-H. Bu, L. L. Grismer, P-P. Li, and Y-Y. Wang. 2021. A sheep in wolf's clothing: *Elaphe xiphodonta* sp. nov. (Squamata, Colubridae) and its possible mimicry to *Protobothrops jerdonii. ZooKeys 1048:* 23–47.

Racca, L., A. Villa, L. C. M. Wencker, M. Camaiti, H. A. Blain, and M. Delfno M. 2020. Skull osteology and osteological phylogeny of the Western Whip snake *Hierophis viridifavus* (Squamata, Colubridae). *Journal of Morphology 281:* 808–836.

Rajabizadeh, M., D. Adriaens, B. De Kegel, A. Avci, Ç. Ilgaz, and A. Herrel. 2021. Body size miniaturization in a lineage of colubrid snakes: Implications for cranial anatomy. *Journal of Anatomy 238:* 131–145.

Ralph, C. L., B. T. Firth, and J. S. Turner. 1979. The role of the pineal body in ectotherm thermoregulation. *American Zoologist 19:* 273–293.

Reichenbach-Klinke, H. and E. Elkan. 1965. *The Principal Diseases of Lower Vertebrates.* London and New York. Academic Press. 612 pp.

Sadeghi, N., S. S. Hosseinian Yousefkhani, N. Rastegar-Pouyani, and M. Rajabizadeh. 2014. Skull comparison between *Eirenis collaris* and *Dolichophis jugularis* (Serpentes: Colubridae) from Iran. *Iranian Journal of Animal Biosystematics 10:* 87–100.

Scanlon, J. D. and M. S. Y. Lee. 2003. Phylogeny of Australasian venomous snakes (Colubroidea, Elapidae, Hydrophiinae) based on phenotypic and molecular evidence. *Zoologica Scripta 33:* 335–366.

Schulz, K. D. 1996. *A Monograph of the Colubrid Snakes of the Genus* Elaphe *Fitzinger*. Havlikuv Brod. Koeltz Scientific Books. 439 pp.

Schulz, K. D. 2013. *Old World Ratsnakes. A Collection of Papers.* Berg. Bushmaster Publications. 432 pp.

Stebbins, R. C. and R. M. Eakin. 1958. The role of the 'third eye' in reptilian behavior. *American Museum Novitates 1879:* 1–39.

Strong, C. R. C., A. Palci, and M. W. Caldwell. 2021. Insights into skull evolution in fossorial snakes, as revealed by the cranial morphology of *Atractaspis irregularis* (Serpentes: Colubroidea). *Journal of Anatomy 238:* 146–172.

Tosini, G. 1997. The pineal complex of reptiles: physiological and behavioral roles. *Ethology Ecology and Evolution 9:* 313–333.

Underwood, G. 1967. A contribution to the classification of snakes. *Trustees of the Natural History Museum, London 653:* 1–179.

Van der Walt, S., N. Hammer, and L. Prigge. 2023. Comparison between the parietal foramina observed in samples of African and European population groups. *International Journal of Morphology 41:* 634–639.

Wagner, P., A. Tiutenko, G. Mazepa, L. J. Borkin, and E. Simonov. 2016. Alai! Alai! – A new species of the *Gloydius halys* (Pallas, 1776) complex (Viperidae, Crotalinae), including a brief review of the complex. *Amphibia-Reptilia 37:* 15–31.

Weinell, J. L., D. J. Paluh, C. D. Siler, and R. M. Brown. 2020. A new, miniaturized genus and species of snake (Cyclocoridae) from the Philippines. *Copeia 108: 907–923*.

Ziegler, T., P. David, A. Miralles, D. van Kien, and N. Q. Truong. 2008. A new species of the snake genus *Fimbrios* from Phong Nha-Ke Bang National Park, Truong Son, central Vietnam (Squamata: Xenodermatidae). *Zootaxa 1729:* 37–48.

Editor: Jaime Bertoluci

Appendix I. *List of preserved and live specimens examined in the current study. Each entry indicates the family to which the specimens belong, the species, the number of individuals analyzed, and the type of analyses performed: "external inspection" refers to inspection of the specimen's cephalic features; "anatomical" refers to a thorough analysis involving dissection and anatomical examination of the soft tissues; "osteological" indicates that the specimen was further prepared for osteological examination of the cranial bones. In the* "in vivo" *specimens only external inspection was performed.*

		Preserved specimens		
Family	**Species**	**Units**	**Stage**	**Analyses**
Colubridae	*D. caspius*	3	adults	ex. inspection, anatomical, osteological
	E. quatuorlineata	2	juveniles	ex. inspection, anatomical, osteological
	H. viridiflavus	7	adults	ex. inspection, anatomical, osteological
	P. guttatus	1	adults	ex. inspection, anatomical, osteological
	Z. longissimus	3	adults	ex. inspection, anatomical, osteological
Dipsadidae	*H. nasicus*	1	adults	ex. inspection, anatomical, osteological
Natricidae	*N. helvetica*	5	adults	ex. inspection, anatomical, osteological
	N. natrix	1	adults	ex. inspection, anatomical, osteological
	N. tessellata	1	adults	ex. inspection, anatomical, osteological
Psammophiidae	*M. moilensis*	1	adults	ex. inspection, anatomical, osteological
Elapidae	*A. lubricus*	1	adults	ex. inspection, osteological
	N. atra	1	adults	ex. inspection, anatomical, osteological
	N. haje	1	adults	ex. inspection, anatomical, osteological
	N. kaouthia	1	adults	ex. inspection, anatomical, osteological
	N. naja	1	adults	ex. inspection, anatomical, osteological
	N. pallida	1	adults	ex. inspection, anatomical, osteological
	N. sputatrix	1	adults	ex. inspection, anatomical, osteological
Viperidae	*V. ammodytes*	1	adult	ex. inspection, osteological
	V. aspis	1	adult	ex. inspection, osteological

Appendix I. *Continued.*

		***In vivo* specimens**	
Family	**Species**	**Units**	**Analyses**
Colubridae	*E. anomala*	1	1 adult
	E. bimaculata	33	15 adults, 18 juveniles
	E. carinata	21	4 adults, 17 juveniles
	E. dione	9	2 adults, 2 subadults, 5 juveniles
	E. quatuorlineata	10	6 adults, 4 juveniles
	G. boulengeri	2	2 adults
	H. hippocrepis	5	5 adults
	H. viridiflavus	6	4 adults, 2 subadults
	O. porhyraceus	2	2 adults
	O. taeniurus	1	1 adult
	P. guttatus	16	16 adults
	P. catenifer	2	2 adults
	Z. longissimus	26	12 adults, 2 subadults, 12 juveniles
	Z. scalaris	2	2 subadults
Natricidae	*N. helvetica*	28	5 adults, 23 juveniles
	T. marcianus	1	1 adult
Psammophiidae	*M. insignitus*	2	2 adults
	M. moilensis	4	4 adults

Phyllomedusa 24(2):223–254, 2025

ISSN 1519-1397 (print) / ISSN 2316-9079 (online)
doi: http://dx.doi.org/10.11606/issn.2316-9079.v24i2p223-254

A partial taxonomic revision of *Atelopus* (Anura: Bufonidae) from the central and eastern Andes of Colombia

Amadeus Plewnia,[1,2] Pedro Henrique dos Santos Dias,[3] Marvin Anganoy-Criollo,[4] Khristian Venegas-Valencia,[5] Kamil Szepanski,[6] Christopher Heine,[1] Philipp Böning,[1,7] Juan P. Ramírez,[8] and Stefan Lötters[1,2]

[1] Trier University, Biogeography Department. 54286 Trier, Germany. E-mail: amadeus.plewnia@t-online.de.

[2] Habitats Conservation. 6990 Hostert, Luxembourg.

[3] Senckenberg Biodiversity and Climate Research Centre (SBiK-F). 60325 Frankfurt am Main, Germany.

[4] Universidade de São Paulo, Instituto de Biociências, Departamento de Zoologia. 05508-090, São Paulo, SP, Brazil.

[5] Instituto de Investigación de Recursos Biológicos Alexander von Humboldt. Villa de Leyva, Colombia.

[6] Hachtel CTmatter GmbH. 73431 Aalen, Germany.

[7] Trier University, Geobotany Department. 54286 Trier, Germany.

[8] Universidad Nacional Autónoma de México, Instituto de Ciencias de la Atmósfera y Cambio Climático. 04510, Ciudad de México, Mexico.

Abstract

A partial taxonomic revision of *Atelopus* (Anura: Bufonidae) from the central and eastern Andes of Colombia. Harlequin toads, genus *Atelopus,* are a species-rich group of Neotropical anurans. Unparalleled declines and extinctions have hampered a thorough understanding of *Atelopus* systematics with numerous species only known from few specimens and a single or few localities. Major knowledge gaps particularly remain in the Cordillera Central and Cordillera Oriental of the Colombian Andes. In the central Andes, the names *Atelopus angelito, A. ebenoides,* and *A. eusebianus* have caused taxonomic confusion because populations can show vast plasticity, and populations assigned to these names were thought to occur in sympatry and parapatry. The virtual disappearance of all populations has prevented an integrative taxonomic assessment and rendered molecular approaches highly challenging. Based on adult and larval morphology, we propose that these populations correspond to a single polymorphic taxon and establish *A. ebenoides* as the senior synonym. In contrast, a form from the northern Cordillera Oriental has been considered a subspecies of the latter, *A. ebenoides marinkellei.* These geographically highly distant populations differ in morphology, particularly in tadpole characters and do not appear to represent conspecifics. We therefore elevate the form *marinkellei* to species rank and provide detailed morphological redescriptions and tadpole accounts for both *A. ebenoides* and *A. marinkellei.*

Keywords: *Atelopus ebenoides, Atelopus marinkellei,* Conservation, Harlequin Toads, Morphology, Synonymy, Tadpoles.

Received 26 February 2025
Accepted 12 September 2025
Distributed December 2025

Resumen

Revisión taxonómica parcial de *Atelopus* (Anura: Bufonidae) de los Andes centrales y orientales de Colombia. Los sapos arlequines, del género *Atelopus*, conforman un grupo de anuros neotropicales rico en especies. Declives y extinciones sin precedentes han dificultado una comprensión profunda de la sistemática de *Atelopus*, ya que numerosas especies se conocen sólo de unos pocos especímenes y una o pocas localidades. En particular, persisten importantes vacíos de conocimiento sobre las especies de la Cordillera Central y la Cordillera Oriental de los Andes colombianos. En los Andes centrales de Colombia, los nombres *Atelopus angelito*, *A. ebenoides* y *A. eusebianus* han causado confusión taxonómica, ya que las poblaciones pueden mostrar una gran variabilidad, además de que se considera que ocurrían en simpatría y parapatría. La desaparición virtual de todas las poblaciones ha impedido hasta ahora una evaluación taxonómica integrativa, resultando en que implementar enfoques moleculares sea altamente desafiante. Utilizando la morfología de adultos y larvas, sugerimos que estas poblaciones corresponden a un único taxón polimórfico y establecemos a *A. ebenoides* como el sinónimo principal. En contraste, una forma del norte de la Cordillera Oriental ha sido previamente considerada como una subespecie de *A. ebenoides*, *A. ebenoides marinkellei*. Sin embargo, estas poblaciones geográficamente muy distantes difieren en morfología, particularmente en caracteres del renacuajo y no parecen ser el mismo taxón. Por tanto, elevamos la forma *A. e. marinkellei* al rango de especie y proporcionamos redescripciones morfológicas detalladas y descripciones de renacuajos tanto para *A. ebenoides* como para *A. marinkellei.*

Palabras clave: *Atelopus ebenoides*, *Atelopus marinkellei*, Conservación, Morfología, Renacuajos, Sapos arlquines, Sinonimia.

Resumo

Revisão taxonômica parcial de *Atelopus* (Anura: Bufonidae) dos Andes centrais e orientais da Colômbia. Sapos-arlequins, gênero *Atelopus*, constituem um grupo diverso de anuros neotropicais. Declínios populacionais sem precedentes e extinções dificultaram uma compreensão abrangente da sistemática do grupo, resultando em diversas espécies conhecidas apenas por poucos espécimes e localidades restritas. Lacunas significativas de conhecimento persistem especialmente na Cordilheira Central e na Cordilheira Oriental dos Andes colombianos. Nos Andes centrais, os nomes *Atelopus angelito*, *A. ebenoides* e *A. eusebianus* geraram confusão taxonômica, uma vez que as populações apresentam grande plasticidade, além de populações atribuídas a esses nomes terem sido consideradas como simpátricas ou parapátricas. O desaparecimento de todas essas populações têm impedido uma avaliação taxonômica integrativa e tornado abordagens moleculares altamente desafiadoras. Com base na morfologia de adultos e larvas, sugerimos que essas populações correspondem a um único táxon polimórfico, estabelecendo *A. ebenoides* como o sinônimo sênior. Em contraste, indivíduos da porção norte da Cordilheira Oriental têm sido considerados uma subespécie deste último, *A. ebenoides marinkellei*. No entanto, essas populações, geograficamente muito distantes, diferem em morfologia, especialmente em características dos girinos, e não parecem pertencer à mesma espécie. Assim, elevamos *marinkellei* ao status de espécie e fornecemos redescrições morfológicas detalhadas e descrições dos girinos para *A. ebenoides* e *A. marinkellei*.

Palavras-chave: *Atelopus ebenoides, Atelopus marinkellei,* Conservação, Girinos, Morfologia, Sapos-arlequins, Sinonímia.

Introduction

Harlequin toads, genus *Atelopus,* are a species-rich group of true toads (Bufonidae) and have radiated over large parts of Central and tropical South America. Harlequin toad diversity peaks in the Andean cloud forests and paramos of Colombia (Lötters 1996, Rueda-Almonacid *et al.* 2005, Lötters *et al.* 2023, 2025, Velásquez-Trujillo *et al.* 2024). In this region, however,

Atelopus taxonomy is particularly poorly resolved and further challenged by the virtual absence of most populations since the 1980s, when unparalleled declines hit the genus (La Marca *et al.* 2005, Lötters *et al.* 2023). As a result, several taxa are known only from a few specimens and a single locality, likely resulting in an underestimation of both within- and between-species diversity (Lötters *et al.* 2023, 2025, Plewnia *et al.* 2025). The problem here is that a limited and spatially restricted sampling favors oversplitting as natural variation along a geographic gradient remains underestimated (Herrera-Lopera *et al.* 2025). Overlooked synonymy could in turn result in an overestimation of the species under serious threat, misguiding conservation prioritization (Dufresnes *et al.* 2023, Mahony *et al.* 2024).

Four species of *Atelopus* have been described from a relatively small area of the Cordillera Central (Figure 1) in the Departments of Cauca and adjacent Huila, east of Popayán (Rivero 1963, Rivero and Granados-Díaz 1993, Ruíz-Carranza and Osorno-Muñoz 1994, Ardila-Robayo and Ruíz-Carranza 1998): (1) *Atelopus angelito* Ardila-Robayo and Ruíz-Carranza, 1998 from "San Sebastián, Inspección de policía Valencia, km 5–6 on mule track from Valencia to Quinchana (Páramo de las Papas)," based on a series of nine individuals; (2) *A. ebenoides* Rivero, 1963 from the "Páramo de las Papas," based on a single specimen; (3) *A. eusebianus*

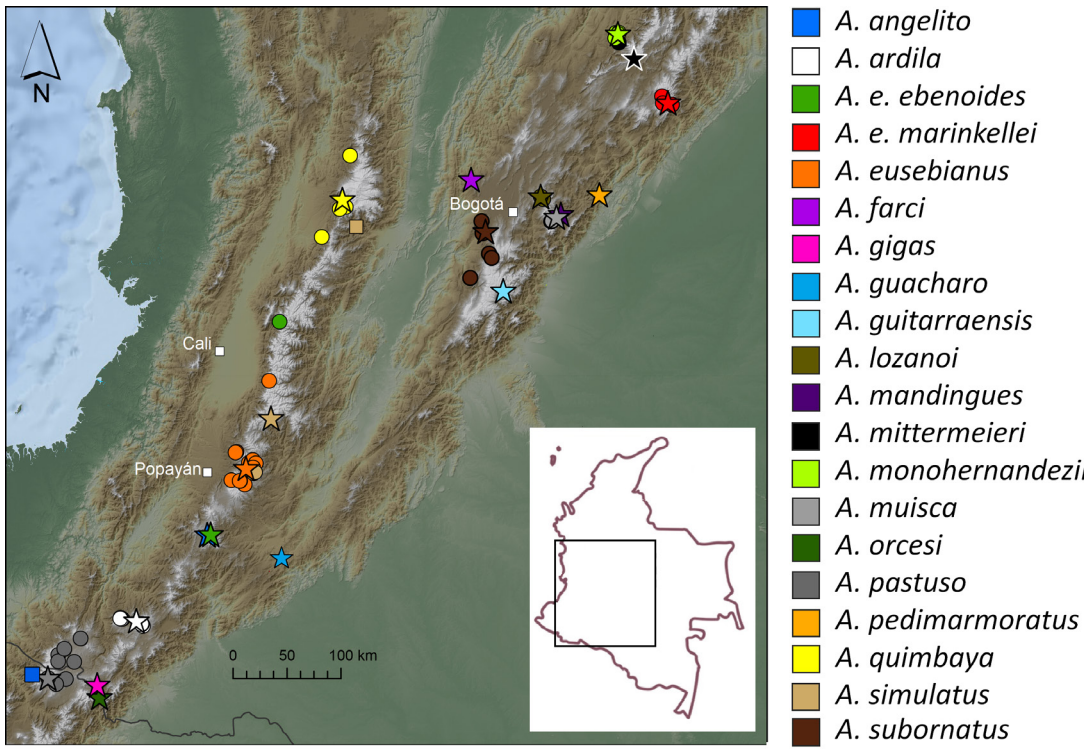

Figure 1. Distribution of species of *Atelopus* from the southern central and eastern Andes of Colombia (inset) and adjacent Ecuador discussed in this paper. Type localities are indicated by stars, additional localities by dots in the same color and localities of uncertain taxonomic status by squares in the color of the closest resembling taxon. Note that the symbols of the type localities of *A. angelito* and *A. ebenoides* partly overlap.

Rivero and Granados-Díaz, 1993 from "Municipio de Totoró, Malvasa," based on ca. 18 specimens (the exact number of specimens remains unclear because of errors with regard to the field number HGD 921, which appears twice under different collection sites and dates; Rivero and Granados-Díaz 1993: 12); (4) *A. simulatus* Ruíz-Carranza and Osorno-Muñoz, 1994 from "Municipio Belalcázar, km 11 on the road from Belalcázar to Tóez," based on a series of 30 specimens. While the latter is a humid montane forest species that is similar to *A. orcesi* Coloma, Duellman, Almendáriz, Ron, Terán-Valdez, and Guayasamin, 2010 and *A. quimbaya* Ruíz-Carranza and Osorno-Muñoz, 1994, the others are all known from paramo and subparamo habitats. They highly resemble each other, and in their original descriptions, taxonomic justifications are only briefly discussed and diagnoses barely consider other species.

For a form from the Páramo de Bijagual in the northern Cordillera Oriental, Department of Boyacá (Figure 1), subspecific status was suggested, *A. ebenoides marinkellei* Cochran and Goin, 1970. Several authors have commented on the taxonomic status either suggesting conspecificy or distinct species status, but without providing comparative evidence or taking formal taxonomic action (Kattan 1986, Rivero and Granados-Díaz 1993, Lötters 1996, Ruíz-Carranza *et al.* 1996, Coloma 1997, Rueda-Almonacid *et al.* 2005, Frost 2025).

The situation is complicated further because taxonomic decisions are best made using an integrative approach. In anuran amphibians, this approach includes external and internal larval and adult characters and bioacoustics, as well as molecular genetic data (cf. Padial *et al.* 2010). For many *Atelopus* that have virtually disappeared, it is highly challenging to obtain molecular genetics from old, formalin-fixed museum material. Particularly for Andean Colombian harlequin toads, (so far) barely any populations have been included in phylogenetic approaches, and topotypic sequences are yet missing for all species. Phylogenetic placement of particular populations is therefore insufficient to resolve taxonomic issues for the Colombian Andean forms (Lötters *et al.* 2025). As a result, forensic taxonomy is limited to external and internal morphology, which is best studied using 'next generation' approaches in anatomy such as synchrotron scanning of soft and hard tissues and electron microscopy of larval forms (cf. Boistel *et al.* 2011, 2013, Dias and Anganoy-Criollo 2024).

We reexamined adult and larval material related to *A. angelito, A. ebenoides ebenoides* Cochran and Goin, 1970, and *A. eusebianus* across their distributional ranges and suggest *A. ebenoides* as a senior synonym for them. In contrast, we elevate the subspecies *A. ebenoides marinkellei* from the Cordillera Oriental, Department of Boyacá, to species rank. We provide redescriptions and tadpole accounts for both *A. ebenoides* and *A. marinkellei.*

Materials and Methods

Specimens examined are in FMNH (Field Museum of Natural History, Chicago), IAvH (Instituto de Investigación de Recursos Biológicos Alexander von Humboldt, Villa de Leyva), ICN (Instituto de Ciencias Naturales, Universidad Nacional, Bogotá), KU (Museum of Natural History, University of Kansas, Lawrence), MHNG (Muséum d'Histoire Naturelle Geneva), NHMW (Naturhistorisches Museum Wien, Vienna), UIS (Universidad Industrial de Santander, Bucaramanga), USNM (National Museum of Natural History, Washington D.C.), and ZFMK (Zoologisches Forschungsmuseum Alexander Koenig, Bonn). Material examined in addition to the redescribed species is provided in Appendix I. We examined all type material of the species revised in this paper. However, for *A. eusebianus,* we could only trace and study two paratopotypes (MCZ-Herp-A-117992, USNM 328737). This is because in the original description, no museum vouchers but only field numbers were provided for all paratypes, rendering the destiny of

paratypes unclear. The holotype, given as ICN 20010 in the original description, could neither be traced during visits at ICN in 1995 (SL) nor in 2017 (JPR), 2022, and 2024 (AP, PB, CH, JPR, SL) and does not appear in the collection files. Actually, this collection number is not attributed to any specimen.

Sex was determined as described in Coloma *et al.* (2000) based on the presence of eggs in females and nuptial pads and vocal slits in males. Measurements were taken to the nearest 0.1 mm with manual calipers and are given in mm as mean ± one standard deviation. Abbreviations are as follows: SVL, snout–vent length; TIBL, tibia length; FOOT, foot length; HLSQ, head length from the squamosal; IOD, interorbital distance; HDWD, head width; EYDM, eye diameter; EYNO, eye to nostril distance; ITNA, internarial distance; FAL, length of flexed forearm; HAND, hand length; THBL, thumb length; SW, sacrum width. FAL and SW were measured according to Bravo-Valencia and Rivera-Correa (2011) and ITNA according to Lötters *et al.* (2025). All other definitions of measurements of adults follow Gray and Cannatella (1985). Tadpole measurements follow the abbreviations for adults where applicable with the addition of LTRF, labial tooth row formula. The foot webbing formula was taken in the manner of Savage and Heyer (1997). Finger nomenclature follows Fabrezi and Alberch (1996) and Coloma *et al.* (2010). We refer to the terms coni and spiculae as defined in Coloma *et al.* (2010).

We further studied external morphology and anatomy of the buccopharyngeal cavity in tadpoles of *Atelopus ebenoides* (from topotypic populations of *A. angelito* and *A. eusebianus*), and *A. marinkellei.* For imaging of buccopharyngeal cavities, one individual per species was manually dissected following Wassersug (1976) and prepared and imaged with scanning electron microscopy (SEM) following Dias and Anganoy-Criollo (2024). Terminology of tadpole characters follows Wassersug (1976, 1980), Lötters *et al.* (2022), and Dias and Anganoy-Criollo (2024).

Results

Atelopus ebenoides Rivero, 1963
Ebony harlequin toad
(Figures 2–5, 6A, 7A–C, E, 8A–B)

Atelopus ebenoides Rivero, 1963: 120, Figures 6, 9, holotype FMNH 69746 from "Páramo de las Papas, 3,600 m [above sea level], [Departamento de] Huila, Colombia." Kattan 1986: 653, Rivero and Granados Díaz 1993: 17, Ruíz-Carranza, Ardila-Robayo and Lynch 1996: 366, Coloma 1997: Appendix IV, Acosta-Galvis 2000: 293, Rueda-Almonacid, *et al.* 2005: 70, Bernal and Lynch 2008: 22, Lötters *et al.* 2023: Appendix 1, Frost 2025, Lötters *et al.* 2025: Appendix 2.

Atelopus ebenoides ebenoides Cochran and Goin 1970: 122, Lynch 1993: 84, Lötters 1996: 24, Rueda-Almonacid, Lynch, and Amézquita 2004: 112.

Atelopus eusebianus Rivero and Granados-Díaz, 1993: 12, Figures 1–3, holotype ICN 20010 from "Malvasa, Municipio de Totoró, [Departamento de] Cauca, Colombia". Ruíz-Carranza and Osorno-Muñoz 1994: 165, Lötters 1996: 26, Ruíz-Carranza, Ardila-Robayo, and Lynch 1996: 366, Coloma 1997: Appendix IV, Ardila-Robayo and Ruíz-Carranza 1998: 283, Acosta-Galvis 2000: 293, Rueda-Almonacid, Lynch, and Amézquita 2004: 185, Rueda-Almonacid *et al.* 2005: 71, Bernal and Lynch 2008: 23, Hernández-Córdoba *et al.* 2014: 682, Lötters *et al.* 2023: Appendix 1, Frost 2025, Lötters *et al.* 2025: Appendix 2.

Atelopus angelito Ardila-Robayo and Ruíz-Carranza, 1998: 281, Figures 1–4, holotype ICN 33408 from "Colombia, Departamento de Cauca, Municipio San Sebastián, Inspección de policía Valencia, ca Km. 5–6 por camino de herradura de Valencia a Quinchana, 2900–3000 m" above sea level. Acosta-Galvis 2000: 293, Osorno-Muñoz, Ardila-Robayo, and Ruíz-Carranza 2001: 517, Rueda-Almonacid *et al.* 2005: 56, Bernal and Lynch 2008: 22, Coloma *et al.* 2010: 34, Lötters *et*

al. 2023: Appendix 1, Frost 2025, Lötters *et al*. 2025: Appendix 2.

Atelopus ebenoides complex—Plewnia *et al.* 2025: 269.

Holotype.—Colombia: Departamento de Huila, Páramo de las Papas (approximately 01.935° N, 76.608° W); approximately 3600 m a.s.l.; Oct. 1951; leg. Philip Hershkovitz; FMNH 69746, an adult female.

Additional material examined.—Colombia: Departamento de Huila, La Plata, Río Bedón, cascada de San Nicólas, IAvH-Am-3920; Departamento de Huila, La Plata, Río Bedón basin, IAvH-Am-6282; Departamento de Huila, 23 km E of Puracé, IAvH-Am-8; Departamento de Cauca, Totoró, Malvasa, MCZ-Herp-A-117992 (field number HGD [= Humberto Granados-Diaz] 702), USNM 328737 (field number 722) (both paratopotypes of *A. eusebianus*); Departamento de Cauca, Totoró, ICN 7597-7608; Departamento de Cauca, Portachuelo, Vereda Loma Alta, Hacienda Alaska, 1 km SW of Laguna de Calvache, ICN 32946–33012, 33128 (tadpoles); Departamento de Cauca, Hacienda Alaska, ICN 33014; Departamento de Cauca, surroundings of Totoró, road from Totoró to Inzá, ICN 393–409; Departamento de Cauca, km 3 on road from Totoró to Inzá, detour to Corrales, ICN 33015, 33126 (tadpoles); Departamento de Cauca, km 3 on road from Totoró to Inzá, vereda Betania, Quebrada Betania, ICN 33208 (tadpoles); Departamento de Cauca, km 7 on road from Totoró to Inzá, vereda La Pedrera, Quebrada Gallinazo, ICN 33207 (tadpoles, not used for morphological description); Departamento de Cauca, Parque Nacional Natural Puracé, San Rafael, IAvH-Am-526, 6284, 6285; Departamento de Cauca, km. 4.5 Northeast of Silvia, IAvH-Am-37, 7882; Departamento de Cauca, [near] Popayán, en páramo, IAvH-Am-9739–9741; Departamento de Cauca, San Sebastián, Parque Nacional Natural Puracé, creek near the headwaters of Rio Caquetá, ICN 33215 (tadpoles, not used for morphological description); Departamento de Cauca, San Sebastián, Parque Nacional Natural Puracé, Páramo de las Papas, km 5–6 on mule track from Valencia to Quinchana, IAvH-Am-6497, ICN 33407 (paratopotypes of *A. angelito*), 33408 (holotype of *A. angelito*), 33410–33415 (paratopotypes of *A. angelito*); Departamento de Valle del Cauca, 7 km NE Tenerife, KU 169259; Departamento de Cauca, Totoro, km 55–56 on the road from Popayán to Inzá, ICN 11303 and 11305 (tadpoles, not used for morphological description).

Definition.—*Atelopus ebenoides* is placed in the genus *Atelopus* based on: presence of supratympanic crest; absence of parotid gland, tympanic membrane; annulus tympanicus not visible or absent; presacrals I and II fused; gastromyzophorous tadpole with LTRF 2/3 (Coloma 1997). It is defined by the combination of the following characters: (1) A large species with SVL 35.0 ± 1.47, $N = 5$, in males and 44.0 ± 5.39, $N = 10$, in females; (2) robust body (SW/SVL 0.28 ± 0.016, $N = 5$, in males and 0.28 ± 0.027, $N = 10$, in females) with (3) relatively short legs (TIBL/SVL 0.37 ± 0.012, $N = 5$, in males and 0.35 ± 0.028, $N = 10$, in females) and (4) projected snout, moderately protruding beyond apex of lower jaw, acuminate in dorsal view in males; truncate snout, barely protruding beyond apex of lower jaw, round in dorsal view in females; (5) columella and tympanic membrane absent, annulus tympanicus not visible; (6) phalangeal formula of hand 2-2-3-3, basal, fleshy webbing present between first two fingers on hand; (7) first finger long (THBL/HAND 0.61 ± 0.030, $N = 5$, in males and 0.66 ± 0.029, $N = 10$, in females); (8) phalangeal formula of foot 2-2-3-4-3, foot webbing formula **I**0 to $^1/_2$—0 to 1**II**0 to 1—$^1/_2$ to 1**III**$^1/_2$ to $1^1/_2$—2 to 3**IV**2 to 3—0 to 2**V**; (9) dorsal and lateral skin on body and limbs densely covered with large, round warts with those on flanks, humerus, and femur bearing conical tips or spiculae in most specimens; ventral surfaces strongly areolate to granular, gular area granular; (10) vertebral

column, neural processes, sacral diapophyses, and urostyle not visible through the skin; (11) in preservative, dark brown to black dorsal surfaces with cream, yellowish, tan, reddish brown, or greenish irregular markings, in some populations light pattern predominant with little, diffuse dark brown to black pattern only, laterally dark brown to black with some intrusions of light dorsal pattern and white to cream warts in some specimens, most specimens present a light band between eye and upper lip, sometimes reduced to a light spot on lower corner of eye; spiculae and conical tips of warts cream to gray; ventrally dark brown to black with whitish, yellowish, or cream irregular marks or bands, palms and soles yellowish cream to cream brown with small dark

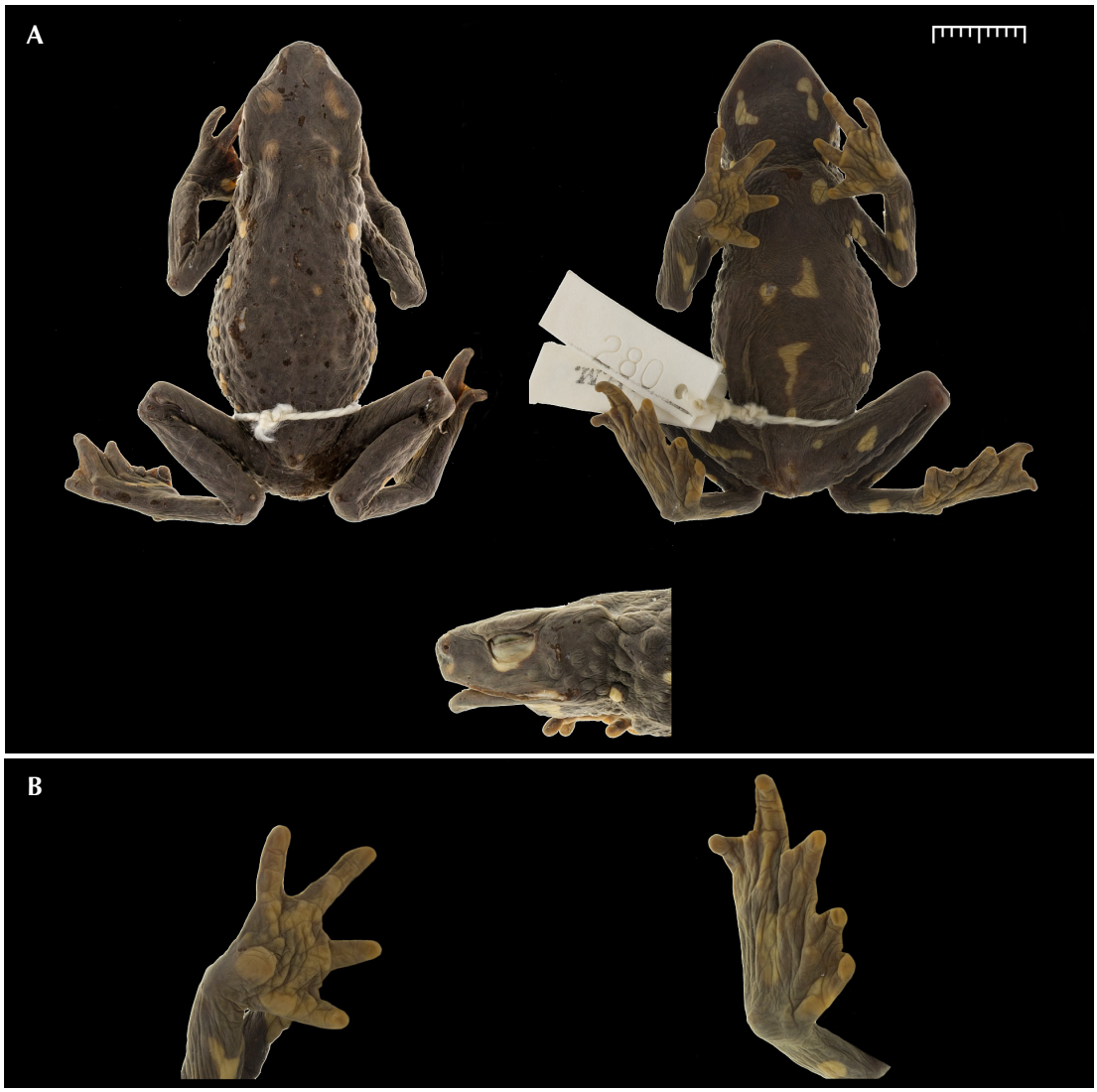

Figure 2. Female holotype of *Atelopus ebenoides* (FMNH 69746) (**A**) in dorsal, ventral and lateral views, scale 10 mm; (**B**) ventral surfaces of right hand and foot. Photographs by Rachunliu Kamei.

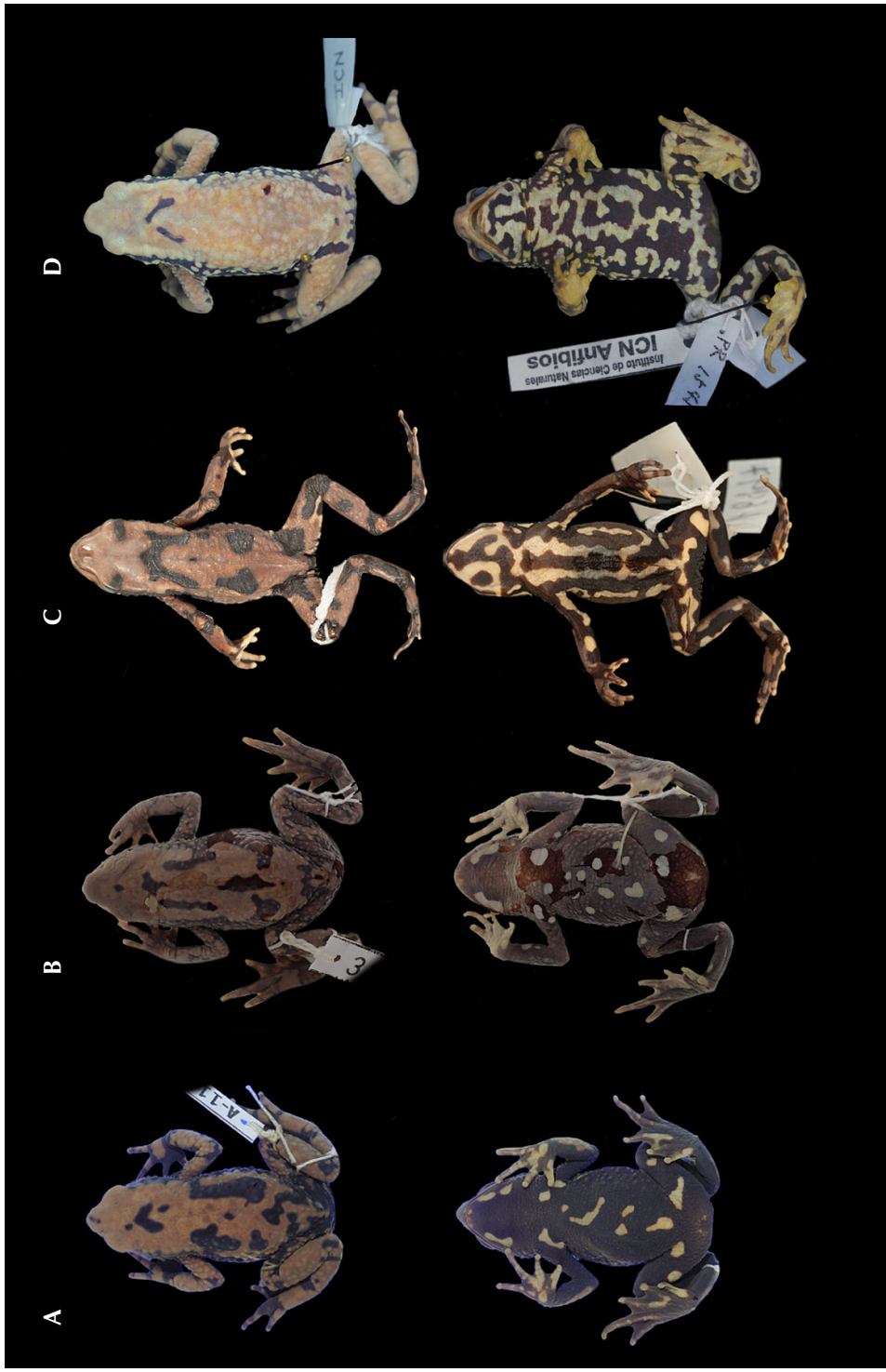

Figure 3. From left to right, female paratopotypes each in dorsal and ventral views of *Atelopus eusebianus:* (**A**) MCZ-Herp-A-117992, (**B**) USNM 328737*;* and *Atelopus angelito:* (**C**) IAvH-Am-6497, (**D**) ICN 33413. Not to scale. Photographs by MCZbase, Harvard University (2024), Addison Wynn, Amadeus Plewnia and Philipp Böning.

Figure 4. Variation of material in dorsal and ventral views attributed to *Atelopus ebenoides:* (**A**) IAvH-Am-3920; and *A. eusebianus:* (**B**) IAvH-Am-6285, (**C**) IAvH-Am-37, (**D**) IAvH-Am-6284, (**E**) ICN 395, (**F**) ICN 394. Not to scale. Photographs by Christopher Heine and Philipp Böning.

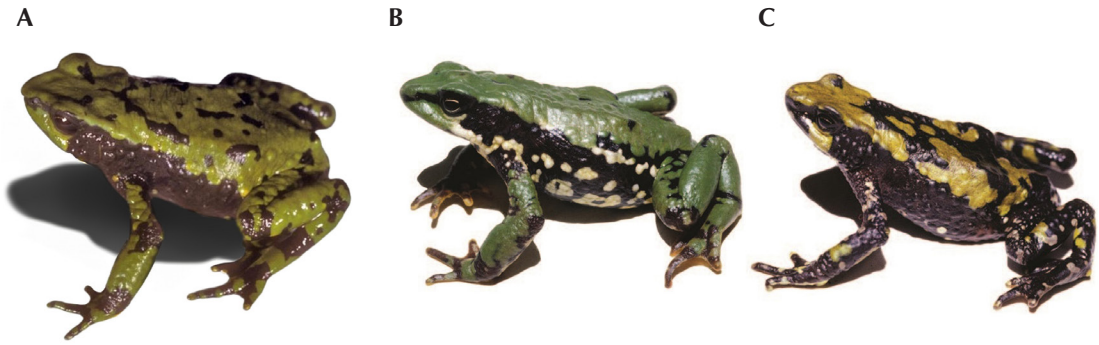

Figure 5. Variation of coloration in *Atelopus ebenoides:* (**A**) Páramo de las Hermosas, Departamento Valle del Cauca (KU 169259); (**B**) Páramo de las Papas, Departamento Cauca (holotype of *A. angelito,* ICN 33408); (**C**) Departamento Cauca (exact locality unknown). Not to scale. Photographs by (A) William E. Duellman, KU Herpetology Digital Archive (KUDA), and (B, C) reproduced from Rueda-Almonacid *et al.* (2005: 56, 74).

irregular markings; tongue whitish to cream; (12) in life, dark pattern black, light dorsal pattern yellow to green; lateral warts white in some specimens; light ventral pattern whitish to yellow; (13) tadpoles in preservative with light markings (some larger than tadpole EYDM) on brownish dorsum.

Diagnosis.—Atelopus ebenoides (Figures 2–5, 6A, 7A–C, E, 8A–B, Table 1) can be readily distinguished from all other described species by the combination of relatively large size, presence of poorly developed fleshy webbing between first and second fingers, truncate, round snout in females; moderately projected, acuminate snout in males, skin covered with large, round warts on dorsum, limbs, and flanks with most specimens having spiculae present on flanks and limbs, and in preservative dark brown to black dorsal surfaces with cream, yellowish, tan, reddish brown, or greenish irregular markings, in some populations light pattern predominant with little diffuse dark brown to black pattern only, laterally dark brown to black with some intrusions of light dorsal pattern and white to cream warts in some specimens, most specimens present a light band between eye and upper lip, sometimes reduced to a light spot on lower corner of eye; spiculae and conical tips of warts cream to gray; ventrally dark brown to black with whitish, yellowish, or cream irregular marks or bands, palms and soles yellowish cream to cream brown with small dark irregular markings.

Atelopus ebenoides is phenotypically most similar to *A. ardila* Coloma, Duellman, Almendáriz, Ron, Terán-Valdez, and Guayasamin, 2010, *A. gigas* Coloma, Duellman, Almendáriz, Ron, Terán-Valdez, and Guayasamin, 2010, *A. ignescens* Cornalia, 1849 (including its junior synonyms *Phryniscus laevis* Günther, 1858 and *A. carinatus* Andersson, 1945), *A. pastuso* Coloma, Duellman, Almendáriz, Ron, Terán-Valdez, and Guayasamin, 2010, *A. quimbaya* and *A. simulatus* from the Cordillera Central of Colombia and Ecuador, as well as *A. guacharo* Plewnia, Venegas-Valencia, Szepanski, Heine, Böning, Ramírez, and Lötters, 2025, and *A. marinkellei* from the Cordillera Oriental of Colombia.

It differs from *A. ardila* in lacking spiculae and coni in gular region (*vs.* present in females), in having large round warts on dorsum (*vs.* dorsum smooth, bearing minute stippling and posteriorly small coni), strongly areolate to granular ventral skin (*vs.* smooth) and light pattern on dark brown, black, or greenish tan dorsum and a dark venter with light markings in preservative (*vs.* uniform pale cream to black dorsum and uniform cream or yellowish venter).

Figure 6. The gastromyzophorous tadpoles of (**A**) *Atelopus ebenoides* (ICN 33126) and (**B**) *A. marinkellei* (ICN 33205) in preservative. Not to scale. Photographs by Philipp Böning.

Atelopus ebenoides is distinguished from *A. gigas* in having large round warts on dorsum (*vs.* dorsum mostly smooth, bearing few warts in some specimens), strongly areolate to granular ventral skin (*vs.* smooth) and light pattern on dark brown, black, or greenish tan dorsum and a dark venter with light markings in preservative (*vs.* uniform yellowish dorsum and uniform cream venter).

It can be distinguished from *A. ignescens* by the absence of spiculae and coni in gular and pectoral region (*vs.* spiculae and coni present in females and some males) and by having light dorsal pattern and a dark venter with light markings in preservative (*vs.* uniform black to dark brown dorsum and uniform cream, yellow, or light brown venter).

It differs from *A. pastuso* in having large round warts on dorsum (*vs.* dorsum mostly smooth, posteriorly bearing few warts in some specimens), strongly areolate to granular venter (*vs.* venter smooth to slightly areolate, but throat areolate) and in the presence of dark pattern on venter (*vs.* venter uniform cream).

Atelopus ebenoides differs from *A. quimbaya* and *A. simulatus* in having, in lateral view, a truncate snout barely protruding apex of lower jaw in females (*vs.* projected snout, protruding beyond apex of lower jaw), large round warts on dorsal surfaces and flanks (*vs.* dorsum smooth, toward flanks bearing small coni and spiculae, flanks bearing conical warts and spiculae, dorsal surfaces of limbs with round warts; some male specimens with warts on dorsum and a dorsolateral row of warts in *A. quimbaya*), ventral skin strongly areolate to granular (*vs.* venter smooth, but gular area areolate), basal fleshy webbing poorly developed between first and second fingers only (*vs.* extensive webbing between first and second fingers and often between third and fourth). In addition, it further differs from *A. quimbaya* in having dark pattern

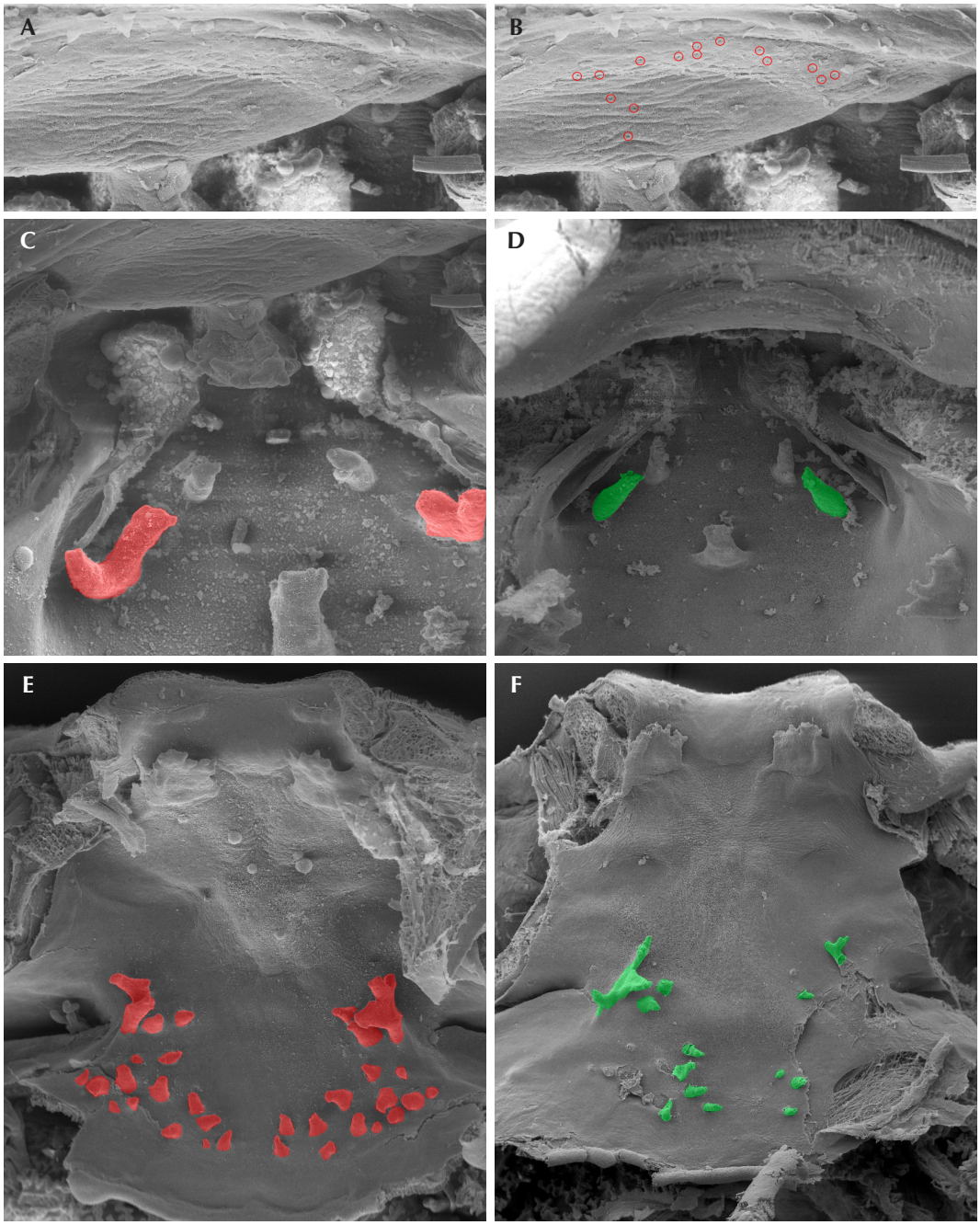

Figure 7. Comparative buccopharyngeal morphology of (**A–C**, **E**) *Atelopus ebenoides* (ICN 33126) and (**D**, **F**) *A. marinkellei* (ICN 34215): (**A**, highlighted in **B**) presence of secretory pits in the anterior region of the buccal roof of *A. ebenoides,* which are absent in *A. marinkellei* (not shown); the shape of postnarial papillae, (**C**) bifurcate in *A. ebenoides* and (**D**) simple in *A. marinkellei;* and the number of buccal floor papillae, (**E**) larger in *A. ebenoides* than in (**F**) *A. marinkellei.*

on venter (*vs.* venter uniform cream, with few small brown spots on throat in some male specimens).

It differs from *A. guacharo* in having a truncate snout, barely protruding apex of lower jaw in females (*vs.* snout projected, protruding beyond apex of lower jaw), adult female size (44.0 ± 5.39, *N* = 10 *vs.* 34.0, *N* = 1 in *A. guacharo*), spiculae present on flanks and limbs in most specimens (*vs.* absent), and by having cream, yellowish, tan, reddish brown, or greenish irregular markings in preservative (*vs.* body entirely dark except on head).

Atelopus ebenoides differs from *A. marinkellei* in coloration and pattern in life (light pattern extended over large part of dorsum in most populations, light pattern yellow to green *vs.* light spots scarce, mostly white, sometimes yellow in *A. marinkellei*), having extensive foot webbing (*vs.* feet only partially webbed; however, considerable within-population variation occurs in *A. ebenoides*) and spiculae restricted to flanks and dorsal surfaces of humerus and femur (*vs.* additionally present on dorsum in most specimens). The two species differ in osteology (sacrum and coccyx fused, posterolateral process of hyoid and scattered pits on dorsal surface of presacrals present *vs.* not fused, absent in *A. marinkellei;* Coloma 1997). The two species differ in larval pattern and coloration (in preservative, presence of light markings on brownish dorsum, always some markings larger than tadpole EYDM *vs.* uniformly dark or with minute light dots, smaller than tadpole EYDM in *A. marinkellei;* Figure 6); and in spiracle shape (conical *vs.* cylindrical in *A. marinkellei*). Further, *A. ebenoides* can be distinguished by having the vent tube distally free (*vs.* completely fused in *A. marinkellei*), the presence of secretory pits situated immediately posterior to the upper jaw sheaths (*vs.* absent in *A. marinkellei*), the presence of bifurcate postnarial papillae (not bifurcate in *A. marinkellei*), and the larger number of buccal roof papillae (16–17 *vs.* 7–8 in *A. marinkellei;* Figure 7).

Redescription of holotype.—Adult female (Figure 2). Body robust (SW/SVL 0.28); head robust, as long as wide (HLSQ/HDWD 0.99); snout truncate, slightly protruding beyond apex of lower jaw, rounded in dorsal view; nostrils directed laterally, protuberant, not visible in dorsal view, situated about four-fifths distance from eye to tip of snout in lateral view, situated above apex of lower jaw; canthus rostralis prominent, concave in dorsal view; loreal region concave; lips slightly flared; choanae large, rounded; tongue long, slightly broadened posteriorly, anterior half attached to floor of mouth; head plain between eyes in frontal view, concave between canthi; eyelid flared; tympanum absent, annulus tympanicus not visible; supratympanic crests well defined, slightly convex in dorsal view, straight in lateral view, longer than EYDM, no externally visible exostosis present, pretympanic crest well defined, about the size of EYDM; vertebral column, neural processes, sacral diapophyses, and urostyle not visible through the skin.

Limbs short (TIBL/SVL 0.36); relative length of toes I < II < III < V < IV, phalangeal formula of foot 2-2-3-4-3, webbing formula of toes **I**0-0**II**0-$^{1}/_{2}$**III**$^{1}/_{2}$-3**IV**3-$^{1}/_{2}$**V**; tarsal fold absent; foot about as long as tibia; outer metatarsal tubercle round, well defined, inner metatarsal tubercle oval, flat; supernumerary plantar tubercles indistinct; subarticular tubercles on toes distinct, rounded; tips of toes rounded, digital pads distinct; toes and fingers lack lateral fringes; relative length of fingers I < II < IV < III; phalangeal formula of hand 2-2-3-3; basal fleshy webbing poorly developed between first two fingers on hand only; palmar tubercle round, large, well defined; thenar tubercle oval, well defined; supernumerary palmar tubercles present; subarticular tubercles of digits poorly defined, evident on third finger only; tips of fingers rounded, not widened.

Dorsal and lateral skin on body and limbs densely covered with large, round warts, coni and spiculae absent; ventral surfaces, palms and soles strongly areolate, granular in gular area, chest and femur.

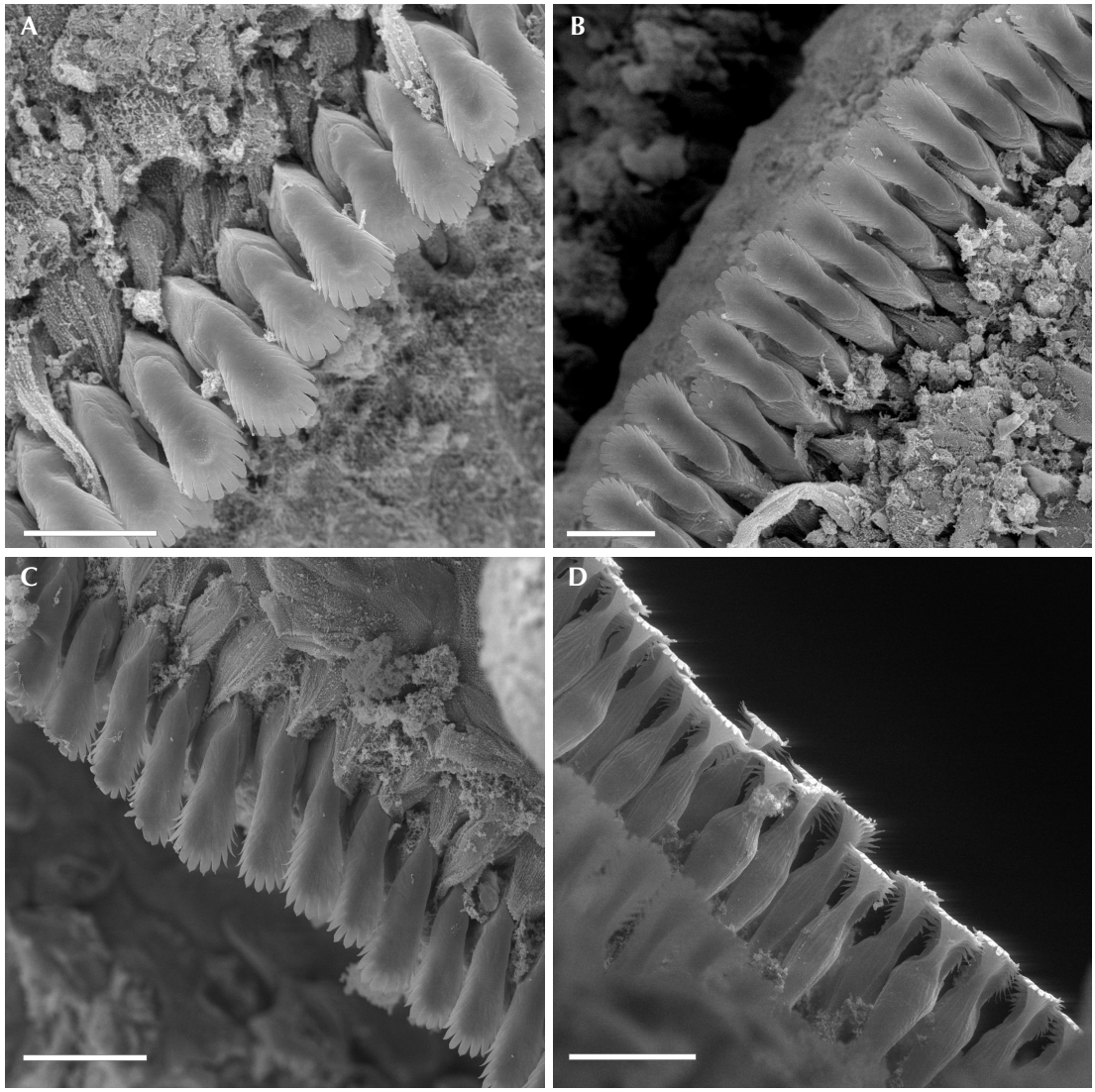

Figure 8. Scanning electron microscope images of the labial teeth (= keratodonts) in (**A**, **B**) dorsal view in *Atelopus ebenoides* (ICN 33126) and in (**C**) dorsal and (**D**) ventral view in *A. marinkellei* (ICN 34215). Scale 20 µm.

Coloration in preservative.—Surfaces of body and limbs brownish black with irregular brownish to yellowish cream spots on dorsum and flanks, cream irregular marks on ventral surfaces of body, limbs and throat; palms and soles brownish cream; tongue cream.

Coloration in life.—Unknown.

Measurements (in mm).—SVL 49.7, TIBL 17.8, FOOT 17.1, HLSQ 13.5, ITOR 4.6, HDWD 13.6, EYDM 5.1, EYNO 3.8, ITNA 9.2, HAND 11.5, THBL 7.7, SW 13.8, FAL 13.4, TIBL/SVL 0.36, SW/SVL 0.28, HLSQ/SVL 0.27, FAL/SVL 0.27, HLSQ/HDWD 0.99, THBL/HAND 0.67.

Variation.—Meristic variation is provided in

Table 1. Specimens from numerous localities in the Puracé area (including the type material of *A. angelito* and *A. eusebianus*) generally correspond to the description above. Sexual dimorphism is apparent with males being smaller than females (Table 1), having keratinized nuptial pads in the dorsal surface of the first and to a lesser extent second fingers and having a projected snout, which protrudes beyond apex of lower jaw, acuminate in dorsal view (*vs.* truncate snout, barely protruding beyond apex of lower jaw, round in dorsal view in females). Considerable variation occurs in foot webbing between specimens (**I**0 to $^{1}/_{2}$-0 to 1**II**0 to 1-$^{1}/_{2}$ to 1**III**$^{1}/_{2}$ to 1$^{1}/_{2}$-2 to 3**IV**2 to 3-0 to 2**V**), which does not follow a geographic signal but can be observed within localities. The large round warts on dorsum are densely distributed in most specimens (with e.g., IAvH-Am-6284 from San Rafael, Parque Nacional Natural Puracé, completely covered in warts) but less dense in some of the specimens from San Sebastián, Parque Nacional Natural Puracé, Páramo de las Papas, km 5–6 on mule track from Valencia to Quinchana, which could be related to a preservation artifact to some extent. Coni and spiculae are present on most specimens but vary in their extent from covering flanks, humerus and femur (e.g., IAvH-Am-37 and 7882 from Silvia) to being restricted to the tympanic area (e.g., ICN 396, 397 from the surroundings of Totoró, road from Totoró to Inzá) or being absent (FMNH 69746, holotype of *A. ebenoides,* IAvH-Am-6284 from San Rafael, Parque Nacional Natural Puracé).

In preservative (Figures 2–4), the dark pattern can vary from almost completely extending over the body (FMNH 69746, holotype of *A. ebenoides,* IAvH-Am-3920 from La Plata, Río Bedón, Cascada de San Nicólas) to being restricted to few small patches only (ICN 33407, paratopotype of *A. angelito,* 33408 holotype of *A. angelito,* 33410–33415 paratopotypes of *A. angelito*); similarly, there is variation in the extent of light markings in ventral coloration; lateral warts black in most specimens but whitish in material from San Sebastián, Páramo de las Papas, km 5–6 on mule track from Valencia to Quinchana (e.g., IAvH-Am-6497, ICN 33407, paratopotypes of *A. angelito,* ICN 33408, holotype of *A. angelito*).

In life (Figure 5), light dorsal markings range from yellow to green.

Tadpoles.—We studied larval series of *A. ebenoides* collected from Portachuelo and the Totoró to Inzá road, Department of Cauca, partially topotypic to its junior synonym *A. eusebianus* (ICN 33126 [used for SEM], 33128, 33208). We further studied a series from San Sebastián, Department of Cauca, topotypic to its junior synonym *A. angelito* (ICN 34211 [used for SEM]). They belong to the gastromyzophorous ecomorphological guild of anuran larvae (*sensu* Altig and Johnston 1989).

External morphology (Figure 6A): in dorsal view, body oval, widest between eye and spiracle; snout rounded. In profile, body depressed (height 2/3 body width), flattened ventrally. Eyes dorsolateral, relatively large (diameter about half of tadpole IOD). Nares large, dorsolateral, elongate, with a weak rim, tadpole ITNA slightly smaller than IOD. Spiracle sinistral, lateral, conical, directed posteroventrally, closer to the vent tube than to the snout, free from the body wall, positioned below midline of body. Digestive tract coiled; switchback point laterally dislocated from the center of abdominal region. Abdominal sucker sub-circular and occupying about three quarters of body length. Vent tube short, medial, cylindrical, distally free from the tail. Tail musculature poorly developed; tail muscle does not reach tail tip. Tail fins about equal in height; dorsal fin originating at the body–tail junction. Tail tip rounded. Oral disc enlarged, positioned and directed ventrally, not emarginate, with a single, continuous, lateral row of rounded, marginal papillae; large gap in papillae present in the lower lip; few submarginal papillae present in both lips. LTRF 2/3 A1 = A2, P1 = P2 = P3. Jaw sheaths present, weakly serrate, keratinized; upper jaw sheath arch-shaped; lower jaw sheath V-shaped. Body and

head of each labial tooth (= keratodont) marked by a constriction; teeth distally enlarged, spatulated, multicuspidate (Figure 8A–B).

According to Marcillo-Lara *et al.* (2020), coloration, especially presence vs. absence of light markings on different parts of the body or tail represent useful characters to distinguish species. All tadpoles of *A. ebenoides* examined possess in preservative numerous irregular light markings (always some markings larger than tadpole EYDM) on a brownish dorsum. The caudal musculature is brown with light dots in some specimens (smaller or equal to tadpole EYDM) and rarely forms a distinct tail band. Tail fins are translucent with thin brown vessels (Figure 6A). In life, coloration was black with cream or white spots or blotches (field notes of P. M. Ruíz-Carranza at ICN on ICN 33207, 33208, 33215, 33126). A more detailed description is available for tadpole lots ICN 11303 and 11305 (field notes of P. M. Ruíz-Carranza at ICN): "Black body with a few white dots, anterior ca. two–thirds of tail black, posterior third transparent (= tail fin) and cream (= musculature). Leg-bearing specimens having cream soles; body dark brown laterally with sagittal region brown, anterior two-thirds of tail metallic dark brown; transparent with abundant black melanophores on the posterior third; the dark-brown musculature continues to the apex."

Buccopharyngeal morphology: buccal roof (Figures 7A–C) triangular. Prenarial arena semi-elliptical, with a pendulum-like papilla and several secretory pits. Internal nares elliptical, transversally oriented; posterior valve free, lacking marginal projection. Vacuities present, circumscribed by margins of inner nares, presenting ciliated cells. Postnarial arena diamond-shaped, two conical, tall postnarial papillae; first pair shorter than second pair; second pair bifurcate. Lateral ridge papillae short, triangular, bifurcated. Median ridge tall, conical, papilla-like. Buccal roof arena poorly defined, completely lacking papillae or pustulation. Dorsal velum medially discontinued, devoid of papillae or projections, arch-shaped. Buccal floor (Figure 7E) triangular. Single pair of flat, wide, infralabial papillae; tip crenulated. Lingual bud poorly defined; lingual papillae absent. Buccal floor arena bell-shaped; 16–17 buccal floor arena papillae present. Buccal floor arena lacking pustulations. Prepocket papillae and pustulation absent. Buccal pockets deep, wide, oblique slit-shaped. Ventral velum present; spicular support inconspicuous; medial notch absent; marginal projections present; secretory pits poorly developed; secretory ridges present. Branchial basket triangular, short, poorly developed, wider than long. Three filter cavities, well-defined, partially covered by ventral velum.

Distribution.—Atelopus ebenoides is known from several localities on the summits of the southern Cordillera Central at approximately 2500–4700 m a.s.l. (Figure 1), where the species inhabits paramo and subparamo environments. The range reaches from Páramo de las Papas northwards to the town of Silvia in the Departamentos de Huila and Cauca (cf. Rivero 1963, Rivero and Granados-Díaz 1993, Ardila-Robayo and Ruíz-Carranza 1998, Rueda-Almonacid *et al.* 2004, Rueda-Almonacid *et al.* 2005), with additional records from Páramo de las Tinajas (Hernández-Córdoba *et al.* 2014) and the Páramo de Las Hermosas (KU 169259; Figure 5A), both in the Departamento de Valle del Cauca as well as a single record from Departamento del Tolima (UIS-A 5510). The entire geographic range from north to south encompasses about 200 km (Figure 1) and it remains to be studied if the species is continuously distributed.

Conservation status and threats.—Atelopus ebenoides as well as its junior synonyms, *A. angelito* and *A. eusebianus,* are currently listed as Critically Endangered (Possibly Extinct) under criterion D of the IUCN Red List of Threatened Species (IUCN SSC Amphibian Specialist Group 2017, 2019, 2021). Despite numerous visits to historic localities, the species has not been seen in any of its localities since 2007 (Lötters *et al.* 2023,

Table 1. Meristic variation in *Atelopus ebenoides* including type and additional material of the species and its junior synonyms *A. angelito* and *A. eusebianus*: mean ± standard deviation followed by the range in parentheses. Measurements are based on males ICN 33408 (holotype of *A. angelito*), 33410-33411 (paratopotypes of *A. angelito*), IAvH-Am-6284, 9740 and females MCZ 117992 (paratopotype of *A. eusebianus*), ICN 33413 (paratopotype of *A. angelito*), IAvH-Am-37, 526, 3920, 6282, 6285, 6497 (paratopotype of *A. angelito*), 7882, 9739. For individual measurements see Appendix II.

	Males (*N* = 5)	**Females (*N* = 10)**
SVL	35.0 ± 1.47 (32.8-36.4)	44.0 ± 5.39 (33.4-55.2)
TIBL	12.9 ± 0.45 (12.3-13.5)	15.4 ± 1.55 (11.5-17.2)
FOOT	14.6 ± 0.75 (13.7-15.3)	16.3 ± 1.99 (12.5-19.3)
HLSQ	10.5 ± 0.97 (8.8-11.1)	12.2 ± 1.15 (10.1-13.7)
IOD	3.7 ± 0.36 (3.3-4.1)	4.5 ± 0.44 (3.8-5.1)
HDWD	10.2 ± 0.58 (9.5-11.0)	11.6 ± 0.88 (9.5-12.6)
EYDM	3.2 ± 0.26 (2.9-3.5)	3.6 ± 0.26 (3.2-4.1)
EYNO	2.7 ± 0.25 (2.3-3.0)	3.3 ± 0.35 (2.8-3.8)
ITNA	3.8 ± 0.16 (3.6-4.0)	4.0 ± 0.37 (3.5-4.4)
FAL	10.2 ± 0.24 (10.0-10.5)	11.7 ± 1.09 (9.4-12.8)
HAND	8.6 ± 0.51 (8.1-9.3)	10.2 ± 1.34 (7.7-11.8)
THBL	5.3 ± 0.51 (4.6-5.8)	6.7 ± 0.75 (5.4-8.0)
SW	9.8 ± 0.21 (9.5-10.0)	12.0 ± 1.56 (9.1-14.0)
TIBL/SVL	0.37 ± 0.012 (0.36-0.39)	0.35 ± 0.028 (0.28-0.38)
SW/SVL	0.28 ± 0.016 (0.26-0.30)	0.28 ± 0.027 (0.22-0.30)
HLSQ/SVL	0.30 ± 0.034 (0.25-0.34)	0.28 ± 0.029 (0.21-0.30)
FAL/SVL	0.29 ± 0.012 (0.27-0.31)	0.27 ± 0.022 (0.22-0.29)
HLSQ/HDWD	1.03 ± 0.085 (0.93-1.12)	1.06 ± 0.059 (0.92-1.11)
THBL/HAND	0.61 ± 0.031 (0.57-0.63)	0.66 ± 0.029 (0.61-0.71)

AP unpublished data 2019, Gustavo Pisso Florez and Jesse Erens, pers. comm. 2024). The majority of the range of this species lies within the well-protected Parque Nacional Natural Puracé. Nearly all Andean harlequin toads from high Andean ecosystems have been proven highly susceptible to chytridiomycosis caused by *Batrachochytrium dendrobatidis* Longcore, Pessier, and Nichols, 1999 (*Bd*), considered a main driver of extinctions in *Atelopus* (e.g., La Marca *et al.* 2005, Lips *et al.* 2008, Flechas *et al.* 2017, Olson *et al.* 2021, Lötters *et al.* 2023). Although *Bd* has not been detected directly from *A. ebenoides,* at least in the year 2021 *Bd* was confirmed on syntopic species in its geographic range (Laura Victoria Rivera Jaimes, pers. comm. 2022) and has likely led to its decline. Climate change may become an additional threat to *Atelopus ebenoides* in the near future (Lötters *et al.* 2023).

Etymology.—Rivero (1963) did not provide a *derivatio nominis.* The epithet *ebenoides* (Greek adjective) means ebony-like or resembling ebony and apparently refers to the almost entirely black coloration of the holotype, resembling ebony wood.

Remarks.—Coloma (1997) studied osteological characters of some species of *Atelopus,* including *A. eusebianus* (syn. ad *A. ebenoides*). The author confirmed fusion of presacrals I and II, absence of a columella, and phalangeal formulae of hand and foot being 2-2-3-3 and 2-2-3-4-3, respectively.

The central and northern Andean paramos and subparamos of Colombia, Ecuador, and Peru are inhabited by species of *Atelopus* with a toad-like appearance. Using molecular genetics and morphology, they are phylogenetically related and can be referred to as an *A. ignescens* clade with various subclades (Guayasamin *et al.* 2010, Lötters *et al.* 2025). However, we lack molecular genetic data for most Colombian Andean harlequin toads.

The coordinates of the type localities for the names *A. angelito* and *A. eusebianus* are likely in error in the original descriptions. In *A. angelito,* the coordinates (01.850° N, 76.783° W) correspond to a site northwest of the town of San Sebastián. Instead, the type locality on the Valencia–Quinchana mule trail is located at the approximate corrected coordinates of 01.9152° N, 76,6248° W. The coordinates for the type locality of *A. eusebianus* (02.05° N, 76.4° W) that were given in the original description correspond to a site in the Departamento del Huila, 51.3 km south of the type locality Totoró. However, this locality is likely incorrect, with the correct type locality of the species being 02.50° N, 76.4° W, close to the village of Totoró.

Coloma *et al.* (2010), Coloma (2002), and Coloma and Duellman (2025) assigned material from Ecuador, Carchi province, Reserva Ecológica El Ángel, Comunidad de Morán, Río La Plata (KU 178417) to *A. angelito* (i.e., syn. ad *A. ebenoides*) based on an examination of the type series. The record lies more than 180 km airline southwest of the type locality of *A. angelito,* separated by the distributional ranges of *A. ardila* and *A. pastuso.* Besides allocation to this species, the authors noted subtle differences in webbing, size, and coloration. We were unable to examine the KU specimens and additional material from the same general area reported as *Atelopus* sp. 14 by Rueda-Almonacid *et al.* (2005). Additional examination is required to confirm its potential conspecificy with *A. ebenoides.*

Atelopus marinkellei Cochran and Goin, 1970
Marinkelle's harlequin toad
(Figures 6B, 7D, F, 8C–D, 9–10)

Atelopus ebenoides marinkellei Cochran and Goin, 1970: 123, plate 18G–H, holotype USNM 150644 from "Páramo [de] Vijagual [= Páramo de Bijagual], [Departamento de] Boyacá, Colombia." Lynch 1993: 84, Lötters 1996: 24, Ruíz-Carranza, Ardila-Robayo, and Lynch 1996: 366, Acosta-Galvis 2000: 293, Rueda-Almonacid, Lynch, and Amézquita 2004: 112, Acosta-Galvis *et al.* 2006: 282, Galvis-Cordoba and Carvajalino-Fernández 2025: 852.

Atelopus ebenoides (non Rivero)—Péfaur and Duellman 1980: 52, Coloma 1997: Appendix IV, Lynch and Mayorga 2011: 239.

Atelopus marinkellei—Rivero and Granados Díaz 1993: 17, Rueda-Almonacid *et al.* 2005: 71, Lötters *et al.* 2023: Appendix 1, Frost 2025, Lötters *et al.* 2025: Appendix 2, Plewnia *et al.* 2025: 269.

Holotype.—Colombia: Departamento de Boyacá, Páramo de Bijagual, between Tunja and Zetaquirá (approximately 05.36° N, 73.28° W); approximately 2660 m a.s.l.; unknown date; leg. Hno. Nicéforo María; USNM 150644, an adult female.

Additional material examined.—Colombia: Departamento de Boyacá, Páramo de Bijagual, USNM 150645–150646 (paratopotypes); NHMW 32716/1; Departamento de Boyacá, Aquitania, Vadamondo [= Vadohondo], Alto Cusiana, IAvH-Am-51; Departamento de Boyacá, Vadohondo, Páramo de Toquilla, IAvH-Am-2324, 9657; KU 169141; Departamento de Boyacá, Páramo de Toquilla, ICN 34215 (tadpoles); Departamento de Boyacá, Toquilla,

Río Cusiana, IAvH-Am-3619, 3622, 3624–3626, 4356; Departamento de Boyacá, Aquitania, Alto Río Cusiana, Páramo de Toquillo, km 53–57 on road from Sogamoso, ICN 33205 (tadpoles); Departamento de Boyacá, Inspección de Policía de Toquilla, Páramo de Siscunsí, IAvH-Am-6042–6055; Departamento de Boyacá, unknown locality, ZFMK 85071, 85072.

Definition.—Atelopus marinkellei is placed in the genus *Atelopus* based on: presence of supratympanic crest; absence of parotid gland and tympanic membrane; annulus tympanicus not visible or absent; presacrals I and II fused; gastromyzophorous tadpole with LTRF 2/3 (Coloma 1997). It is defined by the combination of the following characters: (1) A large species with SVL 32.7 ± 1.10, $N = 5$, in males and 43.5 ± 1.95, $N = 5$, in females; (2) robust body (SW/SVL 0.26 ± 0.007, $N = 5$, in males; 0.28 ± 0.013, $N = 5$, in females) with (3) relatively short legs (TIBL/SVL 0.37 ± 0.0106, $N = 5$, in males; 0.33 ± 0.014, $N = 5$, in females) and (4) projected acuminate snout, protruding beyond apex of lower jaw (most prominent in males); (5) columella and tympanic membrane absent, annulus tympanicus not visible; (6) phalangeal formula of hand 2-2-3-3, basal, fleshy webbing present between first two fingers on hand; (7) first finger long (THBL/HAND 0.61 ± 0.053, $N = 5$, in males; 0.64 ± 0.044, $N = 5$, in females); (8) phalangeal formula of foot 2-2-3-4-3, foot webbing formula **I**0 to $^{1}/_{2}$-$^{1}/_{2}$ to 1**II**0 to 1-1 to 2**III**$^{1}/_{2}$ to 1$^{1}/_{2}$-2 to 3**IV**2 to 3-0 to 1**V**; (9) dorsal and lateral skin on body and limbs densely covered with large, round warts extending to varying extent on dorsum, additionally covered to a variable extent with large spiculae that are often clustered on lateral warts; ventral surfaces areolate with minute coni on venter, chest, and throat in some specimens; (10) vertebral column, neural processes, sacral diapophyses, and urostyle not visible through skin; (11) in preservative, overall brown to black, dorsally with whitish to yellowish cream dots (smaller than eye diameter) and occasionally irregular markings on dorsal surfaces (markings can be absent on extremities), with always a whitish mark immediately below eye; ventrally with whitish to yellowish cream blotches (up to about the size of eye diameter), sometimes including ventral surfaces of extremities; throat sometimes almost entirely whitish cream; sole and palm with whitish cream or yellowish tan marks, metatarsal and metacarpal tubercles always whitish cream or yellowish tan, other tubercles and tips of toes and fingers sometimes whitish cream or yellowish tan; tongue cream; (12) in life, black with white and/or yellowish spot pattern as described; (13) in preservative, tadpoles uniformly dark or with few minute light dots on dorsum (smaller than tadpole EYDM) with cream band on proximal half of tail.

Diagnosis.—Atelopus marinkellei (Figures 6B, 7D, F, 8C–D, 9–10, Table 2) can be readily distinguished from all other described species by the combination of relatively large size, presence of poorly developed fleshy webbing between first and second fingers, truncate, acuminate snout projected (most prominent in males), dorsal and lateral skin on body and limbs densely covered with large, round warts extending to varying extent on dorsum, additionally covered at variable extent with large spiculae that are often clustered on lateral warts; ventral surfaces areolate with minute coni on venter, chest, and throat in some specimens, and in preservative entirely brown to black coloration with whitish to yellowish cream or dots (smaller than eye diameter) and occasionally irregular markings on dorsal surfaces, with always a whitish mark immediately below the eye, and whitish to yellowish cream blotches (up to about the size of eye diameter) on venter.

Atelopus marinkellei is phenotypically most similar to *A. ebenoides, A. guacharo, A. guitarraensis* Osorno-Muñoz, Ardila-Robayo, and Ruíz-Carranza, 2001, and *A. mittermeieri* Acosta-Galvis, Rueda-Almonacid, Velásquez-Álvarez, *et al*., 2006 from the Colombian Andes and *A. arsyecue* Rueda-Almonacid, 1994 from

Figure 9. Female holotype of *Atelopus marinkellei* (USNM 150644) in dorsal (left) and ventral views; scale 10 mm. Photographs by Stefan Lötters.

the Sierra Nevada de Santa Marta, Colombia.

Atelopus marinkellei differs from *A. ebenoides* (including its junior synonyms *A. angelito* and *A. eusebianus*) in coloration and pattern (light spots scarce, mostly white, sometimes yellow *vs.* light pattern extended over large part of dorsum in most populations, light pattern yellow to green in life in *A. ebenoides*) and presence of spiculae on dorsum in most specimens (*vs.* restricted to flanks and dorsal surfaces of humerus and femur). The two species can be distinguished by aspects of osteology (sacrum and coccyx not fused, posterolateral process of hyoid and scattered pits on dorsal surface of presacrals absent *vs.* fused, present in *A. ebenoides;* Coloma 1997).

The two species differ in larval features, i.e., coloration in preservative, uniformly dark or with minute light dots (smaller than tadpole EYDM) *vs.* presence of light markings (always some markings larger than tadpole EYDM) on dorsum in *A. ebenoides* (Figure 6B); and in spiracle shape (cylindrical *vs.* conical in *A. ebenoides*). Further, *A. marinkellei* can be distinguished by having the vent tube completely fused (*vs.* distally free in *A. ebenoides*), absence

of secretory pits situated immediately posterior to the upper jaw sheaths (*vs.* present in *A. ebenoides*), by the postnarial papillae not being bifurcate (bifurcate in *A. ebenoides*), and by the smaller number of buccal roof papillae (7–8 *vs.* 16–17 in *A. ebenoides;* Figure 7).

Atelopus marinkellei can be distinguished from *A. guitarraensis* by having feet only partially webbed (*vs.* fully webbed), dense presence of spiculae in most specimens (*vs.* absent) and, in preservative, presence of light dorsal pattern and light dots on venter up to EYDM size (*vs.* dorsally dark brown to black without pattern, venter in most female specimens yellow with little dark markings, throat, chest, and limbs dark brown).

It differs from *A. guacharo* in adult female size (43.5 ± 1.95, $N = 5$ *vs.* 34.0, $N = 1$ in *A. guacharo*), presence of spiculae in most specimens (*vs.* absent) and, in preservative, presence of light dorsal pattern and light dots on venter (*vs.* body entirely dark except on head).

It differs from *A. mittermeieri* in absence of red ventral coloration in life (*vs.* venter uniformly red with few small cream spots and a brown band on chest) and tadpole coloration [uniformly dark or with few minute light dots (smaller than tadpole EYDM) on dorsum *vs.* presence of light markings (larger than tadpole EYDM) in *A. mittermeieri;* Acosta-Galvis *et al.* 2006].

Atelopus marinkellei differs from *A. arsyecue* by smaller adult size (males ≤ 34.0 *vs.* ≥ 45.2, females ≤ 46.0 *vs.* ≥ 53.0), whitish or yellowish dorsal dots being larger (smaller than *vs.* equal to or larger than eye diameter), and by the presence of a whitish dot immediately below the eye (*vs.* absent).

Redescription of holotype.—Adult female (Figure 9). Body robust (SW/SVL 0.29); head robust, longer than wide (HLSQ/HDWD 1.09); snout acuminate, rounded in dorsal view, moderately protruding beyond apex of lower jaw; nostrils directed laterally, protuberant, not visible in dorsal view, situated about four–fifths distance from eye to tip of snout in lateral view, situated before apex of lower jaw; canthus rostralis prominent, straight in dorsal view; loreal region concave; lips slightly flared; choanae large, rounded; tongue long, slightly broadened posteriorly, anterior half attached to floor of mouth; head plain between eyes in frontal view, concave between canthi; eyelid flared; tympanum absent, annulus tympanicus not visible; supratympanic crests well defined, slightly convex in dorsal view, straight in lateral view, about as long as EYDM, no externally visible exostosis present, pretympanic crest indistinct; vertebral column, neural processes, sacral diapophyses, and urostyle not visible through the skin.

Limbs short (TIBL/SVL 0.34); relative length of toes I < II < III < V < IV, phalangeal formula of foot 2-2-3-4-3, webbing formula of toes **I**0-$^1/_2$**II**0-1**III**$^1/_2$-2**IV**2-0**V**; tarsal fold absent; foot slightly longer than tibia; outer metatarsal tubercle round, well defined, inner metatarsal tubercle oval, well defined; supernumerary plantar tubercles indistinct; subarticular tubercles on toes ill-defined, rounded; tips of toes rounded, digital pads distinct; toes and fingers lack lateral fringes; relative length of fingers I < II < IV < III; phalangeal formula of hand 2-2-3-3; basal fleshy webbing poorly developed between first two fingers on hand only; palmar tubercle round, large, well defined; thenar tubercle oval, well defined; supernumerary palmar tubercles and subarticular tubercles of digits poorly defined; tips of fingers rounded, not widened.

Dorsal skin covered with large spiculae (absent toward head and on arm, and most dense on posterior dorsum and femur); dorsolaterally and on flanks as well as dorsal surfaces of limbs covered with large, flat, and round warts with those on flanks and femur bearing one to many, often clustered, spiculae; ventral surfaces areolate with small coni on venter, chest, and posterior throat.

Coloration in preservative.—Overall brown with dorsally whitish cream dots (smaller than eye diameter) and occasionally irregular markings

Figure 10. *Atelopus marinkellei* in life from Vadohondo (Departamento Boyacá, Colombia, KU 169141). Photograph by William E. Duellman, KU Herpetology Digital Archive (KUDA).

on head, with a whitish mark immediately below the eye, spiculae gray; ventrally with whitish cream dots (most up to about the size of eye diameter) from throat to femur; sole and palm with whitish cream marks, metatarsal and metacarpal tubercles whitish cream, tips of toes and fingers tan.

Coloration in life.—Unknown.

Measurements (in mm).— SVL 43.4, TIBL 15.0, FOOT 17.2, HLSQ 12.9, ITOR 3.8, HDWD 11.8, EYDM 5.1, EYNO 3.1, ITNA 3.2, HAND 9.4, THBL 6.8, SW 12.7, FAL 11.7, TIBL/SVL 0.34, SW/SVL 0.29, HLSQ/SVL 0.30, FAL/SVL 0.27, HLSQ/HDWD 1.09, THBL/HAND 0.72.

Variation.—Meristic variation is provided in Table 2. Considerable variation in skin texture occurs with spiculae almost absent in some specimens (e.g., NHMW 32716), warts almost absent to predominant on dorsum, and ventral coni absent in most specimens with some having flat warts on the lateral parts of the venter (e.g., IAvH-Am-9657). Sexual dimorphism is apparent with males smaller than females, having keratinized nuptial pads in the dorsal surface of the first and to a lesser extent second finger, and having a more projected snout in lateral view.

Color and pattern in preservative show little variation with some specimens bearing irregular markings on dorsal surfaces and light circles instead of dots ventrally (e.g., IAvH-Am-6048). Dark color varies from brown to black.

In life (Figure 10), *A. marinkellei* is black with the light dots on dorsum white to yellow and those on flanks and venter white.

Tadpoles.—We examined larval series of this species from Department of Boyacá, Páramo de Toquilla (ICN 33205, ICN 34215). They belong to the gastromyzophorous ecomorphological guild of anuran larvae (*sensu* Altig and Johnston 1989).

External morphology (Figure 6B): in dorsal view, body oval, widest between eye and spiracle; snout rounded. In profile, body depressed (height 2/3 body width), flattened ventrally. Eyes dorsolateral, relatively large (diameter about half of tadpole IOD). Nares large, dorsolateral, elongate, with a weak rim, tadpole ITNA slightly smaller than IOD. Spiracle sinistral, lateral, cylindrical, directed posteroventrally, closer to the vent tube than to the snout, free from the body wall, positioned below midline of body. Digestive tract coiled; switchback point laterally dislocated from the center of abdominal region. Abdominal sucker sub-circular and occupying about three quarters of body length. Vent tube short, medial, cylindrical, completely fused to tail. Tail musculature poorly developed; tail muscle does not reach tail tip. Tail fins about equal in height; dorsal fin originating at body–tail junction. Tail tip rounded. Oral disc enlarged, positioned and directed ventrally, not emarginate, with a single, continuous, lateral row of rounded, marginal papillae; large gap in papillae present in lower lip; few submarginal papillae present in both lips. LTRF 2/3 A1 = A2, P1 = P2 = P3. Jaw sheaths present, weakly serrate, keratinized; upper jaw sheath arch-shaped; lower jaw sheath V-shaped. Body and head of each labial tooth (= keratodont) marked by a constriction; teeth distally enlarged, spatulated, multicuspidate (Figure 8C–D).

According to Marcillo-Lara *et al.* (2020),

Table 2. Meristic variation in *Atelopus marinkellei:* mean ± standard deviation followed by the range in parentheses. Measurements are based on males IAvH-Am 2324, 4356, 6047, 9657, NHMW 32716 and females IAvH 6045, 6046, 6050, 6055, USNM 150644 (holotype). For individual measurements see Appendix II.

	Males (*N* = 5)	**Females (*N* = 5)**
SVL	32.7 ± 1.10 (31.4–34.0)	43.5 ± 1.95 (41.0–46.0)
TIBL	12.2 ± 0.26 (11.8–12.5)	14.5 ± 0.37 (14.0–15.0)
FOOT	13.1 ± 0.28 (12.8–13.4)	16.2 ± 0.69 (15.3–17.2)
HLSQ	10.4 ± 0.29 (10.0–10.7)	12.6 ± 0.65 (11.5–13.2)
IOD	3.6 ± 0.29 (3.4–4.0)	3.8 ± 0.23 (3.5–4.0)
HDWD	9.4 ± 0.26 (9.0–9.7)	10.9 ± 0.54 (10.4–11.5)
EYDM	3.3 ± 0.28 (3.1–3.8)	3.9 ± 0.70 (3.4–5.1)
EYNO	2.6 ± 0.25 (2.4–3.0)	3.2 ± 0.27 (2.8–3.4)
ITNA	3.2 ± 0.17 (3.0–3.4)	3.7 ± 0.34 (3.2–4.0)
FAL	9.7 ± 0.42 (9.0–10.0)	11.6 ± 0.44 (11.0–12.0)
HAND	8.1 ± 0.44 (7.7–7.8)	10.1 ± 0.50 (9.4–10.6)
THBL	4.9 ± 0.19 (4.6–5.1)	6.5 ± 0.32 (6.0–6.8)
SW	8.5 ± 0.23 (8.3–8.8)	11.9 ± 0.64 (11.0–12.7)
TIBL/SVL	0.37 ± 0.011 (0.36–0.39)	0.33 ± 0.014 (0.32–0.35)
SW/SVL	0.26 ± 0.007 (0.25–0.27)	0.28 ± 0.013 (0.26–0.29)
HLSQ/SVL	0.32 ± 0.011 (0.30–0.33)	0.29 ± 0.008 (0.28–0.30)
FAL/SVL	0.30 ± 0.01 (0.28–0.31)	0.27 ± 0.013 (0.25–0.28)
HLSQ/HDWD	1.11 ± 0.040 (1.08–1.18)	1.16 ± 0.058 (1.09–1.23)
THBL/HAND	0.61 ± 0.053 (0.53–0.66)	0.64 ± 0.044 (0.62–0.72)

coloration, especially presence *vs.* absence of light markings on different parts of the body or tail do represent useful characters to distinguish species. All tadpoles of *A. marinkellei* studied are in preservative uniformly dark or show few minute light dots (always smaller than EYDM). The blackish brown caudal musculature has a complete or partially interrupted cream band on proximal half of tail. Tail fins are blackish brown on proximal half and translucent with blackish vessels on distal half (Figure 6B). In life, they were black with a white band on the proximal half of the tail (field notes of ICN 33205, J. D. Lynch at ICN).

Buccopharyngeal morphology: buccal roof triangular (Figure 7D). Prenarial arena semi-elliptical, with short, pendulum-like papilla; secretory pits absent. Internal nares elliptical, transversally oriented; posterior valve free, lacking marginal projection. Vacuities present, circumscribed by margins of inner nares, presenting ciliated cells. Postnarial arena diamond-shaped, two conical, tall postnarial papillae, subequal in size. Lateral ridge papillae short, triangular, bifurcated. Median ridge tall, conical, papilla-like. Buccal roof arena poorly defined, completely lacking papillae or pustulation. Dorsal velum medially discontinued,

devoid of papillae or projections, arch-shaped. Buccal floor triangular (Figure 7F). Single pair of flat, wide, infralabial papillae; tip crenulated. Lingual bud poorly defined; lingual papillae absent. Buccal floor arena bell-shaped; 7–8 buccal floor arena papillae present. Buccal floor arena lacking pustulations. Prepocket papillae and pustulation absent. Buccal pockets deep, wide, oblique slit-shaped. Ventral velum present; spicular support inconspicuous; medial notch absent; marginal projections present; secretory pits poorly developed; secretory ridges present. Branchial basket triangular, short, poorly developed, wider than long. Three filter cavities, well-defined, partially covered by ventral velum.

Distribution.—Atelopus marinkellei is known from several localities on the eastern versant of the Cordillera Oriental (Department of Boyacá) in the paramo complex comprising the Páramo de Siscunsí, Páramo de Pisba, Páramo de Toquilla, and Páramo de Bijagual, 2600–3650 m a.s.l. (cf. Rueda-Almonacid *et al.* 2004, 2005, Galvis-Cordoba and Carvajalino-Fernández 2025; Figure 1).

Conservation status and threats.—Atelopus marinkellei is currently listed as Critically Endangered under criterion D of the IUCN Red List of Threatened Species (IUCN SSC Amphibian Specialist Group 2024). Despite numerous visits to historic localities in the last 20 years (Lötters *et al.* 2023, AP unpublished data 2024, 2025), the species has only been seen three times in the area of the regional Natural Park of Paramo de Siscunsí-Ocetá at sites above 3,000 m a.s.l.: one individual was discovered each in May and October 2006 and most recently in April 2025 (Galvis-Cordoba and Carvajalino-Fernández 2025). The majority of the range of the species lies outside of protected areas with only Parque Nacional Natural Pisba covering the northernmost range (IUCN SSC Amphibian Specialist Group 2024). All Andean harlequin toads from high Andean ecosystems have been proven highly susceptible to chytridiomycosis caused by *Batrachochytrium dendrobatidis* (*Bd*), which is considered a main driver of extinctions in *Atelopus* (e.g., La Marca *et al.* 2005, Lips *et al.* 2008, Lötters *et al.* 2023). Although *Bd* has not been detected in *A. marinkellei* or syntopic species, wave-like mortality events that were likely induced by the pathogen have been reported (IUCN SSC Amphibian Specialist Group 2024). The species is affected by habitat modification, and invasive trout are widespread in its range (Lötters *et al.* 2023, Galvis-Cordoba and Carvajalino-Fernández 2025, AP unpublished data 2024, 2025). Climate change may become an additional threat to *Atelopus marinkellei* in the near future (Lötters *et al.* 2023).

Etymology.—Cochran and Goin (1970) named this form in honor of Cornelis Johannes Marinkelle (1925–2012), a Dutch-born biologist at the Universidad de Los Andes, Bogotá.

Discussion

Previously, *Atelopus eusebianus* was distinguished from *A. ebenoides sensu stricto* only by coloration in life, i.e., dorsally dark green, bluish green, or yellowish green with bluish markings and ventrally bluish with yellow markings *vs.* uniformly black (Rivero and Granados Díaz 1993). As shown in Figure 2, the only type specimen of *A. ebenoides* (FMNH 69746) is not uniformly black but bears small light markings (cf. Rivero 1963, Cochran and Goin 1970). *Atelopus angelito* was not compared to *A. ebenoides sensu stricto* in its original description, but to *A. eusebianus.* In the original description, it differs in having a slightly larger adult size despite broad overlap between measurements (female 41.0, $N = 1$; males 33.8 ± 0.95, range 33.0–34.8, $N = 6$ *vs.* in *A. eusebianus:* females 39.8 ± 5.24, range 33.0–45.0, $N = 12$; males 34.2 ± 1.4, range 32.5–36.1, $N = 6$ [cf. Rivero and Granado- Díaz 1993]), a slightly more webbed foot, coloration in life (ventrally white with irregular black markings *vs.* ventrally bluish with yellow markings) and lateral warts (large whitish *vs.* small black) (Ardila-Robayo and

Ruíz-Carranza 1998). Based on our comparative reexamination of type material and additional specimens from the general area, we conclude that adult size, webbing, skin texture, and coloration show high intrapopulation variation. We consider differences in these traits as given in the original description as within-species variation and place the names *A. angelito* and *A. eusebianus* in the synonymy of *A. ebenoides,* the oldest available name.

Lötters (1996) mentioned the possible species status of the form originally described as *A. ebenoides marinkellei* based on P. M. Ruíz (pers. comm.). Ruíz-Carranza *et al.* (1996) commented on the taxonomic status ("No hay evidencia que sea una subespecie de *A. ebenoides*" [There is no evidence that it is a subspecies of *A. ebenoides*]) but it is unclear if their intention was to suggest synonymy or to reject conspecificy. Coloma (1997) instead considered *A. ebenoides marinkellei* to be a possible junior synonym of *A. ebenoides,* while other authors gave full species status to it as *A. marinkellei* (e.g., Kattan 1986, Rivero and Granados-Díaz 1993, Rueda-Almonacid *et al.* 2005, Frost 2025). None of these authors provided any arguments based on comparative studies, but Vélez-Rodríguez and Ruíz-Carranza (1997) stated that tadpoles of *A. eusebianus* (syn. ad *A. ebenoides sensu stricto*) can be distinguished from those of *A. ebenoides marinkellei* by coloration. Our reexamination of tadpoles confirmed distinctive coloration and provided additional evidence. Unlike adult coloration, larval pattern and coloration have been considered species-specific discriminatory characters (e.g., Marcillo-Lara *et al.* 2020). Moreover, external larval traits as well as buccopharyngeal morphology clearly differentiate *A. ebenoides* from *A. marinkellei,* both in the presence/absence and number of traits, demonstrating, again, the value of larval morphology for bufonid taxonomy (Dias *et al.* 2024).

Particularly in the Cordillera Oriental, additional taxonomic revisions may become necessary in the future (Plewnia *et al.* 2025). Here, 13 taxa are currently recognized (Figure 1): *Atelopus minutulus* Ruíz-Carranza, Hernández-Camacho, and Ardila Robayo, 1988 and *A. petriruizi* Ardila-Robayo, 1999 from lower elevation forests on the Amazonian versant; *A. farci* Lynch, 1993, *A. guacharo, A. mittermeieri, A. monohernandezii* Ardila-Robayo, Osorno-Muñoz, and Ruíz-Carranza, 2002, and *A. subornatus* Werner, 1899 (with two junior synonyms, *A. echeverrii* Rivero and Serna, 1985 and *A. flaviventris* Werner, 1899) from montane forests on the western versant; and *A. guitarraensis, A. lozanoi* Osorno-Muñoz, Ardila-Robayo, and Ruíz-Carranza, 2001, *A. mandingues* Osorno-Muñoz, Ardila-Robayo, and Ruíz-Carranza, 2001, *A. marinkellei, A. muisca* Rueda-Almonacid and Hoyos, 1992, and *A. pedimarmoratus* Rivero, 1963 from subparamos and paramos (Rueda-Almonacid *et al.* 2005, Lötters *et al.* 2023, 2025, Frost 2025). While most of these species can be distinguished by external morphology, several names were coined for sympatric or parapatric populations from the Bogotá region (cf. Rueda-Almonacid *et al.* 2005), that only differ in adult coloration and pattern, although integrative data are lacking: *A. lozanoi, A. mandingues, A. muisca, A. pedimarmoratus,* and *A. subornatus.* Taxonomic decisions are challenging and best being made using high-throughput sequencing approaches for ancient DNA (e.g., Scherz *et al.* 2020, Grant *et al.* 2025). These types of studies may shed light on the central highland populations from the Cordillera Oriental as a next step in *Atelopus* systematics.

Conclusions

While recent taxonomic work has led to a steady increase of recognized harlequin toad species in some clades, poor morphologic descriptions and the disappearance of most populations have hampered a thorough understanding of alpha taxonomic relationships in Andean species of Colombia. Overlooked synonymy may misdirect conservation priorities. By synonymizing the polymorphic *Atelopus angelito* and *A. eusebianus* with *A. ebenoides sensu stricto* and elevating *A. marinkellei* to species level based on in-depth examination of adult and larval characters, we provide

redescriptions and take taxonomic action as a first step toward resolving the systematics of Andean harlequin toads of Colombia. Additional work, particularly ancient DNA sequencing, osteological examination, and larval morphology, will be required to resolve the remaining taxonomic challenges in the group.

Acknowledgments

We thank Gustavo Pisso Florez for valuable discussion of localities and are grateful for his dedication to conserve habitats of *A. ebenoides*. We are grateful to Andrés R. Acosta-Galvis, Jesse Erens, and Laura Victoria Rivera Jaimes for valuable discussion and insights. We thank Rachunliu Kamei (FMNH), Andrés Aponte and Sandra P. Galeano (IAvH), María C. Ardila-Robayo†, Mauricio Rivera-Correa, Martha Calderon-Espinosa, John D. Lynch, and Pedro Ruíz-Carranza† (ICN), Rafe Brown and William E. Duellman† (KU), Andreas Schmitz (MHNG), Silke Schweiger and Georg Gassner (NHMW), Jenna L. Welch and Addison Wynn (USNM), and Morris Flecks and Wolfgang Böhme (ZFMK) for granting access to museum collections and to David Andrés Velásquez-Trujillo for helping with loan documents.

References

Acosta-Galvis, A. G. 2000. Ranas, salamandras y caecilias (Tetrapoda: Amphibia) de Colombia. *Biota Colombiana 1:* 289–329.

Acosta-Galvis, A., J. V. Rueda, A. A. Velásquez, S. J. Sánchez, and J. A. Peña. 2006. Descubrimiento de una nueva especie de *Atelopus* (Bufonidae) para Colombia: ¿Una luz de esperanza o el ocaso de los sapos arlequines? *Revista de la Academia Colombiana de Ciencias Exactas, Físicas y Naturales 30:* 279–290.

Altig, R. and G. F. Johnston. 1989. Guilds of anuran larvae: relationships among developmental modes, morphologies, and habitats. *Herpetological Monographs 1:* 81–109.

Ardila-Robayo, M. C. and P. M. Ruíz-Carranza. 1998. Una nueva especie de *Atelopus* A. M. C. Dumeril & Bibron 1841 (Amphibia: Bufonidae) de la cordillera central Colombiana. *Revista de la Academia Colombiana de Ciencias Exactas, Físicas y Naturales 83:* 281–285.

Bernal, M. H. and J. D. Lynch. 2008. Review and analysis of altitudinal distribution of the Andean anurans in Colombia. *Zootaxa 1826:* 1–25.

Boistel, R., J. Swoger, U. Kržič, V. Fernandez, B. Gillet, and E. G. Reynaud. 2011. The future of three-dimensional microscopic imaging in marine biology. *Marine Ecology 32:* 438–452.

Boistel, R., T. Aubin, P. Cloetens, F. Peyrin, T. Scotti, P. Herzog, J. Gerlach, N. Pollet, and J.-F. Aubry. 2013. How minute sooglossid frogs hear without a middle ear. *Proceedings of the Academy of Natural Sciences of Philadelphia 110:* 15360–15364.

Bravo-Valencia, L. and M. Rivera-Correa. 2011. A new species of harlequin frog (Bufonidae: *Atelopus*) with an unusual behaviour from Andes of Colombia. *Zootaxa 3045:* 57–67.

Cochran, D. M. and C. J. Goin. 1970. Frogs of Colombia. *Bulletin of the United States National Museum 288:* 1–655.

Coloma, L. A. 1997. Morphology, systematics, and phylogenetic relationships among frogs of the genus *Atelopus* (Anura: Bufonidae). Unpublished Ph.D. Doctoral dissertation. University of Kansas, Lawrence, USA.

Coloma, L. A. 2002. Two new species of *Atelopus* (Anura: Bufonidae) from Ecuador. *Herpetologica 58:* 229–252.

Coloma, L. A. and W. E. Duellman 2025. *Amphibians of Ecuador. Pipidae, Telmatobiidae, Microhylidae, Dendrobatidae, Ranidae, and Hylidae. Volume II.* Boca Raton. CRC Press. 700 pp.

Coloma, L. A., S. Lötters, and A. W. Salas 2000. Taxonomy of the *Atelopus ignescens* complex (Anura: Bufonidae): designation of a neotype of *Atelopus ignescens* and recognition of *Atelopus exiguus. Herpetologica 56:* 303–324.

Coloma, L. A., W. E. Duellman, C. A. Almendáriz, S. R. Ron, A. Terán-Valdez, and J. M. Guayasamin. 2010. Five new (extinct?) species of *Atelopus* (Anura: Bufonidae) from Andean Colombia, Ecuador, and Peru. *Zootaxa 2574:* 1–54.

Dias, P. H. S. and M. Anganoy-Criollo. 2024. Harlequin frog tadpoles—comparative buccopharyngeal morphology in the gastromyzophorous tadpoles of the genus *Atelopus* (Amphibia, Anura, Bufonidae), with discussion on the phylogenetic and evolutionary implication of characters. *Science of Nature 111:* 3.

Dias, P. H. S., J. R. Phillips, M. O. Pereyra, D. B. Means, A. Haas, and P. J. R. Kok. 2024. The remarkable larval morphology of *Rhaebo nasicus* (Werner, 1903) (Amphibia: Anura: Bufonidae) with the erection of a new bufonid genus and insights into the evolution of suctorial tadpoles. *Zoological Letters 10:* 17.

Dufresnes, C., N. Poyarkov, and D. Jablonski 2023. Acknowledging more biodiversity without more species. *Proceedings of the National Academy of Sciences of the United States of America 120:* e2302424120.

Fabrezi, M. and P. Alberch. 1996. The carpal elements of anurans. *Herpetologica 52:* 188–204.

Flechas, S. V., A. Paz, A. J. Crawford, C. Sarmiento, A. A. Acevedo, A. Arboleda, W. Bolívar-García, C. L. Echeverry-Sandoval, R. Franco, C. Mojica, A. Muñoz, P. Palacios-Rodríguez, A. M. Posso-Terranova, P. Quintero-Marín, L. A. Rueda-Solano, F. Castro-Herrera, and A. Amézquita. 2017. Current and predicted distribution of the pathogenic fungus *Batrachochytrium dendrobatidis* in Colombia, a hotspot of amphibian biodiversity. *Biotropica 49:* 685–694.

Frost, D. R. (ed.). 2025. Amphibian Species of the World: An Online Reference. Version 6.2. Electronic Database accessible at https://amphibiansoftheworld.amnh.org/index.php. Captured on 30 August 2025.

Galvis-Cordoba, R. A. and J. M. Carvajalino-Fernández. 2025. *Atelopus marinkellei* Cochran & Goin, 1970 (Amphibia, Anura, Bufonidae): after 20 years, the rediscovery of a Critically Endangered species in the páramo of Siscunsí, a Neotropical high-mountain ecosystem. *Check List 21:* 852–856.

Grant, T., M. L. Lyra, M. Hofreiter, M. Preick, A. Barlow, V. K. Verdade, and M. T. Rodrigues. 2025. Museomics and the systematics of the Atlantic Forest Nurse Frogs (Dendrobatoidea: Aromobatidae: Allobatinae). *Bulletin of the American Museum of Natural History 2025:* 1–76.

Gray, P. and D. C. Cannatella. 1985. A new species of *Atelopus* (Anura, Bufonidae) from the Andes of northern Perú. *Copeia 1985:* 910–917.

Guayasamin, J. M., E. Bonaccorso, W. E. Duellman, and L. A. Coloma. 2010. Genetic differentiation in the nearly extinct harlequin frogs (Bufonidae: *Atelopus*), with emphasis on the Andean *Atelopus ignescens* and *A. bomolochos* species complexes. *Zootaxa 2574:* 55–68.

Hernández-Córdoba, O. D., V. E. Cardona-Botero, and F. Castro-Herrera. 2014. Amphibia, Anura, Bufonidae, *Atelopus eusebianus* (Rivero & Granados-Díaz, 1993): distribution extension for Valle del Cauca, Colombia. *Check List 10:* 682–683.

Herrera-Lopera, J. M., M. Solé, and C. A. Cultid-Medina. 2025. Mapping the missing: assessing amphibian sampling completeness and overlap with global protected areas. *Ecology and Evolution 15:* e71137.

IUCN SSC Amphibian Specialist Group. 2017. *Atelopus ebenoides. The IUCN Red List of Threatened Species 2017: e.T81646342A49535044.* Electronic Database accessible at https://www.iucnredlist.org/species/81646342/49535044. Captured on 17 February 2025.

IUCN SSC Amphibian Specialist Group. 2019. *Atelopus angelito. The IUCN Red List of Threatened Species: e. T54488A49534394*. Electronic Database accessible at https://www.iucnredlist.org/species/54488/49534394. Captured on 17 February 2025.

IUCN SSC Amphibian Specialist Group. 2021. *Atelopus eusebianus. The IUCN Red List of Threatened Species: e. T54507A190204051.* Electronic Database accessible at https://www.iucnredlist.org/species/54507/190204051. Captured on 17 February 2025.

IUCN SSC Amphibian Specialist Group. 2024. *Atelopus marinkellei. The IUCN Red List of Threatened Species: e. T81646204A245672075.* Electronic Database accessible at https://www.iucnredlist.org/species/81646204/245672075. Captured on 17 February 2025.

Kattan, G. 1986. Nueva especie de rana (*Atelopus*) de los Farallones de Cali, Cordillera Occidental de Colombia. *Caldasia 14:* 651–657.

La Marca, E., K. R. Lips, S. Lötters, R. Puschendorf, R. Ibáñez, J. V. Rueda-Almonacid, R. Schulte, C. Marty, F. Castro, J. Manzanilla-Puppo, J. E. García-Pérez, F. Bolaños, G. Chaves, J. A. Pounds, E. Toral, and B. E. Young. 2005. Catastrophic population declines and extinctions in Neotropical harlequin frogs (Bufonidae: *Atelopus*). *Biotropica 37:* 190–201.

Lips, K. R., J. Diffendorfer, J. R. Mendelson III, and M. W. Sears. 2008. Riding the wave: reconciling the roles of disease and climate change in amphibian declines. *PLoS Biology 6:* e72.

Lötters, S. 1996. *The Neotropical Toad Genus* Atelopus. *Checklist – Biology – Distribution*. Cologne. M. Vences & F. Glaw. 154 pp.

Lötters, S., A. Plewnia, A. Hönig, A. Jung, J. Laudor, and T. Ziegler. 2022. The gastromyzophorous tadpole of the pink harlequin frog from Suriname with comments on the taxonomy of Guiana clade *Atelopus* (Amphibia, Bufonidae). *Zootaxa 5087:* 591–598.

Lötters, S., P. Böning, S. Bailon, J. D. B. Castañeda, R. Boistel, A. Catenazzi, J. C. Chaparro, G. Chávez, A. Chujutalli, L. Coen, L. A. Coloma, A. J. Crawford, J. Culebras, J. C. C. Martínez, J. M. Daza, I. De la Riva, D. J. Ellwein, R. Ernst, S. V. Flechas, A. Fouquet, J. M. Guayasamin, C. Heine, R. F. Jorge, A. Jung, K.-H. Jungfer, N. Kaffenberger, H. Krehenwinkel, E. La Marca, M.

Lampo, G. F. M. Rangel, L. Orsen, D. J. Paluh, J. L. P. Gonzales, J. Perrin, A. B. Q. Riera, J. P. Reyes-Puig, B. R.-R. Ross, D. C. Rößler, L. A. R. Solano, D. Salazar-Valenzuela, J. C. S. Vazquez, A. Terán-Valdez, A. Tovar, M. Veith, P. Venegas, R. von May, T. Weitkamp, and A. Plewnia. 2025. A roadmap for harlequin frog systematics, with a partial revision of Amazonian species related to *Atelopus spumarius*. *Zootaxa 5571:* 1–76.

Lötters, S., A. Plewnia, A. Catenazzi, K. Neam, A. R. Acosta-Galvis, Y. A. Vela, J. P. Allen, J. O. A. Segundo, A. L. A. Cabezas, G. A. Barboza, K. R. Alves-Silva, M. Anganoy-Criollo, E. A. Ortiz, J. D. Arpi L., A. Arteaga, O. Ballestas, D. B. Moscoso, J. D. Barros-Castañeda, A. Batista, M. H. Bernal, E. Betancourt, Y. O. C. Bitar, P. Böning, L. Bravo-Valencia, J. F. C. Andrade, D. Cadenas, J. C. C. Auza, G. A. Chaves-Portilla, G. Chávez, L. A. Coloma, C. F. Cortez-Fernandez, E. A. Courtois, J. Culebras, I. De la Riva, V. Diaz, L. C. E. Lara, R. Ernst, S. V. Flechas, T. Foch, A. Fouquet, C. Z. G. Méndez, J. E. García-Pérez, D. A. Gómez-Hoyos, S. C. Gomides, J. Guerrel, B. Gratwicke, J. M. Guayasamin, E. Griffith, V. Herrera-Alva, R. Ibáñez, C. I. Idrovo, A. J. Monge, R. F. Jorge, A. Jung, B. Klocke, M. Lampo, E. Lehr, C. H. R. Lewis, E. D. Lindquist, Y. R. López-Perilla, G. Mazepa, G. F. Medina-Rangel, A. M. Viteri, K. Mulder, M. Pacheco-Suarez, A. Pereira-Muñoz, J. L. Pérez-González, M. A. P. Erazo, A. G. P. Florez, M. Ponce, V. Poole, A. B. Q. Riera, A. J. Quiroz, M. Quiroz-Espinoza, A. R. Guerra, J. P. Ramírez, S. Reichle, H. Reizine, M. Rivera-Correa, B. R.-R. Ross, A. Rocha-Usuga, M. T. Rodrigues, S. R. Montaño, D. C. Rößler, L. A. R. Solano, C. Señaris, A. Shepack, F. R. S. Pesántez, A. Sorokin, A. Terán-Valdez, G. Torres-Ccasani, P. C. Tovar-Siso, L. M. Valencia, D. A. Velásquez-Trujillo, M. Veith, P. J. Venegas, J. Villalba-Fuentes, R. von May, J. F. W. Bernal, and E. La Marca. 2023. Ongoing harlequin toad declines suggest the amphibian extinction crisis is still an emergency. *Communications Earth and Environment 4:* 412.

Lynch, J. D. 1993. A new harlequin frog from the Cordillera Oriental of Colombia (Anura, Bufonidae, *Atelopus*). *Alytes 11:* 77–87.

Lynch, J. D. and Á. M. S. Mayorga. 2011. Clave ilustrada de los renacuajos en las tierras bajas al Oriente de los Andes, con énfasis e n Hylidae. *Caldasia 33:* 235–270.

Mahony, S., R. G. Kamei, R. M. Brown, and K. O. Chan. 2024. Unnecessary splitting of genus-level clades reduces taxonomic stability in amphibians. *Vertebrate Zoology 74:* 249–277.

Marcillo-Lara, A., L. A. Coloma, S. Álvarez-Solas, and E. Terneus. 2020. The gastromyzophorous tadpoles of *Atelopus elegans* and *A. palmatus* (Anura: Bufonidae), with comments on oral and suction structures. *Neotropical Biodiversity 6:* 1–13.

MCZbase, Harvard University. 2024. MCZ Herpetology A-117992, Paratype of *Atelopus eusebianus*. Museum of Comparative Zoology, Harvard University. Electronic Database accessible at https://mczbase.mcz.harvard.edu/guid/MCZ:Herp:A-117992. Captured on 01 Jun. 2024.

Olson, D. H., K. L. Ronnenberg, C. K. Glidden, K. R. Christiansen, and A. R. Blaustein. 2021. Global patterns of the fungal pathogen *Batrachochytrium dendrobatidis* support conservation urgency. *Frontiers in Veterinary Science 8:* 685877.

Osorno-Muñoz, M., M. C. Ardila-Robayo, and P. M. Ruíz-Carranza. 2001. Tres nuevas especies del género *Atelopus* A.M.C. Dumeril & Bibron 1841 (Amphibia: Bufonidae) de las partes altas de la Cordillera Oriental Colombiana. *Caldasia 23:* 509–522.

Padial, J. M., A. Miralles, I. De la Riva, and M. Vences. 2010. The integrative future of taxonomy. *Frontiers in Zoology 7:* 16.

Péfaur, J. E. and W. E. Duellman. 1980. Community structure in high Andean herpetofaunas. *Transactions of the Kansas Academy Science 83:* 45–65.

Plewnia, A., K. Venegas-Valencia, K. Szepanski, C. Heine, P. Böning, J. P. Ramírez, and S. Lötters. 2025. A new harlequin toad from the Cordillera Oriental of the Colombian Andes (Bufonidae: *Atelopus*). *Salamandra 61:* 267–282.

Rivero, J. A. 1963. Five new species of *Atelopus* from Colombia, with notes on other forms from Colombia and Ecuador. *Caribbean Journal of Science 3:* 103–124.

Rivero, J. A. and H. Granados-Díaz. 1993. Nueva especie de *Atelopus* (Amphibia: Bufonidae) del Departamento del Cauca, Colombia. *Caribbean Journal of Science 29:* 12–17.

Rueda-Almonacid, J. V., J. D. Lynch, and A. Amézquita. 2004. *Libro Rojo de los Anfibios de Colombia. Serie Libros Rojos de Especies Amenazadas de Colombia.* Bogotá. Conservación Internacional Colombia, Instituto de Ciencias Naturales, Ministerio del Medio Ambiente, Bogotá. 384 pp.

Rueda-Almonacid, J. V., J. V. Rodríguez-Mahecha, E. La Marca, S. Lötters, T. Kahn, and A. Angulo. 2005. *Ranas Arlequines. Serie Libretas de Campo 5*. Bogotá. Conservación Internacional Colombia. 159 pp.

Ruíz-Carranza, P. M. and M. Osorno-Muñoz. 1994. Tres nuevas especies de *Atelopus* A.M.C. Duméril & Bibron 1841 (Amphibia: Bufonidae) de la cordillera central de Colombia. *Revista de la Academia Colombiana de Ciencias Exactas, Físicas y Naturales 72:* 165–179.

Ruíz-Carranza, P. M., M. C. Ardila-Robayo, and J. D. Lynch. 1996. Lista actualizada de la fauna de Amphibia de Colombia. *Revista de la Academia Colombiana de Ciencias Exactas, Físicas y Naturales 20:* 365–415.

Savage, J. M. and R. W. Heyer. 1997. Digital webbing formulae for anurans: a refinement. *Herpetological Review 28:* 131.

Scherz, M. D., S. M. Rasolonjatovo, J. Köhler, L. Rancilhac, A. Rakotoarison, A. P. Raselimanana, A. Ohler, M. Preick, M. Hofreiter, F. Glaw, and M. Vences. 2020. 'Barcode fishing' for archival DNA from historical type material overcomes taxonomic hurdles, enabling the description of a new frog species. *Scientific Reports 10:* 19109.

Velásquez-Trujillo D. A., F. Castro-Herrera, S. Lötters, and A. Plewnia. 2024. A new species of harlequin toad from the Western Cordillera of Colombia (Bufonidae: *Atelopus*), with comments on other forms. *Salamandra 60:* 67–81.

Vélez-Rodríguez, M. C. and P. M. Ruíz-Carranza. 1997. Una nueva especie de *Atelopus* (Amphibia: Anura: Bufonidae) de la Cordillera Central, Colombia. *Revista de la Academia Colombiana de Ciencias Exactas, Físicas y Naturales 21:* 555–563.

Wassersug, R. J. 1976. Oral morphology of anuran larvae: terminology and general description. *Occasional Papers of the Museum of Natural History of University of Kansas 48:* 1–23.

Wassersug, R. J. 1980. Internal oral features of larvae from eight anuran families: functional, systematic, evolutionary and ecological consideration. *Miscellaneous Publications of the University of Kansas Museum of Natural History 68:* 1–148.

Editor: Vanessa K. Verdade

Appendix I. *Comparative specimens examined.*

Atelopus ardila: Colombia: Nariño, Pasto, Hacienda San Gerardo, ICN 450, 459, 469, 471, 473 (paratypes); Volcán Galeras, ICN 3406 (paratypes); La Laguna, San Fernando, ICN 3636-3638 (paratypes); 12 km E of Pasto, IAvH-Am-21.

Atelopus arsyecue: Colombia: Cesar, Valledupar, Cuenca alta del Río Guatapurí, IAvH-Am-5641 (holotype), 5642, 5643 (paratopoypes); Parque Nacional Natural Sierra Nevada de Santa Marta, cumbre Hato del Medio, surroundings of Lago Curigua, IAvH-Am-5297 (paratype).

Atelopus farci: Colombia, Cundinamarca, Albán, Granja de Padre Luna, ICN 14488 (holotype), ICN 14489–14533 (paratopotypes).

Atelopus guacharo: Colombia, Huila, Parque Nacional Natural Cueva de los Guácharos, trail to cabaña 2, IAvH-Am-544 (holotype).

Atelopus guitarraensis: Colombia, Meta, Macizo de Sumapaz, Laguna La Guitarra, ICN 23348 (holotype), ICN 23349–23351, 32432, 32433 (cleared & stained), ICN 32530 (cleared & stained) (all paratopotypes).

Atelopus laetissimus: Colombia: Magdalena, Parque Nacional Natural Sierra Nevada de Santa Marta, San Lorenzo, IAvH-Am-3199, 3201, 3203, SW of the Estación Experimental San Lorenzo, ICN 410 (holotype), 415, 417, 418, 420, 1196, 1199, 33734–33737 (all paratopotypes).

Atelopus lozanoi: Colombia: Cundinamarca, La Calera, Parque Nacional Natural Chingaza, Páramo de Palacio, Quebrada Caliche, ICN 378–383, 384 (paratopotype), ICN 385, 386 (paratopotype), ICN 387, 388 (paratopotype), ICN 389 (paratopotype), ICN 390, 391, 392 (paratopotype), ICN 1125 (paratopotype), ICN 1126 (paratopotype), ICN 1127, 1128, 1254, 1255, 1296, 1297 (paratopotype), ICN 1299 (paratopotype), ICN 1300, 1301 (holotype), ICN 33376–33378 (paratopotypes); road from La Calera to Guasca, km 24–25 from Chuza, ICN 21147, 21148; Páramo de Palacio, IAvH-Am-3105, 3499; Parque Nacional Natural Chingaza, IAvH-Am-5904, 5905, 7167, 7168, 8635, 8636, 8667, 52, 6633, 14893, 14894, 14896, 14902, 9796, 9797, 9812.

Atelopus mandingues: Colombia, Cundinamarca, Junin, Reserva Biologica Carpanta, ICN 19569, 21155, 22351, 26102, 34286, 34716–34723 (paratopotypes), ICN 34959 (holotype), ICN 34286, 34287, 45149, 45150.

Appendix I. *Continued.*

Atelopus mittermeieri: Colombia: Santander, El Encino, Santuario de fauna y flora Guanentá, Alto Río Fonce, Quebrada Aguas Claras, ICN 52993 (holotype); Gambita, Bogotacito, km 55–56 of Duitama-Charala road, Río Guillermo, ICN 12752–12762, 12765–12769 (paratypes).

Atelopus muisca: Colombia: Cundinamarca, Junin, Reserva Biologica Carpanta, ICN 21158 (paratype), ICN 21159; Parque Nacional Natural Chingaza, surroundings of Laguna de Chingaza, IAvH-Am-16585–16591, 16619–16623; Parque Nacional Natural Chingaza, sector Chuza, IAvH-Am-5398–5407; Chuza reservoir, IAvH-Am-4630 (paratype), IavH-Am 5045–5051 (paratypes); Chuza reservoir, Quebrada Babilonia, IAvH-Am-5091 (paratype); Chuza reservoir, Montaña del Cóndor, IAvH-Am-4648, 4649, 1650 (holotype), IAVH-Am 4652; km 6 from Chuza, sitio La Arboleda, IAvH-Am-4758 (paratype), 5030–5032; Parque Nacional Natural Chingaza, sector Río La Playa, IAvH-Am-5052–5059 (paratypes), 5080–5092 (paratypes).

Atelopus orcesi: Ecuador, Sucumbíos, road from La Alegría to Sibundoy, MHNG 2684.75 (holotype), MHNG 2559.67 (paratopotype).

Atelopus pastuso: Ecuador, Carchi, Tulcán, MHNG 2258.64–2258.74, 2271.39, 2271.40.

Atelopus quimbaya: Colombia: Risaralda, Pereira, Parque Regional Ucumari, Cedral-Ceilan trail, ICN 23339 (holotype), ICN 23340–23347 (paratopotypes); Quindio, Salento, Reserva Forestal del Caño del Quindio, vereda Cocora or Río Arriba, Estación La Montaña, IAvH-Am-5191–5198, 7175, 7178.

Atelopus simulatus: Colombia: Cauca, road from Belalcázar to Cabaña La Termal of INDERENA, banks of Río Paez, ICN 6708–6710 (paratypes); km 41 on road from Belalcázar to Cabaña La Termal of INDERENA, ICN 7259–7260 (paratypes), 7261 (holotype), ICN 7262–7264 (paratopotypes), ICN 7265–7268; Vereda Río Sucio, km 61–67 on road from Popayan to Inzá, ICN 11331, 11332, 11346, 11347 (paratypes).

Atelopus subornatus: Colombia: Cundinamarca, Fusagasugá, ZFMK 28104 (lectotype), 28105 (paralectotype); Alto de Sibaté, ZFMK 28106 (paralectotype), 28107 (holotype of junior synonym *A. flaviventris*); km 7 on road from Bogotá to Sibaté, quebrada Agua Bonita, ICN 34275–34279.

Appendix II. *Individual measurements (in mm) of specimens of* Atelopus *included in Tables 1 and 2. For measurements of holotypes, see the redescriptions.*

Specimen	Species	Type status	Sex	SVL	TIBL	FOOT	HLSQ	IOD	HDWD	EYDM	EYNO	ITNA	FAL	HAND	THBL	SW
MCZ 117992	*A. ebenoides*	paratype (*eusebianus*)	female	43.6	15.4	16.1	12.5	4.2	11.7	3.2	2.9	3.8	10.9	11.1	7.3	12.9
ICN33413	*A. ebenoides*	paratype (*angelito*)	female	43.7	16.6	14.4	10.9	4.7	11.8	3.4	2.9	4.3	11.2	8.9	6	11.9
IAvH 6497	*A. ebenoides*	paratype (*angelito*)	female	33.4	11.5	12.5	10.1	4.1	9.5	3.4	2.8	3.5	9.4	7.7	5.4	9.1
IAvH 6282	*A. ebenoides*	N	female	55.2	15.4	16.1	11.5	3.8	11.7	3.6	3.1	4.2	12	10.5	7	11.9
IAvH 3920	*A. ebenoides*	N	female	46.6	17.2	19.3	13.6	4	12.5	4.1	3.6	4.4	12.7	11.8	8	14
IAvH 37	*A. ebenoides*	N	female	40.7	14.8	15.5	12.1	4.8	10.9	3.8	3.2	3.8	11.3	8.5	6	10.4
IAvH 7882	*A. ebenoides*	N	female	42.6	15.3	18	12	4.4	11.4	3.6	3.3	3.6	11.6	11	6.7	10.8
IAvH 526	*A. ebenoides*	N	female	46	16	16	13.7	4.6	12.6	3.7	3.4	4.4	12.8	10.2	6.7	13.8
IAvH 6285	*A. ebenoides*	N	female	44	15.8	18.4	13	5.1	11.7	3.9	3.8	3.5	12.8	11.2	7.1	12.7
IAvH 9739	*A. ebenoides*	N	female	43.8	16.3	17.1	12.8	5	12	3.7	3.7	4.2	12.6	10.8	7.1	12.9
IAvH 6284	*A. ebenoides*	N	male	36.1	13.2	15	11	4.1	10.5	3.5	3	4	10.5	8.7	5.5	9.8
IAvH 9740	*A. ebenoides*	N	male	32.8	12.8	13.8	11	4	10	3.3	2.6	3.6	10	8.1	4.6	9.8
ICN 33408	*A. ebenoides*	holotype (*angelito*)	male	34.3	12.3	15.3	11.1	3.8	9.9	2.9	2.7	3.9	NA	NA	NA	NA
ICN 33411	*A. ebenoides*	paratype (*angelito*)	male	36.4	13.5	15	10.6	3.3	11	3.2	2.7	3.7	10	9.3	5.8	9.5
ICN 33410	*A. ebenoides*	paratype (*angelito*)	male	35.4	12.9	13.7	8.8	3.4	9.5	2.9	2.3	3.9	10.2	8.4	5.3	10

Appendix II. *Continued.*

Specimen	Species	Type status	Sex	SVL	TIBL	FOOT	HLSQ	IOD	HDWD	EYDM	EYNO	ITNA	FAL	HAND	THBL	SW
IAvH-Am-6045	*A. marinkellei*	N	female	42.5	14.7	16	12.7	4	10.7	3.4	3.4	3.6	12	10.4	6.4	11.9
IAvH-Am-6046	*A. marinkellei*	N	female	44.8	14.4	16.4	12.8	3.6	11	3.6	3.4	4	12	10.2	6.6	11.7
IAvH-Am-6050	*A. marinkellei*	N	female	41	14	15.3	11.5	3.5	10.4	3.5	2.8	3.5	11	9.7	6	11
IAvH-Am-6055	*A. marinkellei*	N	female	46	14.6	16.2	13.2	4	10.7	3.7	3.4	4	11.3	10.6	6.7	12.2
IAvH-Am-2324	*A. marinkellei*	N	male	31.4	12.2	12.8	10	3.4	9.3	3.1	2.7	3.2	9.8	7.7	5.1	8.6
IAvH-Am-4356	*A. marinkellei*	N	male	32.7	12.3	13.3	10.7	3.5	9.5	3.2	2.5	3.4	10	8.7	4.6	8.3
IAvH-Am-6047	*A. marinkellei*	N	male	34	12.5	13	10.3	3.4	9.4	3.2	2.4	3.4	9.5	7.8	5	8.8
IAvH-Am-9657	*A. marinkellei*	N	male	33.6	12.1	13.4	10.6	4	9.7	3.8	2.4	3.2	10	8.4	5	8.7
NHMW 32716	*A. marinkellei*	N	male	31.9	11.8	12.8	10.6	13.6	9	3.4	3	3	9	7.8	5	8.3

Phyllomedusa 24(2):255–269, 2025

ISSN 1519-1397 (print) / ISSN 2316-9079 (online)
doi: http://dx.doi.org/10.11606/issn.2316-9079.v24i2p255-269

Description of the advertisement call of *Dendropsophus frosti* (Anura: Hylidae) as a phenotypic evidence of its phylogenetic relationships

Alexandre P. Almeida,[1,2] Pedro Peloso,[3] Marcelo Gordo,[4] Marcelo J. Sturaro,[5] João Carlos L. Costa,[6] Rommel R. Rojas,[7] Vinícius T. Carvalho,[4] and Robson W. Ávila[2]

[1]Universidade Federal de Santa Catarina, Departamento de Ecologia e Zoologia, Programa de Pós-Graduação em Ecologia. Florianópolis, SC, Brazil. E-mail: alexandre.dealmeida@hotmail.com.

[2]Universidade Federal do Ceará, Núcleo Regional de Ofiologia, Centro de Ciências. Fortaleza, CE, Brazil. E-mail: robsonavila@gmail.com.

[3]California State Polytechnic University, Department of Biological Sciences. Arcata, California, USA. E-mail: pedropeloso@gmail.com.

[4]Universidade Federal do Amazonas, Departamento de Biologia, Instituto de Ciências Biológicas. Manaus, AM, Brazil. E-mail: mgordo@ufam.edu.br.

[5]Universidade Federal de São Paulo, Departamento de Ecologia e Biologia Evolutiva, Instituto de Ciências Ambientais. Diadema, SP, Brazil. E-mail: marcelosturaro@gmail.com.

[6]Museu Paraense Emílio Goeldi, Coordenação de Zoologia, Belém, PA, Brazil. E-mail: joaoclcosta@gmail.com.

[7] Universidad Nacional de la Amazonia Peruana, Departamento de Ecologia y Fauna, Museo de Zoologia. Iquitos, Loreto, Peru. E-mail: rrojaszamora@gmail.com.

Abstract

Description of the advertisement call of *Dendropsophus frosti* (Anura: Hylidae) as a phenotypic evidence of its phylogenetic relationships. For amphibians, gaps in knowledge about natural history and geographic distribution are among the major causes that blur our understanding of their diversity. These key pieces of information contribute to our understanding off taxonomy, systematics, ecology, and conservation. Herein, we provide new information on the geographic distribution and describe for the first time the advertisement call of *Dendropsophus frosti* from western Amazonia. The call consists of two types of short notes, a trilled multipulsed note with a duration ranging from 158 to 297 ms (note type A), and a high-pitched pulsatile note with a duration of about 9 ms (note type B). The dominant frequency of note type A is about 4260 Hz, while that of note type B is around 4330 Hz. The notes are emitted in two call arrangements, a complex call formed by one note type A followed by one or two type B notes or a composite call formed by two to seven type B notes. Overall, the call structure of *D. frosti,* with those two types of notes emitted in complex or composite calls, is shared with closely related species from the *D. parviceps* group, showing a phylogenetic signal. Our results suggest that acoustic characters may represent phylogenetic informative traits for the *Dendropsophus parviceps* group,

Received 15 April 2025
Accepted 20 October 2025
Distributed December 2025

supporting the current taxonomy. Additionally, our findings extended the known geographic distribution by approximately 700 km eastward. Our results highlight once again the necessity of biological surveys in remote areas of Amazonia, where many knowledge gaps persist.

Keywords: Bioacoustics, *Dendropsophus parviceps* group, Raunkiæran shortfall, Wallacean shortfall.

Resumo

Descrição do canto nupcial de *Dendropsophus frosti* (Anura: Hylidae) como uma evidência fenotípica das suas relações filogenéticas. Para os anfíbios, as lacunas no conhecimento sobre a história natural e a distribuição geográfica estão entre as principais causas que obscurecem a nossa compreensão da sua diversidade. Essas são informações fundamentais para a taxonomia, sistemática, ecologia e conservação. Aqui, fornecemos novas informações sobre a distribuição geográfica e descrevemos, pela primeira vez, o canto de acasalamento do *Dendropsophus frosti*, da Amazônia ocidental. O canto consiste em dois tipos de notas curtas, uma nota trilada multipulsionada com duração variando de 158 a 297 ms (nota tipo A) e uma nota pulsante aguda com duração de cerca de 9 ms (nota tipo B). A frequência dominante da nota tipo A é de cerca de 4260 Hz, enquanto a da nota tipo B é de cerca de 4330 Hz. As notas são emitidas em dois arranjos de cantos, um canto complexo formado por uma nota A seguida por uma ou duas notas do tipo B, ou um canto composto formado por duas a sete notas do tipo B. No geral, a estrutura de vocalização de *D. frosti*, com esses dois tipos de notas emitidas em cantos complexos ou compostos, é compartilhada com espécies intimamente relacionadas do grupo *Dendropsophus parviceps*, mostrando sinal filogenético. Os nossos resultados sugerem que as características acústicas podem representar um caráter filogenético informativo para o grupo *D. parviceps*, apoiando a taxonomia atual. Além disso, nossas descobertas ampliaram a distribuição geográfica conhecida em aproximadamente 700 km a leste. Nossos resultados destacam mais uma vez a importância dos levantamentos biológicos em áreas remotas da Amazônia, onde persistem muitas lacunas de conhecimento.

Palavras-chave: Bioacústica, Déficit de Raunkiæran, Déficit de Wallacean, Grupo *Dendropsophus parviceps*.

Introduction

The lack of information on life-history traits and geographic distribution of species, known respectively as the Raunkiæran and Wallacean shortfalls, creates biases in our understanding of biodiversity and compromises knowledge in ecology, evolution, and conservation (Yang *et al.* 2013, Hortal *et al.* 2015). Sampling biases are well-known causes of shortfalls in anuran biodiversity, especially in regions like the Amazon rainforest, which harbors high species richness and encompasses large unexplored areas (Azevedo-Ramos and Gallati 2002, Peloso 2010, Mayer *et al.* 2019, Guerra *et al.* 2020, Moraes *et al.* 2022).

Vocalization and acoustic traits are crucial for studies of behavior, physiology, reproductive biology, ecology, evolutionary history, and taxonomy of amphibians (Wells 1977, Duellman and Trueb 1994, Kohler *et al.* 2017). Among the different acoustic signals, the advertisement call is the most extensively studied acoustic signal emitted by frogs (Wells 1977, Gerhardt 1994). These traits are influenced by various selective pressures and contain phylogenetic signals in frog phylogeny (Gingras *et al.* 2013, Forti *et al.* 2015), which varies in taxonomic scale (e.g. Forti *et al.* 2017). Despite advances in the last decades in the number of studies and described calls, a significant gap in the knowledge of this trait remains. The advertisement call is unknown in about 35% of anuran species (Guerra *et al.* 2018).

Dendropsophus Fitzinger, 1843 comprises 106 recognized species (Frost 2025) and nine species groups (*sensu* Orrico *et al.* 2021). One of these groups, the *Dendropsophus parviceps* group, has received significant attention in recent years, including descriptions of new species (e.g., Motta *et al.* 2012, Fouquet *et al.* 2015, Rivadeneira *et al.* 2018), taxonomic revisions (Fouquet *et al.* 2011, Orrico *et al.* 2013, 2021, Melo-Sampaio 2023), and studies of new natural history data (Forti *et al.* 2015, Orrico *et al.* 2021). Currently, this group includes 19 species: *Dendropsophus bokermanni* (Goin, 1960); *Dendropsophus brevifrons* (Duellman and Crump, 1974); *Dendropsophus counani* Fouquet, Orrico, Ernst, Blanc, Martinez, Vacher, Rodrigues, Ouboter, Jairam, and Ron, 2015; *Dendropsophus frosti* Motta, Castroviejo-Fisher, Venegas, Orrico, and Padial, 2012; *Dendropsophus garagoensis* (Kaplan, 1991); *Dendropsophus giesleri* (Mertens, 1950); *Dendropsophus grandisonae* (Goin, 1966); *Dendropsophus kamagarini* Rivadeneira, Venegas, and Ron, 2018; *Dendropsohus kubricki* Rivadeneira, Venegas, and Ron, 2018; *Dendropsophus luteoocellatus* (Roux, 1927); *Dendropsohus microps* (Peters, 1872); *Dendropsophus padreluna* (Kaplan and Ruiz-Carranza, 1997); *Dendropsophus parviceps* (Boulenger, 1882); *Dendropsophus pauiniensis* (Heyer, 1977); *Dendropsophus praestans* (Duellman and Trueb, 1983); *Dendropsophus subocularis* (Dunn, 1934); *Dendropsophus timbeba* (Martins and Cardoso, 1987); *Dendropsophus virolinensis* (Kaplan and Ruiz-Carranza, 1997); and *Dendropsophus yaracuyanus* (Mijares-Urrutia and Rivero, 2000). It also includes three nominal clades (*D. microps, D. garagoensis,* and *D. subocularis* clades), which highlight morphological similarities or phylogenetic relationships with taxonomic implications (see Orrico *et al.* 2021).

Dendropsophus frosti is a small treefrog in the *D. parviceps* group, closely related phylogenetically to the *D. subocularis* clade (Motta *et al.* 2012, Orrico *et al.* 2021). The species is known only from a few localities in the western Amazonian lowlands. Until recently, it was known to occur only in Colombia and Peru, but Koch *et al.* (2023) reported it from Tabatinga and Japurá municipalites, Amazonas state, Brazil. Despite its relative well-resolved phylogenetic relationship (Motta *et al.* 2012, Fouquet *et al.* 2015, Orrico *et al.* 2021), *D. frosti* does not share any of the known phenotypic synapomorphies of the *D. parviceps* group (Orrico *et al.* 2021). Furthermore, its reproductive biology, vocalization, tadpole morphology, and even its geographic range remain poorly known.

Given the importance of these features for *Dendropsophus* species, natural history, taxonomy, phylogeny and systematics (Orrico *et al.* 2009, Hepp *et al.* 2012, Teixeira *et al.* 2015), herein we describe the advertisement call of *D. frosti,* recorded from males recently collected near the type locality and from a new occurrence in Central Amazonia. Additionally, we reassess its habitat, calling sites, and geographic distribution, and discuss the role of these traits in the taxonomy of the *D. parviceps* group.

Materials and Methods

Study Site and Advertisement Call Recordings

We collected our data from three different expeditions conducted in the Brazilian Amazon, state of Amazonas, over the last ten years. Fieldwork was first carried out on the right bank of Japurá River (01°50'46.10" S, 69°01'46.30" W, 103 m a.s.l.), near Vila Bittencourt village, between 14 August and 20 September 2014, where we collected eight specimens of *D. frosti.* This locality is close to that reported by Koch *et al.* (2023), which is based on a single specimen. We describe the habitat where we found the additional specimens. A second expedition was conducted in the Parque Nacional do Jaú (hereafter PNJ), a protected area in Central Amazonia, about 200 km up the Negro River from Manaus. Fieldwork at PNJ took place from 16 to 28 February 2017, along the sampling sites

on the banks of the Jaú River. On February 24, at one of the sampling sites (02°17'39" S, 62°27'21" W, 41 m a.s.l.), we collected 14 specimens and recorded calling males after a heavy afternoon rainfall. The recordings were made using a Marantz PMD620 recorder with an internal microphone. The final expedition occurred on 5 May 2018 during the rainy season, in a forest fragment in the area of Comando de Fronteira Solimões / 8º Batalhão de Infantaria de Selva of the Brazilian Army (04°14'52.77" S, 69°55'51.05' ' W, 83 m a.s.l.), near the limits of Tabatinga municipality, approximately 15 km straight line from the type-locality of the species. Four specimens were collected and calling males were recorded after rainfall between 19:00 h and 23:00 h, using a Zoom H1/Handy recorder. Additionally, E. Koch provided us with a recording of an unvouchered male specimen from the same locality. Koch's recording was obtained on April 29, 2021, after heavy rainfall, using WavePad free recording app (NCH Software 2015) on a smartphone with an internal microphone. All recordings were made at 44,100 Hz sampling rate and 16-bits resolution. Digital copies of all recordings analyzed are deposited in the Coleção Bioacústica of Universidade Federal de Minas Gerais (CBUFMG), Belo Horizonte, Minas Gerais state, Brazil (Appendix I).

We obtained a total of four recordings, from which we analyzed the calls emitted by seven males (Appendix I). Four individuals were recorded simultaneously by APA in Tabatinga in 2018 (CBUFMG 1119; Appendix I). Only two of the recorded males were collected, while the remaining data came from unvouchered individuals. Specimens were collected following standard procedures and subsequent fixation in formalin. Specimens were deposited in Zoological Collection Paulo Burnheim of Universidade Federal do Amazonas (CZPB-AA), Manaus, Amazonas, Brazil; Collection of Amphibians and Reptiles of Instituto Nacional de Pesquisas da Amazonia (INPA-H), Manaus; and Coleção Herpetológica Osvaldo Rodrigues da Cunha, Museu Paraense Emílio Goeldi (MPEG), Belém, Pará, Brazil (Appendix II). Collecting permits were obtained from Instituto Chico Mendes de Conservação da Biodiversidade (SISBIO-ICMBio).

Acoustic Analysis

We analyzed 17 advertisement calls (N = 7 males) with Raven Pro 1.5 from the Cornell Lab of Ornithology (Bioacoustics Research Program 2017). The call description followed a note-centered approach, with terminology based on Köhler *et al.* (2017). We report temporal features such as call duration, number of notes, note repetition rate (NRR), internote interval, note duration, and number of pulses per note; for spectral features we report lowe and high frequencies, and bandwidth calculated from these variables. Additionally, we measured dominant frequency using the function Peak Frequency option and the bandwidth of the most concentrated energy using the Frequency 5%, Frequency 95% and Bandwidth 90% functions. Temporal variables were taken from oscillograms, and spectral variables were taken from spectrograms with the following settings: window type = Blackman, window size = 256 samples, 3 dB bandwidth filter in 283 Hz, overlap = 80%, hop size 1.16 ms, frequency resolution DFT size = 2048 samples, and grid spacing 21.5 Hz. To avoid overlapping background noises, we measured upper and lower frequencies 20 dB below the peak frequency using the power spectrum tool in Raven. Sound figures were obtained with Seewave package v.2.0.2 (Sueur *et al.* 2008), on R environment (R Development Core Team, 2011). The Seewave settings were Blackman window, 512 points of resolution (FFT) and 80% overlap.

Results

All collected specimens and recorded individuals share morphological characteristics consistent with the diagnosis of *D. frosti* provided by Motta *et al.* (2012). Similarities include

coloration patterns at night (dorsum yellow without contrasting coloration of the flanks; Figure 1A) and during the day (dorsum brown, ventral surface pale yellow, a dark brown coloration, near black, in the thighs, shanks, lateral surface of the body and head and inner parts of feet and hands; Figures 1B, C). These features unequivocally confirm the identification of the specimens, and the calling males recorded in this study.

Advertisement Call Description

The call of *D. frosti* consists of two distinct types of short notes, referred to hereafter as type A and type B notes. These notes are emitted alternately at varying rates in two different arrangements, referred to here as Call type I and Call type II (Figure 2; Table 1). Note type A is a longer trill, i.e., a multipulsed note (χ = 23.3 pulses, SD = 4.4 N = 7), with duration that varies from 158 to 297 ms (χ = 215, SD = 54, N = 7), distinct pulses with amplitude modulation that increase in intensity in the first third of the note to the highest peak in the middle of the note, decreasing during the last pulses (Figure 2). Note type B is a high-pitched pulsatile short note, with duration varying from 8 to 17 ms (χ = 12, SD = 3, N = 8) in the Call type I, and 4 ms to 14 ms (χ = 9 ms, SD = 3, N = 33) in Call type II. As mentioned above, the notes are emitted in two different arrangements: Call type I consists of a complex call formed by one type A note, followed by one or two type B notes, with internote interval varying from 93 to 112 ms (χ = 105, SD = 7, N = 7) and duration ca. 272 to 505 ms (χ = 351 ms, SD = 82 ms, N = 7) resulting in NRR about 3 notes per second (χ = 3.38, SD = 0.54, N = 7) Call type II, which consists of a composite call formed by a series of 2 to 7 uniform pulsatile pitched notes (Figure 2), during ca. 124 to 648 ms depending on the number of notes emitted (see Table 1), and with note repetition rate about eight notes/sec (χ = 8.51, SD = 0.57, N = 10).

Both note types have no frequency modulation and present similar spectral structure (Table 1). Note type A has a dominant frequency between 4048.2 to 4435.8 Hz (χ = 4260.5 Hz, SD = 134,1, N = 7) and the following pulsatile notes observed in Call type I have a dominant frequency varying

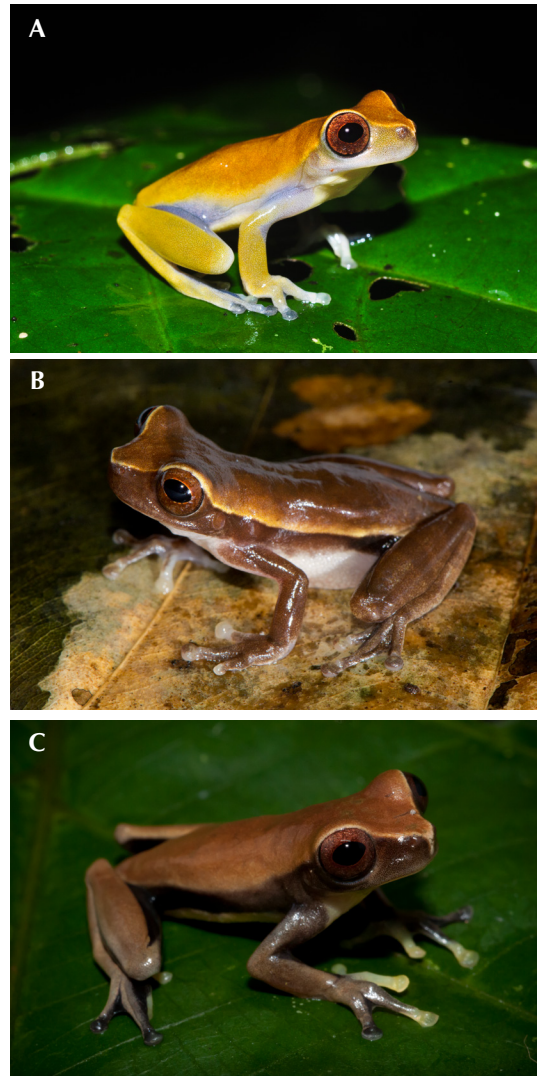

Figure 1. Specimens of *D. frosti* observed and collected from (**A**) Japurá River, near Villa Bittencourt village (INPA-H 38287), (**B**) Parque Nacional do Jaú-PNJ (MPEG 41866), and (**C**) Tabatinga (INPA-H 47002), AM, all localities in the Brazilian Amazon.

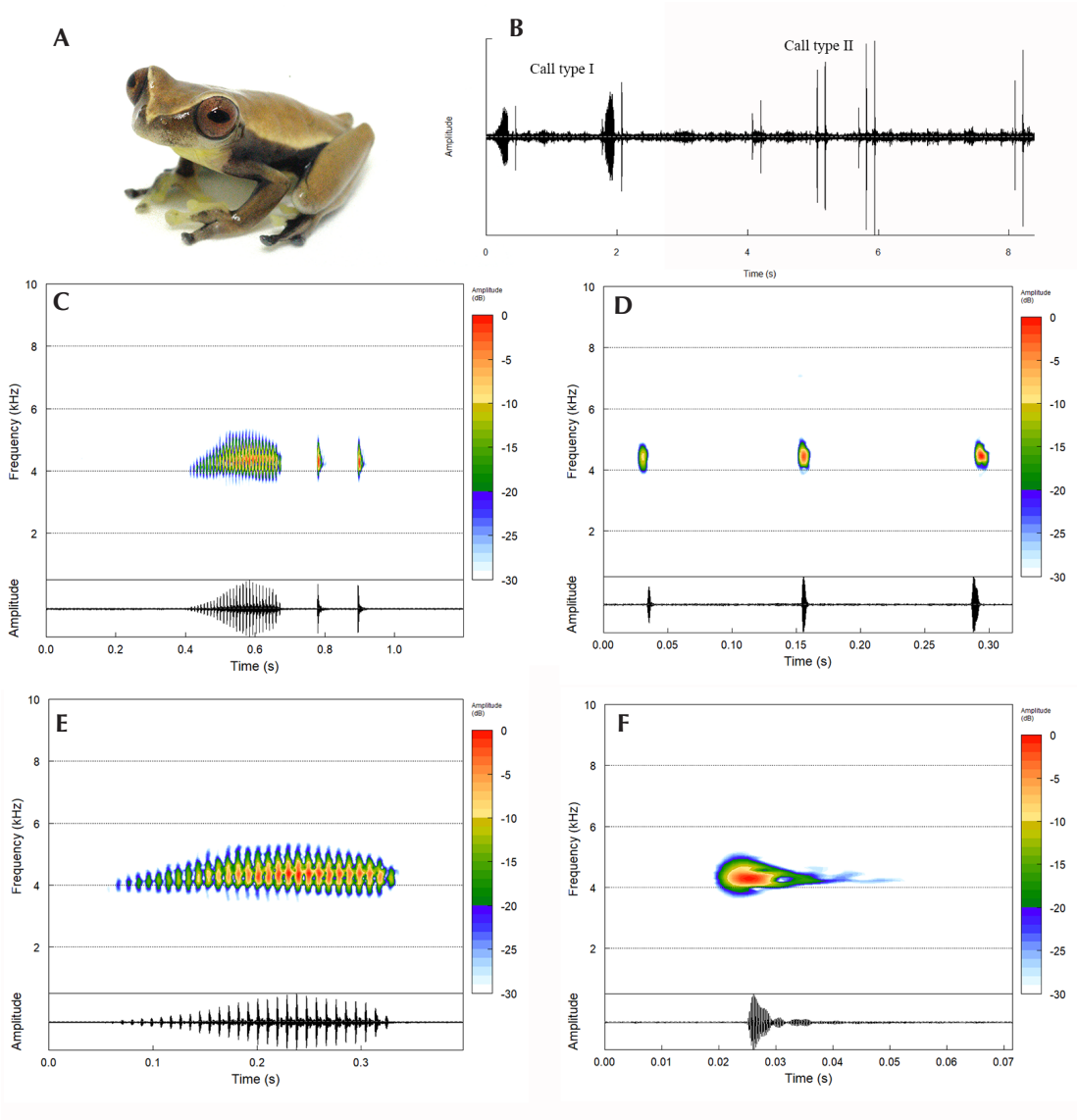

Figure 2. The advertisement call of *D. frosti:* (**A**) a recorded specimen INPA-H 47001; (**B**) Audiospectrogram highlighting the two call arrangements; (**C**) Waveform and spectrogram of Call type I; (**D**) Waveform and spectrogram Call type II; Waveform and spectrogram of notes, type A (**E**) and type B (**F**).

from 4306.6 to 4392.8 (χ = 4332.5 Hz, SD = 38.5, N = 8). In Call type II, the note type B shows a dominant frequency in a similar bandwidth varying from 4199 to 4392.8 Hz along the notes (χ = 4334.2 Hz, SD = 41, N = 19). In two calls recorded from PNJ (CBUFMG #1122; Appendix I) we observed a harmonic structure in both notes of Call type I, with the first harmonic

Table 1. Temporal and spectral traits of the advertisement call of *Dendropsophus frosti*. Call types and notes were recorded from seven males. Temporal traits of Call type II are presented for the three different arrangements (number of notes) observed. (*) denotes values obtained from 19 notes with better resolution on spectrogram (**) denotes values obtained from the notes of Call type I with visible harmonic structure.

Acoustic variables	**Advertisement Call type I Males (*N* = 4) / Call (*N* = 7)**	**Advertisement Call type II Males (*N* = 5) / Call (*N* = 10)**	
Call type	Complex	Composite multinote	
Number of notes	2–3	2–7	
Call duration (ms)	351 ± 82 (272–505)	Two notes (*N* = 5) Three notes (*N* = 3) Seven notes (*N* = 2)	129 ± 4 (124–134) 260 ± 8 (252–267) 646 ± 4 (643–648)
Internote interval (ms)	108 ± 5 (102–112)	112 ± 3 (107–125)	
NRR (notes/sec)	3.4 ± 0.39 (2.8–3.82)	8.26 ± 0.26 (7.81–8.55)	
Note	***N* = 7**	***N* = 8**	***N* = 33**
Note type	(A) Multipulsed	(B) pulsatile	(B) pulsatile
Note duration (ms)	188 ± 33 (158 – 244)	11 ± 3(8–15)	9 ± 3 (4–14)
Number of pulses/note	21 ± 2 (19–25)	Unpulsed	Unpulsed
Low frequency (Hz)	3692.4 ± 63 (3598.1–3752.4)	3882.7 ± 117.9 (3711.7–3987.9)	* 3922.2 ± 94.8 (3644.5–4091.3)
High Frequency (Hz)	4937.0 ± 169.6 (4648.3–5084.6)	4826.5 ± 145.6 (4592.7–4974.4)	* 4795.6 ± 85.8 (4586.6–5023.7)
Bandwidth (Hz)	1244.6 ± 204.7 (921.0–1486.7)	943.8 ± 250 (604.9–1262.7)	* 873.4 ± 163.5 (495.3–1248.1)
Dominant Frequency (Hz)	4310.9 ± 110.2 (4134.4–4435.8)	4332.5 ± 38.5 (4306.6–4392.8)	* 4344.0 ± 41.7 (4199.0–4392.8)
Frequency 5% (Hz)	4013.8 ± 58.2 (3940.6–4069.8)	4091.3 ± 80.6 (3962.1–4177.4)	* 4115.1 ± 41.8 (4005.2–4199.0)
Frequency 95% (Hz)	4646.8 ± 108.1 (4478.9–4758.8)	4578.0 ± 99.4 (4457.4–4715.8)	* 4586.6 ± 50.3 (4543.5–4737.3)
Bandwidth 90% (Hz)	633.1 ± 119.5 (516.8–818.3)	486.7 ± 160.1 (323.0–753.7)	* 471.5 ± 65.3 (409.1–646.0)
2nd Harmonic Frequency (Hz)**	8613 ± 685.2	8089.3 ± 442.5	NA
3rd Harmonic Frequency (Hz)**	11627.8 ± 1279	12511 ± 30.2	NA

and fundamental frequency equal to the dominant frequency of both notes, and secondary harmonics having a frequency ca. 8128 Hz and 11627 Hz, respectively, for the trilled note, and ca. 8089 Hz and 12510 Hz for the pulsatile notes.

Comparisons with Closely Related Species

The overall acoustic structure of the *D. frosti* call, including its complex and composite calls with two types of notes, is similar to those

described for the most closely related species in the *D. parviceps* group (Table 2). The call of *D. frosti* can be distinguished from that of *D. subocularis* by the presence of the pulsatile notes, which are absent in *D. subocularis*. Additionally, the *D. frosti* call is differentiated by its shorter multispulsed note (trill) duration compared to *D. brevifrons* (ca. 460 ms), *D. counani* (ca. 300 ms) and *D. subocularis* (ca. 530 ms). Conversely, the trill note in *D. frosti* is longer (approximately 215 ms) than in *D. bokermani* (approximately 200 ms), *D. parviceps* (approximately 140 ms), *D. kamagarini* (approximately 140), and *D. kubricki* (approximately 190 ms).

Regarding spectral structure, the call of *D. frosti* has a dominant frequency lower than that of *D. parviceps* (around 6300 Hz), but higher than those of *D. subocularis, D. counani,* and *D. kamagarini,* which all have dominant frequencies below 4000 Hz. Among the remaining species, the dominant frequency varies between 4000 Hz and 4600 Hz, which fits with the variation that we described. Besides *D. frosti,* a harmonic structure has been observed in the *D. counani* call (two secondary harmonics with approximately 8000 Hz and 11000 Hz; Fouquet *et al.* 2015), *D. giesleri,* with approximately 6000–10000 Hz harmonics (Heyer 1980), and *D. microps* with harmonics in around 8000 Hz and 11500 Hz (Forti *et al.* 2015).

Habitat and Geographic Distribution

In all our observations of *D. frosti,* individuals were engaged in breeding activity, perched on vegetation above large temporary ponds within "terra-firme" forests (non-seasonally flooded habitat). Calling males were found perched on fallen logs beside the ponds or on vegetation at heights ranging from a few centimeters to 2m above the water, and females were found around the males, in the vegetation. We also found other species of frogs sharing this habitat in all reported sites, including *Dendropsophus sarayacuensis* (Shreve, 1935), *Dendropsophus* cf. *parviceps, Dendropsophus minutus* (Peters, 1872), and *Callimedusa tomopterna* (Cope, 1868).

Two of the localities accessed in this study were recently reported as new occurrences of the species (Koch *et al.* 2023). Here, we present a new record for the species from Central Amazonia, at the PNJ. Our record extends the distribution of *D. frosti* about 733 km east of the nearest known occurrence on the right bank of Japurá River and about 856 km east from the type-locality, in Letícia, Colombia, thereby establishing the easternmost limit of the known geographic range of the species (Figure 3).

Discussion

The lack of information on anuran advertisement calls is tipically associated with species with limited knowledge of their geographic distribution and general biology or with species that occur in remote, hard-to-access areas (Guerra *et al.* 2018). Our findings specifically augment the biological understanding of the poorly documented species *D. frosti,* previously known only from its type series.

The advertisement call structure of *D. frosti* described herein closely resembles that of other species within the *D. parviceps* group. These calls have been characterized as "short insect-like chirps" (*D. brevifrons,* Duellman 1978), "the chirping of a cricket" (*D. microps,* Lutz 1973), "ratling buzz of pulsed notes" (*D. timbeba,* Duellman 2005), "a high-pitched 'creeeek' followed or not by a series of shorter notes, "eek-eek-eek" (*D. pauiniensis = D. koechlini*, Duellman and Trueb 1989), "train" (*D. microps,* Forti *et al.* 2015), "trills" and "clicks" (*D. counani,* Fouquet *et al.* 2015), and characterized by primary and secondary notes (Duellman and Crump 1974, Duellman 1978). These different terminologies describe the acoustic signal of multipulsed and pulsatile notes emitted either randomly, in a series of pulsatile notes, or in a complex combination, similar to that we identified for *D. frosti,* although with variations in temporal and spectral note features. Notably, *D. microps* stands out for having a call structure with two different types of notes: a pulsed note with fused pulses and another

shorter note with evident pulses (Forti *et al.* 2015). The lack of standardized terminology, and analyses of those calls make homology assessments dificult (Hepp *et al.* 2012).

Advertisement call structure and properties within *Dendropsophus* have been reported as a phylogenetically informative trait in *D. marmoratus* (Laurenti, 1768) (Orrico *et al.* 2009,

Table 2. Comparisons of temporal and spectral acoustic traits of closely related species oft he *Dendropsophus parviceps* group. Data obtained from literature ([1]Duellman 1970, [2]Duellman and Crump 1974, [3]Duellman 1978, [4]Martins and Cardoso 1987, [5]Heyer 1980, [6]Duellman and Pyles 1983, [7]Duellman and Trueb 1989, [8]Duellman 2005, [9]Forti *et al.* 2015, [10]Fouquet *et al.* 2015, [11]Rivadaneira *et al.* 2018). Abbreviations: NA = not available; A = the multipulsed note (trill); B = the high-pitched notes (secondary notes); numbers denote the source. * The complex call of *D. microps* described by Forti *et al.* (2015) is formed by one to five notes, and two kinds of notes: a longer note with fused pulses and the other note with evident pulses (B').

Species (Source)	Call type	Call duration (ms)	Note duration (ms)	Dominant frequency (Hz)
D. frosti (present study)	complex	272–502 (2–3 notes)	A = 158–297	A = 4048–4435
	composite multinote	129–646 (2–7 notes)	B = 9–12	B = 4258–4344
D. bokermanni (2, 6, 8,10)	complex	NA	A = 230–280	A = 4000–4652
	composite multinote	620 (5–7 notes)	B = 40	B= 4300
D. brevifrons (2, 3, 6, 8)	complex	750 (4–5 notes)	A = 430–490	4254–5115
	composite multinote		B = ~15	
D. counani (10)	complex	NA	A = 210–350	3780–3970
	composite multinote	330-540 (3–6 notes)	B = NA	
D. giesleri (5)	Single multipulsed note	300	300	3600
D. microps (9)	Single multipulsed note (trill)	670	A = 670	A = 4913
	complex *	8–1930 (1–5 notes)	B' = 340	B' = 4972
D. parviceps (11)	complex	260–2120	A = 60–240	A = 5081–6869
	composite multinote	NA	B = 28–82	B = 4866–6922
D. pauiniensis (7, 8)	complex	NA	A = 220–400	A = 4500
	composite multinote	NA	B = 20	B = NA
D. kamagarini (11)	complex	260–810	A = 90–200	A = 3164–4306
	composite multinote	NA	B = 30–100	B = 3164–4532
D. kubrickyi (11)	complex	230–630	A = 100–300	A = 3542–4394
	composite multinote	NA	B = 30–90	B = 3703–4500
D. subocularis (1)	Single multipulsed note (trill)	530	530	2200
D. timbeba (4, 8)	Single multipulsed note (trill)	400–600	400–600	3000–4200

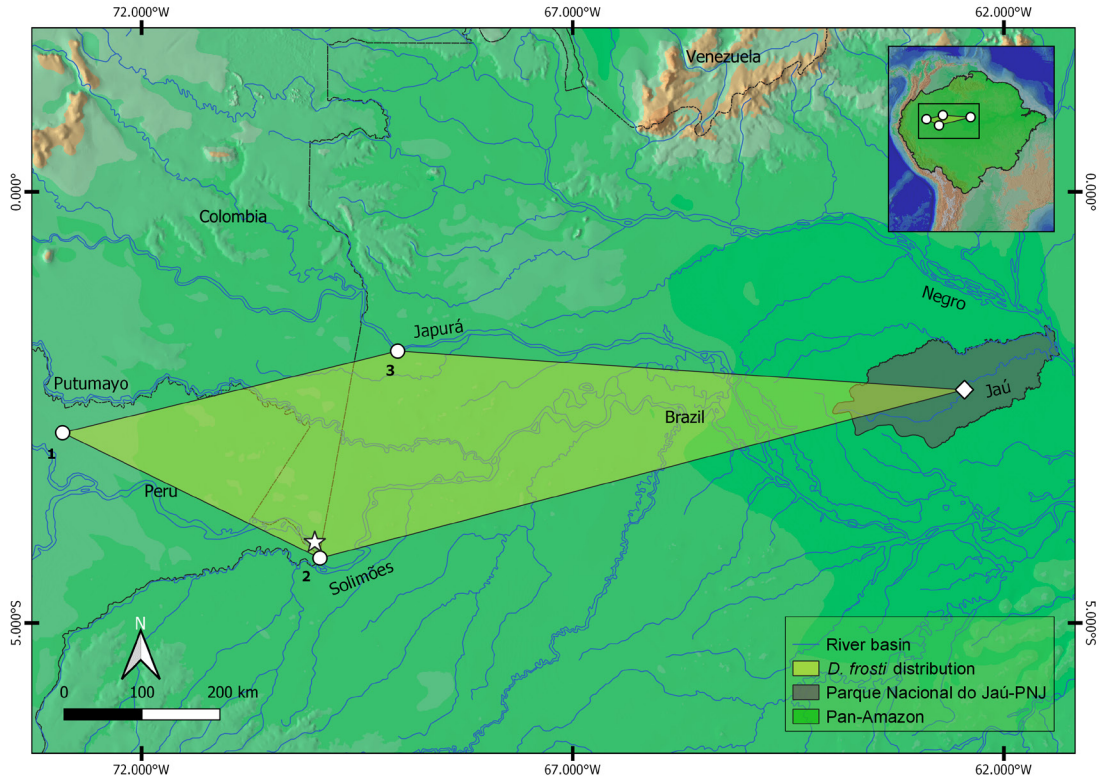

Figure 3. Geographic distribution of *Dendropsophus frosti* in northwestern Amazonia, highlighting the new record in Parque Nacional do Jaú (PNJ), which extends its distribution in ca.733 km to the nearest known occurrence. White star denotes the type locality in Leticia, Colombia (Motta *et al.* 2012); dots denote the known occurrences in (1) Piedras, Peru, near the Putumayo River (Motta *et al.* 2012); (2) Tabatinga municipality, Brazil (Koch *et al.* 2023, this study) and (3) near Vila Bittencourt village, Brazil, on the right bank of Japura River (Koch *et al.* 2023; this study). Diamond denotes the new occurrence in the PNJ.

Hepp *et al.* 2012), *D. microcephalus* (Cope, 1886) (Duellman 1970, Teixeira *et al.* 2013, Teixeira and Giaretta 2015), *D. leucophyllatus* (Beireis, 1783) (Forti *et al.* 2017), and *D. parviceps* groups (Duellman and Crump 1974), indicating it as synapomorphy for these groups, or for the clades with closely related species within the groups (e.g. Hepp *et al.* 2012). Our findings provide the first phenotypic evidence that supports the phylogenetic relationship of *D. frosti* within the *D. parviceps* group, with *D. bokermanni* as the closely related species from *D. subocularis* clade *sensu* Orrico *et al.* (2021). The advertisement call along with a terrestrial egg clutch reported by Koch *et al.* (2023), could be considered as two synapomorphies that *D. frosti* shares with the *D. subocularis* clade (Orrico *et al.* 2021).

Dendropsophus frosti inhabits large temporary ponds within forests, often near major river channels, as reported previously (Motta *et al.* 2012, Koch *et al.* 2023) and corroborated by our study. In all records, we observed the syntopic occurrence of other species of *Dendropsophus* from the *D. leucophyllatus* and *D. microcephalus* groups, as well as closely related species from the *D. parviceps* group (*D. parviceps* complex). This syntopic occurrence has also been noted in

other instances, with sympatric and occasionally syntopic occurrences between *D. parviceps, D. brevifrons, D. bokermanni,* and *D. pauiniensis* (previously recognized as *D. koechlini*) in Ecuador and Peru (Duellman 1978, Duellman and Trueb 1989, Duellman 2005).

Regarding the distribution of species from the *D. parviceps* group, Orrico *et al.* (2021) described it as patchy, with species found in different domains of South America, most notably in Amazonia. *Dendropsophus frosti* was previously known only from the western Amazonian lowlands, with scattered records near its type-locality (Motta *et al.* 2012, Koch *et al.* 2023). The population from PNJ extends the known distribution to the interfluve between the Japurá and Negro rivers, suggesting it may be more widely distributed in northwestern Amazonia, as observed in many other hylid species (e.g. Carvalho *et al.* 2015, Ferrão *et al.* 2019, Almeida *et al.* 2021). Our study once again highlights the necessity of expeditions and fieldwork in remote areas in Amazonia to address knowledge shortfalls, such as the Raunkiæran and Wallacean shortfalls, in anuran biodiversity.

Finally, the overall similarities observed in habitat used by the species (including syntopic and sympatric occurrences), combined with the patterns of acoustic traits observed in the *D. parviceps* group, especially within the *D. subocularis* clade, may offer clues about sympatric speciation driven by sexual selection (Gerhardt 1994, Higashi *et al.* 1999). This ideia has also been suggested for the *D. microps* clade (Forti *et al.* 2015) and could be properly tested in a more comprehensive study.

Acknowledgments

We are thankful for fieldwork assistance from the local communities during all expeditions. APA thanks Fabiano Waldez and Weslei Valteran for logistic assistance during the fieldwork in Tabatinga. Also, APA thanks the Conselho Nacional de Desenvolvimento Científico e tecnológico (CNPq) for a postdoctoral fellowship (CNPq 25/2021 Pós-doutorado Junior PDJ 2021, process #15972/2022-6). RWA thanks CNPq for a research grant (PQ 305988/2018-2, 307722/2021-0). PP was supported by an award from the Maxwell/Hanrahan Foundation. MJS was financially supported by CNPq (process # 434362/2018-2). Fieldwork at Japurá river was financialy supported by CNPq (SISBIOTA Program #533348/2010) and Fundação de Amparo à Pesquisa do Estado do Amazonas—FAPEAM (Edital FAPEAM/SISBIOTA). The expedition to Parque Nacional do Jaú was supported by grants from the National Geographic Society and the Smithsonian Institution. Fieldwork at Tabatinga/AM received financial support from CNPq (Edital Universal #405640/2016-1). This work was suported by the Conselho Nacional de Desenvolvimento Científico e tecnológico (CNPq) under the grants (process #15972/2022-6; #PQ 305988/2018-2, 307722/2021-0; #434362/2018–2; #533348/2010; #405640/2016-1); Fundação de Amparo à Pesquisa do Estado do Amazonas—FAPEAM (#FAPEAM/SISBIOTA), the National Geographic Society and the Smithsonian Institution.

References

Almeida, A. P., L. J. C. L. Moraes, R. R. Rojas, I. J. Roberto, V. T. Carvalho, R. W. Ávila, L. Frazão, A. A. A. Silva, M. Menin, F. P. Werneck, T. Hrbek, I. P. Farias and M. Gordo. 2021. Phylogenetic relationship of the poorly known treefrog *Boana hobbsi* (Cchran & Goin, 1970) (Anura: Hylidae), systematic implications and remarks on morphological variation and geographic distribution. *Zootaxa 4933:* 301–323.

Azevedo-Ramos, C. and U. Galatti. 2002. Patterns of amphibian diversity in Brazilian Amazonia: Conservation implications. *Biological Conservation 103:* 103–111.

Bioacoustics Research Program. 2017. Raven Pro: Interactive sound analysis software. Version 1.5. The Cornell Lab of Ornithology, Ithaca, New York. URL: http://www.birds.cornell.edu/raven.

Carvalho T. R., B. F. V. Teixeira, W. E. Duellman, and A. A. Giaretta. 2015. *Scinax cruentommus* (Anura: Hylidae) in upper Rio Negro drainage, Amazonas state, Brazil, with description of its advertisement call. *Phyllomedusa 14:* 139–146.

Duellman, W. E. 1970. The hylid frogs of Middle America.

Monograph Museum of Natural History 2: 1–753.

Duellman, W. E. 1978. The biology of an Equatorial herpetofauna in Amazonian Ecuador. *Miscellaneous Publications, University of Kansas, Museum of Natural History 65:* 372.

Duellman, W. E. 2005. *Cuzco Amazónico: The Lives of Amphibians and Reptiles in an Amazonian Rainforest*. Ithaca. Cornell University Press. 456 pp.

Duellman, W. E., M. L. Crump, M.L. 1974. Speciation in frogs of the *Hyla parviceps* group in the upper Amazon basin. *Occasional papers of the Museum of Natural History, University of Kansas 23:* 1–40.

Duellman, W. E., and L. Trueb. 1989. Two new treefrogs of *Hyla parviceps* group from the Amazon Basin in southern Peru. *Herpetologica 45:* 1–10.

Duellman, W. E., and L. Trueb. 1994. *Biology of Amphibians.* Baltimore. John Hopkins University Press. 670 pp.

Ferrão M., J. Moravec, L. J. C. L. Moraes, V. T. de Carvalho, M. Gordo, and A. P. Lima. 2019. Rediscovery of *Osteocephalus vilarsi* (Anura: Hylidae): an overlooked but widespread Amazonian spiny-backed treefrog. *PeerJ 7:* e8160.

Forti, L. R., R. Márquez, and J. Bertoluci. 2015. Advertisement call of *Dendropsophus microps* (Anura: Hylidae) from two populations from southeastern Brazil. *Zoologia 30:* 187–194.

Forti, L. R., R. Lingnau, L. C. Encarnação, J. Bertoluci, and L. F. Toledo. 2017. Can treefrog phylogeographical clades and species' phylogenetic topologies be recovered by bioacoustical analyses? *PLoS ONE 12:* e0169911.

Fouquet, A., B. Noonan, M. Blanc, and V. G. D. Orrico. 2011. Phylogenetic position of *Dendropsophus gaucheri* (Lescure and Marty, 2000) highlights the need for an in-depth investigation of the phylogenetic relationship of *Dendropsophus* (Anura: Hylidae). *Zootaxa 3035:* 59–67.

Fouquet, A., V. G. D. Orrico, R. Ernst, M. Blanc, Q. Martinez, J. P. Vacher, M. T. Rodrigues, P. Ouboter, R. Jairam, and S. Ron. 2015. A new *Dendropsophus* Fitzinger, 1843 (Anura: Hylidae) of the *parviceps* group from the lowlands of the Guiana Shield. *Zootaxa 4052:* 39–64.

Frost, D. R. (ed.). 2025. Amphibian Species of the World: an Online Reference. Version 6.2 (25 September 2025). Electronic Database accessible at https://amphibiansoftheworld.amnh.org/index.php. American Museum of Natural History, New York, USA. Captured on 03 March 2025.

Gerhardt, H. C. 1994. The evolution of vocalization on frogs and toads. *Annual Review of Ecology and Systematics 25:* 293–324.

Gingras, B., E. Mohandesan, D. Boko, and T. Fitch. 2013. Phylogenetic signal in the acoustic parameters of the advertisement calls of four clades of anurans. *BMC Evolutionary Biology 13:* 134.

Guerra, V., L. Jardim, D. Llusia, R. Márquez, and R. P. Bastos. 2020. Knowledge status and trends in description of amphibian species in Brazil. *Ecological Indicators 118:* 106754.

Guerra, V., D. Llusia, P. G. Gambale, A. R. de Morais, R. Márquez, and R. P. Bastos. 2018. The advertisement calls of Brazilian anurans: historical review, current knowledge and future directions. *PLoS ONE 13: e0191691.*

Hepp, F. S. F. S., C. De Luna-Dias, L. P. Gonzaga, and S. P. De Carvalho-E-Silva. 2012. Redescription of the advertisement call of *Dendropsophus seniculus* (Cope, 1868) and the consequences for the acoustic traits of the *Dendropsophus marmoratus* species group (Amphibia: Anura: Dendropsophini). *South American Journal of Herpetology 7:* 165–171.

Heyer, W. R. 1977. Taxonomic notes on frogs from the Madeira and Purus rivers, Brazil. *Papéis Avulsos de Zoologia 31:* 141–162.

Higashi, M., G. Takimoto, and A. N. Yamamura. 1999. Sympatric speciation by sexual selection. *Nature 402:* 523–526.

Hortal, J., F. De Bello, J. A. F. Diniz-Filho, T. M. Lewinsohn, J. M. Lobo, and R. J. Ladle. 2015. Seven shortfalls that beset large-scale knowledge of biodiversity. *Annual Review of Ecology, Evolution, and Systematics 46:* 523–549.

Koch, E. D., A. T. Mônico, I. Y. Fernandes, and W. Valteran. 2023. First record of *Dendropsophus frosti* (Amphibia, Anura, Hylidae) in Brazil, with comments on its reproductive behavior. *Herpetologia Brasileira 11:* 106–111.

Köhler, J., M. Jansen, A. Rodríguez, P. J. R. Kok, L. F. Toledo, M. Emmrich, F. Glaw, C. F. B. Haddad, M. O. Rodel, and M. Vences. 2017. The use of bioacoustics in anuran taxonomy: theory, terminology, methods, and recommendations for best practice. *Zootaxa 4251:* 1–124.

Lutz, B. 1973. *The Brazilian Species of Hyla*. Austin. University of Texas Press. 260 pp.

Martins, M. and A. J. Cardoso. 1987. Novas espécies de hilídeos do Estado do Acre (Amphibia: Anura). *Revista*

Brasileira de Biologia 47: 549–558.

Mayer, M., L. F. M. Da Fonte, and S. Lötters. 2019. Mind the gap! a review of Amazonian anurans in Genbank. *Salamandra 55:* 89–96.

Melo-Sampaio, P. R. 2023. On the taxonomic status of *Dendropsophus koechlini* (Duellman & Trueb, 1989). *Journal of Vertebrate Biology 72:* 23022.1-11.

Moraes, L. J. C. L., R. N. Rainha, F. P. Werneck, A. F. S. Oliveira, C. Gascon, and V. T. Carvalho. 2022. Amphibians and reptiles from a protected area in western Brazilian Amazonia (Reserva Extrativista do Baixo Juruá). *Papéis Avulsos de Zoologia 62:* e202262054.

Motta, A. P., S. Castroviejo-Fisher, P. J. Venegas, V. G. D. Orrico, and J. M. Padial. 2012. A new species of the *Dendropsophus parviceps* group from the western Amazon Basin (Amphibia: Anura: Hylidae). *Zootaxa 3249:* 18–30.

Orrico, V. G. D., W. E. Duellman, M. B. Souza, and C. F. B. Haddad. 2013. The taxonomic status of *Dendropsophus allenorum* and *Dendropsophus timbeba* (Anura: Hylidae). *Journal of Herpetology 47:* 615–618.

Orrico, V. G. D., R. Lingnau, and L. O. M. Giasson. 2009. The advertisement call of *Dendropsophus nahdereri* (Anura, Hylidae, Dendropsophini). *South American Journal of Herpetology 4:* 295–299.

Orrico, V. G. D., T. Grant, J. Faivovich, M. Rivera-Correa, M. A. Rada, M. L. Lyra, C. S. Cassini, P. H. Valdujo, W. E. Schargel, D. J. Machado, W. C. Wheeler, C. Barrio-Amarós, D. Loebmann, J. Moravec, J. Zina, M. Solé, M. J. Sturaro, P. L. V. Peloso, P. Suarez, and C. F. B. Haddad. 2021. The phylogeny of Dendropsophini (Anura: Hylidae: Hylinae). *Cladistics 37:* 73–105.

Peloso, P. L.V. 2010. A safe place for amphibians? A cautionary tale on the taxonomy and conservation of frogs, caecilians, and salamanders in the Brazilian Amazonia. *Zoologia 27:* 667–673.

R Development Core Team. 2011. R Foundation for Statistical Computing. Vienna, Austria, 367. URL: http://www.R-project.org.

Rivadeneira, C. D., P. J. Venegas, and S. R. Ron. 2018. Species limits within the widespread amazonian treefrog *Dendropsophus parviceps* with descriptions of two new species (anura, hylidae). *ZooKeys 726:* 25–77.

Sueur, J., T. Aubin, and C. Simonis. 2008. Seewave, a free modular tool for sound analysis and synthesis. *Bioacustics 18:* 213–226.

Teixeira, B. F. V., A. A. Giaretta, and A. Pansonato. 2013. The advertisement call of *Dendropsophus tritaeniatus* (Bokermann, 1965) (Anura: Hylidae). *Zootaxa 3669:* 189.

Teixeira, B. F. V. and A. A. Giaretta. 2015. Setting a fundament for taxonomy: advertisement calls from the type localities of three species of the *Dendropsophus rubicundulus* group (Anura: Hylidae). *Salamandra 51:* 137–146.

Yang, W., K. Ma, and H. Kreft. 2013. Geographical sampling bias in a large distributional database and its effects on species richness-environment models. *Journal of Biogeography 40:* 1415–1426.

Wells, K. D. 1977. The social behaviour of anuran amphibians. *Animal Behaviour 25:* 666–693.

Editor: Ariovaldo Giaretta

Appendix I. *Collection records of the recordings analyzed in the present study with catalog number, recording file identification, and localities where recordings were made. All recordings were deposited in Coleção Bioacústica da Universidade Federal de Minas Gerais (CBUFMG).*

Catalog number	Voucher Number	File-record name	Locality
CBUFMG 1119	INPA-H 470001 INPA-H 470002	DR_APA01_Dendrop frosti_TBT_050518	Tabatinga, Amazonas state, Brazil
CBUFMG 1120	Unvouchered specimen	DR_APA02_EK_D_frosti_Tabatinga_2021	Tabatinga, Amazonas state, Brazil
CBUFMG 1121	Unvouchered specimen	PLPDR 066 - Dendropsophus frosti - Parque Nacional do Jau - PNJAU029_nv	PNJ, Amazonas state, Brazil
CBUFMG 1122	Unvouchered specimen	PLPDR 067 - Dendropsophus frosti - Parque Nacional do Jau - PNJAU031	PNJ, Amazonas state, Brazil

Appendix II. *Museum numbers and occurrence data of the specimens of* Dendropsophus frosti *collected during three fieldwork expeditions in western Amazonia, indicating voucher information, localities, and coordinates. Recorded specimens in bold. Legend to localities:* PNJ, *Parque Nacional do Jaú, AM, Brazil;* T, *Tabatinga, AM, Brazil;* JR, *Japurá River, Vila Bittencourt, AM, Brazil.*

Voucher Number	Field Number	Locality	Geographic Coordinates
MPEG 41861	PLVP 681	PNJ	02°17'39" S, 62°27'21" W
MPEG 41862	PLVP 682	PNJ	02°17'39" S, 62°27'21" W
MPEG 41863	PLVP 683	PNJ	02°17'39" S, 62°27'21" W
MPEG 41864	PLVP 684	PNJ	02°17'39" S, 62°27'21" W
MPEG 41866	PLVP 720	PNJ	02°17'39" S, 62°27'21" W
MPEG 41867	PLVP 721	PNJ	02°17'39" S, 62°27'21" W
MPEG 41868	PLVP 722	PNJ	02°17'39" S, 62°27'21" W
MPEG 41869	PLVP 723	PNJ	02°17'39" S, 62°27'21" W
MPEG 41870	PLVP 724	PNJ	02°17'39" S, 62°27'21" W
MPEG 41865	PLVP 725	PNJ	02°17'39" S, 62°27'21" W
MPEG 41872	PLVP 726	PNJ	02°17'39" S, 62°27'21" W
MPEG 41871	PLVP 727	PNJ	02°17'39" S, 62°27'21" W
MPEG 41873	PLVP 728	PNJ	02°17'39" S, 62°27'21" W
MPEG 41874	PLVP 729	PNJ	02°17'39" S, 62°27'21" W
***INPA-H 47001**	**RSOL 22**	**T**	**04°14'52.77" S, 69°55'51.05" W**
***INPA-H 47002**	**RSOL 24**	**T**	**04°14'52.77" S, 69°55'51.05" W**
INPA-H 47003	RSOL 25	T	04°14'52.77" S, 69°55'51.05" W
INPA-H 47004	RSOL 32	T	04°14'52.77" S, 69°55'51.05" W
CZPB-AA 1555	CTGA-N 1893	JR	01°50'46.10" S, 69°01'46.30" W
INPA-H 38286	CTGA-N 1912	JR	01°50'46.10" S, 69°01'46.30" W
INPA-H 38288	CTGA-N 1935	JR	01°50'46.10" S, 69°01'46.30" W
INPA-H 38287	CTGA-N 2189	JR	01°50'46.10" S, 69°01'46.30" W
CZPB-AA 1554	CTGA-N 2190	JR	01°50'46.10" S, 69°01'46.30" W
CZPB-AA 1552	CTGA-N 2191	JR	01°50'46.10" S, 69°01'46.30" W
CZPB-AA 1553	CTGA-N 2192	JR	01°50'46.10" S, 69°01'46.30" W
INPA-H 38285	CTGA-N 2220	JR	01°50'46.10" S, 69°01'46.30" W

Phyllomedusa 24(2):271–279, 2025

ISSN 1519-1397 (print) / ISSN 2316-9079 (online)
doi: http://dx.doi.org/10.11606/issn.2316-9079.v24i2p271-279

Notes on the distribution and advertisement call of *Nymphargus buenaventura* (Anura: Centrolenidae), with comments on its natural history and conservation

Germán Chávez[1,2] and Alessandro Catenazzi[1,3]

[1] Instituto Peruano de Herpetología. Jirón Augusto Salazar Bondy 136, Lima 33, Peru. E-mail: vampflack@yahoo.com.

[2] Centro de Ornitología y Biodiversidad. Calle Santa Rita 105, urbanización los Huertos de San Antonio, Lima 33, Peru.

[3] Florida International University, Department of Biological Sciences. 11200 SW 8th Street, OE 167. Miami, FL 33199, USA.

Abstract

Notes on the distribution and advertisement call of *Nymphargus buenaventura* (Anura: Centrolenidae), with comments on its natural history and conservation. We provide an update on the distribution of Buenaventura´s glassfrog (*Nymphargus buenaventura*), adding a new locality in Peru. We extend the known geographic range of the species 180 km southward. We report for the first time its advertisement call, which consists of a high-pitched note. Morphological and molecular analyses confirmed the identity of the specimens, with 16S rRNA sequences exhibiting minimal genetic divergence (1.08%) from those of Ecuadorian populations. Additionally, we observed egg clutches exceeding previously reported clutch sizes. Given the extended range and lack of population data, we recommend placing *N. buenaventura* in the Data Deficient category of the IUCN Red List until further studies are conducted.

Keywords: Data Deficient, Glassfrogs, High-pitched note, New locality, Peru, rRNA

Resumo

Notas sobre a distribuição e o canto de advertência de *Nymphargus buenaventura* (Anura: Centrolenidae), com comentários sobre sua história natural e conservação. Fornecemos uma atualização sobre a distribuição da rã-de-vidro-de-buenaventura (*Nymphargus buenaventura*), adicionando uma nova localidade no Peru. Ampliamos a distribuição geográfica conhecida da espécie em 180 km ao sul. Relatamos pela primeira vez seu canto de anúncio, que consiste em uma nota aguda. Análises morfológicas e moleculares confirmaram a identidade dos espécimes, com sequências de rRNA 16S exibindo divergência genética mínima (1,08%) em relação às populações equatorianas. Além disso, observamos ninhadas de ovos excedendo os tamanhos de ninhadas relatados anteriormente. Dada a extensão da distribuição e a falta de dados populacionais, recomendamos incluir *N. buenaventura* na categoria Dados Deficientes da Lista Vermelha da IUCN até que mais estudos sejam conduzidos.

Palavras-chave: Deficiente em Dados, Nova localidade, Notas de alta frequência, Pererecas-de-vidro, Peru, rRNA.

Received 17 March 2025
Accepted 16 September 2025
Distributed December 2025

Introduction

Glassfrogs are a group of Neotropical arboreal frogs renowned for their translucent ventral skin, which often reveals their internal organs—a trait that has fascinated biologists and inspired their common name. Currently, 167 species are recognized as belonging to this family (Frost 2025), most of them inhabiting the eastern side of the Andes. Glassfrogs from the Pacific slopes of northwestern Peru are not as diverse as those from the Andean Amazonian slopes. In contrast to the 17 species distributed in the Amazon River drainage of the northeastern Andes (Catenazzi and Venegas 2012, Twomey *et al*. 2014, Gagliardi-Urrutia *et al*. 2022), only three species have so far been recorded on the Pacific slopes of the Andes of northern Peru: *Centrolene buckleyi (*Boulenger, 1882), *Centrolene hesperia* (Cadle and McDiarmid, 1990), and *Cochranella euhystrix* (Cadle and McDiarmid, 1990) (Duellman and Wild 1993). Further north, the diversity of Glassfrogs on the Pacific drainage of southern Ecuador remains low, with four species recorded: *Espadarana prosoblepon* (Boettger, 1892), *Nymphargus buenaventura* (Cisneros-Heredia and Yañez-Muñoz, 2007) (Guayasamin *et al*. 2020), *Centrolene camposi* Cisneros-Heredia, Yánez-Muñoz, Sánchez-Nivicela, and Ron, 2023, and *C. ericsmithi* Cisneros-Heredia, Yánez-Muñoz, Sánchez-Nivicela, and Ron, 2023. Regarding frogs in the genus *Nympahrgus, N. buenaventura* marks the southernmost geographic limit of the genus in the Pacific drainage of South America (Guayasamin *et al*. 2020).

Nymphargus buenaventura is a small frog (SVL = 20.9–22.4 mm) known from four localities in southwestern Ecuador from 800 to 1925 m a.s.l. (Yáñez-Muñoz *et al*. 2014, Guayasamin *et al.* 2020, Coloma and Duellman 2025). Besides these records, little is known about this species. This lack of knowledge includes its advertisement call and natural history. Additionally, its phylogenetic relationships are controversial due to incongruences in its inferred phylogenetic position, as shown by Portik *et al*. (2023) and Montilla *et al*. (2023). So far, *N. buenaventura* has been found inhabiting vegetation alongside streams in mountain forests (Cisneros-Heredia and Yañez-Muñoz 2007). Although it was originally placed in the Data Deficient category of the IUCN Red List (Cisneros-Heredia 2008), Guayasamin *et al*. (2020) suggested moving it to the Endangered category due to its apparent endemism to southwestern Ecuador and its distribution overlapping a highly deforested area. Later, *N. buenaventura* was placed in the Endangered category after the assessment made by Cisneros-Heredia *et al*. (2022). During fieldwork in the Cordillera de Huancabamba in the northwestern Andes of Peru, we collected a small series of glassfrogs that we assigned to *Nymphargus buenaventura* based on morphological, acoustic, and DNA sequence data. The new geographic record of this glassfrog species is the first report in Peru. The results of this work are described herein.

Materials and Methods

Fieldwork

We conducted Visual Encounter Surveys (Crump and Scott 1994) during both day and night. As a result of our field survey, six adult males (CORBIDI 22316–22318, 22320–22322) and a subadult male (CORBIDI 22319) of *Nymphargus buenaventura* (Figure 1) were caught at Agua Blanca Village, Huancabamba province, Piura department, Peru (05°20'44.0" S, 79°34'1.9" W; 1800 m a.s.l.) on 6 February 2020, from 21:45 to 22:30 h by Luis A. García-Ayachi, Jesus R. Ormeño, and GC. Calling males were approximately 5–10 m apart. All specimens were deposited in the herpetological collection of Centro de Ornitología y Biodiversidad (CORBIDI), Lima, Peru.

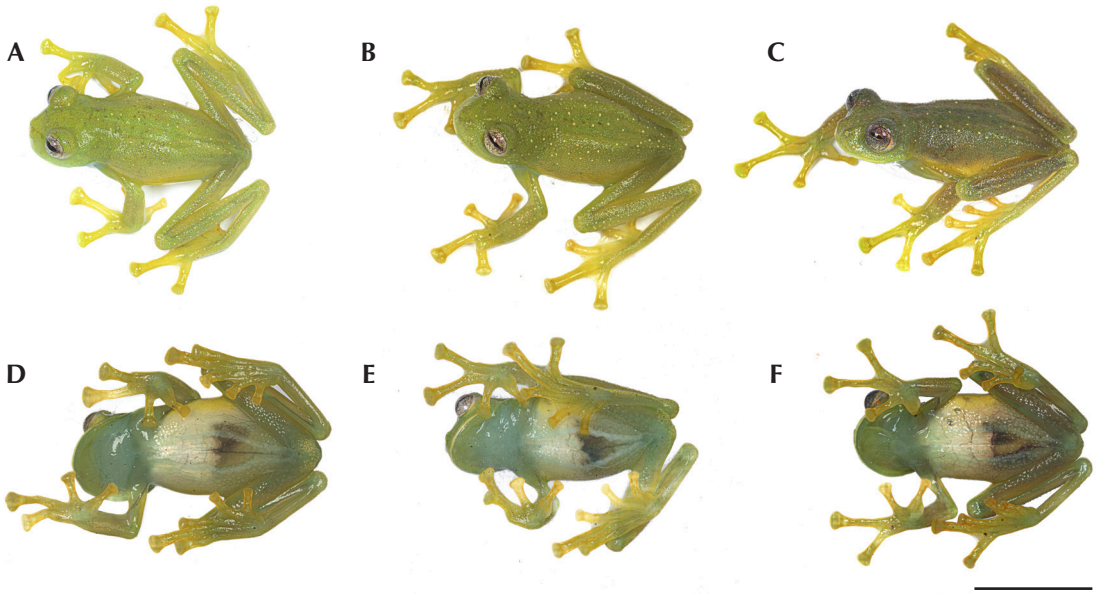

Figure 1. Coloration in life of males of *Nymphargus buenaventura* from Agua Blanca, Piura, northwestern Peru: (**A** and **D**) CORBIDI 22316 (SVL = 22.1 mm), (**B** and **E**) CORBIDI 22318 (SVL = 22.3mm), (**C** and **F**) CORBIDI 22320 (SVL = 22.3 mm). SVL = snout–vent length. Scale bar = 1.2 mm.

Morphology

We follow Guayasamin *et al*. (2020) for systematics of Centrolenidae and nomenclature of morphological characters. Specimens were sexed based on external sexual characteristics (e.g., presence of vocal sac) and by examining gonads. We measured the snout–vent length (SVL) to the nearest 0.1 mm with a digital calliper. Specimens were euthanized with an 8% benzocaine solution, fixed in 10% formalin, and stored in 70% ethanol. We also reviewed photographs of the specimen DHMECN 9471 of *Nymphargus buenaventura* from the type locality, El Oro province, Ecuador.

Bioacoustics

We recorded calls with a Marantz PMD660 digital recorder and a Marantz ME64 shotgun microphone; the resulting digital files were stored in WAV format. Recordings were performed during night surveys at 19°C, 0.5 m from a calling male (CORBIDI 22318) and about 1 m from an unvouchered male. We measured the following variables (as defined by Köhler *et al*. 2017): number of notes per call, note length (NL), and dominant frequency (DoF), which also corresponds to the fundamental frequency in this species, taken with a spectral slice over the entire note. We measured and visualised call variables on oscillograms and spectrograms (Figure 2) using Raven Lite v2.0.5 (K. Lisa Yang Center for Conservation Bioacoustics 2024). Spectrogram parameters included a 512-point window size, Hann window, and 75% overlap, providing a frequency (DFT size) resolution of ~86 Hz and a time (hop size) resolution of ~5.8 ms. Both the oscillogram and spectrogram were extracted directly from the same waveform in Raven and displayed using a logarithmic (dB) color scale.

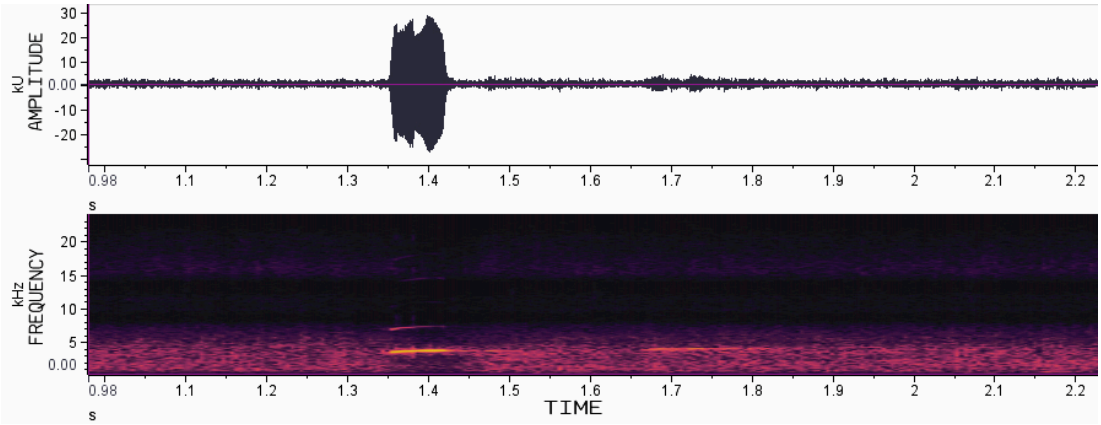

Figure 2. Advertisement call of *Nymphargus buenaventura* from Agua Blanca, Piura, northwestern Peru (CORBIDI 22318). Spectrogram is shown below oscillogram. Air temperature: 19°C.

Molecular Genetics

We sequenced a fragment of the 16S rRNA mitochondrial gene to compare its sequence with the only 16S sequence of *N. buenaventura* of a topotype available in Genbank, from QCAZ 54825 (accession code MT734665). We extracted genomic DNA from muscle tissues of CORBIDI 22316, 22320, and 22322 using the DNA extraction kit of IBI Scientific (Peosta, USA). We followed the standard protocols for amplification and sequencing of DNA (described by Chávez *et al*. 2019). We used the 16Sar forward (5'-3' sequence: CGCCTGTTTATCAAAAACAT) and 16Sbr reverse (5'-3' sequence: CCGGT CTGAACTCAGATCACGT) primers for 16S (Palumbi *et al*. 2002, von May *et al*. 2017). We used the following thermocycling conditions during the polymerase chain reaction (PCR) with a ProFlex thermal cycler (Applied Biosystems): one cycle of 96°C/3 min; 35 cycles of 95°C/30 s, 55°C/45 s, 72°C/1.5 min; one cycle 72°C/7 min. We used Exosap-IT (Affymetrix, Santa Clara, CA) to purify PCR products; MCLAB (San Francisco, CA) performed paired-end Sanger sequencing. We used Geneious R11, version 11.1.5 (Biomatters, http://www.geneious.com/) to assemble pair-end reads, to generate a consensus sequence, and to align our novel and GenBank sequences with the alignment program MAFFT v7.017 (Katoh and Standley 2013). We trimmed aligned sequences to a length of 578 bp, and estimated uncorrected p-distances, the proportion of nucleotide sites at which any two sequences are different, in MEGA X (Kumar *et al*. 2018). The newly generated sequence was deposited in GenBank (accession code for CORBIDI 22316: PV226227; fragments of the two other specimens were identical).

Results

We found all individuals on leaves 1.2–1.9 m above a stream in a small patch of secondary forest dominated by bushes and scattered small trees (3–5 m tall). We noticed some variation in the Peruvian population reported herein. Male CORBIDI 22320 (Figures 1C, 1F) has a darker green background on the dorsum with cream to pale yellow spots. The pale spots on the back are scattered in CORBIDI 22316 (Figures 1A, 1D) and CORBIDI 22320, or densely present in CORBIDI 22318 (Figures 1B, 1E) and CORBIDI 22321. The fragments of 16S of the three specimens are identical (accession code for CORBIDI 22316: PV226227) and similar to

the specimen of *N. buenaventura,* QCAZ 54825, from the type locality (uncorrected p-distance 1.08%). All adult males match the SVL previously documented (Cisneros-Heredia and Yañez-Muñoz 2007) for the species (20.9–22.4 mm).

On the same day we collected the frogs, we recorded two calls: the first one from the male CORBIDI 22318 and the second one from an unvouchered individual, both at 19:40 h. Both individuals were calling from leaves alongside a stream, 19°C air temperature. The call of *Nymphargus buenaventura* is tonal (Figure 2), composed of high-pitched calls (chirps). We analized the two calls. The first one had a duration of 0.59 s with a dominant frequency of 3.66 kHz, while the second was shorter (0.53 s) and peaked at 3.38 kHz (note duration mean = 0.56 ± 0.04 s, N = 2) and a dominant frequency of 3.37–3.65 kHz (mean = 3.51 ± 0.19 kHz, N = 2). The dominant frequency corresponds to the fundamental frequency. This is the first recording and quantitative description of an advertisement call of *N. buenaventura,* which had previously only been described onomatopoeically as a simple "tic" (Cisneros-Heredia and Yañez-Muñoz 2007). We noticed that calling activity ceased upon our approach, suggesting high sensitivity to disturbance. That is why, under these conditions, we recorded one male near us (CORBIDI 22318) and one unvouchered individual from a distant spot.

In the same stream, we also located two egg clutches with 47 and 52 eggs (Figure 3), exceeding the number of 46 eggs for a clutch known from Ecuador (Cisneros-Heredia and Yañez-Muñoz 2007, Guayasamin *et al*. 2020).

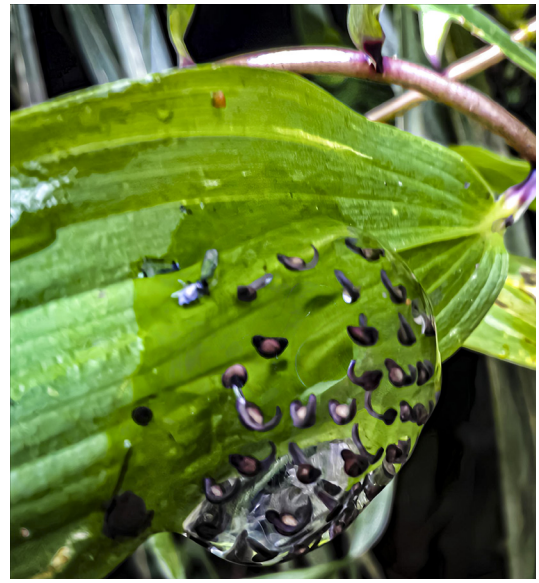

Figure 3. Egg clutch of *Nymphargus buenaventura* with 47 embryos, located at Agua Blanca, Piura, northwestern Peru, locality of the new record.

Discussion

All individuals show the diagnostic characteristics of *Nymphargus buenaventura* (Cisneros-Heredia and Yañez-Muñoz 2007), including green dorsum with small pale yellow to cream spots, reduced webbing between fingers, absence of humeral spine, and absence of iridophores on the digestive visceral peritonea, but with iridophores covering the renal capsules (see Figure 1). Additionally, our genetic analyses yielded a genetic distance of only 1.08% from the topotype QCAZ 54825, which confirms our identification. Also, uncorrected *p*-distance values between QCAZ 54825 and genetically related species (i.e. *Nymphargus cariticommatus, N. lindae,* and *N. sucre*) are more than 4% (Montilla *et al*. 2023). Our results suggest that the Peruvian population reported herein might be ± 1% genetically closer or farther from related samples reported by Montilla *et al*. (2023). Additionally, according to the phylogenetic data published by Guayasamin *et al*. (2020), *N. cariticommatus, N. sucre,* and *N. wileyi* form a clade sister to a clade formed by *N. lindae* and *N. cochranae*. This suggests that *N. buenaventura* may be genetically related to *N. cochranae* and *N. wileyi*. Further genetic research is needed to clarify its phylogenetic position.

We report the first documented occurrence of *Nymphargus buenaventura* in Peru, marking the

fourth glassfrog species recorded from the Pacific versant of the northern Peruvian Andes. This finding significantly expands the known distribution of the species, extending its range 180 km (airline) southward from the southernmost locality reported for this species, which is Marcabelí (Yánez-Muñoz *et al*. 2014), Ecuador, and 190 km (airline) from its type locality (Cisneros-Heredia and Yañez-Muñoz 2007), the Buenaventura Reserve in Guayas Province, Ecuador (see Figure 4). This range extension suggests the potential presence of *N. buenaventura* in intermediate localities, necessitating further field investigations to delineate its precise distribution. Our observations at 1800 m a.s.l. represent one of the few records of this species at altitudes exceeding 1700 m (Cisneros-Heredia and Yañez-Muñoz 2007, Yánez-Muñoz *et al.* 2014, Guayasamin *et al.* 2020, Coloma and Duellman 2025). This is not the first time this species has been recorded at this high elevation. Coloma and Duellman (2025) reported this glassfrog at an elevation of 1925 m a.s.l. The specimen QCAZ 21947 from "Luz María, 0.9 km Oeste de Luz María," Ecuador (geographic coordinates: -2.684 -79.417), reported by Yánez-Muñoz *et al*. (2014) and Guayasamin *et al*. (2020) was found at 1770 m a.s.l., not at 770 m a.s.l. as given therein. The western Andean slopes of northern Peru are characterized by a complex environmental mosaic, transitioning from equatorial dry forests at lower elevations to progressively wetter montane forests at higher altitudes (Koepcke and Koepcke 1958, Brack 1986), with rougher terrain above 300 m a.s.l. (Koepcke and Koepcke 1958, Venegas 2005). The transition to wetter conditions occurs around 1600 m a.s.l. (Koepcke and Koepcke 1958, Venegas 2005). Since the documented altitudinal range of *N. buenaventura* corresponds to the equatorial dry forest zone, updated altitudinal records between 1770–1925 m a.s.l. indicate the upper altitudinal limit of this species and its tolerance to the transitional montane forest environment.

Among *Nymphargus* from the Pacific versant between Peru and Ecuador, the advertisement call of four species have previously been described: *Nymphargus grandisonae* (Cochran and Goin, 1970), *N. griffithsi* (Goin, 1961), *N. lasgralarias* Hutter and Guayasamin, 2012, and *N. manduriacu* Guayasamin, Cisneros-Heredia, Vieira, Kohn, Gavilanes, Lynch, Hamilton, and Maynard, 2019 (all occurring in northwestern Ecuador). We add information on one more species herein. From the aforementioned species, only *N. griffithsi* and *N. manduriacu* emit single-tonal calls, as does *N. buenaventura*. Despite our small sample, we can confirm that the dominant frequency in the advertisement call of *N. buenaventura* is considerably lower: 3.37–3.65 kHz (vs 3.79–4.30 kHz in *N. griffithsi,* and 4.05–4.44 kHz in *N. manduriacu*). Additionally, only *N. manduriacu* has a combination of a single tonal call with a chirp-like sound (Guayasamin *et al*. 2019) as observed in *N. buenaventura*. Among genetically related species mentioned earlier in this section, the call is only known for *N. cochranae,* which was described as a high-pitched note by Lynch and Duellman (1973). Despite the description matching the sound we recorded from *N. buenaventura* (high-pitched note), the lack of data about spectral and temporal variables of the call of *N. cochranae* prevents us from performing additional analyses on this topic.

A negative correlation between SVL and peak frequency in glassfrogs was observed by Escalona-Sulbarán *et al*. (2018). Due to the lack of quantitative acoustic data, it is not possible to analyse genetically related species. *Nymphargus buenaventura,* which is smaller (SVL range = 20.9–22.4 mm) than *N. griffithsi* (SVL range = 20.9–22.4 mm) and *N. manduriacu* (SVL range = 20.9–22.4 mm), two species from southern Ecuador, has a lower dominant frequency range, something that does not support the hypothesis provided by Escalona-Sulbarán *et al*. (2018). This hypothesis needs to be tested using a larger dataset based mainly on genetically related species as suggested by Escalona-Sulbarán *et al*. (2018).

We noticed that embryos inside clutches are dark grey (see Figure 3), whereas embryos reported

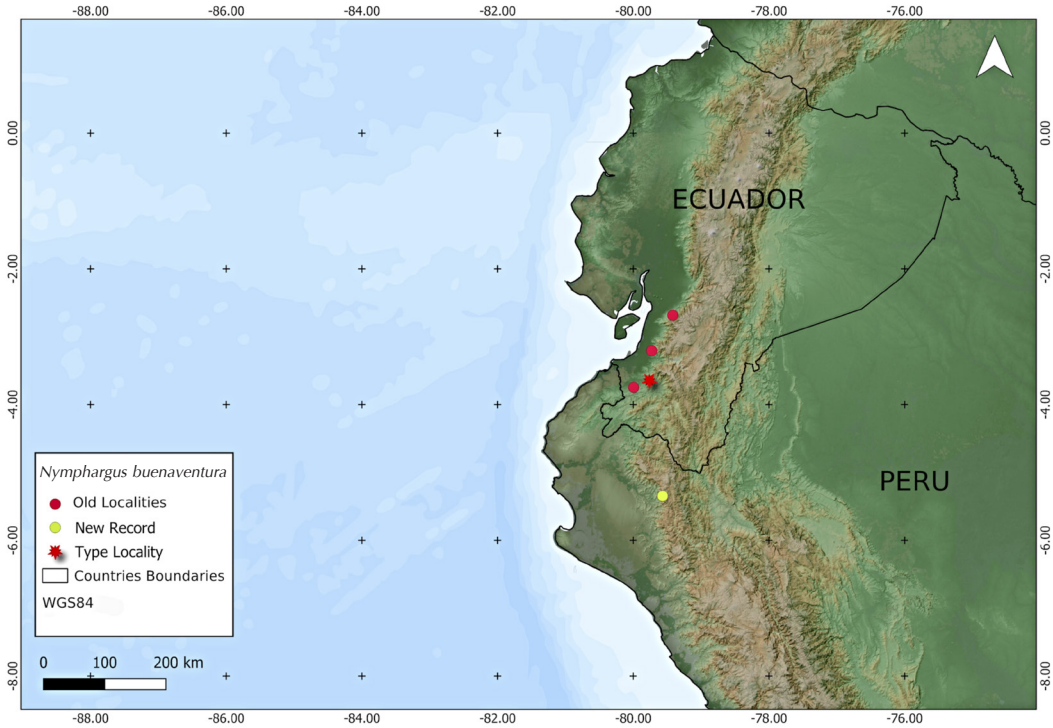

Figure 4. Map showing the distribution of *Nymphargus buenaventura*.

for Ecuadorian populations are yellow (Cisneros-Heredia and Yañez-Muñoz 2007). The ages of the clutches we located are unknown, which may explain the color differences. As reported by Cisneros-Heredia and Yañez-Muñoz (2007), both egg clutches were on the upper side of the leaf and seemed to glide toward its edge.

Despite the suggestion of Gayasamin *et al.* (2020) and Cisneros-Heredia *et al.* (2022) that *N. buenaventura* should be categorized as Endangered, we suggest keeping *N. buenaventura* in the Data Deficient category until future studies focused on its population status are conducted.

Acknowledgments

We thank Moisés Escalona and Thiago R. Carvalho for their insightful revisions and particularly Fernando Rojas-Runjaic for his accurate comments and thoughtful suggestions that have helped us to improve this manuscript. We are also grateful to Janalee P. Caldwell for her revision to the latest version of this work. The Servicio Nacional Forestal y de Fauna Silvestre de Peru issued the collecting permit RJ Nº 003-2014-SERFOR-RCS-JEF029-2016-SERFORDGGSPFFS. This study would not have been possible without the economic support of the Chicago Board of Trade (CBOT) Fund for Endangered Species and Nature and Culture International (NCI). AC is the Half-Earth Chair and was supported by a grant from the E. O. Wilson Biodiversity Foundation. GC thanks the Cornell University Ornithology Lab for providing acoustic equipment and software. We also thank Kathy Carillo, Elio Nuñez-Cortez, and all the

people working in NCI who helped us during every field survey. GC also thanks Ivan Wong, who helped him build the graphics. We are grateful to the staff of Cafeteria Pajarero and La Cortez Restaurant for their hospitality and logistical support during our fieldwork.

References

Brack, A. 1986. Las ecorregiones del Perú. *Boletín de Lima 44:* 57–70.

Catenazzi, A. and P. J. Venegas. 2012. Anfibios y reptiles. Pp. 106–116 *in* N. Pitman, E. Ruelas-Inzunza, D. Alvira, C. Vriesendorp, D. K. Moskovits, A. del Campo, T. Wachter, D. F. Stotz, S. Noningo-Sesén, E. Tuesta-Cerrón, and R. C. Smith (eds.), *Perú: Cerros de Kampankis. Rapid Biological and Social Inventories Report 24*. The Field Museum.

Chávez, G., R. Pradel, and A. Catenazzi. 2019. Integrative taxonomy reveals first country record of *Hyalinobatrachium mondolfii* Señaris and Ayarzagüena 2001, and distribution range extensions for *Cochranella nola* Harvey 1996, and *Rulyrana spiculata* Duellman 1976 (Anura: Centrolenidae) in Peru. *Zootaxa 4691:* 541–560.

Cisneros-Heredia, D. F. 2008. *Nymphargus buenaventura*. The IUCN Red List of Threatened Species 2008: e. T135767A4198831. Eletronic Database accessible at https://dx.doi.org/10.2305/IUCN.UK.2008.RLTS.T135767A4198831.en. Accessed on 15 June 2025.

Cisneros-Heredia, D. F. and M. H. Yánez-Muñoz. 2007. A new species of glassfrog (Centrolenidae) from the southern Andean foothills on the west Ecuadorian region. *South American Journal of Herpetology 2:* 1–10.

Cisneros-Heredia, D. F., M. Yánez-Muñoz, M. Ortega-Andrade, and P. Bejarano-Muñoz. 2022. *Nymphargus buenaventura*. The IUCN Red List of Threatened Species 2022: e. T135767A98656893. Eletronic Database accessible at https://dx.doi.org/10.2305/IUCN.UK.2022-2.RLTS.T135767A98656893.en. Captured on 15 June 2025.

Coloma, L. A., and W. E. Duellman. 2025. *Amphibians of Ecuador. Volume 4. Phyllomedusidae, Leptodactylidae, Ceratophryidae, Hemiphractidae, Eleutherodactylidae, Centrolenidae, Gymnophiona, and Caudata.* Boca Raton. CRC Press. 496 pp.

Crump, M. L. and N. Y. Scott Jr. 1994. Visual encounter surveys. Pp. 84–91 *in* W. R. Heyer, M. A. Donnelly, R. A. McDiarmid, L. C. Hayek, and C. M. Foster (eds.), *Measuring and Monitoring Biological Diversity: Standard Methods for Amphibians*. Smithsonian Institution, USA.

Duellman, W. E. and E. R. Wild. 1993. Anuran amphibians from the Cordillera de Huancabamba, northern Peru: Systematics, ecology, and biogeography. *Occasional Papers of the Museum of Natural History, The University of Kansas 157*: 1–53.

Escalona-Sulbarán, M. D., P. I. Simões, A. Gonzalez-Voyer, S. Castroviejo-Fisher. 2018. Neotropical frogs and mating songs: the evolution of advertisement calls in glassfrogs. *Journal of Evolutionary Biology 32:* 63–176.

Frost, D. R. 2025. Amphibian Species of the World: an Online Reference. Version 6.2 (15th July, 2025). Electronic Database accessible at https://amphibiansoftheworld.amnh.org/index.php. American Museum of Natural History, New York, USA.

Gagliardi-Urrutia, G., C. R. García-Dávila, A. Jaramillo-Martinez, O. Rojas-Padilla, E. Ríos-Alva, R. Aguilar-Manihuari, P. E. Pérez-Peña, P. Tupinambá, and S. Castroviejo-Fisher. 2022. *Anfibios de Loreto*. Iquitos, Peru. Instituto de Investigaciones de la Amazonía Peruana. 203 pp.

Guayasamin, J. M., D. F. Cisneros-Heredia, J. Vieira, S. Kohn, G. Gavilanes, R. L Lynch, P. S. Hamilton, R. J. Maynard. 2019. A new glassfrog (Centrolenidae) from the Chocó-Andean Río Manduriacu Reserve, Ecuador, endangered by mining. *PeerJ 7:* e6400.

Guayasamin, J. M., D. F. Cisneros-Heredia, and R. W. McDiarmid. 2020. Glassfrogs of Ecuador: Diversity, evolution, and conservation. *Diversity 6:* 222.

Katoh, K. and D. M. Standley. 2013. MAFFT multiple sequence alignment software version 7: Improvements in performance and usability. *Molecular Biology and Evolution 30:* 772–780.

K. Lisa Yang Center for Conservation Bioacoustics at the Cornell Lab of Ornithology. 2024. Raven Pro: Interactive sound analysis software. https://ravensoundsoftware.com/software/raven-pro.

Koepcke, H. W. and M. Koepcke. 1958. Los restos de bosques en las vertientes occidentales de los Andes peruanos. *Boletín del Comité Nacional para la Protección a la Naturaleza (Peru) 16:* 22–30.

Köhler, J., M. Jansen, A. Rodriguez, P. J. R. Kok, L. F. Toledo, M. Emmrich, F. Glaw, C. F. B. Haddad, M. O. Rodel, and M. Vences. 2017. The use of bioacoustics in anuran taxonomy: Theory, terminology, methods and recommendations for best practice. *Zootaxa 4251:* 1–124.

Kumar, S., G. Stecher, M. Li, C. Knyaz, and K. Tamura. 2018. MEGA X: Molecular evolutionary genetics

analysis across computing platforms. *Molecular Biology and Evolution 35:* 1547–1549.

Lynch, J. D. and W. E. Duellman. 1973. A review of the centrolenid frogs of Ecuador, with descriptions of new species. *Occasional Papers of the Museum of Natural History*, *The University of Kansas:* 1–66

Montilla S. O., L. F. Arcila-Pérez, M. P. Toro-Gómez, F. Vargas-Salinas, and M. Rada. 2023. A multidisciplinary approach reveals a new species of Glassfrog from Colombia (Anura: Centrolenidae: *Nymphargus*). *Zootaxa 5271:* 1–48.

Palumbi, S. R., A. Martin, S. Romano, W. O. McMillan, L. Stice, and G. Grabawski. 2002. *The Simple Fool's Guide to PCR, Version 2.0.* Privately published, University of Hawaii, USA. 45 pp.

Portik, D.M., J.W. Streicher, J.J. Wiens. 2023. Frog phylogeny: A time-calibrated, species-level tree based on hundreds of loci and 5,242 species. *Molecular Genetics and Evolution 188:* 107907.

Twomey, E., J. Delia, and S. Castroviejo-Fischer. 2014. A review of northern Peruvian glassfrogs (Centrolenidae), with the description of four new remarkable species. *Zootaxa 3851:* 1–87.

Venegas, P. 2005. Herpetofauna del bosque seco ecuatorial de Perú: Taxonomía, ecología y biogeografía. *Zonas Áridas 9:* 9–26.

von May, R., A. Catenazzi, A. Corl, R. Santa-Cruz, A. C. Carnaval, and C. Moritz. 2017. Divergence of thermal physiological traits in terrestrial breeding frogs along a tropical elevational gradient. *Ecology and Evolution 7:* 7187–7202.

Yánez-Muñoz, M. H., J. C. Sánchez-L., K. López-Hervas, E. Rea-S., P. Meza-Ramos, L. A. Oyagata-C., and P. Guerrero. 2014. Expansion of the distributional range of some species of amphibians and reptiles in southwestern Ecuador/Ampliaciones del rango de distribución de algunas especies de anfibios y reptiles en el suroccidente de Ecuador. *Avances en Ciencias e Ingeníerias. Sección B. Quito 6:* 2–5.

Editor: Thiago R. Carvalho

Phyllomedusa 24(2):281–294, 2025

ISSN 1519-1397 (print) / ISSN 2316-9079 (online)
doi: http://dx.doi.org/10.11606/issn.2316-9079.v24i2p281-294

Population observations and microhabitat use of *Isthmohyla tica* (Anura: Hylidae) in San Ramón, Costa Rica

Pablo Marín Pacheco,[1] Jerson Santamaría Martínez,[2] José Manuel Mora,[3,4] Jennifer L. Stynoski,[5] and Randall Arguedas[6,7]

[1] Universidad Técnica Nacional, Sede Atenas, Ingeniería Forestal y Vida Silvestre. Atenas, Costa Rica. E-mail: pablomarin95@hotmail.com.

[2] Life Monteverde. Monteverde, Puntarenas, Costa Rica. E-mail: jsantamaria@lifemonteverde.com.

[3] Universidad Técnica Nacional, Sede Central. Carrera de Gestión Ecoturística, Alajuela, Costa Rica. E-mail: josemora07@gmail.com.

[4] Portland State University, Department of Biology and Museum of Vertebrate Biology. Portland, Oregon, USA.

[5] Instituto Clodomiro Picado, Universidad de Costa Rica, Coronado, Costa Rica. E-mail: stynoski@gmail.com.

[6] Universidad Técnica Nacional, Sede Atenas. Alajuela, Costa Rica.

[7] División de Especies Exóticas y Fauna Silvestre, VetLab. Curridabat, San José,Costa Rica. E-mail: ranarg@gmail.com.

Abstract

Population observations and microhabitat use of *Isthmohyla tica* (Anura: Hylidae) in San Ramón, Costa Rica. *Isthmohyla tica,* the Tica Frog, is a critically endangered species endemic to Costa Rica and supposedly Panama that has only been seen in a few sites in recent decades. To aid in its conservation, we assessed the population status and microhabitat preferences of this frog in a section of the Danta stream at Rancho Alegre farm, San Ramón, Costa Rica. We conducted 18 nocturnal surveys and collected data on perch types, vegetation associations, stream characteristics, and environmental variables for each sighting of the Tica Frog. To identify potential microhabitat preferences, we compared these features between sites with or without frogs as well as between sites with juvenile or adult individuals. We recorded 13 individuals, comprising three juveniles and 10 adults. Nine adults were male and one female, with the disparity likely due to the conspicuous vocalizations of males. Juvenile and adult frogs occupied areas with similar stream widths (t = 0.91; p = 0.38). However, juveniles were found closer to the water (t = 5.14, p = 0.01) and adjacent to shallower areas of the stream compared to adults (t = 2.50, p = 0.03). Frogs predominantly perched on *Piper* sp. (30.7%) and on the upper surface of leaves (69.2%). The height at which the Tica Frog was recorded (0.1 to 2.2 m) was similar for both age groups (t = 0.86, p = 0.44). We did not find significant differences in canopy cover (average = 74.6%), diameter at breast height (≤ 3.14 cm), vegetation density (5.0 plants/m²), or plant richness (1–4 species) between juveniles and adults. Similarly, we did not observe differences in environmental variables between these groups. Furthermore, vegetation characteristics and environmental variables did not differ between sites with the

Received 30 September 2024
Accepted 25 September 2025
Distributed December 2025

Tica Frog and nearby sites without them. Our findings suggest that the measured variables do not significantly influence the microhabitat selection of the Tica Frog. This novel information on the population status and microhabitat use of *I. tica* is needed for the development of management strategies for the conservation of this critically endangered species.

Keywords: Amphibians, Conservation, Critically endangered, Environmental variables, Microhabitats, Population, Vegetation characteristics.

Resumen

Observaciones poblacionales y uso del microhábitat de *Isthmohyla tica* (Anura: Hylidae) en San Ramón, Costa Rica. *Isthmohyla tica,* la rana Tica, es una especie en peligro crítico de extinción, endémica de Costa Rica y supuestamente de Panamá que solo ha sido avistada en unos pocos sitios en las últimas décadas. Para contribuir a su conservación, evaluamos el estado de la población y las preferencias de microhábitat de esta rana en un tramo de la quebrada Danta en Rancho Alegre, San Ramón, Costa Rica. Realizamos 18 censos nocturnos y recolectamos datos sobre tipos de perchas, asociaciones vegetales, características de la quebrada y variables ambientales para cada avistamiento de esta rana. Comparamos estas características entre individuos juveniles y adultos, así como entre sitios con y sin la presencia de la rana, con el fin de identificar posibles preferencias de microhábitat. Registramos 13 individuos, tres juveniles y 10 adultos, nueve machos y una hembra. Esta disparidad posiblemente se deba a que los machos son más fáciles de detectar debido a sus vocalizaciones. Tanto juveniles como adultos ocuparon áreas con similares anchos de la quebrada (t = 0.91; p = 0.38). Sin embargo, los juveniles se encontraron más cerca del agua (t = 5.14, p = 0.01) y en zonas laterales más superficiales de la quebrada (t = 2.50, p = 0.03). Las ranas se posaron predominantemente en *Piper* sp. (30.7%) y en la superficie superior de las hojas (69.2%). La altura a la que se registró la rana Tica (0.1 a 2.2 m) fue similar para ambos grupos (t = 0.86, p = 0.44). No encontramos diferencias significativas en la cobertura de dosel (promedio = 74.60%), diámetro a la altura del pecho (≤ 3.14 cm), densidad de vegetación (5.0 plantas/m²) o riqueza de especies entre juveniles y adultos. Del mismo modo, no observamos diferencias en las variables ambientales entre estos grupos. Además, no encontramos diferencias en las características de la vegetación o en las variables ambientales entre los sitios con y sin ranas. Nuestros hallazgos sugieren que las variables medidas no influyen significativamente en la selección de microhábitat de la rana Tica. Esta información es crucial para desarrollar estrategias de manejo y conservación para esta especie críticamente amenazada.

Palabras clave: Anfibios, Características de la vegetación, Conservación, Microhábitats, Peligro crítico, Población, Variables ambientales.

Resumo

Observações populacionais e uso de micro-hábitats de *Isthmohyla tica* (Anura: Hylidae) em San Ramón, Costa Rica. *Isthmohyla tica* é uma espécie criticamente ameaçada de extinção, endêmica da Costa Rica e, supostamente, do Panamá, que só foi vista em algumas localidades nas últimas décadas. Para contribuir para sua conservação, avaliamos o estado da população e as preferências de micro-hábitat dessa perereca em um trecho do riacho Danta, fazenda Rancho Alegre, em San Ramón, Costa Rica. Realizamos 18 observações noturnas e coletamos dados sobre tipos de poleiros, associações com a vegetação, características do riacho e variáveis ambientais para cada observação. Para identificar potenciais preferências de micro-hábitat, comparamos essas características entre localidades com ou sem as pererecas, bem como entre locais com indivíduos juvenis ou adultos. Registramos 13 indivíduos, incluindo três juvenis e 10 adultos. Nove adultos eram machos e um era fêmea, com a disparidade provavelmente devida às vocalizações conspícuas dos machos. As rãs juvenis e adultas ocupavam áreas com larguras do curso d'água semelhantes (t = 0,91; p = 0,38).

No entanto, os juvenis foram encontrados mais perto da água (t = 5,14, p = 0,01) e adjacentes a áreas mais rasas do riacho em comparação com os adultos (t = 2,50, p = 0,03). As pererecas empoleiraram-se predominantemente em *Piper* sp. (30,7%) e na superfície superior das folhas (69,2%). A altura em que os animais foram registrados (0,1 a 2,2 m) foi semelhante para ambas as faixas etárias (t = 0,86, p = 0,44). Não encontramos diferenças significativas na cobertura do dossel (média = 74,6%), diâmetro à altura do peito (≤ 3,14 cm), densidade da vegetação (5,0 plantas/m²) ou riqueza de plantas (1–4 espécies) entre juvenis e adultos. Da mesma forma, não observamos diferenças nas variáveis ambientais entre esses grupos. Além disso, as características da vegetação e as variáveis ambientais não diferiram entre os locais com a espécie e as localidades próximas sem a espécie. Nossas descobertas sugerem que as variáveis medidas não influenciaram significativamente a seleção de micro-hábitats por essa espécie. Essas novas informações sobre o estado populacional e o uso de micro-hábitats de *I. tica* são necessárias para o desenvolvimento de estratégias de manejo para a conservação dessa espécie criticamente ameaçada.

Palavras-chave: Anfíbios, Características da vegetação, Conservação, Criticamente ameaçada, Micro-hábitats, População, Variáveis ambientais.

Introduction

Amphibians are the most endangered class of vertebrates globally, with approximately 41% of described species classified as threatened and an increasing number facing a high risk of extinction (Carné and Vieites 2024). In Costa Rica, declines in numerous amphibian species have been observed. The country is home to 221 amphibian species, of which about 100 are listed under some threat category and four are considered extinct (Zumbado-Ulate *et al.* 2019, Rodríguez *et al.* 2020, BiodataCR 2024, Sasa *et al.* 2025).

Frogs of the genus *Isthmohyla* are second among groups of anurans with the highest number of critically endangered species in Costa Rica; some are observed only rarely and are listed among priority species for conservation (Bolaños 2009, Chaves-Acuña *et al.* 2020). *Isthmohyla tica* (Starrett, 1966) is one of these priority species.

Populations of *I. tica* have declined dramatically since the late 1980s, to the point that the species was reported absent from many sites with historic populations. By 2007, it was feared to be extinct (Bolaños 2009). Declines of *I. tica* populations have been attributed to chytridiomycosis, a disease caused by the fungus *Batrachochytrium dendrobatidis* Longcore, Pessier, and D. K. Nichols, 1999 (Gratwicke *et al.* 2016). No evidence of this pathogen was found in 26 *I. tica* (collected between 1961 and 2011) specimens at the Museum of Zoology at the University of California-Berkeley and the University of Costa Rica (De León *et al.* 2018). Therefore, the population decline of this tree frog remains enigmatic and has occurred despite the availability of protected areas with preserved forests (Cheng *et al.* 2011, Rodríguez *et al.* 2020).

Isthmohyla tica is endemic to Costa Rica and supposedly Panama, meaning its distribution is limited, which heightens its vulnerability to extinction. In Costa Rica, it was historically found in the mid-elevations of the Tilarán, Central, and Talamanca mountain ranges, at altitudes ranging from 720 to 1750 m above sea level (Sasa *et al.* 2010). Since 2007, it has only been reported in the Bosque Eterno de los Niños in Monteverde along with a single individual that was sighted at Tapantí National Park (Abarca 2016, IUCN SSC Amphibian Specialist Group and NatureServe 2020, Hidalgo-Mora *et al.* 2022). According to the information we compiled, stable populations have only been reported in the Chutas sector of the Bosque Eterno de los Niños (Hidalgo-Mora *et al*. 2022).

In Panama, the species was "rediscovered" in 2010, with sightings of three individuals at two sites within the Parque Internacional La Amistad (Hertz *et al.* 2012, IUCN SSC Amphibian

Specialist Group and NatureServe 2020). It is thought that the populations in Monteverde, Costa Rica and western Panama are likely not the same species (IUCN SSC Amphibian Specialist Group and NatureServe 2020). Similarly, another population described in the Los Santos region of Costa Rica likely represents a different, undescribed species (G. Chaves pers. comm.).

In the current scenario, the species has been reported at only two localities in Costa Rica, and the records are sporadic with a small number of individuals observed during each visit (Rodríguez *et al.* 2020). Due to this situation, the IUCN SSC Amphibian Specialist Group and NatureServe (2020) have classified the *I. tica* as a critically endangered species with declining populations for over two decades. It is estimated that there are no more than five subpopulations throughout its range, and it is likely that each subpopulation has fewer than 50 mature individuals (IUCN SSC Amphibian Specialist Group and NatureServe 2020). If the Los Santos population in Costa Rica and the Panama populations are indeed different species, then the species' status is even more concerning.

The first recent sighting of *Isthmohyla tica* in Costa Rica occurred in Monteverde in 2010, after 15 years without any reports (García-Rodríguez *et al.* 2012, Hertz *et al.* 2012). In 2020, we also identified *I. tica* at the Rancho Alegre farm in San Ramón de Alajuela, Costa Rica. We aimed to study this population in order to generate baseline information on biological and ecological characteristics, which in turn could contribute to future management plans and conservation strategies for this species. To this end, our objective was to assess the status and microhabitat use of the population in terms of the vegetation, perch types, and environmental variables in a section of the Danta stream at Rancho Alegre farm. Additionally, we sought to compare microhabitat variables between sites with *I. tica* and nearby sites that did not have individuals of this species in this same section of the stream.

Materials and Methods

Study Species

Isthmohyla tica has a short, truncated snout in profile. The dorsum and upper body surfaces display visible greenish-brown tubercles, and the hind limbs are marked with dark transverse bands (Savage 2002). Adult males range from 27 to 34 mm in snout–vent length, while females range from 33 to 42 mm. The toes are relatively short and broad, and digits III and IV bear large, wide discs that are equal to, or slightly larger than, the diameter of the tympanum (Savage 2002).

Savage (2002) suggested that *I. tica* lays its eggs beneath rocks in streams, and that the tadpoles adhere to the substrate using a large oral funnel. Nevertheless, many fundamental aspects of its reproductive and developmental biology, such as type of amplexus, oviposition behavior, parental care, hatching time, microhabitat preferences, feeding, and duration of metamorphosis, remain unknown (Savage 2002, IUCN SSC Amphibian Specialist Group and NatureServe 2020).

Study Area

The study area is located in the western part of San Ramón Canton, Alajuela Province, within the Peñas Blancas District, specifically along the Danta Stream (10°20'13" N, 84°46'21" W; 1,492 m a.s.l.; Figure 1). The site lies within the Lower Montane Rain Forest life zone (Calvo 1989). The climate is humid, with average annual precipitation exceeding 5,000 mm, and March being the only dry month. Temperatures vary between 9 and 24°C (Calvo 1989). Common vegetation includes ferns, epiphytes, and a variety of trees from the Lauraceae, Meliaceae, Melastomataceae, Rubiaceae, and Sapotaceae families (Calvo 1989). The Danta Stream is 2,303 m long with lotic waters; however, for this study, we focused on a 1,200 m section. A waterfall blocked access upstream to the

northeast and served as a natural reference point marking the start of our sampling transect.

Data Collection

We conducted 18 sampling sessions, each consisting of two nights in a row per month from December 2020 to August 2021. Visits to the study site between September and November were not conducted because they are risky due to severe storms and flash floods. We established defined band transects to estimate presence or absence, relative abundance, microhabitat association, and activity patterns of anuran species (Heyer *et al.* 2014). This method involves limited searches for individuals per unit of time along permanent transects (Heyer *et al.* 2014). We divided the selected section of the Danta stream into three 400 m long sectors, designated as A, B, and C (Figure 1). During each sampling night, we surveyed all three sectors, but we randomized the order in which the sectors were surveyed to avoid biases in the behavior and distribution of the species according to its activity peaks.

We marked 24 defined band transects, with eight transects per sector. Each transect measured 2 m perpendicularly from the stream's edge on both sides by 50 m along the stream. We systematically surveyed the transects, alternating between odd-numbered transects (1, 3, 5, 7… 23) on the first night and even-numbered transects (2, 4, 6, 8… 24) on the following night. To cover both sides of the stream, we always surveyed both banks simultaneously for 30 min. We used a stopwatch to control the time, pausing it each time we found a frog to record the respective data. Each survey included both visual searches to locate individual *I. tica* and auditory searches to find males.

We conducted surveys from 17:30 h to approximately midnight (between 23:30 and 24:00 h). For each individual, we recorded the geographical coordinates, time, date, activity (calling, amplexus, or resting), stage (juvenile or adult), and sex (determined by vocalizations and the presence of nuptial pads in males). In cases where the sex of an individual was uncertain, we captured the frog to accurately determine its characteristics and subsequently released it at the same location where it was found. Capture was conducted using gloves to minimize the risk of disease transmission, although we acknowledge that certain types of gloves may negatively affect amphibians (Gutleb *et al.* 2001, Cashins *et al.* 2008).

For each record of *Isthmohyla tica,* we noted the following biophysical habitat characteristics: type of perch (leaf, branch, vine, stem, sand, soil, leaf litter, pebble, or stone), position on vegetative substrate (upper or lower leaf surface), plant species, height above ground, and distance of the perch from the stream edge. Additionally, we recorded data on the width and depth of the water at the center of the stream.

To characterize the vegetation, we marked 2 × 5 m plots for the tree stratum (diameter at breast height; DBH > 10 cm) and 1 × 1 m plots for the herbaceous stratum (DBH <10 cm). These plots were established in locations where *I. tica* was present and were also paired randomly with plots in locations where the frogs were absent (Tocher *et al.* 1997). We characterized the vegetation according to the following variables: (a) species richness, defined as the number of plant species; (b) vegetation density of the tree and herbaceous strata, measured as abundance per unit area; (c) DBH of each individual plant; and (d) canopy cover, estimated using a densiometer (Tocher *et al.* 1997).

Regarding climatic variables, we used a Be8910 Ontranki® multifunction anemometer to measure air temperature (°C), relative humidity (%), and wind speed (m/s). We collected these data at a height of 1.50 m above the ground. We obtained precipitation values (mm) from the meteorological station in Monteverde, 3.41 km from the Danta stream. Additionally, we gathered data on moonlight percentage using the website of the Astronomical Applications Department of the United States Naval Observatory (https://aa.usno.navy.mil/data/index). Meteorological variables

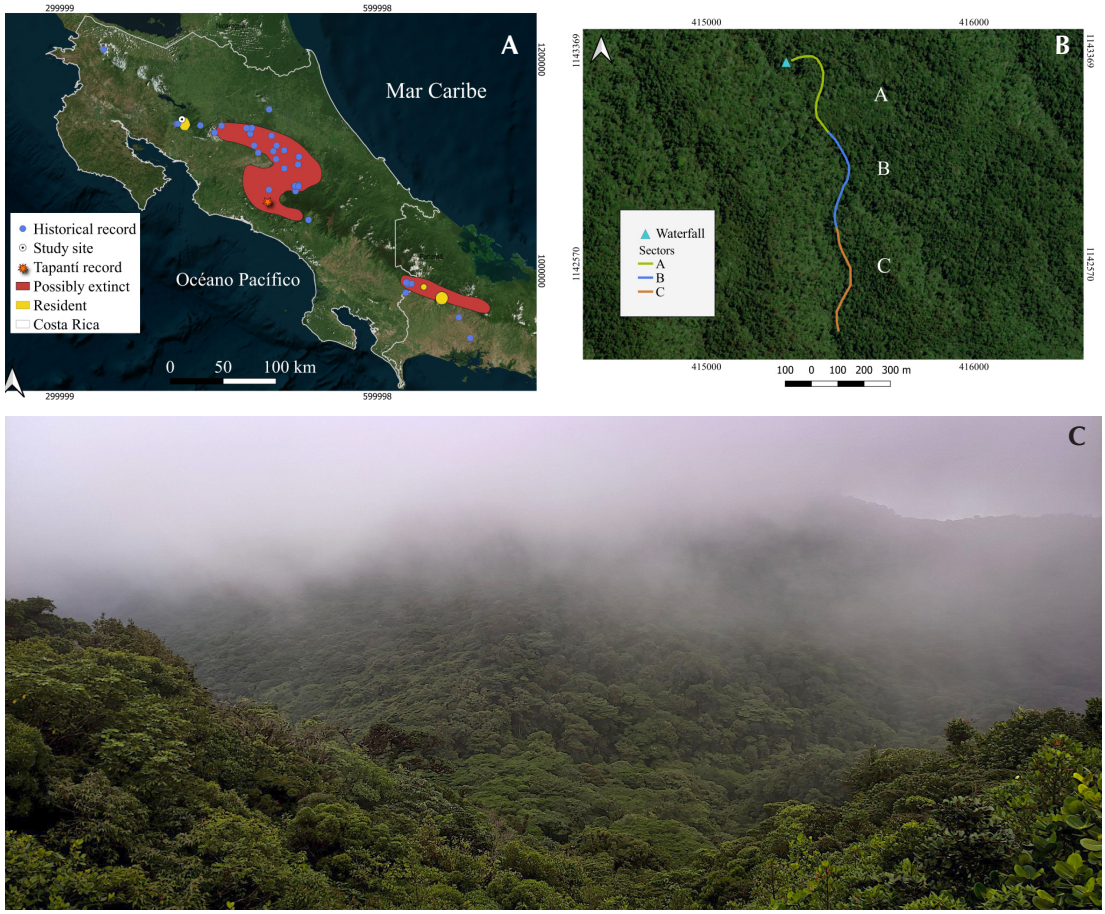

Figure 1. (**A**) Historical records (red; IUCN SSC Amphibian Specialist Group and NatureServe 2020), and current known areas of *Isthmohyla tica* in Costa Rica and Panama. (**B**) Sampling sectors along the Danta stream at the study site. (**C**) General view of the study site at Rancho Alegre, San Ramón, Alajuela, Costa Rica.

were recorded in locations where *I. tica* was present, as well as during sampling sessions in which no individuals were found.

Data Analysis

To analyze the microhabitat characteristics of Tica Frog, *Isthmohyla tica,* we calculated descriptive statistics of each variable, including the mean, standard deviation, and range, as well as created contingency tables for count data. We tested whether any vegetation or environmental variables predicted the presence or absence of *I. tica* using generalized linear models (GLM) with a binomial error distribution. We attempted to include random variables to account for different transects and sampling nights, but with low sample size and the fact that we typically only found a single frog on a given night or transect (with a single exception of a metamorph and a male both located on 25 March 2021), mixed models led to non-convergence due to singularity. Additionally, inclusion of interactions between different vegetation and environmental variables

in models led to model non-convergence, likely due to low sample sizes and high co-linearity among fixed model predictors (|r| = 0.37 to 0.71), so here we report the results of GLMs with individual predictors. Separately, we compared sites with adult and juvenile individuals with respect to vegetation, environmental, perch, and stream characteristics using either a *t*-test or Mann-Whitney U test as appropriate after testing each variable for normality with a Shapiro-Wilk test. All statistical analyses were performed using R 4.1.2 (R Core Team 2021).

Results

We obtained 13 records of *Isthmohyla tica,* of which three were juvenile individuals and 10 were adults. Among the adults there were nine males and one female. The most commonly used substrate for perching was the upper surface of leaves, accouting for 69.23% of observations (Figure 2). Candelillos (*Piper* spp.) were the most frequently used substrate plants (30.76%), while *Cyathea* sp. and *Heliconia tortuosa* Griggs were used less often (15.38% each). Other plant species were recorded only once each (Figure 3).

Perch height ranged from 0.1 to 2.2 m above the ground, and the distance from the stream ranged from 0.1 to 2.1 m (Table 1). Stream depth ranged from 3 to 60 cm (Table 1). Forest canopy cover averaged 74.6% (Table 2). Sites with *I. tica* had an average plant density of 5.0 plants/ m^2 (Table 2), and a low average DBH (≤ 3.14 cm), characteristic of an herbaceous stratum (Table 2).

The average temperature at the study site was 22.42 (± 1.81°C SD), with values ranging from 19.6°C to 24.8°C (Table 3). Both precipitation and relative humidity were high (Table 3). Sixty-two percent of *I. tica* observations were associated with the presence of rain or drizzle at the time of encounter, while 38% were made on nights without precipitation (Table 3). Additionally, 38% of encounters included males vocalizing in the presence of rain or drizzle.

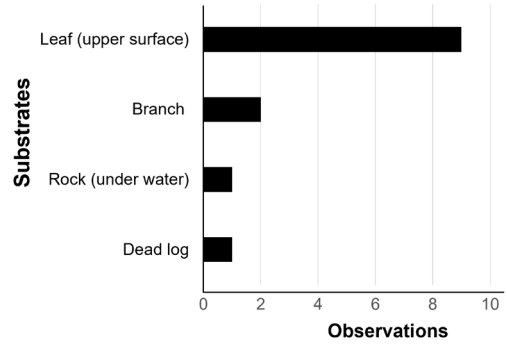

Figure 2. Types of substrates upon which *Isthmohyla tica* was found adjacent to the Danta stream, San Ramón, Costa Rica (*N* = 13).

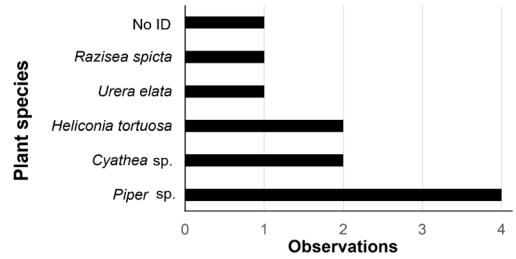

Figure 3. Plant species upon which *Isthmohyla tica* was found perching adjacent to the Danta stream, San Ramón, Costa Rica (*N* = 11).

Males vocalized at wind speeds of up to 8.2 km/h (Table 3). Forty-six percent of sightings occurred during the waxing crescent moon, followed by 31% during the full moon, and 15% during the new moon. There was a single sighting during the waning crescent moon. Males vocalized during the full moon, new moon, and waxing crescent moon.

Vegetation association variables did not predict the presence or absence of *I. tica* in transects (vegetation density: Z = -0.64, p = 0.56; plant richness: Z = -0.92, p = 0.35; canopy cover: Z = 0.69, p = 0.48; plant DBH: Z = -0.63, p = 0.52). Similarly, environmental variables did not differ between sites with and without frogs (temperature: Z = 0.50, p = 0.61; humid-

ity: Z = -0.41, p = 0.67; moonlight illumination: Z = 0.52, p = 0.60; precipitation: Z = -1.30, p = 0.54), with the exception of a trend suggesting that as wind speed increases, the likelihood of the presence of *I. tica* decreases (Z = 1.85, p = 0.06).

Juveniles were found closer to the water (t = 5.14, p = 0.01) and in shallower areas of the stream (t = 2.50, p = 0.03) than adults, but stream width did not differ between sites with juveniles or adults (t = 0.91; p = 0.38). Perch height was similar between juveniles and adults (t = 0.86, p = 0.44). We did not find differences between sites with juveniles or adults in either vegetation parameter (canopy cover: t = -1.01, p = 0.36; plant DBH: t = 0.30, p = 0.77; vegetation density: t = -1.12, p = 0.34; plant richness: t = -0.06, p = 0.95), or environmental parameters (temperature: t = 0.28, p = 0.78; humidity: t = -0.30, p = 0.77; precipitation: U = 13, p = 0.79; moonlight illumination: t = 0.51, p = 0.63; wind speed: t = 1.26, p = 0.26).

Table 1. Characteristics of the perches and the Danta stream where *Isthmohyla tica* was found in San Ramón, Costa Rica (N = 13).

Variable	Average ± SD	Range
Height above ground (m)	0.89 ± 0.70	0.1–2.2
Distance from the stream (m)	0.95 ± 0.75	0.1–2.1
Stream depth (cm)	21.54 ± 15.97	3–60
Stream width (m)	2.33 ± 0.93	0.78–4.17

Table 2. Characteristics of the plants in plots at the sites where *Isthmohyla tica* was found in the Danta stream, San Ramón, Costa Rica (N = 13).

Variable	Average ± SD	Range
Canopy cover (%)	74.60 ± 10.76	57–92
DBH (cm)	1.82 ± 0.74	0.90–3.14
Plant richness (number of species)	2.61 ± 1.28	1–4
Vegetation density (plants/m^2)	5.00 ± 2.88	1–10

Table 3. Characterization of the environmental variables at the sites where *Isthmohyla tica* was found in the Danta stream, San Ramón, Costa Rica (N = 13).

Variable	Average ± SD	Range
Humidity (%)	82.21 ± 6.29	71.8–91.5
Temperature (°C)	22.42 ± 1.74	19.6–24.8
Wind speed (km/h)	5.47 ± 2.63	1–10.1
Precipitation (mm)	4.97 ± 5.33	0–15.2
Moon illumination (%)	54.28 ± 35.58	3.3–99.7

Discussion

This study provides fundamental ecological data on *Isthmohyla tica,* an endemic Costa Rican frog species listed as Critically Endangered by the IUCN (IUCN SSC Amphibian Specialist Group and NatureServe 2020). Although individual frogs have been observed on vegetation along stream edges during both the rainy and dry seasons (Duellman 1970), we present some of the first data on the microhabitat characteristics and population dynamics of *I. tica,* based on 13 individuals encountered at Quebrada Danta, San Ramón, Costa Rica.

Of the 10 adult *I. tica* individuals we encountered, nine were males, and only one was a female. This disparity is likely due to the males' distinctive vocalizations, which increase their detectability compared to females (Emerson and Boyd 1999). We recorded an average of 0.72 frogs per night, a relatively low count, but consistent with findings from other locations (Abarca 2016, Hidalgo-Mora *et al.* 2022). For instance, only a single individual was observed in Tapantí National Park in 2012 (Abarca 2016). Similarly, very few sightings and individuals per visit have been reported in the Bosque Eterno de los Niños in Monteverde (Rodríguez *et al.* 2020).

Apparently, *Isthmohyla tica* primarily used leaves as perches, consistent with its arboreal behavior (Savage 2002). Frogs were predominantly found on leaves of *Piper* spp. This preference may be associated with its ability to camouflage and blend into its surroundings, particularly given the green tones of its skin (Figure 4). A choice-behavior study would be necessary to draw conclusions about substrate preferences.

The proximity of *I. tica* to the stream in terms of height and horizontal distance may be necessary for accessing food, such as arthropods near the water, and could serve as a means of escape from predators (Restrepo 2018). Additionally, proximity to appropriate water bodies is crucial during the breeding season for the development of tadpoles (Savage 2002), and may explain why we found juveniles closer to the edge of the stream than adults. Juveniles recently metamorphosized from tadpoles, which is a transition that requires an adaptation process from aquatic to terrestrial environments and may require them to stay closer to the water than adults that are already acclimated to the terrestrial environment. However, it could simply be that the metamorphs were leaving the water when we found them. The height at which we found frogs could represent an estimation bias, because we sampled at ground level, which makes it difficult to find frogs above 2 m. Thus, frogs at greater heights may not have been detected. However, 46.15% of the detections occurred while following vocalizations, and in none of those cases did we find frogs at heights exceeding 2.20 m, unlike frogs in other clades such as centrolenids that frequently vocalize at heights above 2 m (Duarte-Marín *et al.* 2023).

Canopy cover at sites used by *Isthmohyla tica* was high (74.6%), which likely helps reduce desiccation by limiting solar exposure, maintaining moisture, and providing camouflage within the surrounding vegetation (McDiarmid 1978, Stückler *et al.* 2023, Spranger *et al.* 2024). Plant DBH is not as well studied in relation to amphibian microhabitats, but may indicate the types of perches available to *I. tica,* such as stems or trunks. Some studies have found that the presence of trees with large diameters and woody debris affect the presence of certain frog species (Acosta-Chaves *et al.* 2015, Pabijan *et al.* 2023). The average DBH at sites with *I. tica* was low ($\leq$ 3.14 cm), characteristic of an herbaceous layer. This may be because within the 2 m sampled on each side of the river, the area is prone to increased flow. Certain sectors of this microhabitat regenerate annually due to the increased stream flow during the rainy season, which washes away some vegetation. For example, on a visit after the study in September 2021, we found that part of the microhabitat where we had previously sighted *I. tica* had been washed away by the strong current after a storm (Figure 4).

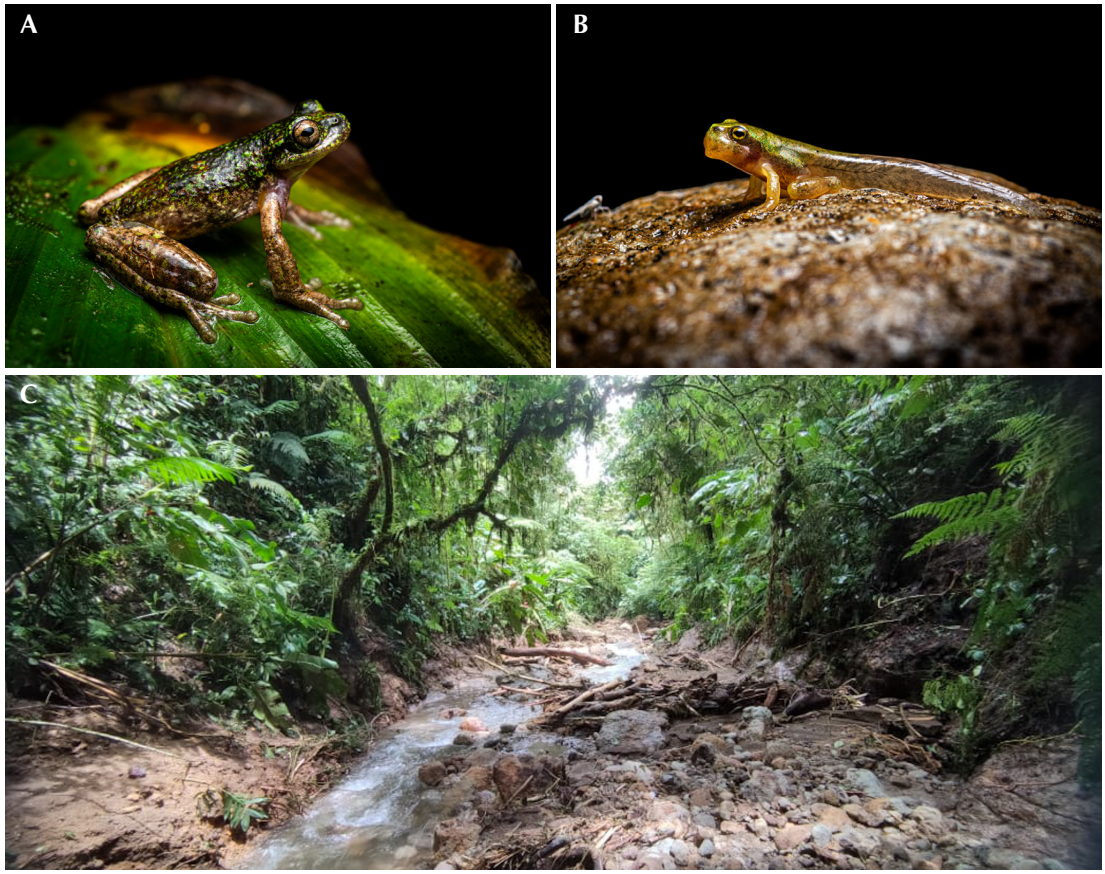

Figure 4. (**A**) Adult *Isthmohyla tica,* (**B**) metamorphosing tadpole of *I. tica,* (**C**) the Danta stream after a storm in September 2021. San Ramón, Alajuela, Costa Rica.

We observed a tendency for *I. tica* to be more abundant and for males to vocalize more when wind speeds were lower, although this pattern was not statistically supported. Wind speed can influence relative humidity, calling activity, and desiccation risk in amphibians (Burggren and Moalli 1984, Prasad *et al.* 2022). Other studies suggest that tolerance to desiccation varies among species, with some hylids being relatively resilient (Ralin and Rogers 1972), while abundance and calling activity in related species may be more strongly linked to rainfall and temperature (Arguedas *et al.* 2022).

Lunar phases can affect the activity and detection of anuran species (Acosta-Chaves *et al.* 2015, Pérez and Medina 2018). A study in Brazil found a positive correlation between amphibian vocalization and darker lunar phases (Lima *et al.* 2021). Two tree frogs, *Agalychnis spurrelli* Boullenger, 1913 and *A. saltator* Taylor, 1955, are explosive breeders that may be influenced by lunar phases (Ortega-Andrade *et al.* 2011, Arguedas *et al.* 2022, 2023). Our limited observations suggest that lunar phases may also influence the behavior of *I. tica,* although further studies are needed to understand this aspect of its ecology.

In the case of *I. tica,* reproduction is concentrated in the dry season when precipitation is lower (Duellman 1970, Savage 2002, Leenders

2016). Accordingly, we found juveniles in March, April, and May, the least rainy months. The study site has an average annual precipitation greater than 5000 mm, and the stream maintains its flow year-round (Calvo 1989), providing this frog with suitable ecological conditions for reproduction during the dry season. Tadpoles of *I. tica* have oral disc adaptations that allow them to cling to rocks and avoid being swept away by the current (Savage 2002). When water flow increases and currents are stronger, tadpoles would need to expend more energy to cling to rocks or could be carried away by the current. Tadpoles may be more likely to survive to metamorphosis during the dry season when the current flow is slower. The reproductive activity of amphibians is strongly influenced by exogenous factors such as rainfall and air temperature (Bertoluci and Rodrigues 2002), and is commonly associated with the rainy season in the Neotropics (e.g., Wells 2007). Reproductive activity of Neotropical species can indeed increase or decrease during either the rainy or dry seasons (Bertoluci and Rodrigues 2002).

We found a low relative abundance of juveniles compared to adults across the months of sampling. Given that the breeding period of this species is in the dry season from February to May (Duellman 1970, Savage 2002, Leenders 2016) and most of the sampling took place outside of this period, this phenology and relative abundance of life phases is to be expected.

Although our analyses are limited by a small sample size ($N = 13$), the absence of significant differences in microhabitat variables between sites with and without *I. tica* suggests that the species may rely on streams in general, rather than on specific microhabitat features (Duellman 1970). By contrast, some amphibians show strong habitat specialization, such as *Craugastor rhyacobatrachus* (Campbell and Savage 2000), which depends on streams and inhabits clear, cascading mountain streams in humid montane forests, often associated with rocky sections of torrential watercourses (Savage 2002), and *Atelopus varius* (Lichtenstein and Martens, 1856), which prefers rocky substrates and log accumulations in streams and shows higher encounter rates in forested habitats than in pastures (Leenders 2016, Gómez-Hoyos *et al.* 2020). Future studies should assess the degree of microhabitat flexibility in *I. tica* and examine additional factors not measured here, including food availability, predator pressure, and disease dynamics. Such work is urgently needed to clarify the ecological requirements of this critically threatened species and to inform conservation strategies for its persistence and recovery.

Conclusion

This study represents the first documentation of the microhabitat use of the critically endangered frog *Isthmohyla tica* in Costa Rica. Our findings reveal a remnant population with low relative abundance in the riparian forest of Rancho Alegre farm, San Ramón. The presence of both juvenile and adult individuals indicates active reproduction in the study area, offering encouraging evidence for the species' persistence. These values are important as a baseline; however, long-term monitoring over several years will be essential to determine whether the population trends are positive or negative and to assess how this information can best guide conservation actions. We therefore recommend the implementation of a sustained monitoring program in the Danta stream and other known populations to ensure the long-term survival and potential recovery of this species.

Acknowledgments

We thank SINAC for granting permission for this research (Resolution Nº M-P-Sinac-PNI-ACAT-024-2020). We extend our gratitude to Monteverde Brewing, Instituto Monteverde, Tytira Lodge, and Marco Vinicio Zamora for their financial support and contribution of equipment. We thank E. Rodríguez, J. Rodríguez, J. Alpízar, J. Rojas, S. Gallo, S. Rojas, C. Acuña,

J. Gamboa, and D. Coto for valuable field assistance. JMM acknowledges Emilce Rivera, department head, Carrera de Gestión Ecoturística, Sede Central, Universidad Técnica Nacional (UTN), for her academic support.

References

Abarca, J. G. 2016. In Searching for Missing Frog Species in Costa Rica: Rediscovery of Critically Endangered Species in a Time of Extinction. Final Report. The Rufford Foundation. Electronic Database accessible at https://www.rufford.org/projects/juan-g-abarca-a/in-searching-of-missing-frog-species-in-costa-rica-rediscovery-critically-endangered-species-in-a-time-of-extinction. Captured on 02 September 2024.

Acosta-Chaves, V. J., G. Chaves, J. G. Abarca, A. García-Rodríguez, and F. Bolaños. 2015. A checklist of the amphibians and reptiles of Río Macho Biological Station, Provincia de Cartago, Costa Rica. *Check List 11:* 1784–1784.

Arguedas, V., M. D. Barquero, and J. M. Mora. 2022. Population structure and dynamics, breeding activity and phenology of the blue-sided treefrog (*Agalychnis annae*). *Biotropica 54:* 455–466.

Arguedas, V., J. M. Mora, and M. D. Barquero. 2023. Habitat use by *Agalychnis annae* (Anura: Hylidae) at an urban green space in Costa Rica. *Revista Latinoamericana de Herpetología 6:* 180–187.

Bertoluci, J. and M. T. Rodrigues. 2002. Seasonal patterns of breeding activity of Atlantic rainforest anurans at Boracéia, southern Brazil. *Amphibia-Reptilia 23:* 161–167.

BiodataCR. 2024. Lista taxonómica de referencia de anfibios. Electronic Database accessible at https://biodatacr.github.io/lista-taxonomica-referencia-anfibios/#referencias. Captured on 02 September 2024.

Bolaños, F. 2009. Situación de los anfibios de Costa Rica. *Biocenosis 22:* 95–108.

Burggren, W. W. and R. Moalli. 1984. Active regulation of cutaneous gas exchange by capillary recruitment in amphibians: experimental evidence and a revised model for skin respiration. *Respiratory Physiology 55:* 379–392.

Calvo, A. 1989. *Departamento de Avalúos.* San José. Ministerio de Hacienda, República de Costa Rica.

Carné, C. and D. R. Vieites. 2024. A race against extinction: the challenge to overcome the Linnean amphibian shortfall in tropical biodiversity hotspots. *Diversity and Distributions 30:* e13912.

Cashins, S. D., R. A. Alford, and L. F. Skerratt. 2008. Lethal effect of latex, nitrile, and vinyl gloves on tadpoles. *Herpetological Review 39:* 298–301.

Chaves-Acuña, W., G. Chaves, J. Klank, E. Arias, F. Bolaños, A. Shepack, T. Leenders, J. Cossel, and F. Faivovich. 2020. Recent findings of *Isthmohyla pictipes* (Anura: Hylidae) in Costa Rica: variation and implications for conservation. *Zootaxa 4881:* 499–514.

Cheng, T. L., S. M. Rovito, D. B. Wake, and V. T. Vredenburg. 2011. Coincident mass extirpation of neotropical amphibians with the emergence of the infectious fungal pathogen *Batrachochytrium dendrobatidis. Proceedings of the National Academy of Sciences 108:* 9502–9507.

De León, M. E., H. Zumbado-Ulate, A. García-Rodríguez, G. Alvarado, H. Sulaeman, F. Bolaños, and V.T. Vredenburg. 2018. Prevalence of the fungal pathogen *Batrachochytrium dendrobatidis* in amphibians of Costa Rica predated first-known epizootic. *BioRxiv: 482968*.

Duarte-Marín, S., M. Rada, M. Rivera-Correa, V. Caorsi, E. Barona, G. González-Durán, and F. Vargas-Salinas. 2023. Tic, Tii and Trii calls: advertisement call descriptions for eight glass frogs from Colombia and analysis of the structure of auditory signals in Centrolenidae. *Bioacoustics 32:* 143–180.

Duellman, W. E. 1970. *The Hylid Frogs of Middle America.* Volume 2, Monograph. Lawrence. Museum of Natural History, University of Kansas. 448 pp.

Emerson, S. B. and S. K. Boyd. 1999. Mating vocalizations of female frogs: control and evolutionary mechanisms. *Brain Behavior and Evolution 53:* 187–197.

García-Rodríguez, A., G. Chaves, C. Benavides-Varela, and R. Puschendorf. 2012. Where are the survivors? Tracking relictual populations of endangered frogs in Costa Rica. *Diversity and Distributions 18:* 204–212.

Gómez–Hoyos, D. A., R. Seisdedos de Vergara, R., J. Schipper, R. Allard, and J. F. González–Maya. 2020. Potential effect of habitat disturbance on reproduction of the critically endangered harlequin frog *Atelopus varius* in Las Tablas, Costa Rica. *Animal Biodiversity and Conservation 43:* 1–7.

Gratwicke, B., H. Ross, A. Batista, G. Chaves, A. J. Crawford, L. Elizondo, A. Estrada, M. Evans, D. Garelle, J. Guerrel, A. Hertz, M. Hughey, C. A. Jaramillo, B. Klocke, M. Mandica, D. Medina, C. L. Richards-Zawacki, M. J. Ryan, A. Sosa-Bartuano, J. Voyles, B. Walker, D. C. Woodhams, and R. Ibáñez. 2016. Evaluating the probability of avoiding disease-related

extinctions of Panamanian amphibians through captive breeding programs. *Animal Conservation 19:* 324–336.

Gutleb, A. C., M. Bronkhorst, J. H. J. van den Berg, and A. J. Murk. 2001. Latex laboratory-gloves: an unexpected pitfall in amphibian toxicity assays with tadpoles. *Environmental Toxicology and Pharmacology 10:* 119–121.

Hertz, A., S. Lotzkat, A. Carrizo, M. Ponce, G. Köhler, and B. Streit. 2012. Field notes on findings of threatened amphibian species in the central range. *Amphibian and Reptile Conservation 6:* 9–30.

Heyer, R., M. A. Donnelly, M. Foster, and R. McDiarmid. 2014. *Measuring and Monitoring Biological Diversity: Standard Methods for Amphibians*. Washington D.C. Smithsonian Institution. 364 pp.

Hidalgo-Mora, E., J. Navarro-Picado, and J. G. Abarca. 2022. Notes on geographic distribution, advertisement call and habitat of the Starrett's Tree Frog *Isthmohyla tica* (Hylidae) in the Zona de los Santos, Costa Rica. *Revista Latinoamericana de Herpetología 5:* 112–120.

IUCN SSC Amphibian Specialist Group and NatureServe. 2020. *Isthmohyla tica.* The IUCN Red List of Threatened Species 2020: e.T55675A54347781. Electronic Database accessible at https://dx.doi.org/10.2305/IUCN.UK.2020-3.RLTS.T55675A54347781.en. Captured on 12 July 2024.

Leenders, T. 2016. *Amphibians of Costa Rica.* Ithaca. Zona Tropical Publication. 544 pp.

Lima, M. S., J. Pederassi, U. Caramaschi, K. D. Sousa, and C. A. S. Souza. 2021. Frog vocalization is influenced by moon phases: Brazilian frogs tend to prefer low-albedo phases. *Web Ecology 21:* 1–13.

McDiarmid, R. W. 1978. Evolution of parental care in frogs. Pp. 127–147 *in* G. M. Burghardt and M. Bekoff (eds.), *The Development of Behavior: Comparative and Evolutionary Aspects.* New York. Garland STPM Press.

Ortega-Andrade, H. M., C. Tobar-Suárez, and M. Arellano. 2011. Tamaño poblacional, uso del hábitat y relaciones interespecíficas de *Agalychnis spurrelli* (Anura: Hylidae) en un bosque húmedo tropical remanente del noroccidente de Ecuador. *Papéis Avulsos de Zoologia 51:* 1–19.

Pabijan, M., S. Bąk-Kopaniarz, M. Bonk, S. Bury, W. Oleś, W. Antoł, I. Dyczko, and B. Zając. 2023. Amphibian decline in a Central European forest and the importance of woody debris for population persistence. *Ecological Indicators 148:* 110036.

Pérez, C. and G. Medina. 2018. Influencia de algunas variables ambientales sobre la abundancia relativa y características corporales de la rana de lluvia *Pristimantis renjiforum* (Lynch, 2000) en Cundinamarca, Colombia. *Revista Biodiversidad Neotropical 8:* 157–167.

Prasad, V. K., M. F. Chuang, A. Das, K. Ramesh, Y. Yi, K. P. Dinesh, and A. Borzée. 2022. Coexisting good neighbours: acoustic and calling microhabitat niche partitioning in two elusive syntopic species of balloon frogs, *Uperodon systoma* and *U. globulosus* (Anura: Microhylidae) and potential of individual vocal signatures. *BMC Zoology 7:* 1–12.

R Core Team. 2021. R: A language and environment for statistical computing. R Foundation for Statistical Computing, Vienna, Austria. URL: https://www.R-project.org/.

Ralin, D. B. and J. S. Rogers. 1972. Aspects of tolerance to desiccation in *Acris crepitans* and *Pseudacris streckeri. Copeia 1972:* 519–525.

Restrepo, E. 2018. Descripción del hábitat de la rana cristal *Sachatamia punctulata* (Ruíz-Carranza y Lynch, 1995), en el municipio de Victoria, Caldas, Colombia. Unpublished M.Sc. Dissertation. Universidad Distrital Francisco José Caldas, Colombia.

Rodríguez, J., G. Chaves, K. Neam, J. Luedtke, L. Carrillo, F. Bolaños, and Y. Matamoros. 2020. *Taller de Evaluación de las Necesidades de Conservación de Anfibios - Arca de los Anfibio y de la Lista Roja de la UICN: Un Esfuerzo para la Segunda Evaluación Global de Anfibios. 9–13 Septiembre 2019.* Grupo de Especialistas en Anfibios UICN SSC y Grupo de Especialistas en Planificación para la Conservación UICN SSC (CPSG Mesoamérica). San José. Parque Zoológico y Jardín Botánico Nacional Simón Bolívar, San José, Costa Rica. 40 pp.

Sasa, M., G. Chaves, and L. W. Porras. 2010. The Costa Rican herpetofauna: conservation status and future perspectives. Pp. 510–60 *in* L. D. Wilson, J. H. Townsend, and J. D. Johnson (eds.), *Conservation of Mesoamerican Amphibians and Reptiles.* Eagle Mountain City. Eagle Mountain Publications.

Sasa, M., E. Arias, and G. Chaves. 2025. Annotated list of amphibians and reptiles of Costa Rica: the role of the Museum of Zoology in cataloging the country's herpetological diversity. *Revista de Biología Tropical 73:* e64536.

Savage, J. M. 2002. *The Amphibians and Reptiles of Costa Rica: A Herpetofauna Between Two Continents, Between Two Seas.* Chicago. The University of Chicago Press. 934 pp.

Spranger, R. R., T. R. Raffel, and B. R. Sinervo. 2024. Canopy coverage, light, and moisture affect

thermoregulatory trade-offs in an amphibian breeding habitat. *Journal of Thermal Biology 122:* 103864.

Stückler, S., X. I. Dawkins, M. J. Fuxjager, and D. Preininger. 2023. From masquerading to blending in: ontogenetic shifts in antipredator camouflage in Wallace's flying frogs. *Behavioral Ecology and Sociobiology 77:* 102.

Tocher, M., C. Gascon, and B. L. Zimmerman. 1997. Fragmentation effects on a central Amazonian frog community: a ten-year study. Pp. 124–137 *in* W. F. Laurance and R. O. Bierregaard (eds.), *Tropical Forest Remnants: Ecology, Management, and Conservation of Fragmented Communities.* Chicago. University of Chicago Press.

Wells, K. 2007. *The Ecology and Behavior of Amphibians.* Chicago. The University of Chicago Press. 1148 pp.

Zumbado-Ulate, H., K. N. Nelson, A. García-Rodríguez, G. Chaves, E. Arias, F. Bolaños, S. M. Whitfield, and C. L. Searle. 2019. Endemic infection of *Batrachochytrium dendrobatidis* in Costa Rica: implications for amphibian conservation at regional and species level. *Diversity 11:* 129.

Editor: Jaime Bertoluci

Phyllomedusa 24(2):295–312, 2025

ISSN 1519-1397 (print) / ISSN 2316-9079 (online)
doi: http://dx.doi.org/10.11606/issn.2316-9079.v24i2p295-312

Discovery of a new species of *Gegeneophis* (Gymnophiona: Grandisoniidae) highlights hidden diversity and implications for regional endemism in the Western Ghats, India

K. P. Dinesh,[1] Sahil Shikalgar,[1] Pranjal Adhav,[2] Bapurao Vishnu Jadhav,[3] and Nirmal U. Kulkarni[4]

[1] Zoological Survey of India, Western Regional Center, Pune, Maharashtra. E-mails: kpdinesh.zsi2@gmail.com, sahilshikalgar72276@gmail.com.

[2] Savitribai Phule Pune University, Department of Zoology. Pune, Maharashtra. E-mail: pranjaldhav.01@gmail.com.

[3] Silvernest Building, Flat No. 5, Near Jagdam Chowk, Shahunagar, Satara 415001, Maharashtra, India. E-mail: drbvjadhav@gmail.com.

[4] Mhadei Research Centre. C/o Hiru Naik Building, Dhuler Mapusa 403507, Goa. E-mail: nirmalukulkarni@gmail.com.

Abstract

Discovery of a new species of *Gegeneophis* (Gymnophiona: Grandisoniidae) highlights hidden diversity and implications for regional endemism in the Western Ghats, India. A new species of *Gegeneophis* is described from the base of the lateritic plateaus of Satara, Maharashtra, India. The new species is described based on morphological characters, metric and meristic measurements, phylogenetic analysis, genetic distances, ASAP analysis, and geographic isolation. Phylogenetic and ASAP analyses suggest the presence of an additional six lineages representing potential new species from the northern and central Western Ghats. The affinities of spatial and temporal distribution of *Gegeneophis* in the northern and central Western Ghats are discussed.

Keywords: Annulocylix caecilian, Legless amphibian, New species description, Northern Western Ghats, Tailless caecilians, Taxonomy.

Resumo

A descoberta de uma nova espécie de *Gegeneophis* (Gymnophiona: Grandisoniidae) destaca a diversidade oculta e as implicações para o endemismo regional nos Ghats Ocidentais, India. Uma nova espécie de *Gegeneophis* é descrita a partir da base dos planaltos lateríticos de Satara, Maharashtra, Índia. A nova espécie é descrita com base em várias linhas de evidência, incluindo características morfológicas, medições métricas e merísticas, análise filogenética, distâncias genéticas, análise ASAP e isolamento geográfico. As análises filogenéticas e ASAP sugerem a presença de seis linhagens adicionais que representam potenciais novas espécies do norte e centro dos Ghats Ocidentais. São discutidas as afinidades da distribuição espacial e temporal de *Gegeneophis* no norte e no centro dos Ghats Ocidentais.

Palavras-chave: Anfíbio ápode, Cecílias sem cauda, Descrição de espécie nova, Ghats Ocidentais setentrionais, Taxonomia.

Received 25 August 2025
Accepted 07 November 2025
Distributed December 2025

Introduction

In India the legless amphibian family Grandisoniidae is represented by two genera, *Gegeneophis* Peters, 1880 "1879" and *Indotyphlus* Taylor, 1960 (Dinesh *et al.* 2024, Frost 2025). The genus *Gegeneophis* is endemic to peninsular India and is represented by 12 species. One species is endemic to the Eastern Ghats, and 11 species are endemic to the Western Ghats (Dinesh 2020, Ramakrishna *et al.* 2023) (Figure 1, Table 1). The two species in the genus *Indotyphlus* are endemic to the northern Western Ghats (Dinesh *et al.* 2024).

The first species of *Gegeneophis* described from the Western Ghats was *Gegeneophis carnosus* (Beddome, 1870) (described as *Epicrium carnosum* Beddome, 1870) from the Periah Peak region of Wayanad, Kerala (Table 1). The species is endemic and has a restricted distribution around the Wayanad hill ranges (Dinesh 2025).

Taylor (1964) described *Gegeneophis ramaswamii* Taylor, 1964 from the Tenmalai forest region of Kollam, Kerala (Table 1). This species is endemic to the southern Western Ghats and has abundant populations south of Shencotah pass (Dinesh 2025).

The first lower-elevation (below 100 m) species of *Gegeneophis* was described as *Gegeneophis krishni* Pillai and Ravichandran, 1999 from Krishna Farms, Gurpur, Dakshina Kannada, Karnataka (Pillai and Ravichandran 1999) (Table 1). The species is a central Western Ghats endemic confined to habitats in the vicinity of the type locality (Dinesh 2025).

The earliest species of *Gegeneophis* lacking secondary annuli was described as *Gegeneophis seshachari* Ravichandran, Gower, and Wilkinson, 2003 from the reaches of Dorle Village, Ratnagiri, Maharashtra (Ravichandran *et al.* 2003) (Table 1). The species is a northern Western Ghats endemic confined to the regions surrounding the type locality (Gower *et al.* 2007, Dinesh 2025).

The first species of *Gegeneophis* having secondaries in the anterior half of the body was described by Giri *et al.* (2003) as *Gegeneophis danieli* Giri, Wilkinson, and Gower, 2003 from the Amboli region of Sindhudurg, Maharashtra (Table 1). *Gegeneophis nadkarnii* Bhatta and Prashanth, 2004 was described from vicinities of the Bondla Wildlife Sanctuary, Goa, by Bhatta and Prashanth in 2004. Because of genetic homogeneity *G. nadkarnii* was treated as a junior synonym of *G. danieli* by Gower *et al.* (2013). *Gegeneophis danieli* is a northern Western Ghats endemic known to inhabit the Amboli region of Maharashtra to northeastern Goa (Dinesh 2025).

Bhatta and Srinivasa (2004) described *Gegeneophis madhavai* Bhatta and Srinivasa, 2004 from lower elevations (150 m) of Doddinaguli, Mudur, Kundapura, Udupi, Karnataka (Table 1). This species is endemic to the central Western Ghats and is known only from the type specimens (Dinesh 2025).

In 2007 two species of *Gegeneophis* were described from northern Western Ghats. *Gegeneophis goaensis* Bhatta, Dinesh, Prashanth, and Kulkarni, 2007 was described from the lower elevations of Ganv Kond, Keri, Sattari, North Goa, Goa (Bhatta *et al.* 2007a), and *Gegeneophis mhadeiensis* Bhatta, Dinesh, Prashanth, and Kulkarni, 2007 was described from the surrounding areas of Rameshwar temple, Chorla, Khanapur, Belgaum, Karnataka (Bhatta *et al.* 2007b) (Table 1). Both species are northern Western Ghats endemics with good populations near the type localities (Bhatta *et al.* 2010, Dinesh 2025).

Gegeneophis pareshi Giri, Gower, Gaikwad, and Wilkinson, 2011, a species with a worm-like pinkish head, was described by Giri *et al.* (2011) from the lower-elevation villages of Kuske near Cotigaon Wildlife Sanctuary, Canacona, South Goa, Goa (Table 1). This endemic species is known primarily from areas adjacent to the type locality (Dinesh 2025).

Kotharambath *et al.* (2012) described *Gegeneophis primus* Kotharambath, Gower, Oommen, and Wilkinson, 2012 from the Cardamom state in the Sugandhagiri region, near Vythiri,

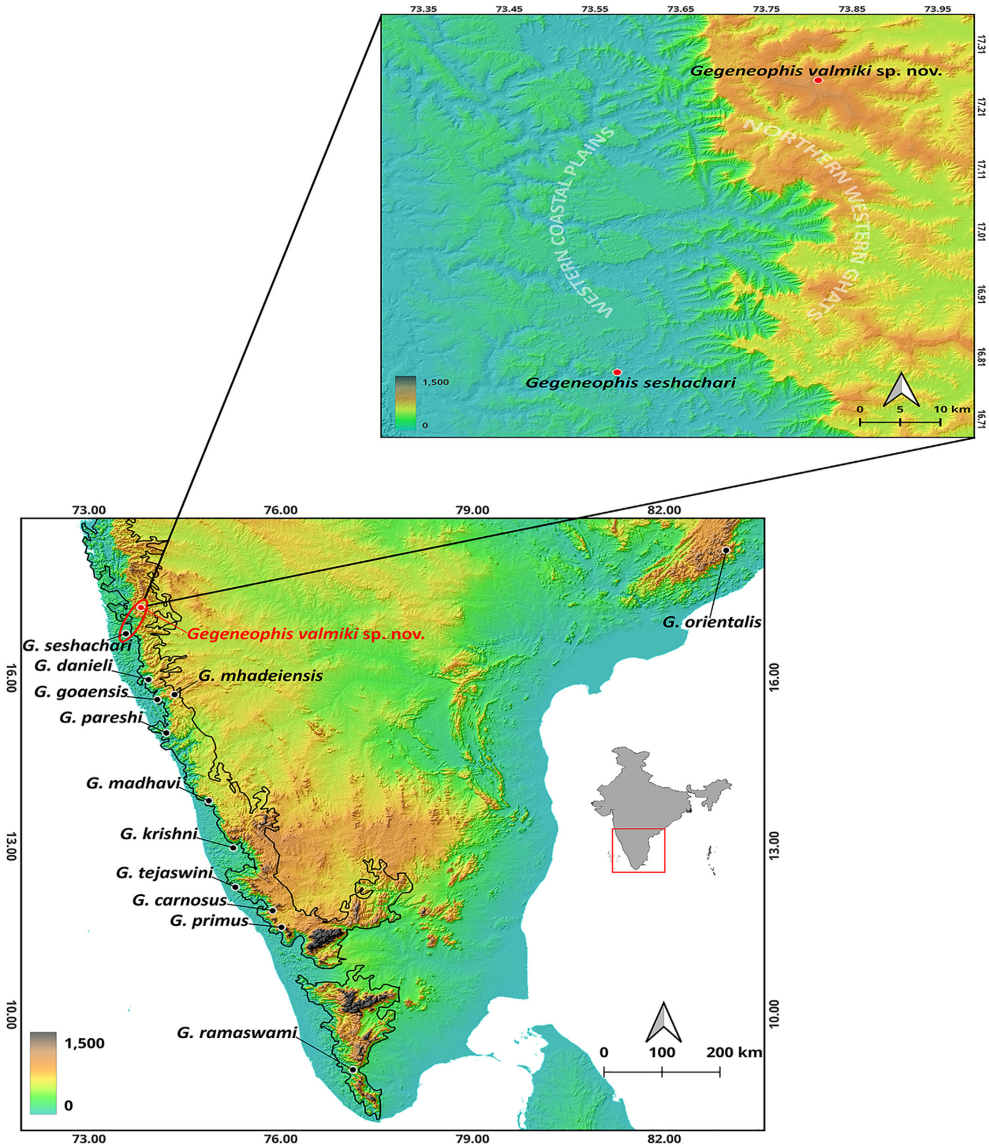

Figure 1. Map showing the type localities of the extant species of *Gegeneophis* in peninsular India and the type localities of phylogenetic sister species *Gegeneophis valmiki* sp. nov. and *Gegeneophis seshachari*.

Pozhuthana, Vythiri, Wayanad, Kerala (Table 1). This endemic species is limited to the locations around the Wayanad hill ranges (Dinesh 2025).

Outside the Western Ghats, the first species of *Gegeneophis* was described from the Eastern Ghats (near Beespuram, Visakhapatnam, Andhra Pradesh) as *Gegeneophis orientalis* Agarwal, Wilkinson, Mohapatra, Dutta, Giri, and Gower, 2013 (Agarwal *et al.* 2013) (Table 1). This species is an Eastern Ghats endemic with a localized distribution in the Andhra Pradesh and Orissa regions (Agarwal *et al.* 2013, Dinesh 2025).

Kotharambath *et al.* (2015) described *Gegeneophis tejaswini* Kotharambath, Wilkinson, Oommen, and Gower, 2015 from Bedoor, Kakkadav Bridge, Cheemeni, Hosdurg, Kasaragod, Kerala (Table 1). This species is endemic to the central Western Ghats and is known only from the type specimens (Dinesh 2025).

A unique pattern occurs among the 11 species of *Gegeneophis* reported from the Western Ghats (Dinesh 2020, Ramakrishna *et al.* 2023). Five species, *G. danieli, G. seshachari, G. goaensis, G. mhadeiensis,* and *G. pareshi* are restricted to the northern Western Ghats region, while another five species, *G. carnosus, G. krishni, G. madhavai, G. primus,* and *G. tejaswini,* are restricted to the central Western Ghats. *Gegeneophis ramaswamii* is the only species restricted to the southern Western Ghats (Table 1).

Table 1. Type locality and annuli (primary and starting of secondary grooves) information for the extant species of *Gegeneophis* from the peninsular India.

Sl. No	Species	Total primary	Secondary starts between	Type locality in peninsular India	Geographic zones
1	*Gegeneophis valmiki* sp. nov.	137–145	absent	Maharshi Valmiki Mandir, Valmiki Plateau, Palashi, Pathan, Satara, Maharashtra	Northern Western Ghats
2	*Gegeneophis seshachari*	122–127	absent	Dorle, Sindhudurg, Maharashtra	
3	*Gegeneophis danieli*	112	5–34	Amboli, Sawanthwadi, Maharashtra	
4	*Gegeneophis mhadeiensis*	117–125	87–98	Chorla Ghats, Surla, Karnataka	
5	*Gegeneophis goaensis*	125–126	38–48	Kheri village, Goa	
6	*Gegeneophis pareshi*	145–150	absent	Kuske near Cotigaon Wildlife Sanctuary, Canacona, South Goa	
7	*Gegeneophis madhavai*	96–97	63–70	Mookambika wild life sanc. Karnataka	Central Western Ghats
8	*Gegeneophis krishni*	125–127	110–114	Gurupur, Dakshina Kannada, Karnataka	
9	*Gegeneophis carnosus*	105–112	99–105	Periah Peak, Wayanad, Kerala	
10	*Gegeneophis primus*	108–112	absent	Sugandhagiri, Vythiri, Wayanad Kerala	
11	*Gegeneophis tejaswini*	125–131	105–115	Bedoor, near Cheemeni, Hosdurg Taluk, Kasaragod Kerala	
12	*Gegeneophis ramaswamii*	109–114	98–103	Tenmalai Bonakad estate, Kerala	Southern Western Ghats
13	*Gegeneophis orientalis*	104–106	95–99	Beespuram, Visakhapatnam District, Andhra Pradesh	Eastern Ghats

Koyna Wildlife Sanctuary in the northern Western Ghats, which is known for tropical evergreen forests and the surrounding Koyna reservoir mosaic-forested ecosystem, is one of the well-suited habitats for caecilians. No species of the genus *Gegeneophis* have been reported previously further north of the Amboli region. During a field survey conducted in and around Koyna Wildlife Sanctuary (Dinesh 2021), a population of *Gegeneophis* was encountered that did not correspond morphologically to any of the extant congeners. Integrative taxonomic studies involving DNA barcode data, and meristic and morphometric studies confirmed the novelty, and this species is herein described as a new species supported with a single gene phylogeny and ASAP (Assemble Species by Automatic Partitioning) species delimitation.

Materials and Methods

Study Species

The field survey was one of the faunistic surveys conducted in search of amphibians in and around the Koyna Wildlife Sanctuary (Dinesh 2021). The specimens were collected from decaying leaf litter in the vicinity of Shri Maharshi Valmiki Mandir during heavy rain in July 2017. A total of seven specimens were collected by hand during daytime searches, which involved digging the soil using a trident and spade. Photographs of live specimens were taken using a Canon camera. The specimens were euthanized using MS-222, and liver tissues were extracted prior to preservation and stored in molecular-grade alcohol for subsequent molecular analysis. The specimens were then fixed in 70% ethanol for morphological studies.

Morphometry

Morphometric measurements were taken using Mitutoyo vernier calipers and an Olympus SZ61 camera-mounted stereomicroscope, except for body length and body circumference, which were measured using a piece of thread and a ruler. Abbreviations and terminology follow Bhatta *et al.* (2007ab). The studied specimens are registered in the National Zoological Collections of the ZSI, WRC, Pune (ZSI/WRC/V/A2782 to 2784).

Principal Component Analysis (PCA) was conducted for eight morphometric characters to compare the new species (N = 7) with morphologically similar species lacking secondary annuli, including *G. seshachari* (N = 3), *G. pareshi* (N = 16), and *G. primus* (N = 8) (data taken from original descriptions of *G. seshachari, G. pareshi,* and *G. primus*). All parameters were normalized by dividing the total body length of the specimen (TBL), except for one ratio (length divided by width). PCA was performed using PAST software 4.03 (Hammer *et al.* 2001).

DNA Barcoding

Genomic DNA was extracted from liver tissue using the QIAGEN kit, following the manufacturer's protocol. The gDNA was eluted in 100 µl of AE buffer and quantified using the dsDNA HS Assay Kit (Invitrogen) on a Qubit 2.0 fluorometer. The mitochondrial 16S gene was targeted and amplified using the primers 16SarL (5′-CGCCTGTTTATCAAAAACAT-3′) and 16SbrH (5′-CCGGTCTGAACTCAGATCACG-3′) (Palumbi *et al.* 2002). PCR reactions were carried out in a 25 µl volume, consisting of 2 µl of gDNA (> 100 ng), 12.5 µl of 2X Hot Start Master Mix (Promega), 2.0 µl of $MgCl_2$, 1.0 µl each of forward and reverse primers (10 pmol), and nuclease-free water to reach the final volume.

The thermocycling profile included an initial denaturation at 95°C for 2 min, followed by 35 cycles of 30 s at 95°C, 30 s at 47–52°C, and 30 s at 72°C, with a final extension at 72°C for 5 min. Amplification success was confirmed by gel electrophoresis on a 1.2% agarose gel stained with 0.6 µl of ethidium bromide. PCR products were purified using Invitrogen's PureLink PCR Purification Kit and subsequently outsourced for Sanger sequencing.

Phylogenetic Analysis

The resulting chromatogram files were visualized and manually edited using Chromas v2.6.5 software (Technelysium Pty. Ltd. 2018). A total of 47 sequences provided in Gower *et al.* (2011), along with outgroup sequences, were downloaded from NCBI GenBank. These sequences were aligned and trimmed using the MUSCLE algorithm in MEGA X (Kumar *et al.* 2018). Maximum Likelihood analysis was performed on a dataset comprising 53 sequences of 562 bp, including those generated in this study, using the IQ-TREE multicore version 1.6.12 web server (Trifinopoulos *et al.* 2016). The analysis was conducted with 1000 ultrafast bootstrap replicates under default parameters, and the GTR+F+I+G4 substitution model was auto-selected based on the Bayesian Information Criterion (BIC). The final consensus tree was visualized in FigTree v1.4.0, with *Grandisonia, Praslinia,* and *Hypogeophis* treated as outgroups (Gower *et al.* 2011).

Species delimitation was conducted using the ASAP (Assemble Species by Automatic Partitioning) online tool (Puillandre *et al.* 2021), employing Kimura (K80) genetic distances with a default transition/transversion ratio of 2.0. Partitions were assessed based on the lowest ASAP scores, which indicate well-differentiated and statistically supported groups. The best partition with the lowest ASAP is marked with a red frame. An elevation map was generated using QGIS v3.24 (QGIS Development Team). The sequences generated in this study were submitted to NCBI GenBank (PX475275.1).

Results

The proposed new species, collected from the Valmiki Plateau, Palashi, is geographically located in the central plateau hills of the northern Western Ghats at an elevation of 1000 m (Figure 1). It is isolated by at least 70 km (aerial distance) from one of its sister clade members, *G. seshachari,* which is reported from an elevation of 200 m (Figure 1).

Phylogenetically, the populations from Valmiki Plateau, Palashi were recovered as sister to the clade comprising two unnamed lineages from Kolhapur, one unnamed lineage from Ratnagiri, and the extant species *G. seshachari* (Figures 2 and 3). For the uncorrected pairwise genetic distance the new species was 3.5% divergent from the unnamed lineage from Ratnagiri, 3.9% divergent from *G. seshachari,* 4.8% from one of the unnamed lineages from Kolhapur, and 7% divergent from another unnamed lineage from Kolhapur (Figures 2 and 3). Furthermore, analysis using ASAP indicates that the new lineage is a distinct phylogenetic lineage, supported by the best partition identified with a minimum value (Figure 3).

The populations from Valmiki Plateau were assigned to *Gegeneophis* as done by Peters (1879) and Pillai and Ravichandran (2005). Morphologically, the new species has a unique combination of characters, including primary annular grooves ranging from 137 to 145, absence of secondary grooves, and unsegmented terminal keel (Figures 4, 5, 6). Due to the absence of secondary grooves and a greater number of primary annular grooves, field identification of the new species is easy.

Taxonomy

Gegeneophis valmiki sp. nov.
lsid:zoobank.org:act:7D8A404D-6AC2-4347-8FB5-A12A17B1B13A

Holotype.—An adult male (ZSI/WRC/V/A/2782), collected on 16 July 2017 around the Maharshi Valmiki Mandir (17.2518° N, 73.8104° E, 1000 m); Valmiki Plateau, Paneri, Palashi, Patan, Satara, Maharashtra, collected by A.S. Kalawate and team.

Paratype.—An adult male (ZSI/WRC/V/A/2783), collection details same as holotype.

Etymology.—The species is named after the Maharshi Valmiki temple near the Valmiki Plateau,

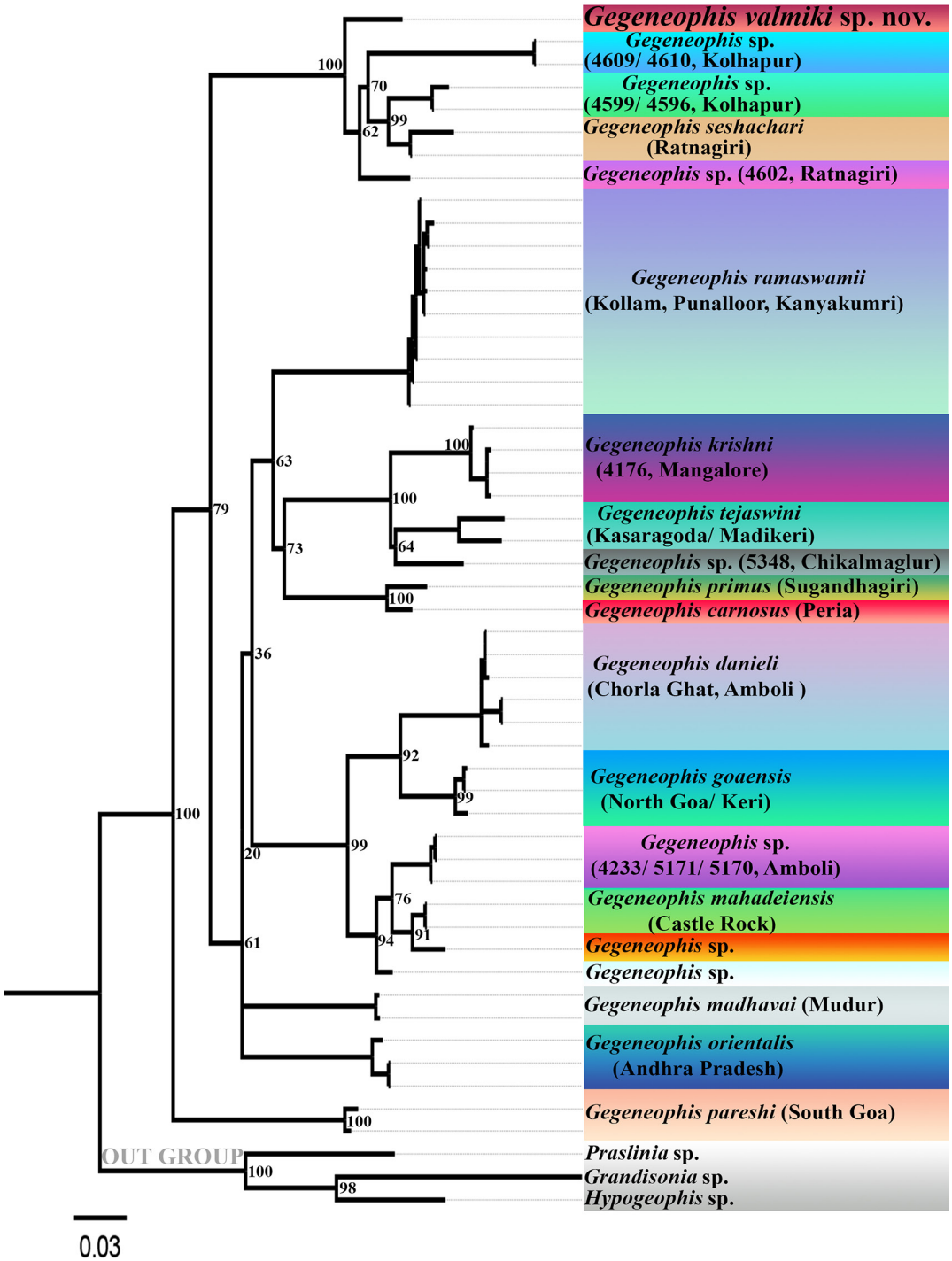

Figure 2. Maximum likelihood tree for the members of *Gegeneophis* based on the mt 16S rRNA (590 bp).

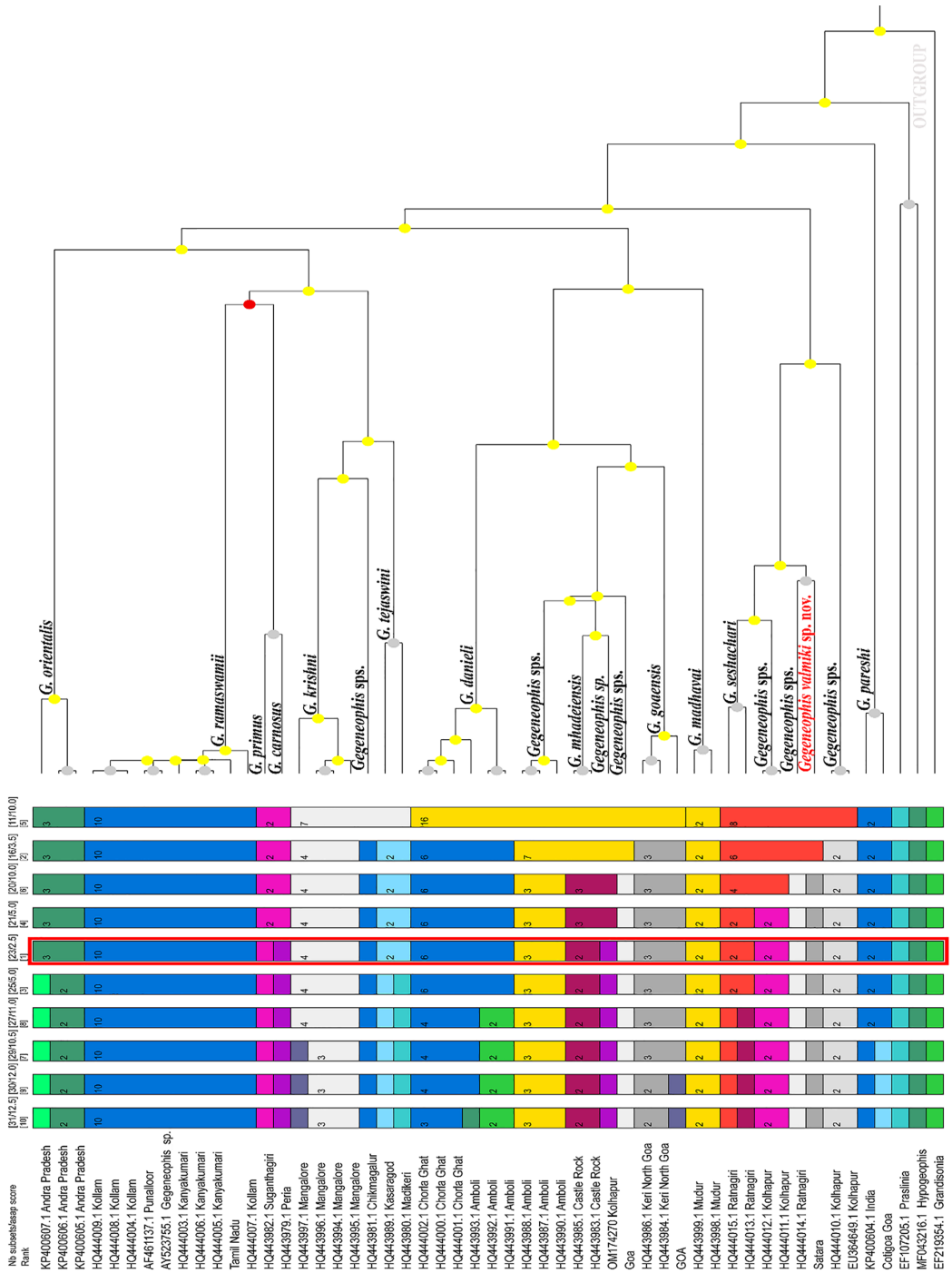

Figure 3. ASAP species delimitation for the genus *Gegeneophis* based on mt 16S rRNA sequences included in this study. The best partition with the lowest ASAP is marked with a red frame.

type locality. Species epithet '*valmiki'* is treated as a noun in apposition to the generic name.

Morphological diagnosis.—A slender vermiform teresomatan *Gegeneophis* having a tentacle between eye and naris, narial plugs open and small. Only primary annuli are distinct and distinguishable with no secondary annular grooves. *Gegeneophis valmiki* sp. nov. has 135 to 145 primary annuli. Diastemata absent between vomerine and palatal teeth. Unsegmented terminal shield without keel and 1 mm long from the last primary groove, transverse vent close to terminal shield (0.2 mm).

Description of the holotype (ZSI/WRC/A/2782) (Figures 5 and 6).—Morphometric and metric details provided in Table 1. Adult male, 192 mm total length, in well-preserved condition. Skin of the fixed specimen soft, smooth, and glandular, slightly glossy due to preservation artefacts. A mid-ventral incision anterior to vent was made for extraction of tissue sample and determination of sex. A few scratches visible on skin on anterodorsal body (made during search for scales). In life body sub-cylindrical, after fixation became slightly dorsoventrally compressed. Circumference at midbody 10.0 mm, with length by circumference ratio of 19.2. Body width almost uniform throughout length; in preserved state body 3.0 mm wide at first annular groove and 4.1 mm at midbody at widest part. Body width decreases to 2.5 mm at region of vent. Body width at 1st nuchal groove 3.2 mm, 2nd nuchal groove 3.1 mm. Distance from tip of snout tip to 1st nuchal groove 4.6 mm, 2nd nuchal groove 4.7 mm, 3rd nuchal groove 5.6 mm. Laterally width of 1st nuchal groove 0.4 mm, 2nd nuchal groove 0.5 mm. Nuchal region broader when compared to another nuchal collar and annular region. Three distinct nuchal grooves visible between the two nuchal collars.

In dorsal view, head tapers obtusely from region of eye to tentacular aperture. Anteriorly head rounded at tip of snout. Head at jaw angle slightly narrower than nuchal region, head length 4.5 mm, head width at jaw angle 2.9 mm. Laterally, top of head straight without protuberances (preservation artefacts). Margin of upper lip slightly arched, snout projects 0.6 mm beyond mouth (Figure 6A). Distance between jaw angle and top of head (1.8 mm) more than distance between the jaw angle and ventral surface of lower jaw (0.9 mm). Anterior margin of lower jaw more narrowly rounded than anterior margin of snout in ventral view. Tiny sub-circular nostrils closer to level of tip of snout (0.2 mm). Internarial distance 1.0 mm, visible laterally but not ventrally, whitish rim around nostrils visible laterally.

In life, tentacles visible laterally (Figure 4), globular in position, 2.9 mm apart. Tentacles situated 1.2 mm from snout, 0.8 mm from nostril, 0.4 mm from margin of upper lip, 0.7 mm from top of head, 2.4 mm from jaw angle (Figure 6B). Tiny eyes situated under bone (width of eye 0.3 mm), visible evidently in life (Figure 4) but not clearly in preserved specimen (Figures 5 and 6B). Eyes dorsolateral in position, interorbital distance 2.6 mm. Distance from eye to nostril 1.9 mm, to tentacle 0.9 mm, to tip of snout 2.2 mm.

Two rows of teeth in upper jaw, two rows of teeth in the lower jaw, all recurved and monocusped. Compared to posterior teeth, anterior teeth smaller. Teeth in posterior region of premaxillary–maxillary and vomeropalatine series almost parallel, vomeropalatine teeth series lacks diastemata. Total premaxillary–maxillary teeth 20, 18 vomeropalatine teeth, 17 dentary teeth, 3 splenial teeth. The premaxillary–maxillary and vomeropalatine tooth rows clearly extend posterior to region of choanae. In anterior view dentary teeth appear larger when compared to premaxillary–maxillary and vomeropalatine teeth, splenials are smallest. Sub-circular choanae smaller in upper palate. Tongue broadly rounded, unattached anteriorly, close to splenial teeth that are separated by a groove from gingivae.

Laterally, second collar region 0.5 mm, equal to first collar region (0.4 mm). First and second nuchal grooves complete around body when compared to third incomplete nuchal groove. One short transverse middorsal groove on

Figure 4. *Gegeneophis valmiki* sp. nov in life from Maharshi Valmiki Mandir, Valmiki Plateau, Paneri, Palashi, Pathan, Satara, Maharashtra, India.

dorsum of first collar between first and second nuchal groove. Middorsal groove present over entire dorsum between second and third nuchal grooves.

Dorsal surface of body dark brown, ventral region light brown. Anterior part of body lighter in color compared to rest of the midbody and posterior part of body. Entire body glandular in texture, annuli marked by whitish grooves. Primary grooves more conspicuous on lateral sides of body when compared dorsally and ventrally. 145 primary annuli present to terminal shield that is 1.0 mm (Figure 6C). Transverse vent 0.2 mm wide, vent surrounded by 11 denticles (Figure 6D).

In life, dorsum and lateral sides of holotype dark slate brown, ventrally lighter brown, anterior part of head light brown, glossy, where tentacles and eyes visible. Annuli and annular groves prominent on lateral sides of body, annular grooves clearly demarcated with distinct glandular dots. In preservation, head region dorsally and ventrally light brown compared to dark brown body color. Annular grooves lighter in color and clearly distinguishable. Disc in vent region whitish both in life and preservation.

Figure 5. Holotype of *Gegeneophis valmiki* sp. nov. (ZSI/WRC/V/A/2782).

Other Variations

The paratype is similar to the holotype in all morphological features except for body size and the number of primary annuli. Variation among the reference collections is provided in Table 2.

Comparisons

Multivariate Principal Component Analysis (PCA) was used for the species of *Gegeneophis* without secondary annular groves (*G. seshachari, G. pareshi, G. tejaswini,* and *Gegeneophis valmiki* sp. nov.). Morphological character separation was analyzed using PC2 and PC3 (Figure 7). In the Principal Component analysis, PC2 accounted for 18.7% variance, and PC3 accounted for 10.4% variance. The combination of total primaries and the appearance of secondaries on the primaries are graphically illustrated (Figure 8) for ease of museum specimen identification.

Among the congeners, *Gegeneophis valmiki* sp. nov. differs from *G. seshachari* in having 137 to 145 primary annuli (*vs.* 122 to 127); *G. valmiki* is known from high-elevation mountain plateaus of 1000 m at Palashi, Pathan, Satara, Western Ghats (*vs.* known from coastal plains with an elevation of 30 m at Dorle village, Ratnagiri, Maharashtra).

Figure 6. (**A**) Head, ventral profile; (**B**) Head, lateral side profile; (**C**) Dorsal view of terminal shield, (**D**) Ventral side of body terminus of *Gegeneophis valmiki* sp. nov.

Gegeneophis valmiki sp. nov. differs from *G. pareshi* in having 137 to 145 primary annuli (*vs.* 145 to 150); known from high-elevation mountain plateaus of 1000 m at Palashi, Pathan, Satara, Western Ghats (*vs.* known from elevation of of 200 m at Kuske village, Cotigao Wildlife Sanctuary, Goa).

Gegeneophis valmiki sp. nov. differs from *G. primus* in having 137 to 145 primary annuli (*vs.* 108 to 112); known from higher-elevation mountain plateaus of 1000 m at Palashi, Pathan, Satara, Western Ghats (*vs.* known from elevations of 800 m at Vythiri Taluk, Wayanad District, Kerala).

Gegeneophis valmiki sp. nov. differs from *G. danieli* in having 137 to 145 primary annuli and the absence of secondary annuli (*vs.* 112 to 114 primary annuli and secondaries starting between 5th to 34th annuli); known from higher-elevation mountain plateaus of 1000 m at Palashi, Pathan, Satara, Western Ghats (*vs.* known from elevations

Table 2. Morphometric (in mm) and meristic data for the type series of *Gegeneophis valmiki* sp. nov. #ZSI/WRC/V/; *eight characters used for Principal Component Analysis (PCA).

Reg no.#		**A/2782**	**A/2783**	**A/2784a**	**A/2784b**	**A/2784c**	**A/2784d**	**A/2784e**
Sex		Holotype	Paratype					
Total length	TBL	192	195	190	99	77	146	146
Head length	HDL	4.5	4.5	4.8	3.2	2.2	3.0	2.3
Head width at jaw angle*	HWJ*	2.9	3.0	2.7	1.8	1.7	2.3	1.9
Circumference at mid body*	CMB*	10.0	11.0	10.0	7.0	7.0	10.0	11.0
Width of the body at 1st annular groove	WFA	3.0	3.0	2.7	1.8	1.7	2.4	2.4
Width of the body at broadest region	WBB	4.1	3.9	3.1	1.9	1.8	3.0	2.8
Width of the body at the level of vent*	WBV*	2.5	2.6	2.4	1.3	1.2	2.0	1.8
Length divided by width	LDW	19.2	17.7	19.0	14.1	11.0	14.6	13.3
Length of snout projecting beyond mouth	LSP	0.6	0.7	0.5	0.4	0.7	0.2	0.4
Distance between jaw angle and top of head	DJH	1.8	1.6	1.6	1.3	1.9	0.7	1.5
Distance between jaw angle and ventral surface of lower jaw	DJV	0.9	1.6	1.1	0.7	1.7	1.4	0.8
Distance between jaw angle and tip of lower jaw	DJJ	3.3	3.3	2.9	1.8	3.2	0.9	2.4
Distance between nostrils*	DBN*	1.0	0.7	1.4	0.7	0.6	0.6	0.7
Distance between nostril and snout tip	DNS	0.2	0.3	0.2	0.3	0.3	0.3	0.2
Distance between tentacles*	DBT*	2.9	2.1	3.2	1.6	1.3	1.4	1.8
Distance between tentacle and snout tip*	DTS*	1.2	1.3	1.0	0.9	1.2	1.1	0.9
Distance between tentacle and jaw angle*	DTJ*	2.4	2.5	2.4	1.5	2.7	2.2	1.9
Distance between tentacle and nostril	DTN	0.8	0.8	0.6	0.5	0.7	0.6	0.7
Distance between tentacle and margin of upper lip	DTU	0.4	0.4	0.4	0.3	0.5	0.3	0.2
Distance between tentacle and top of head	DTH	0.7	0.5	0.6	0.6	0.7	0.6	0.7

Table 2. Continued.

Reg no.#		A/2782	A/2783	A/2784a	A/2784b	A/2784c	A/2784d	A/2784e
Width of eye	WOE	0.3	0.2	0.2	0.1	0.3	0.2	0.2
Distance between eyes	DBE	2.6	2.7	2.7	1.0	1.6	1.0	2.0
Distance from eye to nostril	DEN	1.9	1.7	2.0	1.0	1.7	1.5	1.4
Distance from eye to tentacle	DET	0.9	0.7	1.1	0.3	0.7	0.5	0.5
Distance from eye to snout tip	DES	2.2	2.2	2.3	1.4	2.2	1.8	1.7
Width at 1st nuchal groove	WFN	3.2	3.0	2.9	1.9	1.9	2.9	2.5
Width at 2nd nuchal groove	WSN	3.1	2.8	2.7	1.6	1.5	2.5	2.3
Width at 2nd nuchal groove	LFN	0.4	0.7	0.3	0.3	0.3	1.2	1.0
Length of 2nd nuchal collar (Laterally)	LSN	0.5	0.5	0.3	0.3	0.9	1.5	1.6
Distance between snout tip and 1st nuchal groove	DFN	4.6	4.5	4.5	3.0	3.0	3.9	4.1
Distance between snout tip and 2nd nuchal groove	DSN	4.7	5.1	4.8	3.3	3.4	4.6	4.3
Distance between snout tip and 3rd nuchal groove	DST	5.6	6.0	4.9	3.8	4.5	5.8	5.1
Width of disc surrounding vent*	WDV*	1.2	1.4	3.1	0.6	0.6	1.0	1.2
Length of disc surrounding vent	WDV*	1.1	1.4	2.0	0.5	0.5	1.1	1.2
width of vent	WOV	0.1	0.1	0.1	0.1	0.1	0.1	0.1
Number of denticles surrounding the vent	DSV	11	11	12	6	10	5	6
Number of premaxillary-maxillary teeth	NPM	20	18	19	15	16	17	16
Number of vemoropalantine teeth	NVT	18	18	17	12	14	18	18
Number of dentary teeth	NDT	17	15	19	14	12	17	15
Number of splenial teeth	NST	3	3	4	3	2	3	2
Total number of primary annuli	TPA	145	143	144	137	137	141	144

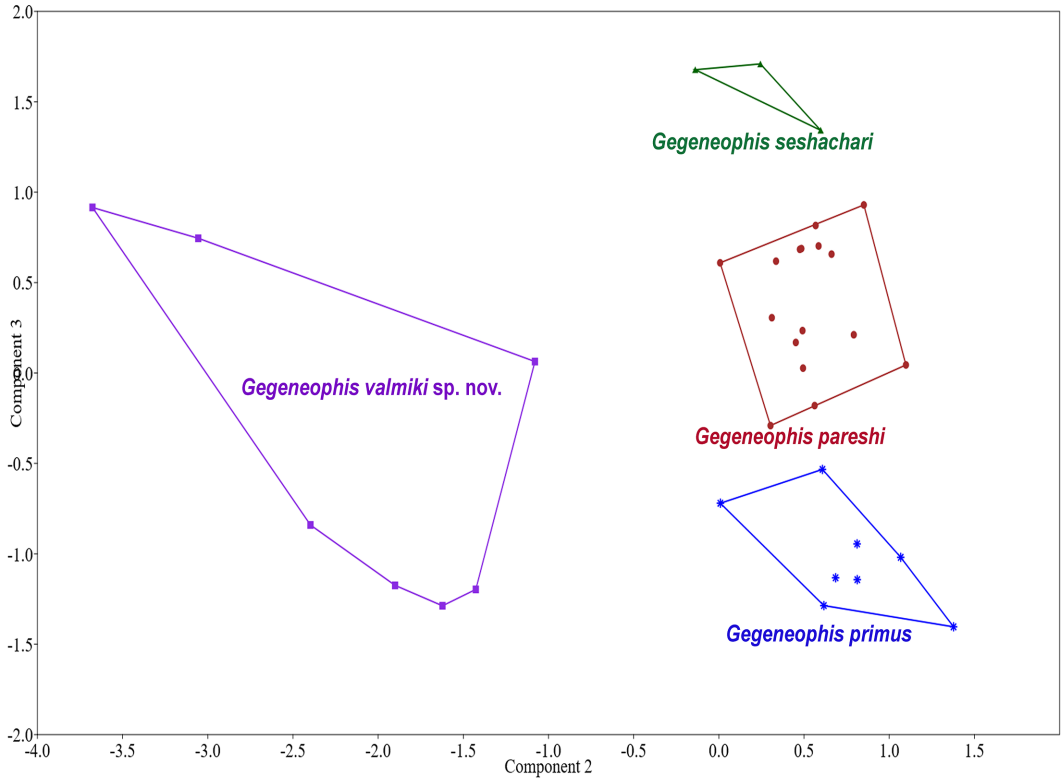

Figure 7. Multivariate Principal Component Analysis scatter plot for the members of *Gegeneophis* without secondary annuli (*Gegeneophis valmiki* sp. nov, *G. seshachari, G. pareshi,* and *G. primus*).

of 850 m at Amboli forest of Western Ghats in Sindhudurg, Maharashtra).

Gegeneophis valmiki sp. nov. differs from *G. goaensis* in having 137 to 145 primary annuli and absence of secondary annuli (*vs.* 125 to 126 primary annuli and secondaries starting between 38th to 48th annuli); known from higher-elevation mountain plateaus of 1000 m at Palashi, Pathan, Satara, Western Ghats (*vs.* known from elevations of 50 m at Keri Village, Goa).

Gegeneophis valmiki sp. nov. differs from *G. mhadeiensis* in having 137 to 145 primary annuli and absence of secondary annuli (*vs.* 117 to 125 primary annuli and secondaries starting between 87th to 98th annuli); known from higher-elevation mountain plateaus of 1000 m at Palashi, Pathan, Satara, Western Ghats (*vs.* known from elevations of 700 m at Chorla Village, Belgaum, Karnataka).

Gegeneophis valmiki sp. nov. differs from *G. madhavai* in having 137 to 145 primary annuli and absence of secondary annuli (*vs.* 96 to 97 primary annuli and secondaries starting between 63rd to 70th annuli); known from higher-elevation mountain plateaus of 1000 m at Palashi, Pathan, Satara, Western Ghats (*vs.* known from elevations of 50 m at Mudur Village, Kundapura, Udupi, Karnataka).

Gegeneophis valmiki sp. nov. differs from *G. krishni* in having 137 to 145 primary annuli and absence of secondary annuli (*vs.* 125 to 127 primary

annuli and secondaries starting between 110th to 114th annuli); known from higher-elevation mountain plateaus of 1000 m at Palashi, Pathan, Satara, Western Ghats (*vs.* known from elevations of 40 m at Krishna Farms, Gurpur, Dakshina Kannada, Karnataka).

Gegeneophis valmiki sp. nov. differs from *G. tejaswini* in having 137 to 145 primary annuli and absence of secondary annuli (*vs.* 125 to 131 primary annuli and secondaries starting between 105th to 115th annuli); known from higher-elevation mountain plateaus of 1000 m at Palashi, Pathan, Satara, Western Ghats (*vs.* known from elevations of 40 m at Bedoor, Cheemeni, Hosdurg, Kasaragod, Kerala).

Gegeneophis valmiki sp. nov. differs from *G. carnosus* in having 137 to 145 primary annuli and absence of secondary annuli (*vs.* 105 to 112 primary annuli and secondaries starting between 99th to 105th annuli); known from higher-elevation mountain plateaus of 1000 m at Palashi, Pathan, Satara, Western Ghats (*vs.* known from elevations of 1500 m at Periah Peak, Wayanad, Kerala).

Gegeneophis valmiki sp. nov. differs from *G. ramaswami* in having 137 to 145 primary annuli and absence of secondary annuli (*vs.* 109 to 114 primary annuli and secondaries starting between 98th to 103rd annuli); known from higher-elevation mountain plateaus of 1000 m at Palashi, Pathan, Satara, Western Ghats (*vs.* known from elevations of 200 m at Tenmalai forests, Kollam, Kerala).

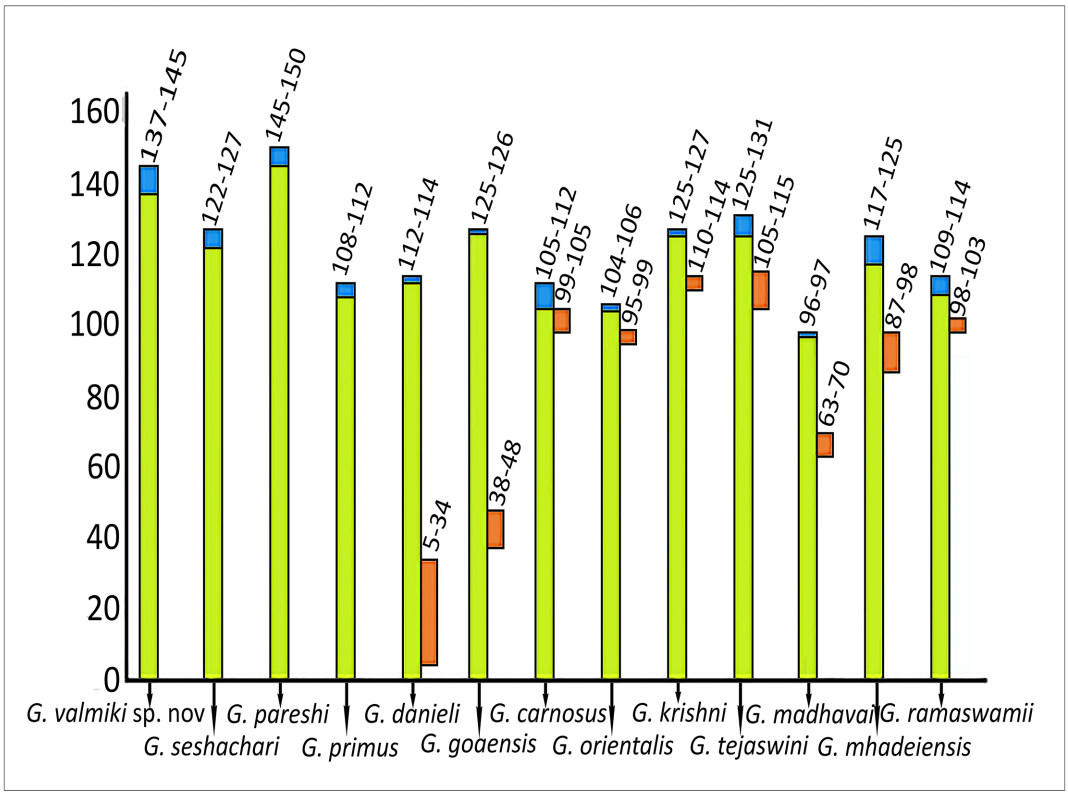

Figure 8. Graphic illustration of number of primary annular grooves and the initiation of secondary annular grooves for the extant 13 species of *Gegeneophis* in the peninsular India. Green bars: primary annuli; Blue bars: range of primary annuli; Orange bars: secondary annular groove starting range.

Gegeneophis valmiki sp. nov. differs from *G. orientalis* in having 137 to 145 primary annuli and absence of secondary annuli (*vs.* 104 to 106 primary annuli and secondaries starting between 95th to 99th annuli); known from higher-elevation mountain plateaus of 1000 m at Palashi, Pathan, Satara, Western Ghats (*vs.* known from elevations of 1200 m at Beespuram, Visakhapatnam, Andhra Pradesh and Deomali, Koraput, Odisha region of the Eastern Ghats).

Discussion

The distribution and patterns of species descriptions in *Gegeneophis* are unique in peninsular India. Among the 13 extant species (including the new species), six have their type localities and ranges in the northern Western Ghats, followed by five species in the central Western Ghats (Table 1, Figure 1). The southern Western Ghats and the Eastern Ghats are each represented by a single species.

Another six new lineages (Figures 2 and 3) are awaiting formal description, of which four are from the northern Western Ghats. This pattern of higher concentration of *Gegeneophis* species in the northern Western Ghats needs to be examined in context of this region as a potential center of origin for species diversity.

Considering the taxonomy of Indian caecilians, tooth count as a reliable taxonomic character is questionable. The number of teeth in caecilians varies with life stage, physiological condition, and dietary preferences within their habitat. For example, Giri *et al.* (2003) reported 30 premaxillary–maxillary, 33 vomeropalatine, 24 dentary, and 6 splenial teeth in their description of *G. danieli.* In contrast, Bhatta *et al.* (2004) documented 20 premaxillary–maxillary, 18 vomeropalatine, 10 dentary, and 5 splenial teeth in the description of *G. nadkarni.* Subsequently, based on molecular data presented by Gower *et al.* (2011), *G. nadkarni* was treated as a junior synonym of *G. danieli* (Gower *et al.* 2013). Now, dentition details for *G. danieli* are 20 to 30 premaxillary–maxillary, 18 to 33 vomeropalatine, 10 to 24 dentary, and 5 to 6 splenial teeth. Similarly, Ravichandran *et al.* (2003) reported 21 premaxillary–maxillary, 20 vomeropalatine, 18 dentary, and 3 splenial teeth in the original description of *G. seshachari.* Gower *et al.* (2007), in their redescription of the species, documented a range of 21 to 23 premaxillary–maxillary, 20 to 22 vomeropalatine, 16 to18 dentary, and 2 to 3 splenial teeth. Age, habitat preference, and diet composition are crucial factors influencing tooth retention in adult caecilians. Under these circumstances the utility of tooth count as a taxonomic character is challenging.

Since 2003, in descriptions of new species of *Gegeneophis* and *Indotyphlus,* more than 20 measurable (metric) characters have been considered. Only a few characters such as the position of the tentacles relative to the nostrils and eyes have proven to be reliable for generic-level differentiation between *Gegeneophis* and *Indotyphlus* (Giri *et al.* 2004). It is apparent that the remaining measurable characters were included as part of formal species descriptions rather than being taxonomically reliable or diagnostic (Figure 7). In contrast, meristic characters, such as the number of primary annuli and the presence or initiation of secondary annular grooves, have proven to be useful (Figure 8). High resolution field photographs are expected to facilitate the use of meristic characters for species identification in the field. Understanding the high species richness in northern Western Ghats using the total number of primaries and secondary annular grooves on the body in combination with geography (Dinesh 2025) may be reliable identification characters for Western Ghats caecilians.

The challenging part of caecilian studies in Western Ghats is the limited number of museum specimens for morphological studies and the limited knowledge of geographical distribution. In India, most of the members of the *Gegeneophis* are treated as either Data Deficient or Not Assessed categories for IUCN Red List status (Ramakrishna *et al.* 2023).

The type locality of *Gegeneophis valmiki* sp.

nov. lies in the vicinity of a temple characterized by perennial streams that provide suitable microhabitats for caecilians. Small scale agricultural practices in the surrounding areas involve the use of cow dung manure in paddy fields. Our field surveys discovered a higher frequency of caecilian encounters around cow manure pits next to forested areas, which are generally rich in organic matter and moisture (Dinesh *et al.* 2024). Because this study represents the northernmost distributional limit of *Gegeneophis* in the Western Ghats, further field explorations are warranted to uncover the potential hidden diversity and to better delineate the distributional range of the genus. Because *Gegeneophis valmiki* sp. nov. is known from only from a single locality, it is recommended that the species be treated as Data Deficient, warranting further field studies.

Acknowledgments

We thank the Director, Zoological Survey of India (ZSI), Kolkata; the Officer-in-Charge, ZSI, WRC, Pune for support and facilities. We are grateful to Mr. Ajay Sagar, Mr. Ram Sundarkanth Salve, and the staff of ZSI, WRC, Pune for their help during field work. We thank Priyanka Swami and Varsha V Kumar, Kartik Shankers lab, CES, IISc, Bangalore, and Shabnam Ansari ZSI, WRC Pune for the wet lab support. KPD is deeply grateful to Dr. Gopalakrishna Bhatta for his guidance and mentorship in caecilian research. The authors are grateful to the anonymous reviewers, Prof. Janalee Caldwell and the Editor-in-Chief for their critical comments that helped improve an earlier version of this manuscript.

References

Agarwal, I., M. Wilkinson, P. P. Mohapatra, S. K. Dutta, V. B. Giri, and D. J. Gower. 2013. The first teresomatan caecilian (Amphibia: Gymnophiona) from the Eastern Ghats of India—a new species of *Gegeneophis* Peters, 1880. *Zootaxa 3696:* 534–546.

Bhatta, G. and P. Prashanth. 2004. *Gegeneophis nadkarnii* – a caecilian (Amphibia: Gymnophiona: Caeciliidae) from Bondla Wildlife Sanctuary, Western Ghats. *Current Science. Bangalore 87:* 388–392.

Bhatta, G. and R. Srinivasa. 2004. A new species of *Gegeneophis* Peters (Amphibia: Gymnophiona: Caeciliidae) from the surrounds of Mookambika Wildlife Sanctuary, Karnataka, India. *Zootaxa 644:* 1–8.

Bhatta, G., K. P. Dinesh, P. Prashanth, and N. U. Kulkarni. 2007a. A new species of *Gegeneophis* Peters (Amphibia: Gymnophiona: Caeciliidae) from Goa, India. *Zootaxa 1409:* 51–59.

Bhatta, G., K. P. Dinesh, P. Prashanth, and N. U. Kulkarni. 2007b. A new species of the Indian caecilians genus *Gegeneophis* Peters (Amphibia: Gymnophiona: Caeciliidae) from the surrounds of Mahadayi Wildlife Sanctuary, Western Ghates. *Current Science. Bangalore 93:* 1442–1445.

Bhatta, G., K. P. Dinesh, P. Prashanth, N. U. Kulkarni, and C. Radhakrishnan. 2010. New site records of *Gegeneophis goaensis* and *G. mhadeiensis* (Gymnophiona: Caeciliidae) from the Western Ghats of Goa and Karnataka. *Journal of Threatened Taxa 2:* 1105–1108.

Dinesh, K. P. 2020. Amphibia. Pp. 647–662 *in* K. Chandra, C. Raghunathan, P. M. Sureshan, K. A. Subramanian, and A. N. Rizvi (eds.), *Faunal Diversity of Biogeographic Zones of India: Western Ghats.* Volume 24. Kolkata. Zoological Survey of India.

Dinesh, K. P. 2021. Amphibians. Pp. 54–67 *in* D. Banerjee (ed.), *Fauna of Koyna Wildlife Sanctuary, Maharashtra. Conservation Area Series 66*. Kolkata. The Director, Zoological Survey of India.

Dinesh, K. P. 2025. Taxonomic studies on the Amphibians of the Western Ghats. *Records of the Zoological Survey of India, Occasional Papers 429:* 1–148.

Dinesh, K.P., B. V. Jadhav, S. Shikalgar, and P. Adhav. 2024. Additional records of *Indotyphlus maharashtraensis* Giri, Wilkinson and Gower, 2004 (Amphibia: Gymnophiona: Grandisonidae) from Pune District, Maharashtra. *Records of the Zoological Survey of India 124:* 367–378.

Frost, D. R. (ed.). 2025. Amphibian Species of the World: An online Reference. Version 6.2. Electronic Database accessible at https://amphibiansoftheworld.amnh.org/index.php. American Museum of Natural History, New York, USA. Captured on 20 August 2025.

Giri, V. B., M. Wilkinson, and D. J. Gower. 2003. A new species of *Gegeneophis* Peters (Amphibia: Gymnophiona: Caeciliidae) from southern Maharashtra, India, with a key to the species of

the genus. *Zootaxa 351:* 1–10.

Giri, V. B., D. J. Gower, and M. Wilkinson. 2004. A new species of *Indotyphlus* Taylor (Amphibia: Gymnophiona: Caeciliidae) from the Western Ghats, India. *Zootaxa 739:* 1–9.

Giri, V. B., D. J. Gower, K. Gaikwad, and M. Wilkinson. 2011. A second species of *Gegeneophis* Peters (Amphibia: Gymnophiona: Caeciliidae) lacking secondary annular grooves. *Zootaxa 2815:* 49–58.

Gower, D.J., V. B. Giri, and M. Wilkinson. 2007. Rediscovery of *Gegeneophis seshachari* Ravichandran, Gower and Wilkinson, 2003 at the type locality. *Herpetozoa 19:* 121–127.

Gower, D.J., D. San Mauro, V. Giri, G. Bhatta, V. Govindappa, R. Kotharambath, O. V. Oommen, F. A. Fatih, J. A. Mackenzie-Dodds, R. A. Nussbaum, and S. D. Biju. 2011. Molecular systematics of caeciliid caecilians (Amphibia: Gymnophiona) of the Western Ghats, India. *Molecular Phylogenetics and Evolution 59:* 698–707.

Gower, D.J., V. Giri, V. R. Torsekar, K. Gaikwad, and M. Wilkinson. 2013. On the taxonomic status of *Gegeneophis nadkarnii* Bhatta & Prashanth, 2004 (Amphibia: Gymnophiona: Indotyphlidae). *Zootaxa 3609:* 204–212.

Hammer, O., D. T. A. Harper, and P. D. Ryan. 2001. PAST: Paleontological statistics software package for education and data analysis. *Palaeontologia Electronica 4:* 9.

Kumar, S., G. Stecher, M. Li, C. Knyaz, and K. Tamura. 2018. MEGA X: Molecular evolutionary genetics analysis across computing platforms. *Molecular Biology and Evolution 35:* 1547–1549.

Kotharambath, R., D. J. Gower, O. V. Oommen, and M. Wilkinson. 2012. A third species of *Gegeneophis* Peters (Amphibia: Gymnophiona: Indotyphlidae) lacking secondary annular grooves. *Zootaxa 3272:* 26–34.

Kotharambath, R., M. Wilkinson, O. V. Oommen, and D. J. Gower. 2015. A new species of Indian caecilian highlights challenges for species delimitation within *Gegeneophis* Peters, 1879 (Amphibia: Gymnophiona: Indotyphlidae). *Zootaxa 3948:* 60–70.

Peters, W. C. H. 1880 "1879". Über die Eintheilung der Caecilien und insbesondere über die Gattungen *Rhinatrema* und *Gymnopis*. *Monatsberichte der Königlichen Preussische Akademie des Wissenschaften zu Berlin 1879:* 924–945.

Palumbi, S. R., P. A. Martin, L. S. Romano, O. W. McMillan, L. Stice, and G. Grabowski. 2002. *The Simple Fool's Guide to PCR Ver. 2.0.* Honolulu. Special Publications Department of Zoology, University of Hawaii. 24 pp.

Pillai, R. S., and M. S. Ravichandran. 1999. Gymnophiona (Amphibia) of India. A taxonomic study. *Records of the Zoological Survey of India, Occasional Papers 172:* 1–117.

Pillai, R. S., and M. S. Ravichandran. 2005. ''Gymnophiona (Amphibia) of India. A taxonomic study. *Records of the Zoological Survey of India 172:* 1–126.

Puillandre N, S. Brouillet, and G. Achaz. 2021. ASAP: Assemble Species by Automatic Partitioning. *Molecular Ecology Resources 21:* 609–620.

Ravichandran, M. S., D. J. Gower, and M. Wilkinson. 2003. A new species of *Gegeneophis* Peters (Amphibia: Gymnophiona: Caeciliidae) from Maharashtra, India. *Zootaxa 350:* 1–8.

Ramakrishna, P., P. Deepak, and K. P. Dinesh. 2023. Status of amphibian diversity in the Western Ghats. Pp. 219–240 *in* T. Pullaiah (ed.), *Biodiversity Hotspot of the Western Ghats and Sri Lanka.* Palm Bay and Boca Raton. Taylor and Francis Group, CRC Press and Apple Academic Press.

Taylor, E. H. 1964. A new species of caecilian from India (Amphibia, Gymnophiona). *Senckenbergiana Biologica 45:* 227–231.

Trifinopoulos, J., L. T. Nguyen, A. von Haeseler, and B. Q. Minh. 2016. W-IQ-TREE: a fast online phylogenetic tool for maximum likelihood analysis. *Nucleic Acids Research 44:* 232–235.

Editor: Jaime Bertoluci

Phyllomedusa 24(2):313–318, 2025

ISSN 1519-1397 (print) / ISSN 2316-9079 (online)
doi: http://dx.doi.org/10.11606/issn.2316-9079.v24i2p313-318

Short Communication

Notes on saxicolous habits of *Aspidoscelis communis* (Squamata: Teiidae) in an isolated population

Eduardo A. Gómez-Hernández[1,2] and Armando H. Escobedo-Galván[1]

[1] Universidad de Guadalajara, Centro Universitario de la Costa. Puerto Vallarta 48280, Jalisco, Mexico. E-mail: elchorvis@gmail.com.

[2] Current address: El Colegio de la Frontera Sur, Unidad Villahermosa. Villahermosa 86280, Tabasco, Mexico.

Keywords: Behavior shift, Habitat use, Insularity, Jalisco.

Palabras clave: Cambio de comportamiento, Insularidad, Jalisco, Uso de habitat.

Palavras-chave: Insularidade, Jalisco, Mudança de comportamento, Uso de hábitat.

The Whiptail Lizards of the genus *Aspidoscelis* are characterized by their elongated, slim bodies, sharp-pointed snouts, and notably long tails (Duellman and Zweifel 1962). These lizards predominantly exhibit diurnal terrestrial behavior and employ an energetic hunting approach, which enables them to traverse expansive territories and maintain prolonged periods of activity (Anderson and Karasov 1981, Brown and Nagy 2007). Surprisingly, some species of *Aspidoscelis* inhabit isolated ecosystems such as atolls [*Aspidoscelis maslini* (Fritts, 1969) (Charruau *et al.* 2015)], land-bridge islands [*A. lineattissimus* (Cope, 1878); (Siliceo-Cantero *et al.* 2023)], oceanic islands [*A. costatus* (Cope, 1878) (Cruz-Elizalde *et al.* 2014)], and lake islands [*A. tigris* (Baird and Girard, 1852) (Keehn *et al.* 2013)]. This isolation has resulted in populations occupying broader niches, with behavioral shifts being the most noticeable change compared to mainland populations. For example, some isolated populations have expanded their trophic niches by increasing prey diversity (Hernández-Salinas *et al.* 2022, Barraza-Soltero *et al.* 2024), or by using different perches and habitat types other than the ground (Hernández-Salinas *et al.* 2022, Siliceo-Cantero *et al.* 2023). Despite these ecological and behavioral differences in isolated populations compared to their mainland counterparts, the lake islands could be subject to more intense deterioration than an island in the ocean due to their proximity to the mainland and the presence of human settlements, which lead to changes in native vegetation and the presence of non-native species (Harris 1984).

Received 06 January 2025
Accepted 05 June 2025
Distributed December 2025

The Colima Giant Whiptail *Aspidoscelis communis* (Cope, 1878) is endemic to Mexico and is widely distributed throughout the country along the Pacific slope from Sinaloa to Guerrero (Van Denburgh 1897, Castro-Franco and Bustos-Zagal 2004, Loc-Barragán *et al.* 2024), including some island populations reported along the coast of Jalisco (Siliceo-Cantero *et al.* 2023), and Nayarit (Nolasco-Luna *et al.* 2022). This species was assessed as Least Concern by the IUCN (Ponce-Campos and García Aguayo 2007). Wilson *et al.* (2013) gave it a high environmental vulnerability score (EVS = 14), and this species is placed in the special protection category by NOM-059-2010 (SEMARNAT 2010).

Regarding the behavior and habitat use of *C. communis* on isolated populations, Stejneger (1899) reported that five individuals were captured from a small detached rock on María Cleofas Island. Siliceo-Cantero *et al.* (2023) observed that *A. communis* used perches at ground level in a mainland population, while some individuals used different perch types such as grass, herbs, shrubs, cacti, and trees on two island populations. The above observations were conducted on land-bridge islands; in the first study, the island was isolated approximately 87.5 km from San Blas, Nayarit (Stejneger 1899), while in the second study the islands were located at distance of 1.2 km and 1.4 km from the mainland (Siliceo-Cantero *et al.* 2023). Information on ecology and life history from lake islands remains somewhat limited. Herein, we present additional information on the habitat use of *A. communis* on an island within Chapala Lake, Jalisco, Mexico, in which human activities have occurred for half a century.

On 27–28 March and 17–18 August 2024, we visited Mezcala Island, which is located in Chapala Lake, Jalisco, Mexico (20°17'28.47" N, 103°01'24.10" W; 1551 m a.s.l.; Figure 1). The island has a surface area of approximately 0.2 km^2, and it lies 5 km from the dock at the town of Mezcala. This island has degraded vegetation of tropical deciduous forest (e.g., *Guazuma ulmifolia* Lam., *Spondia* sp., *Bursera* sp.) interspersed with human activities such as agriculture of *Sicyos edulis* Jacq, and *Opuntia* sp., the presence of introduced pigs, cats, and dogs, as well as recently established tourism activities. In some parts of the island, rock buildings date back to 1280, and some others were built during the time of the Mexican Independence where they were used as cells for prisoners. Some buildings are still standing, while others have collapsed over time (Pedroza-Gutiérrez and Catalán-Romero 2017).

During the first visit to Mezcala Island on 27–28 March 2024, which corresponds to the dry season, we observed three lizard species: *Anolis nebulosus* (Wiegmann, 1834), *Sceloporus melanogaster* Cope, 1885, and *Aspidoscelis communis.* Of the last species, we observed 20 individuals foraging actively in different ground microhabitats, including trunks, rocks, grass, and leaf litter. We began seeing individuals around 09:45 h. We captured nine individuals on the ground to measure the snout–vent length (SVL) from the tip of the snout to the anterior margin of the cloaca (Williams 1995), which ranged from 42.2 to 59.4 mm, with a mean ± SD of 52.5 ± 5.5 mm.

On the second visit, 17–18 August 2024 (rainy season), we observed 15 individuals of *A. communis* with different behavior and habitat use. Specifically, seven were observed on rock piles or walls, some at heights greater than 1 m (Figure 2A). Some individuals were seen beginning around 09:30 h, and, as shown in Figure 2, many were perched on rocks (Figure 2B), while others were climbing or descending walls (Figures 2C and 2D). As we attempted to capture the lizards, we anticipated they would descend to the ground and flee. Instead, they climbed vertically along the walls, moving to higher locations. Capturing specimens was more difficult due to their facultative saxicolous habits; therefore, we only captured two individuals that had SVLs of 73.4 mm and 83.2 mm.

Our observations on the saxicolous habits of *A. communis* provide insight into the behavioral plasticity in isolated environments, which has been observed in several species of *Aspidoscelis*.

Specifically, the use of rock buildings and walls by *A. communis* on Mezcala Island may be associated with the interplay among low prey availability, microclimate conditions, non-native predators, and foraging strategy (Hernández-Salinas *et al.* 2022, Siliceo-Cantero *et al.* 2023). Species of *Aspidoscelis* usually invest more time and effort in covering larger distances while searching for food across various microhabitats, in contrast with other lizard species (Cooper 1995). The abundance of rocky constructions on the island may make foraging on and using them a common behavior for *A. communis.*

The rocky constructions could provide shaded spaces due to the absence of vegetation on Mezcala Island. These constructions would help maintain the microclimatic conditions that an actively foraging species such as *A. communis* needs for thermoregulation and feeding. Siliceo-Cantero *et al.* (2023) observed that temperature and humidity on island population were different between shaded and sunny sites, which could promote more efficient thermoregulation for physiological processes. Nevertheless, this idea must be evaluated in greater detail in future studies.

The limited predation and absence of interspecific competition on island ecosystems allow island species to spend more time searching for food in various microhabitats, in contrast to mainland populations (Siliceo-Cantero *et al.* 2016). For example, Siliceo-Cantero *et al.* (2023)

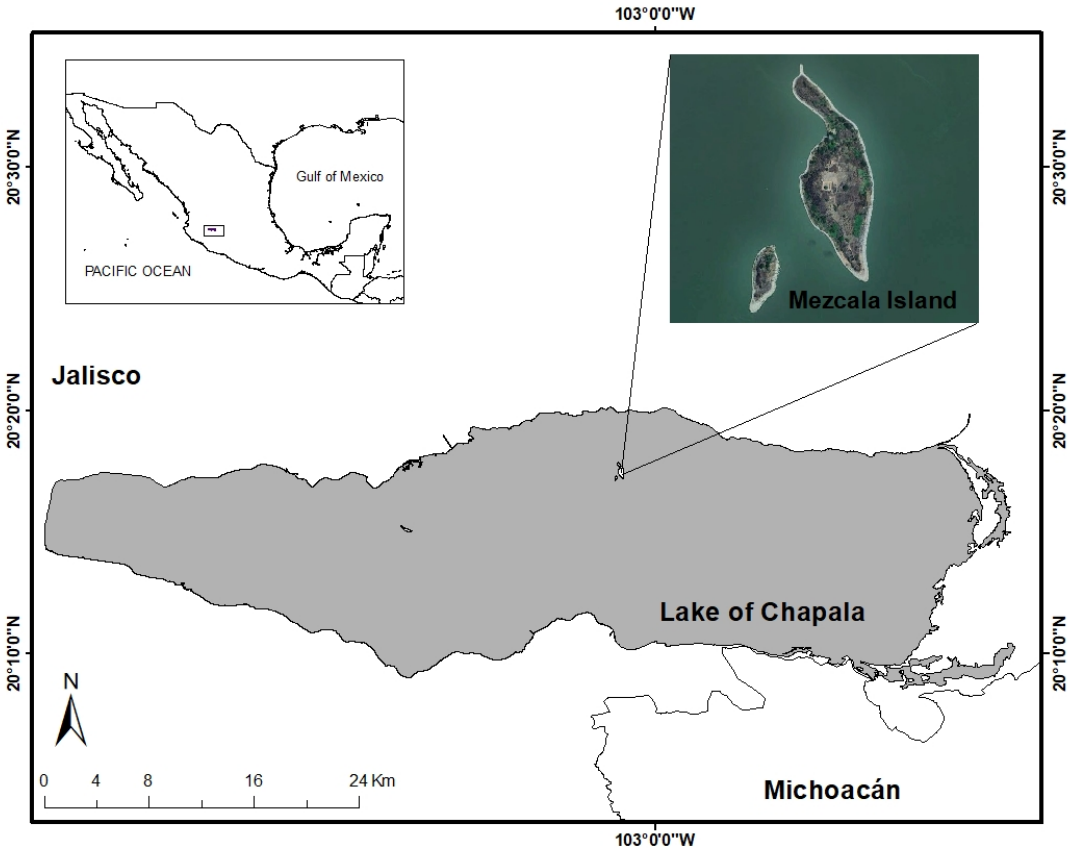

Figure 1. Map showing the location of Mezcala Island in Chapala Lake, Jalisco, Mexico.

Figure 1. Individuals of *Aspidoscelis communis* perched on rocks and descending walls on Mezcala Island, Mexico.

observed 80 individuals of *A. communis* using ground-level perches on the mainland. On islands, of 93 individuals, 75 used ground-level perches, 13 perched on grass, shrubs, and herbs, and five perched on cacti and trees. In the same study, the authors observed 32 individuals of *A. lineattissimus* using ground-level perches on the mainland, while on islands, of 108 individuals, 85 used ground-level perches, 16 perched on grass, shrubs, and herbs, and seven perched on cacti and trees. Hernández-Salinas *et al.* (2022) compared the diet composition of *A. lineattissimus* between mainland and island populations. During their fieldwork, individuals from the island population were collected in three types of habitat: tropical dry forest, desert cliff scrub, and coastal dunes, while individuals from the mainland population were collected only from tropical dry forest. These observations suggest that *A. communis* dedicates more time to foraging and exploring different microhabitats due to low prey availability and absence of interspecific competition on Mezcala Island.

The presence of non-native fauna could be a factor affecting the behavior of *A. communis* on the island. Specifically, predation pressure by cats could force *A. communis* to seek protection on rock buildings and walls; however, since non-native fauna were present during both visits, we expected that the habitat use of the species would be similar between visits. During the first visit, the species was foraging actively in different

ground microhabitats, while in the second visit, the species primarily used rock structures. These observations suggests that the interplay between the presence of non-native fauna and climatic conditions (dry season *vs.* rainy season) could have affected not only habitat use but also foraging behavior of *A. communis;* indeed, some studies have shown that native species can modify their foraging behavior in response to invasive species (e.g. Peck *et al.* 2014, Wilson Rankin *et al.* 2018). Further studies should be conducted to explore how the aforementioned factors may influence habitat use and foraging strategy of this species on the lake island.

Acknowledgments.—The first author received a scholarship from the Universidad de Guadalajara (PROSNI-2024) to work as a research assistant. This research was conducted by SEMARNAT permit SGPA/DGVS/01208/17. We thank Ismael Huerta de la Barrera for his support in editing figures. Finally, we thank the anonymous reviewers for their valuable comments and suggestions to improve this manuscript.

References

Anderson, R. A. and W. H. Karasov. 1981. Contrast in energy intake and expenditure in sit and wait and widely foraging lizards. *Oecologia 49:* 67–72.

Barraza-Soltero, I. K., F. G. Cupul-Magaña, and A. H. Escobedo-Galván. 2024. Food web of lizard species in a land-bridge island from Western Mexico. *Food Webs 38:* e00330

Brown, T. K. and K. A. Nagy. 2007. Lizard energetics and the sit-and-wait vs. wide-foraging paradigm. Pp. 120–140 *in* S. Reilly, L. McBrayer, and D. Miles (Eds.), *Lizard Ecology*. Cambridge, New York. Cambridge University Press.

Castro-Franco, R. and M. G. Bustos-Zagal. 2004. Additional records and range extensions of reptiles from Morelos, Mexico. *Herpetological Review 35:* 196.

Charruau, P., A.H. Díaz de la Vega Pérez, and F.R. Méndez de la Cruz. 2015. Reptiles of Banco Chinchorro: updated list, life history data, and conservation. *Southwestern Naturalist 60:* 299–312.

Cooper, W. E. Jr. 1995. Prey chemical discrimination and foraging mode in gekkonoid lizards. *Herpetological Monographs 9:* 120–129.

Cruz-Elizalde, R., A. Ramírez-Bautista, U. Hernández-Salinas, C. Sosa-Vargas, J. Johnson, and V. Mata-Silva. 2014. Sexual dimorphism and natural history of the Western Mexico Whiptail, *Aspidoscelis costata* (Squamata: Teiidae), from Isla Isabel, Nayarit, Mexico. *North-Western Journal of Zoology 10:* 374–381.

Duellman, W. E. and R. G. Zweifel. 1962. A synopsis of the lizards of the *sexlineatus* group (genus *Cnemidophorus*). *Bulletin of the American Museum of Natural History 123:* 155–210.

Harris, L. D. 1984. *The Fragmented Forest: Island Biogeography Theory and the Preservation of Biotic Diversity.* Chicago. The University of Chicago Press. 230 pp.

Hernández-Salinas, U., A. Ramírez-Bautista, R. Cruz-Elizalde, and L. A. Torres-Hernández. 2022. Feeding niche and predator-prey size relationship in the Whiptail lizard *Aspidoscelis lineattissima* (Squamata: Teiidae) in insular and continental populations of the Mexican Pacific. *Ichthyology & Herpetology 110:* 737–749.

Keehn, J. E., N. C. Nieto, C. R. Tracy, C. M. Gienger, and C. R. Feldman. 2013. Evolution on a desert island: body size divergence between the reptiles of Nevada's Anaho Island and the mainland around Pyramid Lake. *Journal of Zoology 291:* 269–278.

Loc-Barragán, J. A., G. R. Smith, G. A. Woolrich-Piña, and J. A. Lemos-Espinal. 2024. An updated checklist of the amphibians and reptiles of Nayarit, Mexico with conservation status and comparison with adjoining states. *Herpetozoa 37:* 25–42.

Nolasco-Luna, J. R., I. K. Barraza-Soltero, M. A. López-Montes, J. A. Moreno-López, and A. H. Escobedo-Galván. 2022. An updated checklist of the herpetofauna from Isla María Cleofas, Mexico. *Check List 18:* 241–252.

Peck, H. L., H. E. Pringle, H. H. Marshall, I. P. F. Owens, and A. M. Lord. 2014. Experimental evidence of impacts of an invasive parakeet on foraging behavior of native birds. *Behavioral Ecology 25:* 582–590.

Pedroza-Gutiérrez, C. and J. M. Catalán-Romero. 2017. Evolución histórica y ambiental en los procesos de trasformación del lago Chapala. *Ambiente y Desarrollo 21:* 9–25.

Ponce-Campos, P. and A. García Aguayo. 2007. *Aspidoscelis communis*. The IUCN Red List of Threatened Species 2007: e.T64258A12759166. https://dx.doi.org/10.2305/IUCN.UK.2007.RLTS.T64258A12759166.en. Captured

on 02 December 2024.

SEMARNAT (Secretaría de Medio Ambiente y Recursos Naturales) (2010) NORMA Oficial Mexicana NOM-059-SEMARNAT-2010, Protección ambiental-Especies nativas de México de flora y fauna silvestres-Categorías de riesgo y especificaciones para su inclusión, exclusión o cambio-Lista de especies en riesgo. Diario Oficial de la Federación, Ciudad de México. https://dof.gob.mx/nota_detalle_popup.php?codigo=5173091. Captured on 20 September 2024.

Siliceo-Cantero, H. H., J. Benítez-Malvido, and I. Suazo-Ortuño. 2023. Lizard species on three islands off the Mexican Pacific coast: effects of insularity. *Revista Mexicana de Biodiversidad 94:* e944068.

Siliceo-Cantero, H. H., A. García, R. G. Reynolds, G. Pacheco, and B. C. Lister. 2016. Dimorphism and divergence in island and mainland Anoles. *Biological Journal of the Linnean Society 118:* 852–872.

Stejneger, L. 1899 Reptiles of the Tres Marias and Isabel islands. *North American Fauna 14:* 63–71

Van Denburgh, J. 1897. Reptiles from Sonora, Sinaloa and Jalisco, Mexico, with a description of a new species of *Sceloporus*. *Proceedings of the Academy of Natural Sciences of Philadelphia 49:* 460–464.

Williams, E. E. 1995. A computer approach to the comparison and identification of species in difficult taxonomic groups. IV. The morphological characters used in the Anole key described, defined, and illustrated. *Breviora 502:* 15–37.

Wilson, L. D., J. D. Johnson, and V. Mata-Silva. 2013. A conservation reassessment of the amphibians of Mexico based on the EVS measure. Contribution to Special Mexico Issue. *Amphibian and Reptile Conservation 7:* 97–127.

Wilson Rankin, E. E., J. L. Knowlton, D. S. Gruner, D. J. Flaspohler, C. P. Giardina, D. R. Leopold, A. Buckardt, W. C. Pitt, and T. Fukami. 2018. Vertical foraging shifts in Hawaiian forest birds in response to invasive rat removal. *PLoS ONE 13:* e0202869.

Editor: Jaime Bertoluci

Phyllomedusa 24(2):319–325, 2025

ISSN 1519-1397 (print) / ISSN 2316-9079 (online)
doi: http://dx.doi.org/10.11606/issn.2316-9079.v24i2p319-325

Short Communication

Rediscovery of *Dipsas peruana* (Serpentes: Dipsadidae) in Bolivia and extension of its distribution

Oliver Quinteros-Muñoz,[1] Paola De la Quintana,[2,3] Pedro Gómez-Murillo,[1] Rodrigo Aguayo,[4] and Konrad Mebert[3,5]

[1] Museo de Historia Natural Alcide d' Orbigny. Casilla 843, Cochabamba, Bolivia. E-mail: ohlisin@gmail.com, pedrosquamata@gmail.com.

[2] Red de Investigadores en Herpetología. La Paz, Bolivia. E-mail: paola.d.c.1186@gmail.com.

[3] Universidade Estadual de Santa Cruz, Departamento de Ciências Biológicas (PVE). Rodovia Jorge Amado, km 16, Ilhéus, BA, CEP 45662-900, Brazil. E-mail: paola.d.c.1186@gmail.com.

[4] Universidad Mayor de San Simón, Centro de Biodiversidad y Genética. Casilla 538, Cochabamba, Bolivia. E-mail: rodrigoaguayo.v@fcyt.umss.edu.bo.

[5] Institute of Development, Ecology, Conservation and Cooperation. 00144 Rome, Italy; IUCN Viper Specialist Group (committee member), Waldmattstrasse 15, 5242 Birr, Switzerland. E-mail: konradmebert@gmail.com.

Keywords: Dipsadini, New record, Peruvian Snail-Eater, Range extension.

Palabras clave: Ampliación de rango, Dipsadini, Nuevo récord, Serpiente caracolera peruana.

Palavras-chave: Dipsadini, Extensão de área de distribuição, Novo registro, Serpente-comedora-de-caracóis-peruana.

The genus *Dipsas* is one of the most diverse groups of snakes and includes more than 50 species distributed throughout Central and South America. Most of them are arboreal, nocturnal, and specialized in feeding on gastropods (Harvey and Embert 2008, Lima and Prudente 2009, Arteaga *et al.* 2018, Uetz *et al.* 2025). Information on systematics about species of *Dipsas* remains poor, resulting in a lack of understanding of their morphological variation from scales to color pattern (Silva *et al.* 1985, Cadle and Myers 2003, Cadle 2005). In Bolivia, 10 species of the genus *Dipsas* are currently recognized: *D. bucephala* (Shaw, 1802), *D. catesbyi* (Sentzen, 1796), *D. chaparensis* Reynolds and Foster, 1992, *D. cisticeps* (Boettger, 1885), *D. indica* Laurenti, 1768, *D. lavillai* (Scrocchi, Porto and Rey, 1993), *D. pavonine* Schlegel, 1837, *D. peruana* (Boettger, 1898), *D. turgida* (Cope, 1868), and *D. variegata* (Duméril, Bibron and Duméril, 1854) (Gonzáles and Reichle 2003, Aguayo 2009, Arteaga *et al*. 2018, Reichle 2019, Gómez-Murillo *et al*. *in press*). However, very little is known about the biology and distribution of these 10 species, in contrast to their congenerics in other South American countries.

Originally, Boettger (1898) described *Leptognathus peruana* Boettger, 1898 from the

Received 17 September 2024
Accepted 24 January 2025
Distributed December 2025

Santa Ana region, Cuzco, Peru, and Werner (1901, 1909) followed by describing *Leptognathus boettgeri* Werner, 1901, and later added *Leptognathus boliviana* Werner, 1909 (= *Dipsas peruana*) from Beni River, Bolivia. Decades later, Peters (1960) synonymized *L. boliviana* with *L. boettgeri*. Similarly, Peters and Orejas-Miranda (1970) placed *L. boliviana* within *Dipsas boettgeri* and continued to recognize *Dipsas peruana* (*L. peruana)* as a distinct taxon. Harvey and Embert (2008) placed *L. boettgeri* as a synonym of *D. peruana.* Amaral (1929) synonymized *L. praeornata* Werner, 1909, from Venezuela with *Sibynomorphus*. Fernandes *et al*. (2002) synonymized *D. latifasciata* with *D. polylepis*. Harvey and Embert (2008) resurrected the name *D. praeornata* (Werner, 1909) for the Venezuelan coastal range population and relegated *D. latifrontalis* (Boulanger, 1905) to a synonym of *D. peruana*. Arteaga *et al*. (2018) removed *D. palmeri* (Boulanger, 1912) (as well as *D. latifasciata* and *D. latifrontalis*) from the synonymy of *D. peruana* (Uetz *et al*. 2025). Therefore, the specimen (*L. boliviana*) described by Werner in 1909 was the first specimen of *D. peruana* recorded in Bolivia, which was subsequently housed at the Museum für Tierkunde in Dresden, Germany. Although the type specimen was destroyed during World War II, it remained the only documented specimen from Bolivia for many years and served as the reference for all subsequent records of it (Harvey and Embert 2008, Aguayo 2009, Arteaga *et al.* 2018, Reichle 2019). Until this publication, no other specimen attributable to this species could be located in a Bolivian or external collection aside from those deposited by us.

During several field trips between 2016 and 2025, six new specimens of *Dipsas peruana* have been found in Bolivia after more than 100 years since its last observation. All the specimens were captured while active at night between 19:00 and 24:00 h. Four specimens from the Department of Cochabamba (Figures 1A and 2) were collected on an unpaved road adjacent to a mature secondary mountain forest in the Yungas ecoregion, Chaquisacha, Carrasco National Park (17°25'30.73" S, 65°14'5.41" W; 1800 m a.s.l.). Two additional specimens were captured from the Departments of Beni and La Paz. One, a male, was found under a rock on an unpaved road near the Waicani Hill, Coripata, (16°11'47.9" S, 67°53'38.1"

Figure 1. Specimens of *Dipsas peruana*, (**A**) MNHC-R 3082 from Chaquisacha (Carrasco National Park), Cochabamba, Bolivia, and (**B**) CBF 4521 from Coripata, La Paz, Bolivia. Photographs by Oliver Quinteros-Muñoz (A) and James Aparicio (B).

Figure 2. Female specimen (MHNC-R 3082) of *Dipsas peruana* in preservative, from Chaquisacha Carrasco National Park, Cochabamba, Bolivia. (**A**) Dorsal view; (**B**) ventral view; (**C**) dorsal view of the head; (**D**) ventral view of head; (**E**) right view of the head; (**F**) left view of the head. Scale bar (head only) = 10 mm.

W; 2750 m a.s.l.), which is located in the Yungas ecoregion of La Paz (Figure 1B). The other, a female, from the Department of Beni, Municipality of San Borja (14°50'21.8" S, 66°44'25.2" W; 200 m a.s.l.), was collected near a road between the branches of a small tree, interestingly representing the only low elevation record from the Amazon ecoregion. Specimens from Cochabamba were

collected under permit MMAYANMABCCGDF/DGBAP/MEG No. 0053/2019 and deposited in the herpetological collection at the Museo de Historia Natural Alcide d'Orbigny (MHNC-R 3081; MHNC-R 3082; MHNC-R 3142; MHNC-R 3143), Cochabamba, Bolivia. Specimens from Beni and La Paz were deposited in the Colección Boliviana de Fauna (CBF 4352; CBF 4521), La Paz, Bolivia.

All specimens fit the diagnosis of Arteaga *et al.* (2018). *Dipsas peruana* differs from all described species of *Dipsas* by the following combination of characters (Table 1). Scales: (1) 15/15/15 smooth dorsals with moderately enlarged vertebral row; (2) one loreal and one preocular in contact with orbit; (3) 8–9 supralabials with 4–6 or 3–5 contacting orbit; (4) one pair of infralabials in contact behind symphysial; (5) 177–200 ventrals in males, 180–203 in females; (6) 75–127 divided subcaudals in males, 79–105 in females; color pattern: (7) dorsal and ventral ground color brown to dark brown (light brown in juveniles) with 33–43 blackish brown to complete black, white to cream-edged circular to vertically elliptical blotches that are longer than interspaces; head dark brown with dirty cream reticulations and different degrees of whitish edging on labial scales, and a thin (1–3 scales long) white to light grayish brown irregular nuchal collar; dorsal blotches extending marginally onto ventrals and rarely fusing midventrally; (8) 199 mm SVL in males, 610–725 mm in females; (9) 85 mm TL in males, 155–241 mm in females.

The distribution of *D. peruana* includes the Andes Mountains, throughout Venezuela, Colombia, Ecuador, Peru, and Bolivia (Harvey and Embert 2008, Harvey *et al*. 2008, Pazmiño-Otamendi and Rodríguez-Guerra 2019). Wallach (2014: 237) reported the distribution of this species in the Departments of La Paz and Pando in Bolivia, without citing any evidence for the presence of this species in these Departments. Arteaga *et al*. (2018) restricted the distribution of the populations of *D. peruana* to the eastern slopes of the Peruvian and Bolivian Andes south of the Huancabamba Depression at elevations between 1279 and 2671 m a.s.l. These authors mentioned no evidence for this species in Bolivia. Literature data and the new specimens presented herein also allow us to confirm the presence of the species in the Department of

Table 1. Meristic characters of all collected specimens of *Dipsas peruana* from Bolivia.

Characters	MHNC-R 3081 (Female)	MHNC-R 3082 (Female)	CBF-4352 (Female)	CBF-4521 (Male)	MHNC-R 3142 (Female)	MHNC-R 3143 (Male)
SVL (mm)	368	568			795	715
TL (mm)	500	780			1067	99
Maxillary teeth	12	14				
Dorsals	15/15/15	15/15/15	15/15/15	15/15/15	15/15/15	15/15/15
Ventrals	203	201	200	199	197	204
Subcaudals	106	111	101	115	94	99
Preoculars	1/1	1/1	1/1	1/1	1/1	2/2
Postoculars	3/3	2/2	2/2	2/2	2/2	3/2
Temporals	2+3/2+1+2	2+3/2+3	2+3/1+3	2+3/2+3	2+3/1+3	2+3/2+3
Supralabials	9/10	9/8	9/9	9/10	9/9	8/8
Infralabials	13/13	12/13	13/12	12/12	12/12	10/10
Anal Plate	Undivided	Undivided	Undivided	Undivided	Undivided	Undivided

Beni, Bolivia, with a new low altitude record of 200 m a.s.l. Furthermore, our records extend the geographic distribution of *D. peruana* to the Departments of Cochabamba and La Paz, respectively (Figure 3).

In Bolivia, *Dipsas peruana* appears to be a rare species, known only from the holotype of *Leptognathus boliviana* (Harvey and Embert 2008). Although *D. peruana* has consistently been cited as a species present in Bolivia, no specimens have been deposited in any Bolivian collection to date. This report represents the first formal record of the species after more than 100 years since this species was reported for the first time in Bolivia. In addition, this record extends the distribution of the species by 640 km in a southwest direction from Peru (Puno) to Bolivia. The record from the Cochabamba Department is the southernmost record of *D. peruana* in South America (Figure 3).

Dipsas peruana was classified as Least Concern (LC) in the IUCN Red List of Threatened Species by Caicedo *et al.* (2016), but an update is necessary because its categorization considered the wide distribution proposed by Harvey and Embert (2008). Nonetheless, the

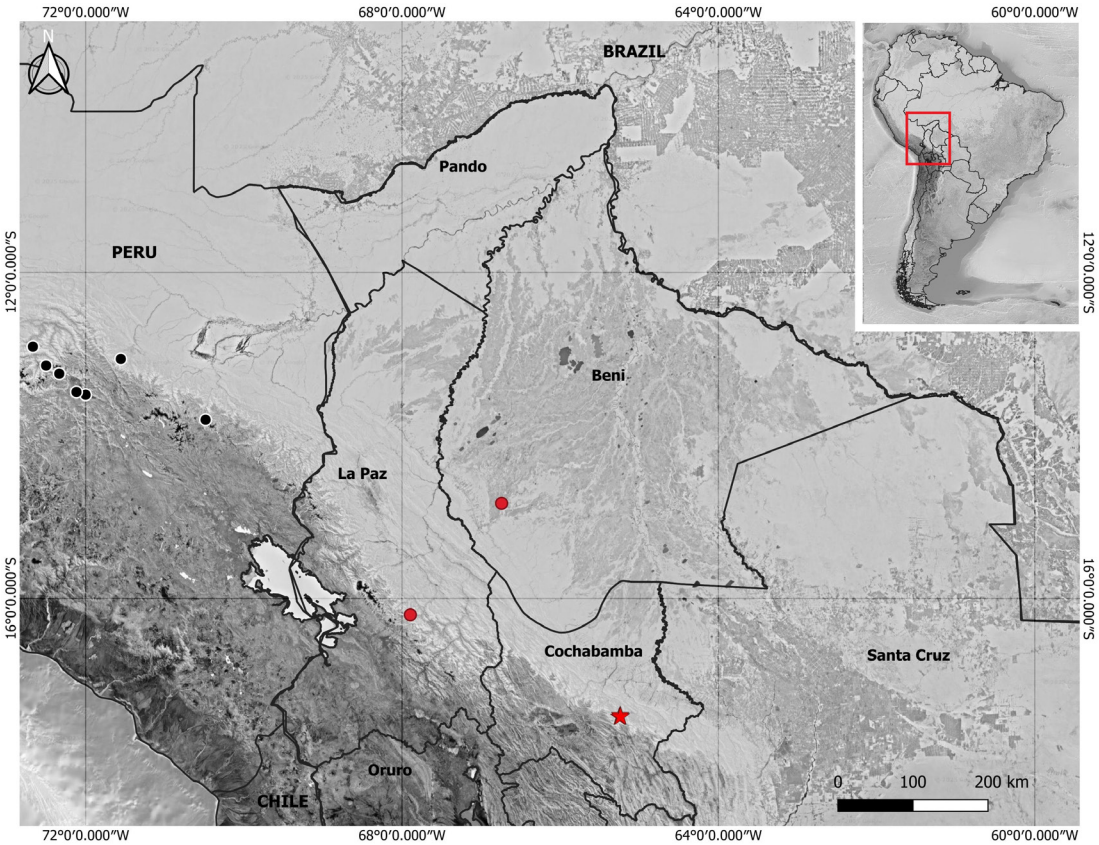

Figure 3. Geographic distribution of *Dipsas peruana* in Bolivia. Red star corresponds to the southernmost record of the species in South America (Cochabamba, Bolivia); red circles correspond to records in the Departments of Beni and La Paz. Black circles represent records of *D. peruana* in Peru reported by Harvey and Embert (2008).

presence of *Dipsas peruana* in Bolivia is confirmed. We suggest that further morphological and molecular evidence is necessary to better understand and clarify its relationship with other *Dipsas* species and evaluate its geographic variation throughout its entire distribution.

Acknowledgments.—The authors thank J. Aparicio (†) and M. Ocampo for sharing their information, Mirco Solé for their comments on the manuscript, Janalee Caldwell for English review. Anonymous reviewers critically read and commented on the manuscript. We thank the Carrasco National Park and its rangers for their support and interest in the research and conservation of our biological wealth.

References

Aguayo, R. 2009. *Reptiles de Bolivia. Edición Bolivia Ecológica 53.* Santa Cruz. Centro de Ecología y Difusión, Fundación Simón I. Patiño. 32 pp.

Amaral, A. 1929. Estudos sobre ophídios neotrópicos. XVIII – Lista remissiva dos ophídeos da região neotrópica. *Memórias do Instituto Butantan 4:* 129–271.

Arteaga, A., D. Salazar-Valenzuela, K. Mebert, N. Peñafiel, G. Aguiar, J. C. Sánchez-Nivicela, R. A. Pyron, T. J. Colston, D. F. Cisneros-Heredia, M. H. Yánez-Muñoz, P. J. Venegas, J. M. Guayasamin, and O. Torres-Carvajal. 2018. Systematics of South American snail-eating snakes (Serpentes, Dipsadini), with the description of five new species from Ecuador and Peru. *ZooKeys 766:* 79–147.

Boettger, O. 1898. *Katalog der Reptilien-Sammlung im Museum der Senckenbergischen Naturforschenden Gesellschaft in Frankfurt am Main. I. Teil (Rhynchocephalen, Schildkröten, Krokodile, Eidechsen, Chamäleons)*. Frankfurt. Druck von Gebrüder Knauer. 151 pp.

Cadle, J. E. and C. W. Myers. 2003. Systematics of snakes referred to *Dipsas variegata* in Panama and western South America, with revalidation of two species and notes on defensive behaviors in the Dipsadini (Colubridae). *American Museum Novitates 3409:* 1–47.

Cadle, J. E. 2005. Systematics of snakes of the *Dipsas oreas* complex (Colubridae: Dipsadinae) in western Ecuador and Peru, with revalidation of *D. elegans* (Boulenger) and *D. ellipsifera* (Boulenger). *Bulletin of the Museum of Comparative Zoology 158:* 67–136.

Caicedo, J., M. Calderón, M. Harvey, A. Ines-Hladki, M. Ramírez-Pinilla, J. Renjifo, G. Rivas, N. Urbina, D. F. Cisneros-Heredia, G. Gagliardi, and A. Catenazzi. 2016. *Dipsas peruana.* The IUCN Red List of Threatened Species 2016: e.T176796A44949677. Electronic Database accessible at https://dx.doi.org/10.2305/IUCN.UK.2016-1.RLTS.T176796A44949677.en. Captured on 05 May 2025.

Fernandes, R., D. S. Fernandes, and P. Passos. 2002. *Leptognathus latifasciatus* Boulanger, 1913, a Junior synonym of *Dispas polylepis* (Boulanger, 1912) (Serpentes, Colubridae). *Boletim do Museu Nacional, Nova Série Zoologia 493:* 1–7.

Gómez-Murillo, P., O. Quinteros-Muñoz, E. Domic, T. Camacho-Badani, R. Rojas-Estrada, I. Arellano-Martín, R. Aguayo, L. Gonzales, L.F. Esqueda, C. Urdiales, D.E. Lizarro, E. Cortez, M. Ocampo, S. Reichle, O. Jiménez-Robles, R. Carpio, O.M. Entiauspe-Neto, L.R. Rivas, A. Llobet, A. B. Miranda-Calle, A. J. Aguilar-Kirigin, and I. De la Riva. *Cuadernos de Herpetología* (in press).

Gonzales, L. and S. Reichle. 2003. Anexo 3. Lista de reptiles presentes en Bolivia. Pp. 586–589 in P.L. Ibisch and G. Mérida (eds.), *Biodiversidad: La Riqueza de Bolivia, Estado de Conocimiento y Conservación.* Santa Cruz de la Sierra. Editorial FAN.

Harvey, M. B. and D. Embert. 2008. Review of Bolivian *Dipsas* (Serpentes: Colubridae), with comments on other South American species. *Herpetological Monographs 22:* 54–105.

Harvey, M. B., G. R. Fuenmayor, J. R. C. Portilla, and J. V. Rueda-Almonacid. 2008. Systematics of the enigmatic dipsadine snake *Tropidodipsas perijanensis* Alemán (Serpentes: Colubridae) and review of morphological characters of Dipsadini. *Herpetological Monographs 22:* 106–132.

Lima, A. C. and A. L. C. Prudente. 2009. Morphological variation and systematics of *Dipsas catesbyi* (Sentzen, 1796) and *Dipsas pavonina* Schlegel, 1837 (Serpentes: Dipsadinae). *Zootaxa 2203:* 31–48.

Pazmiño-Otamendi, G. and A. Rodríguez-Guerra. 2019. *Dipsas peruana in* Torres-Carvajal, O., G. Pazmiño-Otamendi, and D. Salazar-Valenzuela (eds.), Reptiles del Ecuador. Museo de Zoología, Pontificia Universidad Católica del Ecuador. Version 2019.0. Electronic Database accessible at https://bioweb.bio/faunaweb/reptiliaweb/FichaEspecie/Dipsas%20peruana. Captured on 25 June 2020.

Peters, J. A. 1960. The snakes of the subfamily Dipsadinae. *Miscellaneous Publications Museum of Zoology,*

University of Michigan 114: 1–224.

Peters, J. A. and B. Orejas-Miranda. 1970. *Catalogue of the Neotropical Squamata. Part I. Snakes*. Washington D.C. Smithsonian Institution Press. 347 pp.

Reichle, S. 2019. Serpientes de Bolivia. Centro de Ecología y Difusión Simón I. Patiño. *Revista Bolivia Ecológica 87:* 1–36.

Silva, J. L, J. Valdez, and J. Ojasti. 1985. Algunos aspectos de una comunidad de ofidios del norte de Venezuela. *Biotropica 17:* 112–125.

Uetz, P. P, Freed, and J. Hošek. 2025. The Reptile Database. Electronic Database accessible at http://www.reptile-database.org. Captured on 19 June 2020.

Wallach, V., K. L. Williams, and J. Boundy. 2014. *Snakes of the World: A Catalogue of Living and Extinct Species*. Boca Raton. Taylor and Francis, CRC Press. 1237 pp.

Werner, F. 1901. Reptilien und Batrachier aus Peru and Bolivia. *Abhandlungen Berichte Ko¨ niglichen Zoologischen und Anthropolisch-Ethnographischen Museums zu Dresden 9:* 1–14.

Werner, F. 1909. Über neue oder seltene Reptilien des Naturhistorischen Museums in Hamburg. *Mitteilungen aus dem Naturhistorischen Museum in Hamburg 26:* 206–244.

Editor: Francisco L. Franco

Phyllomedusa 24(2):327–331, 2025

ISSN 1519-1397 (print) / ISSN 2316-9079 (online)
doi: http://dx.doi.org/10.11606/issn.2316-9079.v24i2p327-331

Short Communication

Contribution to the natural history of *Ninia sebae* (Serpentes: Dipsadidae) from an urban area in Veracruz, Mexico

Arleth Reynoso-Martínez[1] and Víctor Vásquez-Cruz[2]

[1] Independent researcher. Córdoba, Veracruz, Mexico.

[2] Universidad Veracruzana, Facultad de Ciencias Biológicas y Agropecuarias, Área de Colecciones Zoológicas. Camino Viejo Peñuela-Amatlán de los Reye, s/n. CP 94950, Amatlán de los Reyes, Veracruz, Mexico. E-mail: victorbiolvc@gmail.com.

Keywords: Ecological niche, *Indotyphlops braminus,* Predator-prey interaction, Melanism, Urban herpetofauna.

Palabras clave: Herpetofauna urbana, *Indotyphlops braminus,* Interacción depredador-presa, Melanismo, Nicho ecológico.

Palavras-chave: Herpetofauna urbana, *Indotyphlops braminus,* Interação predador-presa, Melanismo, Nicho ecológico.

The redback coffee snake, *Ninia sebae* (Duméril, Bibron, and Duméril, 1854) is widely distributed from central Veracruz on the Atlantic slope and from southern Oaxaca on the Pacific side, extending southward to Costa Rica (Heimes 2016). It can be found in rainforests, savannas, cloud forests, and even marginally in pine-oak forests (Heimes 2016). It also inhabits peri-urban and urbanized areas (Köhler *et al.* 2016), occurring in small green islands within cities such as gardens, parks, and vacant lots (V. Vásquez-Cruz pers. observ.). It seeks refuge under any natural cover, such as logs, rocks, and leaf litter, as well as under artificial cover, including rubble, tarps, tires, and plastic (Pérez-Higareda *et al*. 2007). *Ninia sebae* exhibits a Batesian mimetic pattern with bright colors (Hinman *et al*. 1997) that resemble specimens of coral snakes of the genus *Micrurus* (De la Torre-Loranca *et al*. 2006). The coffee-colored snake is nocturnal and is often observed at night on roads after heavy rains. Reproduction occurs during the rainy season (July–September), when females lay 1 to 4 eggs (Burger and Werler 1954, Álvarez del Toro 1982). The incubation period is approximately 75 to 79 days, and the hatchlings measure between 85 and 135 mm in total length at birth (Greene 1975).

In the scientific literature, a few cases of which *N. sebae* are included in trophic chains, being reported as prey of tarantulas (*Schizopelma* sp.; Aguilar López *et al*. 2014), birds [*Quiscalus mexicanus* (Gmelin, 1788) (Vásquez-Cruz 2019)], coral snakes [*Micrurus diastema* (Duméril, Bibron, and Duméril, 1854) and *M. nigrocinctus* (Girard, 1854) (Savage 2002, West et al. 2019)], and false coral snakes [*Erythrolamprus mimus* (Cope, 1868)

Received 08 August 2025
Accepted 06 October 2025
Distributed December 2025

and *Lampropeltis polyzona* Cope, 1860 (Schmidt 1932, Villegas-Castillo and Vásquez-Cruz 2024)]. As a predator, it specializes in invertebrates such as earthworms, leeches, slugs, and snails (Greene 1975, Seib 1985), and arthropods (Köhler *et al*. 2016). Landy *et al*. (1966) reported a caecilian in the stomach of a specimen from Chiapas, which remains the only known vertebrate prey for *N. sebae*.

In this study, we document two relevant observations that contribute to the understanding of the trophic and adaptive ecology of *N. sebae* in urban environments, and we briefly discuss their possible relationship to the species' adaptation to anthropogenic settings. These records were obtained near train tracks, close to the old railway station in the municipality of Fortín de las Flores, in the central-western region of the state of Veracruz, Mexico (18°54'06.1" N, 97°00' 00.4" W; WGS 84; 1010 m a.s.l.).

On 22 January 2025, around 17:00 h, we found a "dead on road" (DOR) adult specimen of *N. sebae*, which had part of its stomach exposed due to crushing (Figure 1A). From the stomach, we extracted an individual (apparently subadult) of the Brahminy blindsnake, *Indotyphlops braminus* (Daudin, 1803) (Figure 1B-C). *Indotyphlops*

Figure 1. (**A**) Dorsal view of the DOR specimen of *Ninia sebae* with its stomach exposed. (**B**) *Ninia sebae* with its prey. (**C**) The specimen of *Indotyphlops braminus* found in the stomach of *Ninia sebae*. Photos: VVC.

Figure 2. (**A**) Dorsal view of *Ninia sebae* with melanism of. (**B**) Dorsal view of the typical coloration of *Ninia sebae*. Photos: VVC.

braminus was recognized by its ocular scale separated from the lip by a supralabial and 20 scale rows around the body (Canseco-Márquez and Gutiérrez-Mayén 2010, Heimes 2016). This specimen was deposited in the vertebrate collection of the Facultad de Ciencias Biológicas y Agropecuarias at Universidad Veracruzana (collection code: FCBA-CH-503).

On 13 July 2025, around 11:00 h, we found approximately 12 individuals of *N. sebae*; one of them exhibited a noticeably dark coloration on its body (Figure 2A). This adult individual had a black head; with a faint collar of dark yellow tones; the body had dark red and black dorsal scales. In contrast, the typical coloration of *N. sebae* (Figure 2B) shows a yellow band around the back of the head and the beginning of the dorsal scales, sometimes extending to the labial scales; the body features intense red scales that may be immaculate, blotched, or have small black bands occasionally bordered by yellow hues (Heimes 2016). A photovoucher was deposited in the digital herpetological collection of the Facultad de Ciencias Biológicas y Agropecuarias at Universidad Veracruzana (collection code: FCBA-CHD-111).

Habitat loss and modification caused by the expansion of urban sprawl has not only resulted in the local extinction of species but also in the adaptation of some individuals, possibly leading to changes in their behavior, life cycles, or diet (e.g. Caspi *et al*. 2022). Previously, Ariano-Sánchez (2024) reported the first case of melanism in *N. sebae* and hypothesized that the survival of cryptic individuals (such as melanistic ones) may be present—and even favored—in populations where the aposematic venomous species, *Micrurus diastema* in this case, has been extirpated from the study area. Our observations may be consistent with the hypothesis proposed

by Ariano-Sánchez (2024), which suggests that in urban environments without *Micrurus,* cryptic individuals could have a selective advantage. It is also possible that cryptic individuals have a camouflage advantage against visual predators such as birds and domestic species like cats.

Additional hypotheses have been proposed to explain melanism in snakes. The thermal melanism hypothesis—although recent evidence suggests that this mechanism has limited support—proposes that darker individuals gain an advantage by warming more efficiently in cold environments (Sahlean *et al*. 2025). Another alternative hypothesis is Gloger's rule, which predicts that melanistic forms are more common in humid regions (Delhey 2019), with precipitation recently identified as a significant predictor of melanism prevalence (Sahlean *et al*. 2025). Neutral evolutionary forces such as phenotypic plasticity or genetic drift could also contribute to the occurrence of melanistic individuals. While our observation is consistent with the hypothesis proposed by Ariano-Sánchez (2024), multiple ecological and evolutionary mechanisms could influence the persistence of melanistic morphs in urban landscapes.

Regarding diet, vertebrate consumption appears to be unusual in *N. sebae;* nevertheless, the caecilians prey (Dermophiidae) and the blindsnake *I. braminus* share certain similarities with a common prey of *N. sebae* (earthworms), which could explain these occurrences as cases of mistaken prey identity under conditions of limited foraging or reduced availability of invertebrates. It is worth noting that *I. braminus* is an introduced species in Mexico, and recent reports indicate an increase in populations of this species in the country. All these reports were made in urban areas (e.g., Vásquez-Cruz *et al*. 2021, Vásquez-Cruz and Vásquez-Espinoza 2025), suggesting that *I. braminus* may represent a food resource for *N. sebae* in anthropogenic environments. Although this idea requires additional study, it could constitute an example of a novel interaction facilitated by urbanization.

Other cases of predation on *I. braminus* have been documented and have shown that the predator has difficulty digesting this snake; it has even been reported that *I. braminus* can be expelled through the predator's cloaca (O'Shea *et al*. 2013, Zlotnik *et al*. 2017, Yang and Mori 2018). The Loggerhead shrike, *Lanius ludovicianus* Linnaeus, 1766, also preys on *I. braminus*, which may be impaled for up to 85 days, the longest retention time reported, similar to that observed with hard-bodied insects (Zerega-Contreras and Sánchez-Velázquez 2024). Yang and Mori (2018) hypothesized that *I. braminus* may have specialized scaly structures that delay digestion by predators, giving it time to escape the predator's digestive system. In contrast, our observation suggests partial digestion of *I. braminus* by *N. sebae;* however, we cannot rule out the possibility that the apparent "damage" to the prey was caused by the predator. These observations highlight the need to document cases of predation on *I. braminus* and its potential role in the food chain outside of its distribution area.

Acknowledgments.—Thanks to Luis Canseco Márquez for verifying the identification of the snakes.

References

Aguilar-López, J. L., E. Pineda, and R. Luría-Manzano. 2014. Depredación de tres especies de herpetozoos por arañas en la región tropical de Veracruz, México. *Revista Mexicana de Biodiversidad 85:* 965–968.

Álvarez del Toro, M. 1982. *Los Reptiles de Chiapas.* 3rd ed. Tuxtla Gutiérrez, Chiapas, Mexico. Instituto de Historia Natural. 248 pp.

Ariano-Sánchez, D. 2024. Primer registro de melanismo parcial en la serpiente de espalda roja del café *Ninia sebae* (Squamata: Dipsadidae). *Revista Latinoamericana de Herpetología 7:* 88–89.

Burger, W. L. and J. E. Werler. 1954. The subspecies of the ring-necked coffee snake, *Ninia diademata*, and a short biological and taxonomic account of the genus. *University of Kansas Science Bulletin 36:* 643–672.

Canseco-Márquez, M. L. and M. G. Gutiérrez-Mayén. 2010. *Anfibios y Reptiles del Valle de Tehuacán-Cuicatlán.*

Primera edición. CONABIO, Fundación para la Reserva de la Biosfera Cuicatlán A.C. y Benemérita Universidad Autónoma de Puebla, México. 302 pp.

Caspi, T., J. R. Johnson, M. R. Lambert, C. J. Schell, and A. Sih. 2022. Behavioral plasticity can facilitate evolution in urban environments. *Trends in Ecology and Evolution 37:* 1092–1103.

De la Torre-Loranca, M. A., G. Aguirre-León, and M. A. López-Luna. 2006. Coralillos verdaderos (Serpentes: Elapidae) y coralillos falsos (Serpentes: Colubridae) de Veracruz, México. *Acta Zoológica Mexicana 22:* 11–22.

Delhey, K. 2019. A review of Gloger's rule, an ecogeographical rule of colour: Definitions, interpretations and evidence. *Biological Reviews 94:* 1294–1316.

Greene, H. W. 1975. Ecological observations on the red coffee snake, *Ninia sebae*, in southern Veracruz, Mexico. *American Midland Naturalist 93:* 478–484.

Heimes, P. 2016. *Herpetofauna Mexicana. Vol. 1. Snakes of Mexico*. Frankfurt am Main, Germany. Edition Chimaira. 572 pp.

Hinman, K. E., H. L. Throop, K. L. Adams, A. J. Dake, K. K. McLauchlan, and M. J. McKone. 1997. Predation by free-ranging birds on partial coral snake mimics: the importance of ring width and color. *Evolution 51:* 1011–1014.

Köhler, G., J. R. Cedeño-Vázquez, M. Spaeth, and P. M. Beutelspacher-García. 2016. The Chetumal Snake census: generating biological data from road-killed snakes. Part 3. *Leptodeira frenata*, *Ninia sebae*. *Mesoamerican Herpetology 3:* 930–947.

Landy, M. J., D. A. Langebartel, E. O. Moll, and H. M. Smith. 1966. A collection of snakes from Volcán Tacaná, Chiapas, Mexico. *Journal of the Ohio Herpetological Society 5:* 93–101.

O'Shea, M., A. Kathriner, S. Mecke, C. Sanchez, and H. Kaiser. 2013. 'Fantastic Voyage': a live blindsnake (*Ramphotyphlops braminus*) journeys through the gastrointestinal system of a toad (*Duttaphrynus melanostictus*). *Herpetology Notes 6:* 467–470.

Pérez-Higareda, G., M. A. López-Luna, and H. M. Smith. 2007. *Serpientes de la Región de Los Tuxtlas, Veracruz, México. Guía de Identificación Ilustrada*. México D.F. Universidad Nacional Autónoma de México. 189 pp.

Sahlean, T. C., R. A. Martin, P. Spaseni, I. Gherghel, and A. Strugariu. 2025. Melanism in polymorphic terrestrial snakes: A meta-analysis and systematic review. *Journal of Biogeography 52:* 27–41.

Savage, J. M. 2002. *The Amphibians and Reptiles of Costa Rica. A Herpetofauna Between Two Continents, Between Two Seas*. Chicago. The University of Chicago Press. 934 pp.

Schmidt, K. P. 1932. Stomach contents of some American coral snakes, with the description of a new species of *Geophis. Copeia 1932:* 6–9.

Seib, R. L. 1985. *Feeding Ecology and Organization of Neotropical Snake Faunas*. Unpubl. Ph.D. Dissertation. University of California, Berkeley. 245 pp.

Vásquez-Cruz, V. 2019. *Ninia sebae*. (Coffee Snake). Predation. *Herpetological Review 50:* 806.

Vásquez-Cruz, V. and V. Vásquez-Espinoza. 2025. *Virgothyphlops braminus*. Geographic Distribution. *Herpetological Review 55:* 221.

Vásquez-Cruz, V., A. Reynoso-Martínez, A. Fuentes-Moreno, E. M. Pérez-Gámez, A. Kelly-Hernández, S. M. Rovito, and J. L. Castillo-Juárez. 2021. Nuevos registros de la serpiente introducida *Indotyphlops braminus* (Squamata: Typhlopidae) en el estado de Veracruz, México. *Revista Latinoamericana de Herpetología 4:* 192–196.

Villegas-Castillo, J. and V. Vásquez-Cruz. 2024. False coral snake versus false coral snake in Veracruz, Mexico: first record of *Ninia sebae* (Squamata: Colubridae) as prey of *Lampropeltis polyzona* (Squamata: Colubridae). *Bulletin of the Chicago Herpetological Society 59:* 102–103.

West, T. R., T. D. Schramer, Y. Kalki, and D. B. Wylie. 2019. Dietary notes on the variable coral snake, *M. diastema* (Duméril, Bibron, and Duméril, 1854). *Bulletin of the Chicago Herpetological Society 54:* 4–8.

Yang, C. and A. Mori. 2018. *Indotyphlops braminus* (Brahminy Blindsnake) and *Dinodon rufozonatum* (= *Lycodon rufozonatus*) (Red-banded Snake). Predation and Diet. *Herpetological Review 49:* 549.

Zerega-Contreras, M. and O. A. Sánchez-Velázquez. 2024. Nuevo registro de depredación de especies exóticas por el verdugo americano (*Lanius ludovicianus*) en México. *Huitzil 25:* e-675.

Zlotnik, S., B. C. Leavell, and J. H. Peniston. 2017. *Indotyphlops braminus* (Brahminy Blind Snake) Predation. *Herpetological Review 48:* 675.

Editor: Jimena Fernández

Phyllomedusa 24(2):333–337, 2025

ISSN 1519-1397 (print) / ISSN 2316-9079 (online)
doi: http://dx.doi.org/10.11606/issn.2316-9079.v24i2p333-337

Short Communication

First record of dicephalism in *Epicrates cenchria* (Serpentes: Boidae) from Brazil

Maisa Jampauli Bernardes,[1,2] Alícia Giolo Hippólito,[2] Alexandre Luiz da Costa Bicudo,[1] Cláudia Cristina da Costa Ladeira,[2] and Lígia Souza Lima Silveira da Mota[1]

[1] Universidade Estadual Paulista (UNESP), Faculdade de Medicina Veterinária e Zootecnia, Programa de Pós-graduação em Animais Selvagens. Rua Prof. Doutor Walter Mauricio Correa s/n, 18618-681, Botucatu, SP, Brazil. E-mail: pgselvagens.fmvz@unesp.br

[2] Parque Zoológico Municipal de Bauru. Rodovia Comandante João Ribeiro de Barros (SP-225), km 232, 17035-245, Bauru, SP, Brazil. E-mail: zoologicodebauru@gmail.com

Keywords: Bicephalic snake, Congenital anomalies, Herpetology, Teratology, Vertebrate zoology.

Palavras-chave: Anomalias congênitas, Herpetologia, Serpente bicefálica, Teratologia, Zoologia de vertebrados.

Although the factors responsible for malformations in wild animals are still poorly understood, the embryonic development of most animals comprises critical periods during which the embryo is more sensitive to harmful influences. Each organ or system has its own critical period, which varies among species. Significant interference from exogenous forces during these stages can compromise proper embryonic formation, resulting in relevant morphological alterations (Haschek *et al.* 2010).

Dicephalism, also referred to as axial bifurcation or bicephaly, is the most frequently reported malformation in snakes, characterized by total or partial duplication of the head. It is a rare condition (Wallach 2007), with an estimated occurrence of 1:100,000 (Belluomini 1959), although more recent studies indicate a higher prevalence, around 73:100,000 (Sant'Anna *et al.* 2013). The condition has been described in several snake families, including viperids (Belluomini *et al.* 1977, Andrade and Abe 1992, Sant'Anna *et al.* 2013, Esqueda *et al.* 2016), colubrids (Prado 1943, Albuquerque *et al.* 2013) and boids (Cunha 1968, Albuquerque *et al.* 2010).

This study reports the first case of dicephalism in *Epicrates cenchria* (Linnaeus, 1758) (Serpentes: Boidae) born under human care, with a description of its external morphological characteristics, internal anatomy, birth history, and biological implications. Dicephalism in the genus *Epicrates* is not unprecedented, as Wallach (2018) documented previous occurrences.

Epicrates cenchria, commonly known as the rainbow boa, red boa, or salamanta, belongs to the family Boidae, is viviparous, and produces litters of 8 to 15 offspring per gestation. It is a non-venomous snake that subdues its prey by constriction. Its diet is broad, including mammals,

Received 28 August 2025
Accepted 02 October 2025
Distributed December 2025

birds, bird eggs, and lizards. It exhibits both diurnal and nocturnal activity. Adult individuals can reach approximately 1.5 m in length (Vanzolini *et al.* 1980). The species is endemic to the Neotropical region, occurring in forest formations of the Amazon Basin in Colombia, Ecuador, Peru, Bolivia, Venezuela, Guyana, Suriname, French Guiana, and Brazil. A disjunct population occurs in the Atlantic Forest of Brazil, from the state of Alagoas to Rio de Janeiro (Passos and Fernandes 2008).

The animal was born in 2023 from the mating of two individuals of the same species that had been kept at the Bauru Municipal Zoo (São Paulo state, Brazil) since 2019. The litter consisted of nine offspring, with only one exhibiting malformation. The parents originated from the illegal wildlife trade and, therefore, had no known genetic history. They were housed in a terrarium with controlled temperature and humidity. After birth, the offspring were transferred to individual terrariums.

Regarding external morphology, the dicephalic specimen exhibited bifurcation of the axial column in the cervical region, with two necks and two independent skulls arranged laterally. The left head was slightly larger and more aligned with the body axis. Coloration was similar to the characteristic pattern of the species.

During the observation period, the left head was consistently dominant over the right. Both heads ingested water and food (neonatal mice), but only the left performed constriction, while the right had greater difficulty swallowing. We observed feeding competition, which required intervention with physical barriers. The dominant head typically controlled locomotion; however, the right head occasionally assumed control when the left remained inactive. During ecdysis, we recorded skin retention at the bifurcation site, which required manual removal of the retained skin.

The specimen survived for eight months. After death, we radiographed and dissected the animal. At necropsy, it had a body mass of 35 g and a total length of 51 cm. The bifurcation began 5.5 cm from the cephalic extremity.

Radiographs and dissections revealed duplication of the tracheae, functional and independent hearts, livers, gallbladders, spleens, pancreases, and stomachs. The systems merged at the initial portion of the small intestine (Figure 1). The individual also had two lungs of similar extension and two kidneys.

Among the classification systems for duplications in reptiles, the one proposed by Nakamura (1938) stands out and is widely adopted in the specialized literature. According to this classification, the specimen is categorized as a teratodymus derodymus, characterized by bifurcation of the vertebral column in the cervical region, resulting in the presence of two heads. The organ duplication observed in this case is consistent with other reports in snakes of the family Boidae (Albuquerque *et al.* 2010).

According to Nakamura (1938), in snakes, duplication of the axial skeleton is restricted to the anterior portion of the body. In the most common cases of teratodymus derodymus, the bifurcation occurs in the cervical region, forming two distinct heads, as observed in the present study.

In addition to Nakamura's (1938) system, Smith and Pérez-Higareda (1991) proposed a classification comprising seven categories of axial bifurcations. Within this system, the present case is classified as proarchodichotomous, characterized by individuals with two heads, two elongated necks, and a single body.

Cases of dicephalism in snakes reported in the literature show considerable variability in the degree of duplication of internal structures. Nakamura (1938) described four teratodymus derodymus with a single functional heart but varying degrees of duplication of digestive system organs. Albuquerque *et al.* (2013) reported a dicephalic specimen of *Philodryas patagoniensis* (Girard, 1858) with duplication restricted to the esophagus and trachea, while the other organs remained identical in number and position. In a study with *Eunectes notaeus* Cope, 1862, Albuquerque *et al.* (2010) observed

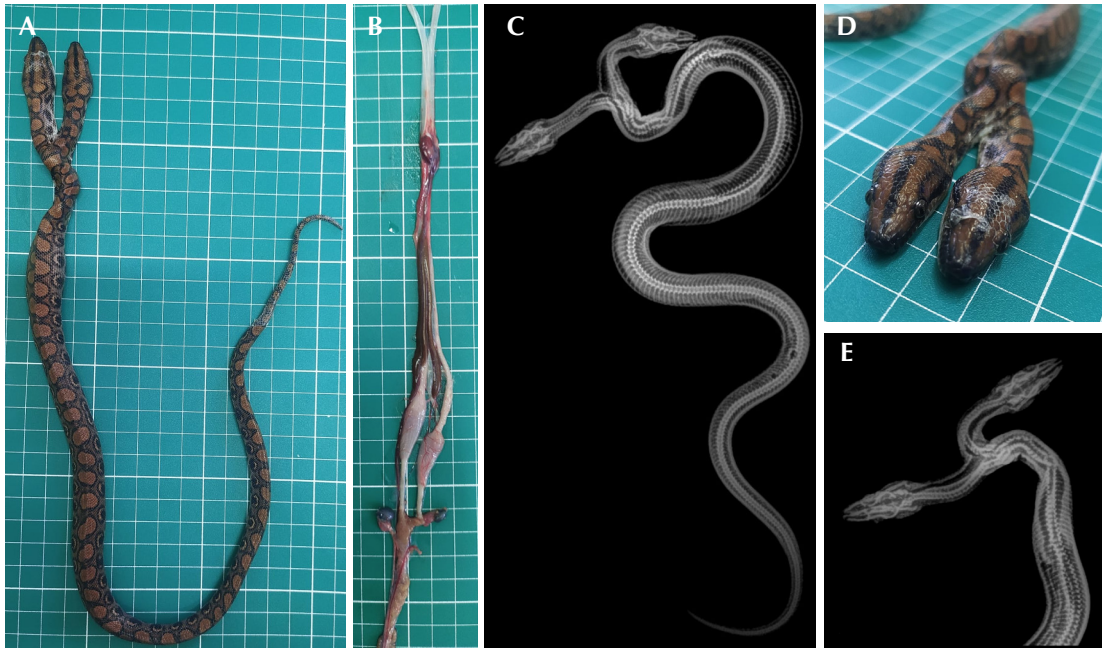

Figure 1. Morphological and anatomical aspects of a dicephalic *Epicrates cenchria*. (**A**) Dorsal view of the entire body of the specimen, showing cephalic duplication. (**B**) Dissection and arrangement of the organs, showing duplication of internal structures. (**C**) Dorsoventral radiograph showing bifurcation of the vertebral column in the cervical region. (**D**) Frontal view detail of the two heads. (**E**) Dorsoventral radiograph of the cephalic region, highlighting the separation of the skulls and cervical vertebrae.

duplication of the heart, lung, liver, and stomach. Cunha (1968) described a case of *Boa constrictor* Linnaeus, 1758 in which the individual on the right side had all vital organs complete, while the one on the left was anatomically and physiologically incomplete, and was dependent on the other to survive. These reports, together with the present case, highlight significant morphological heterogeneity among dicephalic individuals, with no clearly defined pattern of internal duplication.

Functional dominance of one head, as observed in this study, was also described by Cunha (1968) and Wallach (2007). According to these authors, dominance influences both locomotion and feeding behavior. In the case reported here, the left head showed greater activity, performing constriction and guiding body movements, which possibly contributed to the animal's physiological maintenance during its survival.

Dicephalism in snakes is predominantly observed in neonates or very young individuals (Nakamura 1938, Cunha 1968, Albuquerque *et al.* 2010) which are commonly short-lived (Cunha 1968, Wallach 2018). This condition can impair essential functions, such as predation and predator avoidance, leading to premature death by starvation or predation in natural environments. Under human care, however, survival can be prolonged due to assisted management, although most affected individuals still haave a short life expectancy (Wallach 2018).

According to Wallach (2007), dicephalic individuals with heads of similar size and development tend to survive longer. This condition is presumed to be associated with the proper formation of muscular, visceral, and neurological connections between the duplicated regions and the rest of the body. In the case described, the dominance of one head, combined with the absence of severe motor dysfunctions, may have favored the specimen's relatively prolonged survival.

Several etiological factors have been proposed for the occurrence of dicephalism in snakes: (1) incomplete division of a single embryo; (2) partial fusion of two embryos; (3) exposure to extreme temperatures during incubation or gestation; (4) regeneration following embryonic injury; (5) anoxia during embryonic development; (6) toxic effects of metabolic secretions associated with prolonged retention in the oviduct; (7) inbreeding in populations with reduced genetic diversity; (8) interspecific hybridization; (9) environmental pollution; (10) exposure to toxic substances in captivity; and (11) ionizing radiation (Wallach 2007).

Although it was not possible to determine the exact cause of the malformation in this case, several hypotheses can be considered. According to Wallach (2007), significant thermal changes during gestation are among the factors most frequently associated with dicephalism. The breeders involved were kept under controlled environmental conditions, making this hypothesis less likely—although not entirely dismissible. Developmental disturbances during embryogenesis are also potential causes of this anomaly. Nevertheless, the absence of specific data on the gestation of the individual prevents a conclusive assessment.

Both parents originated from the illegal wildlife trade, having been rescued and later kept at the Bauru Municipal Zoo. Given the lack of prior genetic information, it was not possible to determine the degree of relatedness between the progenitors. It is noteworthy, however, that clandestine breeding facilities often neglect proper genetic management practices, thereby promoting inbreeding to maximize offspring production for illegal trade.

Inbreeding has been identified as a factor associated with increased incidence of congenital anomalies, including dicephalism, in snakes bred in captivity. The rise in reports of axial bifurcation in these animals over the past decade may be primarily related to genetic depression resulting from inbreeding between individuals bred in captivity as a consequence of repeated crosses between siblings or between parents and offspring (Wallach 2018). This association is supported by studies such as that of Federsoni Júnior (1979), which identified a high occurrence of teratogenesis and mortality in inbred litters of *Bothrops atrox* (Linnaeus, 1758).

Studies have shown that organochlorine environmental contaminants, such as polychlorinated biphenyls, have bioaccumulative potential and can cross the placental barrier in viviparous snakes (Fontenot *et al.* 2000). Thus, the possibility cannot be excluded that the parents were exposed to chemical toxins, pollutants, or ionizing radiation prior to rescue, which could have contributed to the occurrence of the malformation observed in the offspring.

Although it was not possible to precisely determine the etiology of the malformation observed in the specimen of *E. cenchria* described in this study, it is plausible that its origin is related to the interaction of multiple factors, both genetic and environmental. Documenting rare cases such as this is relevant for advancing knowledge of morphological anomalies in wild animals, especially in species with scarce available literature.

In addition to contributing relevant anatomical and behavioral data, reports such as this can support future comparative studies, assist in identifying possible etiological patterns, and foster investigations into the effects of inbreeding, captive conditions, and environmental contaminants on the embryonic development of reptiles. The continued reporting and detailed

analysis of similar cases are essential for a more profound understanding of the occurrence of congenital malformations in snakes and other vertebrates.

Acknowledgments.—The authors thank the Bauru Municipal Zoo for providing the specimen and for the institutional support for development of this research.

References

Albuquerque, N. R., L. Piatti, and V. Wallach. 2013. Dicephalism in the green racer snake, *Philodryas patagoniensis* (Serpentes, Colubridae), from southeastern Brazil. *Herpetology Notes 6:* 85–87.

Albuquerque, N. R., W. S. Arruda, A. S. Costa, R. C. V. Galhart, L. G. H. Vargas, and I. H. Moreno. 2010. A dicephalic yellow anaconda snake, *Eunectes notaeus* (Serpentes: Boidae), from Southern Pantanal, Brazil. *Journal of Natural History 44:* 1989–1994.

Andrade, D. A. and A. S. Abe. 1992. Malformações em ninhadas de caiçara, *Bothrops moojeni* (Serpentes, Viperidae). *Memórias do Instituto Butantan 54:* 61–67.

Belluomini, H. E. 1959. Bicefalia em *Xenodon merremii* (Wagler 1824) (Serpentes) (1957–1958). *Memórias do Instituto Butantan 28:* 85–90.

Belluomini, H. E., P. Biasi, G. Puorto, and V. Borelli. 1977. Bicefalia em *Crotalus durissus terrificus* (Laurenti). [Serpentes: Viperidae, Crotalinae]. *Memórias do Instituto Butantan 40:* 117–121.

Cunha, O. R. 1968. Um teratódimo deródimo em jiboia (*Constrictor constrictor constrictor* (Linn., 1766)). (Ophidia; Boidae). *Boletim do Museu Paraense Emílio Goeldi 67:* 1–25.

Esqueda, L. F., J. Perdomo, and J. Rodríguez. 2016. Un caso de cascabel bicefálica (*Crotalus* Linnaeus, 1758) para Venezuela. *Saber 28:* 626–630.

Federsoni Júnior, P. A. 1979. Casos teratogênicos em *Bothrops atrox* (Serpentes: Viperidae: Crotalinae). *Memórias do Instituto Butantan 43:* 49–64.

Fontenot, L. W., G. P. Noblet, J. M. Akins, M. D. Stephens, and G. P. Cobb. 2000. Bioaccumulation of polychlorinated biphenyls in ranid frogs and northern water snakes from a hazardous waste site and a contaminated watershed. *Chemosphere 40:* 803–809.

Haschek W. M., C. G. Rousseaux, and M. A. Wallig (eds.). 2010. *Fundamentals of Toxicologic Pathology.* San Diego. Academic Press. 691 pp.

Nakamura, K. 1938. Studies on some specimens of Double Monsters of snakes and tortoises. *Memoirs of the College of Science, Kyoto Imperial University 14:* 171–191.

Passos, P. and R. Fernandes. 2008. Revision of the *Epicrates cenchria* complex (Serpentes: Boidae). *Herpetological Monographs 22:* 1–30.

Prado, A. 1943. Um novo caso de bicefalia em serpente. *Memórias do Instituto Butantan 17:* 7–11.

Sant'Anna, S. S., K. F. Grego, C. A. B. Lorigados, A. C. B. C. Fonseca-Pinto, W. Fernandes, L. C. Sá-Rocha, and J. L. Catão-Dias. 2013. Malformations in neotropical viperids: qualitative and quantitative analysis. *Journal of Comparative Pathology 149:* 503–508.

Smith, H. M. and G. Pérez-Higareda. 1987. The literature on somatodichotomy in snakes. *Bulletin of the Maryland Herpetological Society 23:* 139–153.

Vanzolini, P. E., A. M. M. Ramos-Costa, and L. J. Vitt (eds.). 1980. *Répteis das Caatingas.* Rio de Janeiro. Academia Brasileira de Ciências. 161 pp.

Wallach, V. 2007. Axial bifurcation and duplication in snakes. Part I. A synopsis of authentic and anecdotal cases. *Bulletin of the Maryland Herpetological Society 43:* 57–95.

Wallach, V. 2018. Axial bifurcation and duplication in snakes. Part VI. A 10-year update on authentic cases. *Bulletin of the Chicago Herpetological Society 53:* 1–20.

Editor: Jaime Bertoluci

INSTRUCTIONS TO AUTHORS

General Information. *Phyllomedusa* publishes articles dealing with the entire field of herpetology. The journal also maintains sections for Short Communications and Book Reviews. Manuscripts are considered on the conditions that they: (1) have not been published elsewhere; (2) are not under consideration for publication, in whole or in part, in another journal or book; and (3) are submitted by the authors in the format and style of *Phyllomedusa* and in accordance with the specifications included in the Instructions to Authors. Manuscripts should be submitted as a single Microsoft Word document via e-mail. High-quality color images are accepted. Manuscripts must be written in English with appropriate abstracts in alternate languages. If English is not your primary language, arrange to have your manuscript reviewed for English usage before you submit it. Direct any questions about manuscript submission to the primary editor. Publication in *Phyllomedusa,* including color images, is free of charge.

Scope. Manuscripts must contain significant new findings of fundamental and general herpetological interest. Surveys and taxonomic descriptions are published only if there is sufficient new biological information or taxonomic revision to render the paper of general herpetological interest. Lower priority is accorded confirmatory studies, investigations primarily of localized interest, range extensions, technique papers with narrow application, descriptions of phenomena based on insufficient data, and descriptive work that is not placed in a significant context. Manuscripts should include a clear statement of the purpose of the study or the hypothesis that was tested.

Peer Review. At least two referees, an Associate Editor, and the Editor will review each manuscript that is deemed to fall within the scope of *Phyllomedusa.* Authors will be notified of the status of their manuscript within 90 days. Revised manuscripts accepted for publication will be edited for English usage and syntax prior to final acceptance for publication.

Manuscript Style and Format. Use the active voice when possible; thus, you should write "I/we studied the frog," rather than "The frog was studied by me/us" (passive voice). Use American spelling and punctuation. Double space the entire manuscript, including references, tables, table captions, and legends for illustrations. Use Times New Roman 12-point font, and set up document with margins of at least 2.54 cm (1 in.) on each side. Do not justify the text; it should be left aligned and ragged right. Number manuscript pages consecutively and lines continuously, **followging the arrangement and format outlined below exactly.**

- **Title:** Bold-faced caps and lower-case Roman; sentence capped, left aligned; use colons to separate ranked taxonomic names.
- **Name(s) of author(s):** Bold-faced caps and lower-case Roman; left aligned; use serial commas. Follow example:

José Wellington Alves dos Santos[1,2], Roberta Pacheco Damasceno[1,2], and Pedro Luís Bernardo da Rocha[2,3]

- **Institutional affiliation(s):** Light-faced caps and lower-case Roman; left aligned. Follow example:

[1] University of Kansas, Department of Ecology and Evolutionary Biology. Lawrence. Kansas 66045-7580, USA. E-mail: trueb@ku.edu.

[2] Universidade de São Paulo, Escola Superior de Agricultura Luiz de Queiroz, Departamento de Ciências Biológicas. 13.418-900, Piracicaba, SP, Brazil. E-mail: jaime.bertoluci@usp.br.

[3] Universidad Nacional Autónoma de México, Centro de Ciencias Genómicas. Cuernavaca, Morelos, Mexico. E-mail: delibasanta@gmail.com.

- **Abstract:** Should not exceed 350 words (including lead title) and one paragraph and only is included in regular articles. Alternate-language abstracts may be included, but these must match the content of the English abstract. See example:

Abstract

Title of paper in bold-faced Roman. Content of abstract follows in light-faced Roman; left alignment.

- **Keywords:** Light-faced Roman; separate words with commas; capitalize only proper nouns; include descriptors not contained in the title in alphabetical order.
- **Body of Article:** The text of the article will include the following parts indicated by **primary headings in bold-faced Roman aligned to the left (except for References, which should be centered).**

Introduction
Materials and Methods
Results
Discussion
Acknowledgments
References

Secondary headings within major sections are title-capped, italics aligned left. **Tertiary headings** follow a paragraph indentation; they are sentence capped, and set in italics. Tertiary headers are followed by a point and an em-dash. Follow example:

Material and Methods [Primary header]

Study Site [Secondary header]

Selection of site.—This is a Tertiary, or third-level, heading. Note that it is indented and lacks a hard return. The heading is followed by a point or period and a long (em-dash).

- **Body of Short Communication or Book Review:** These shorter articles do not include the primary headings Introduction, Materials and Methods, Results, and Discussion. "Acknowledgments" is treated as a third-level, or tertiary header.
- **Tables:** Number tables consecutively with Arabic numbers. Refer to tables in text as Table 1, Tables 2 and 3, and Tables 2–5. Exceedingly long tables should be placed in appendices. Table captions should be placed above the table. Horizontal rules may be used in the table header and at the foot of the table. No rules (horizontal or vertical) should appear in the body of a table. Consult Vol. 20 (2) of *Phyllomedusa* for proper format of table captions and contents.
- **Appendices:** Number appendices consecutively with Roman numerals. Refer to tables in text as Appendix I, Appendices II and III, and Appendices II–V. Appendix captions should be placed above the appendix content. Most appendices should follow the format instructions for tables. Extensive lists of specimens examined should be included as an appendix. Consult Vol. 18 (2) of *Phyllomedusa* for proper format and arrangement of specimens examined.
- **Figure captions or legends:** All figures must be numbered consecutively and their legends or captions formatted in *Phyllomedusa* style (Vol. 18, No. 2). The captions should be listed in order separate from the images. Refer to figures in text as Figure 1, Figures 2 and 3, Figures 2–5, Figure 4A, and Figure 4A, B. "Figure" or "Figures" are always spelled out—even in parentheses. Figures must be cited in order in the text. See specific instructions for preparation of figures.
- **Figures for review:** Embed all figures in order at the end of the Word document as PNG (Portable Network Graphic) files. Identify each with the figure number and a short caption, and **indicate whether the figure is intended for reproduction at column or page width, or as a broadside.**

Preparation of Figures for Publication. All figures should be submitted digitally as TIF files with LZW compression, **separately from the files embedded in the manuscript** for review. Each figure should be submitted at **the exact size** intended for publication. There are three choices: **page width** (34 picas, 145 mm, 5 and 11/16 in.), **column width** (16.5 picas, 70 mm, 2 and 3/4 in.), or **broadside** (193 mm × 145 mm). All illustrations must **allow room for a caption to be printed below the figure,** while conforming to these measurements.

- **Labeling figures:** Labels must be consistent on a figure and among all figures included in the article. **Use a sans serif font** that is common to Windows and Macintosh platforms (e.g., Arial). Subunits of multipart figures must be labeled with capital letters (A, B, C) placed in the **upper, left-hand area** of each unit. The letters **should be about 10 points large** (not to exceed 12 pt); they must be identical in size and typeface on each figure included in the manuscript.

INSTRUCTIONS TO AUTHORS

Labeling within figures (e.g., anatomical parts, legends on axes of graphs, etc.) **should be in the range of 8–9 pt and in a sans serif font, such as** Arial. Scale bars should be labeled with their values on the face of the figure (e.g., 5 mm); **the minimal size of lettering that may be used is 7 points** in a sans serif font for scale bars, longitude and latitude on maps, etc.

- **Vector graphics:** *Maps, graphs, and line drawings* should be prepared with an illustration program such as Adobe Illustrator, CorelDRAW, or Deneba Canvas. Graphs and maps generated in other programs (e.g., Sigma Plot, Excel) can be imported into these illustration programs and manipulated (or used as a template to produce a new drawing) to produce an acceptable figure at the size intended for publication. Similarly, drawings executed by hand, should be scanned (300–600 dpi) and imported into an illustration program in which they can be sized and labeled for publication. Follow the instructions for labeling provided above, along with the following guidelines for illustrations at column and page widths.
  - ✓ Sized for publication, lines (strokes) should be between 0.25 and 2 points wide.
  - ✓ Tick marks on graphs should be on the outside of the axis line. Sized for publication, they are between 3 and 5 points in length and 0.25 pt in weight. Longitude and latitude marks should be on the inside of the map border.
  - ✓ All maps must have an appropriate scale in kilometers.
  - ✓ Overlapping symbols and lines must be counter shadowed with white.
  - ✓ Export completed image as a TIF document for submission.
- **Raster graphics:** *Photographs (color and gray-scale [black & white]) and tone (gray-scale) renderings* should be submitted as a RGB document in TIF format sized for publication (described above) at a resolution between 300 and 600 dpi (after reduction/sizing). To label raster images, import them into a vector graphic program, follow the directions above, and export the completed image as a TIF document for submission.

Editorial conventions.

- **Taxonomy.** All generic and specific names must appear in italics. At the first mention of a species in any paragraph, provide its complete binomial name; in subsequent references to the same species, the generic name may be abbreviated. The first citation of a species must include the authority and date, but the authority does not have to be cited in the References. Hierarchical taxa are separated with colons (e.g., Anura: Leptodactylidae). New taxonomic names should not appear in the Abstract or Keywords.
- **Dashes.** There are three kinds of dashes. Short dashes (-) are used as hyphens. En-dashes (–) are used to denote ranges (e.g., 5–10, May–September) and the minus sign in mathematics. Em-dashes (—) are used in Tertiary Headings, and frequently as a substitute for parentheses and colons. There should be no space on either side of any of these dashes.
- **Numbers and units.** All measurements are noted in Arabic, unless the number starts a sentence.
  - ✓ Measurements include distances, areas, dimensions, volumes, weights, time (e.g., hours, days, seconds, minutes), temperatures, etc. **Standard SI units are used**—e.g., time: 08:16 h; distances and areas: 7 km, 12.5 mm, 17,840 ha; geographic coordinates: 04°43'23" S; temperature: 24°C. To indicate degrees, use a degree sign (°), not a superscript oh (º). Note that degrees and minutes are straight quotation marks or prime signs; do not use curly quotes.
  - ✓ Use the **double-digit rule** for numbers other than measurements. Numbers less than 10 are spelled out—e.g., "… nine animals were sampled"; numbers of 10 and more are denoted in Arabic—e.g., "… but 10 larvae were collected."
- **Citations.** Authorities are cited in text as follows. Single: (Caballero 1944); double: (Bursey and Goldberg 2006); three or more (Goldberg *et al.* 2002). Note use of "and" and italics for "et al." Multiple text citations should be listed in chronological order and separated by commas—thus: (Crump 1974, Duellman 1978a–c, 1980, Duellman and Trueb 1986). Two or more publications by the same author should be cited in the following pattern: (Vanzolini 1991, 1992) or Cadle (1984a, b, 1985).
- **References.** All publications cited in the text (except taxonomic authorities) must be included in the References in alphabetical order. "Gray literature" (e.g., technical reports, theses, dissertations that have limited distribution or are difficult to identify and acquire) should be avoided. Follow the formats shown below.

  ✓ **Normal journal articles:**

  Vanzolini, P. E. 1993. A new species of turtle, genus *Trachemys,* from the state of Maranhão, Brazil (Testudines, Emydidae). *Revista Brasileira de Biologia 55:* 111–125.

  ✓ **Two authors in a journal series:**

  Zamudio, K. R. and H. W. Greene. 1997. Phylogeography of the bushmaster (*Lachesis muta:* Viperidae): implications for Neotropical biogeography, systematics, and conservation. *Biological Journal of the Linnean Society 62:* 421–442.

  ✓ **More than two authors in a journal series:**

  Hero, J.-M., W. E. Magnusson, C. F. D. Rocha, and C. P. Catterall. 2001. Antipredator defenses influence the distribution of amphibian prey species in the central Amazon rain forest. *Biotropica 33:* 131–141.

  ✓ **Chapter in an edited volume:**

  Hedges, S. B. 1999. Distribution patterns of amphibians in the West Indies. Pp. 211–254 *in* W. E. Duellman (ed.), *Patterns of Distribution of Amphibians. A Global Perpective.* Baltimore and London. The Johns Hopkins University Press.

  ✓ **Unpublished thesis or dissertation:**

  Verdade, V. K. 2001. Revisão das espécies de *Colostethus* Cope, 1866 da Mata Atlântica (Anura, Dendrobatidae). Unpublished M.Sc. Dissertation. Universidade de São Paulo, Brazil.

  ✓ **Book:**

  McDiarmid R. W. and R. Altig (eds.). 1999. *Tadpoles. The Biology of Anuran Larvae.* Chicago and London. The University of Chicago Press. 633 pp.

  ✓ **Material from the World Wide Web:**

  Frost, D. R. (ed.). 2010. Amphibian Species of the World: an Online Reference. Version 5.4 (8 April 2010). Electronic Database accessible at http: // research.amnh.org/vz/herpetology/amphibia/American Museum of Natural History, New York, USA. Captured on 22 August 2010.

  ✓ **Software:**

  Maddison, W. P. and D. R. Madison. 2010. Mesquite. A Modular System for Evolutionary Analysis. Version 2.73. URL: http://mesquiteproject.org

- **Animal care and permits.** The editorial staff of *Phyllomedusa* subscribes to humane and ethical treatment of all animals; all contributors to the journal must comply with this principle. In addition, all required state and federal permits must have been obtained and must be cited in the Acknowledgments.
- **Proofs.** The publisher will undertake proofreading, unless specifically advised otherwise by the corresponding author when the contribution is accepted for publication.
- **Reprints.** Authors will receive a PDF of their contribution and are invited to distribute it freely.
- **Submission.** Send your manuscript as a single Microsoft Word file (.doc or .docx) containing the main text followed by Appendices, Tables and Figures with their respective captions via e-mail to the Editor: phyllomedusa@usp.br.

Jaime Bertoluci
Editor-in-Chief


PHYLLOMEDUSA
Journal of Neotropical Herpetology
PHYLLOMEDUSA
Journal of Neotropical Herpetology
PHYLLOMEDUSA
Journal of Neotropical Herpetology
PHYLLOMEDUSA
Journal of Neotropical Herpetology
PHYLLOMEDUSA
Journal of Neotropical Herpetology
PHYLLOMEDUSA
Journal of Neotropical Herpetology
PHYLLOMEDUSA
Journal of Neotropical Herpetology
PHYLLOMEDUSA
Journal of Neotropical Herpetology
PHYLLOMEDUSA
Journal of Neotropical Herpetology
PHYLLOMEDUSA
Journal of Neotropical Herpetology
PHYLLOMEDUSA
PHYLLOMEDUSA
PHYLLOMEDUSA
Journal of Herpetology
PHYLLOMEDUSA
Journal of Herpetology
PHYLLOMEDUSA
PHYLLOMEDUSA
Journal of Herpetology
PHYLLOMEDUSA
Journal of Herpetology
PHYLLOMEDUSA
Journal of Herpetology
PHYLLOMEDUSA
Journal of Herpetology

Contents

Volume 24 Number 2
July-December 2025

Articles

Short Communications

Articles published in Phyllomedusa are indexed in the following databases: Web of Science (Science Citation Index Expanded), SCOPUS, Dimensions, Zoological Record, BIOSIS Previews, CABI Publishing, Current Contents (Agriculture, Biology & Environmental Sciences), and DOAJ (Directory of Open Access Journals).

www.revistas.usp.br/phyllo
www.phyllomedusa.esalq.usp.br